Spring 1993

Mechanism of pneumatic fracturing

Trevor Compton King
New Jersey Institute of Technology

Copyright Warning & Restrictions

The copyright law of the United States (Title 17, United States Code) governs the making of photocopies or other reproductions of copyrighted material.

Under certain conditions specified in the law, libraries and archives are authorized to furnish a photocopy or other reproduction. One of these specified conditions is that the photocopy or reproduction is not to be "used for any purpose other than private study, scholarship, or research." If a, user makes a request for, or later uses, a photocopy or reproduction for purposes in excess of "fair use" that user may be liable for copyright infringement,

This institution reserves the right to refuse to accept a copying order if, in its judgment, fulfillment of the order would involve violation of copyright law.

Please Note: The author retains the copyright while the New Jersey Institute of Technology reserves the right to distribute this thesis or dissertation

Printing note: If you do not wish to print this page, then select "Pages from: first page # to: last page #" on the print dialog screen

ABSTRACT

Mechanism of Pneumatic Fracturing

by
Trevor Compton King

This thesis investigates the mechanism of pneumatic fracturing in geologic materials such as soil and rock. Pneumatic fracturing is a recently developed technique for increasing the permeability of geologic formations by the controlled injection of high pressure air. Present applications are focusing on the in situ remediation of contaminated soil and ground water, although pneumatic fracturing has other geotechnical uses such as pumping well enhancement.

A comprehensive literature review of a related technology known as hydraulic fracturing is presented, which serves as background for development of a pneumatic fracturing model. Pressure-time histories from actual pneumatic injections are analyzed in detail to understand the failure mechanism. Several distinct stages of a typical fracture event are identified including: fracture initiation, fracture extension, fracture maintenance, and fracture residual. Reinjection behavior of previously fractured formations is also investigated. The entire fracture event was consistently found to be quite rapid, lasting only several seconds, leading to the conclusion that the formations will respond brittlely.

Based on these pressure-time analyses, an original analytical model is developed for the prediction of fracture initiation pressure and fracture maintenance pressure. The model describes the stress conditions leading to failure in and around a discrete section of borehole during pneumatic injection. The model has a linear form, and assumes the geologic medium is brittle-elastic, uniformly stratified, overconsolidated, horizontally isotropic, and semi-porous. The two dominant terms found to influence fracture pressure are overburden stress and apparent tensile strength of the formation. The effects of pieozometric head are also incorporated, so that the model is applicable to both the

vadose zone and saturated zone.

Validation of the model is made with actual field data from several different research test sites. The trends of the data show reasonable agreement with the model, and numerical coefficients are determined by regression. Tentative relationships were developed for two types of geologic media: clayey silt and siltstone/sandstone. Overburden gradients for the clayey silt, siltstone and sandstone ranged from 1.0 to 2.5 psi per foot of depth. Apparent cohesive/tensile strengths for these materials ranged from 5 to 23 psi, 41 to 130 psi and 42 to 52 psi respectively. Sample computations with the model are presented, and the thesis concludes with recommendations for future study.

MECHANISM OF PNEUMATIC FRACTURING

by
Trevor Compton King

A Thesis
Summitted to the Faculty of
New Jersey Institute of Technology in Partial Fulfillment of the
Requirements for the Degree of
Master of Science in Environmental Engineering

Department of Civil and Environmental Engineering

May 1993

APPROVAL PAGE
Mechanism of Pneumatic Fracturing

by
Trevor Compton King

Dr. John R. Schuring, Thesis Advisor
Associate Professor of Civil and Environmental Engineering, NJIT

Dr. Paul C. Chan, Committee Member
Professor of Civil and Environmental Engineering, NJIT

Dr. Dorairaja Raghu, Committee Member
Professor of Civil and Environmental Engineering, NJIT

BIOGRAPHICAL SKETCH

Author: Trevor Compton King

Degree: Master of Science in Environmental Engineering

Date: May 1993

Undergraduate and Graduate Education:

- Master of Science in Environmental Engineering,
  New Jersey Institute of Technology, Newark, NJ, 1993

- Bachelor of Science in Mechanical Engineering,
  Wolverhampton Polytechnic and Harper Adams College,
  Shropshire, England, 1982

Major: Environmental Engineering

This thesis is dedicated to
Fleurette, Jean and Trevayne.

ACKNOWLEDGMENTS

The author wishes to express his sincere gratitude to his advisor, Dr. John Schuring. By his valuable help, guidance and patience throughout the writing of this thesis, the author has been able to improve his research, technical, analytical and writing skills.

Special thanks are also extended to Dr. Paul Chan and Dr. Dorairaja Raghu for serving as members of the committee and for their careful review and helpful suggestions.

Recognition is also made to his colleagues and friends, Conan Fitzgerald, Dr. Prasanna Ratnaweera, Firoz Ahmed, Deepak Nautiyal, Yuan Ding, Osualdo Rodriguez, Sheridan Quarless, Renee Crawley and Lois Chipepo-Hodges, for their constant corporation, useful suggestions and encouragement throughout this study.

Finally, he would like to thank his wife and son for their love, patience and support.

TABLE OF CONTENTS

TABLE OF CONTENTS

LIST OF TABLES

LIST OF FIGURES

Figure **Page**

Figure **Page**

EQUATION NOMENCLATURE

a = constant of porous-elastic material

A_f = Skempton's pore pressure parameter

b = One-half major axis of ellipse

c_i = Cohesive strength intercept

C_b = Rock bulk compressibility

C_r = Rock matrix compressibility

E = Young's modulus

h = Height of overburden

h_w = Height of saturated zone

K = Principal stress ratio

K_o = Coefficient of lateral earth pressure

m = Rate of change of fracture pressure with horizontal stress

P_a = Pressure on the borehole wall due to the injected air

P_b = Fracture initiation pressure

P_b^p = Fracture initiation or breakdown pressure in permeable formation

P_b^i = Fracture initiation or breakdown pressure in impermeable formation

P_e = Excess pressure

P_l = Fracturing pressure of liquid

P_m = Fracture maintenance pressure

P_o = Initial pore pressure of formation

P_s = Fracture shut-in pressure

P_w = Pressure on the borehole wall due to the injected liquid

Δp = Fluid pressure difference between the formation and the wellbore.

R = Critical stress

EQUATION NOMENCLATURE

r = Radius at the end of the ellipse

t_a = Apparent tensile strength

t_o = Tensile strength of material

t_r = Tensile strength of rock

t_s = Tensile strength of soil

β = Angle between major and minor principal stress

γ_r = Unit weight of rock

γ_s = Unit weight of soil

γ_w = Unit weight of water

ν = Poisson's ratio

$\sigma_{\max.}$ = Maximum stress

$\overline{\sigma}$ = Average stress

$\sigma_{rr}, \sigma_{\theta\theta}, \sigma_{zz}$ = Tectonic (in-situ) stresses

$\sigma'_{rr}, \sigma'_{\theta\theta}, \sigma'_{zz}$ = Effective (in-situ) stresses

σ_{11} = Maximum principal stress

σ_{22} = Intermediate principal stress

σ_{33} = Minimum principal stress

σ'_{11} = Effective maximum principal stress

σ'_{22} = Effective intermediate principal stress

σ'_{33} = Effective minimum principal stress

σ^h_{11} = Maximum horizontal principal stress

σ^h_{22} = Minimum horizontal principal stress

σ_h = Principal horizontal stress

σ'_h = Effective horizontal stress

EQUATION NOMENCLATURE

σ_{ta} = Apparent tensile stress

σ_v = Principal vertical stress

$\sigma_v^{'}$ = Effective vertical stress

σ_{11}^h = Maximum horizontal principal stress

σ_{22}^h = Minimum horizontal principal stress

τ = Shear stress

τ_f = Shear strength at failure

θ = Angle measured clockwise from radius in the direction of the smaller horizontal tectonic stress.

ϕ = Angle of internal friction

λ = Constant $(1 - a\frac{1-2\nu}{1-\nu})$

λ_1 = constant representing overburden stress term

λ_2 = constant representing residual tensile strength

λ_3 = constant representing the apparent breakdown tensile strength term

η = $\frac{1+\sin\theta}{1-\sin\theta}$ (Equation 3.41)

ψ = $2c_i \tan\left(45+\frac{\theta}{2}\right)$ (Equation 3.41)

CHAPTER 1

INTRODUCTION

1.1 General Information

The concept of "pneumatic fracturing" grew out of a need to enhance the capability of current remediation technologies to remove volatile organic compounds (VOC's) from soil and rock formations. The pneumatic fracturing process focuses on in-situ treatment of the vadose zone, and the current technologies targeted for enhancement include vacuum extraction, bioremediation, and thermal injection.

A review of the available literature for current in-situ remediation technologies reveals a major limitation, i.e. their success is significantly impaired in soils with low permeabilities ($K<10^{-5}$ cm/sec). This occurs since in-situ remediation depends on the pore fluid exchange rate of the geologic formation being treated. It was clear, therefore, that essentially all in-situ technologies require some type of enhancement in low permeability formations; otherwise treatment rates would be unacceptably slow, and in most cases satisfactory regulatory requirements could not be achieved.

In response to the above, the new technology, pneumatic fracturing was conceived. This technology has similarities to hydraulic fracturing techniques which have been extensively used in the petroleum industry for decades. The primary function of pneumatic fracturing is to increase fluid flow rates in low permeability formations, but it also has the potential to deliver nutrients, moisture, microorganisms and other substrates to the geologic formation for in-situ bioremediation. To date, investigative studies have focused on the vadose zone, but plans are underway to extend this technology to the saturated zone.

The concept and technique of pneumatic fracturing are straightforward and is shown conceptually in Figure 1. The process consists of injecting high pressure air or a gas into the geologic formation through a borehole. The injection is done at a controlled pressure and flow rate. The compressed air is used to pressurize an interval which has been

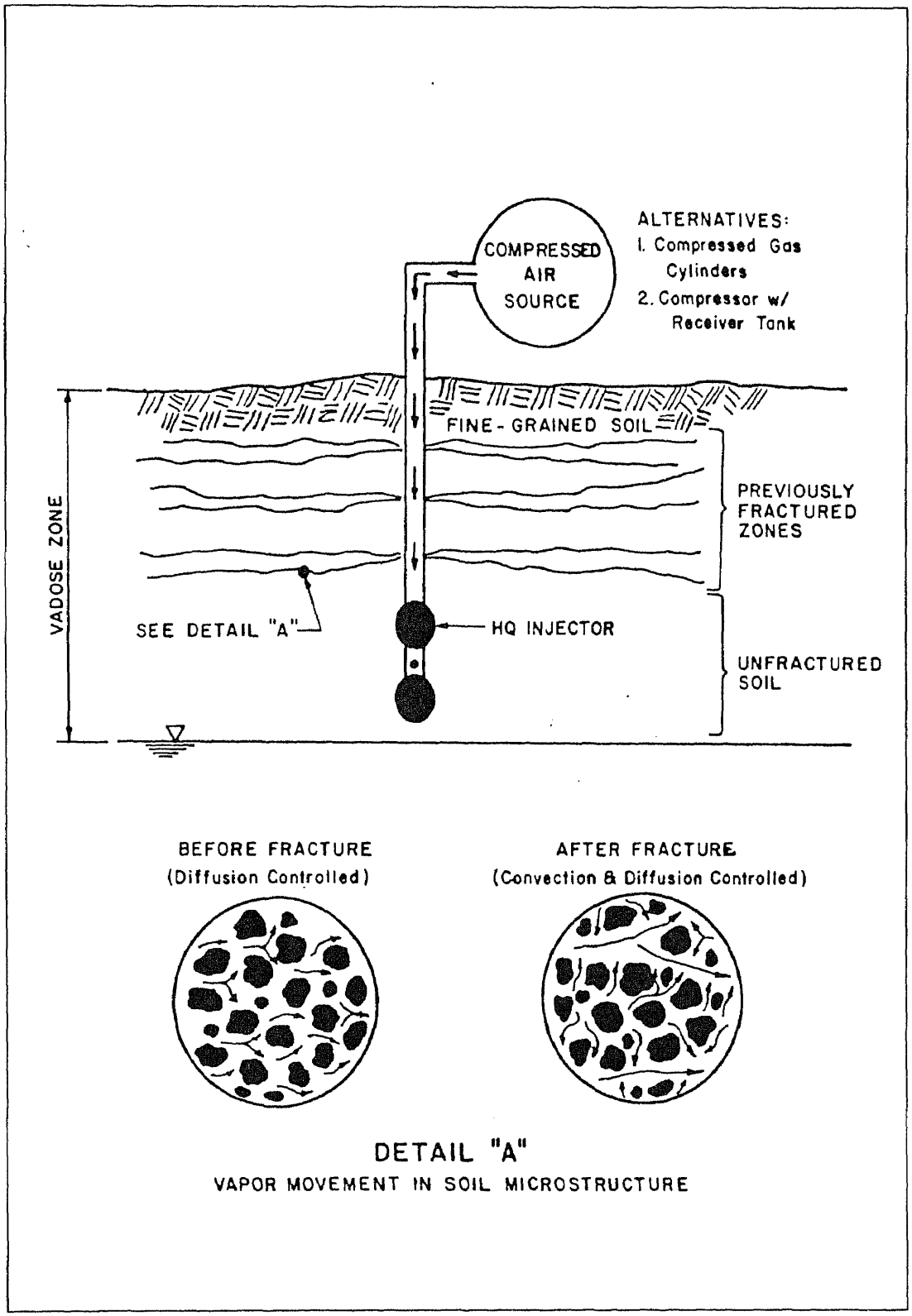

Figure1 Schematic of Pneumatic Fracturing Process.

isolated with inflatable packers. The pressure within the interval is increased until it exceeds a value which causes failure of the geologic formation in that region. The result is a fractured zone extending radially from the point of injection.

The feasibility and the economic success of the pneumatic fracturing technology can only be realized if the engineering parameters are clearly understood, and can be easily applied during the design of a clean up action. The present study addresses the theoretical aspects of pneumatic fracturing by analyzing experimental data collected during the last four years. By using its counterpart technology, hydraulic fracturing, as a starting point, theoretical models for pneumatic fracturing mechanisms are developed. The information presented will not only describe the mechanism of pneumatic fracturing, but more importantly will also provide practical relationships for applying this technology in the field.

1.2 Objectives and Scope

Research work done during the last four years has resulted in the accumulation of field data, which has been obtained through numerous pneumatic fracture injections performed in a variety of geologic formations. The results of these tests are quite encouraging, since they have consistently demonstrated that the permeability of these geologic formations are enhanced.

The commercial success of this technology will depend on the ability to create controlled fractures in contaminated geologic formations. This requires that accurate estimates of key process parameters be made during the design phase. These parameters include: fracture initiation pressure, fracture propagation pressures, fracture orientation and fracture dimensions. The ultimate goal of this study is to develop procedures for design and optimization of pneumatic fracture applications.

The objectives of this study are therefore to

1. Describe the physical mechanism of pneumatic fracturing in geologic formations.

2. Develop analytical models which can be used to predict pneumatic fracture behavior.
3. Organize the accumulated field data in a manner which can be easily managed and manipulated.
4. Verify the proposed analytical model with field data and
5. Identify future design criteria which are essential for applying and understanding this technology.

CHAPTER 2

BACKGROUND INFORMATION

2.1 Project History

Pneumatic fracturing has been under development since Spring 1988 at the Hazardous Substance Management Research Center (HSMRC) located in New Jersey Institute of Technology (NJIT). In the first two years, the investigative work involved mostly bench scale experiments which were conducted in the laboratory. A first series of experiments were conducted with Plexiglas vats which were filled with soil containing a surrogate contaminant of known concentration and density (Papanicolaou, 1989; Shah, 1991). Simulated vapor extraction was conducted on vats which had been pneumatically fractured, as well as unfractured vats. The results consistently showed that contamination removal efficiencies were 100% to 360% higher in the fractured soil compared with the unfractured soil. These encouraging results subsequently led to the on-going prototype development activities and pilot demonstrations.

A second series of laboratory studies investigated the flow characteristics and mass transport rate of a single fracture with known dimensions (Ng, 1991). Experiments were conducted with a custom fabricated horizontal infiltrometer. Experimental results proved that the improved mass flow rate in fractured soil was attributable to enhanced subsurface air-flow. In addition, they confirmed that flow rate through a fracture is proportional to the cube of the aperture. Bench scale and theoretical studies are continuing to investigate new phenomena and design variations.

During the last two years, the pneumatic fracturing prototype has been extensively tested and demonstrated in the field at a number of "clean" and contaminated sites along the East Coast.(Schuring, Jurka and Chan (1991)), Pisciotta, Schuring, et al. (1991) and Schuring, Chan, et al. (1992). This has permitted study of various system parameters, e.g., fracture length, injection pressures, and orientations in a variety of geologic

formations. These field tests provide valuable insight into the system's operational capabilities, and have resulted in subsequent improvements. The first commercial version of the pneumatic fracturing technology has been built by Accutech Remedial Systems of Keyport, New Jersey, and production operation began in April 1993.

In July 1991 the technology was patented, and in August 1992, it was evaluated by the U.S. EPA under its SITE Demonstration Program. The purpose of the SITE project was to scientifically evaluate the technical claims of the technology and to determine its suitability for Superfund sites. A full report on the results of the demonstration is due in late Spring 1993.

Current research activities are focusing on the application of the pneumatic fracturing technology to enhance bioremediation. The former study involves the injection of acclimated microbes, as well as the stimulation of indigenous microbes. The pneumatic fracturing prototype has been modified to permit injection of biological supplements, e.g. buffers, and nutrients in liquid or granular form into the fractured formation. Laboratory studies are also being conducted to investigate the ability of microorganisms to survive the pressures and stresses associated with pneumatic fracturing.

2.2 Methodology of Pneumatic Fracturing

Figure 2 shows the prototype pneumatic fracturing system. The first step in applying the pneumatic fracturing technology, consists of drilling boreholes to predetermined depths in a selected area. The location and depths of these boreholes is determined by the hydrogeology of the site, as well as the distribution of the contaminant.

Next, a pneumatic device known as an "HQ injector" is inserted into the borehole to a predetermined elevation. The nozzle can be positioned at any elevation within the hole depending on the desired number of fractures, and degree of aeration required. The seals of the HQ injector are inflated using nitrogen gas which isolates an approximate two foot borehole section for the injection.

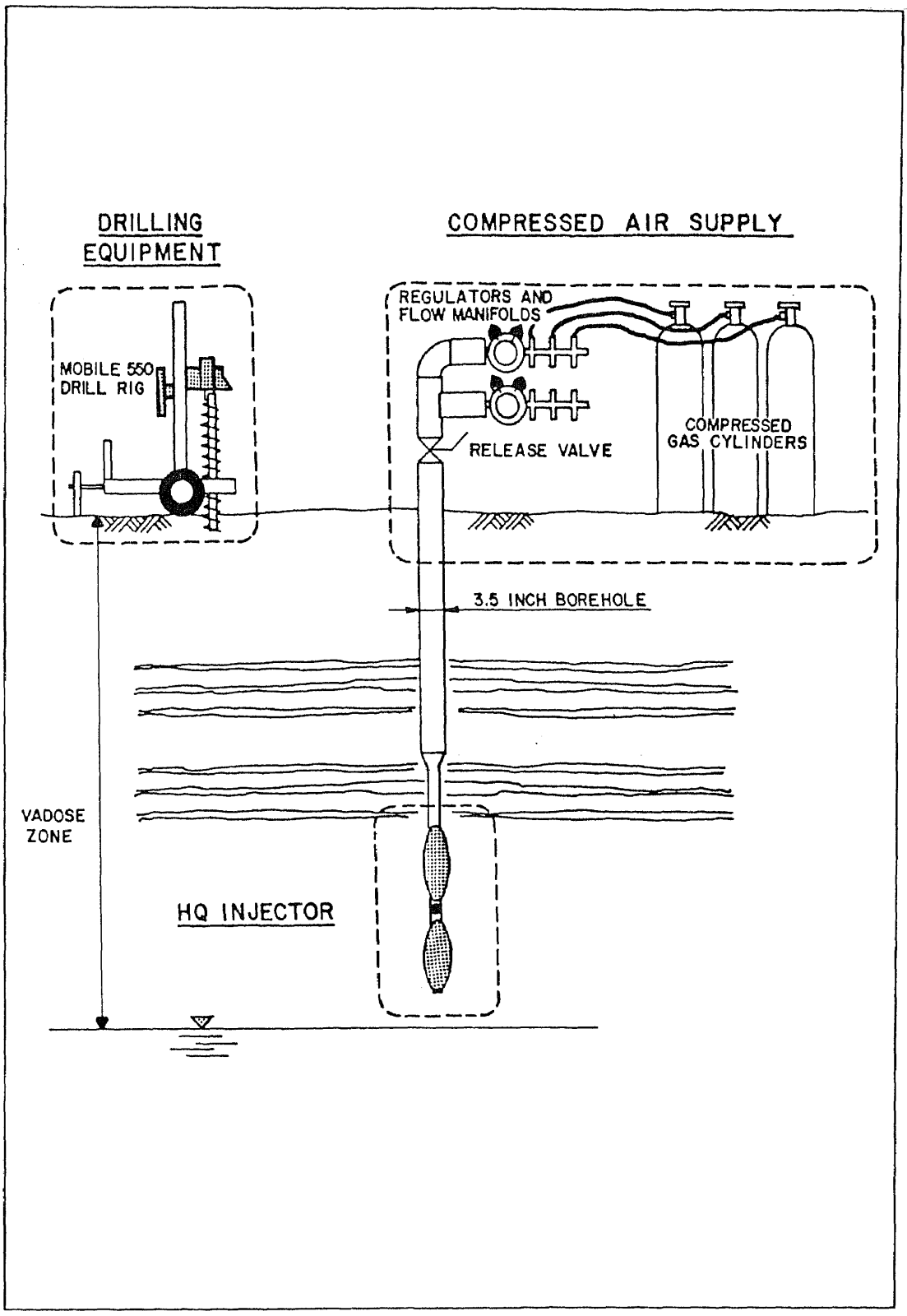

Figure 2 Prototype Pneumatic Fracturing System.

The inflation pressure of the packers is important from a fracturing efficiency and safety perspective. It has been found that during pressurization of the interval, there is a tendency for the pressure to force the packers away from the interval. This movement is counteracted both by the frictional forces that exist between the seals and the borehole, as well as the attaching rod between the two seals.

A packer friction test is conducted prior to any fracture operation to determine the proper inflation pressure of the packer for the particular formation. For most formations the packer is inflated to at least twice the anticipated injection pressure.

The fracturing process involves the injection of high-pressured air or other gas through the HQ injector and into the geologic formation for a specific time period. The pressurized air required to initiate pneumatic fractures is controlled by a pressure manifold system. This system consists of regulators, valves, pressure gauges and a compressed air source.

The injection pressures and flow rates are selected so that they exceed material in-situ stresses and the permeability of the formations. The fracture initiation pressures have been found to be relatively modest and to range below 100 psi for the soils tested and below 200 psi for rock formations tested. To date, fracturing has been conducted at depths ranging from 3 to 21 ft.

The response of geologic formations to pneumatic fracturing and the potential benefits which may be derived, depend on the nature of the deposit. In fine-grained soils, which naturally have low permeability values, pneumatic injections create conductive channels which increase the permeability and exposed surface area of the formation. Application of pneumatic fracturing to fine-grained soils is shown conceptually in Figure 3.

For coarse-grained soils e.g. sand and gravel, whose natural permeability is already high, the ability to create new fractures is limited. However, the process provides a means for rapidly aerating the formation under aerobic and anaerobic conditions. As

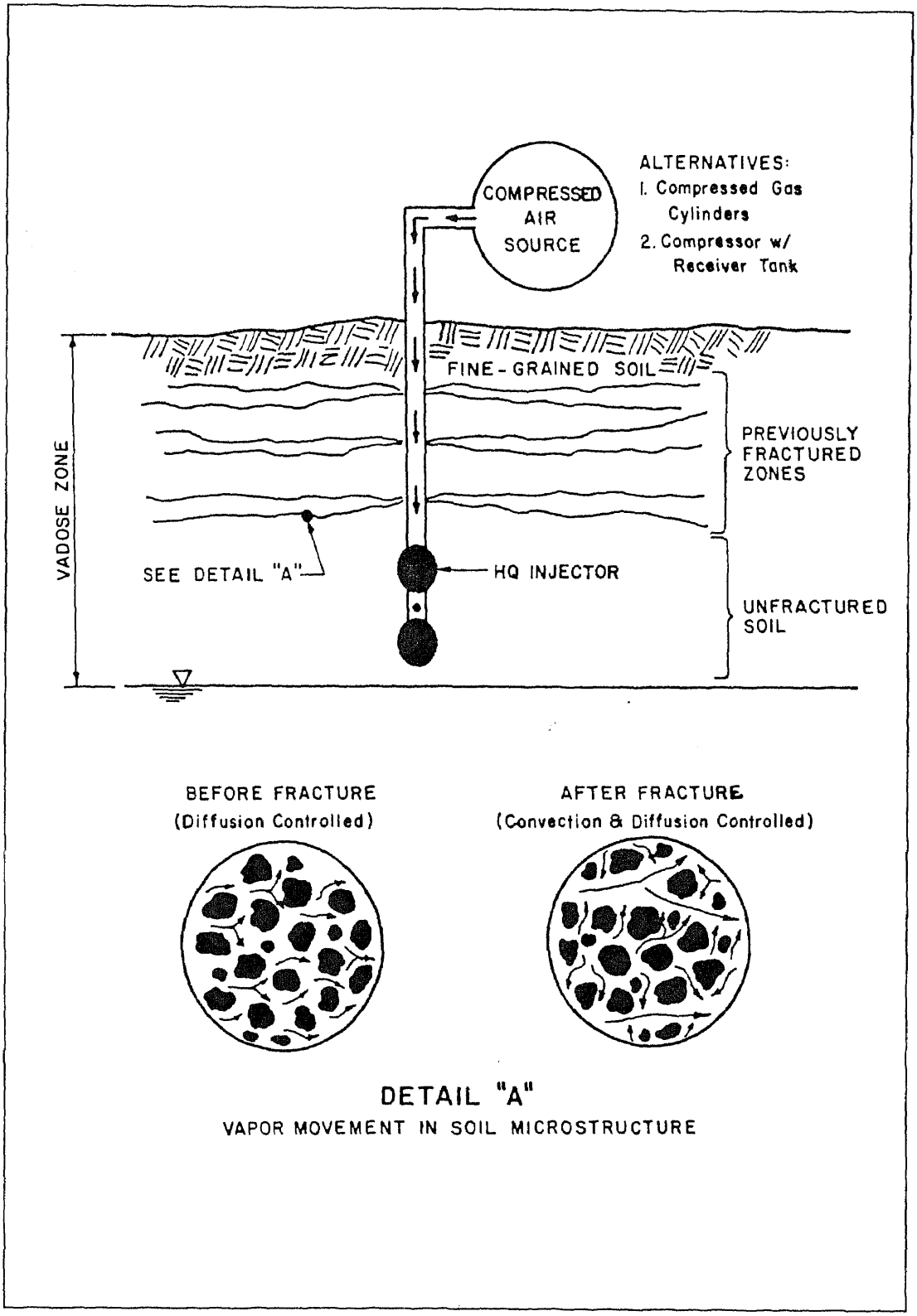

Figure 3 Pneumatic Fracturing Concept for Fine-Grained Soils.

indicated in Figure 4, an injection of two minutes in duration can affect a radius of up to 18 feet from the borehole.

For sedimentary rocks, such as shale and sandstone, pneumatic fracturing can enhance formation permeability by widening the apertures of existing discontinuities and/or clearing soil fillings from primary joints. It may also create a minor amount of new fractures. The application of pneumatic fracturing to sedimentary rock is depicted in Figure 5.

Although the response of different geologic conditions to pneumatic fracturing will vary, the net effect remains the same, i.e. acceleration of the rate at which pore gases and liquids can move through the formation. This will result in reduction of in-situ remediation times and also extension of current technologies to more difficult geologic conditions.

2.3 Monitoring Methods for Pneumatic Fracturing

Evaluation of the pneumatic fracturing technology requires the measurement of a number of system parameters relating to fracture initiation and dimensions. As a result, several methods and monitoring techniques have been developed for the detection and measurement of pneumatically induced fractures. Those pertinent to the present study will now be summarized and include: reference beam, tiltmeters, borehole camera, borehole pressure transducer and monitoring wells.

2.3.1 Reference Beam

Ground surface heave has been one of the primary methods used to detect fractures and estimate fracture dimensions. Initially, measurements were made with optical levels and graduated heave rods. These were subsequently complemented by the use of a custom fabricated reference beam system. Details of the reference beam are shown in Figure 6.

The reference beam system provides a more comprehensive method of monitoring

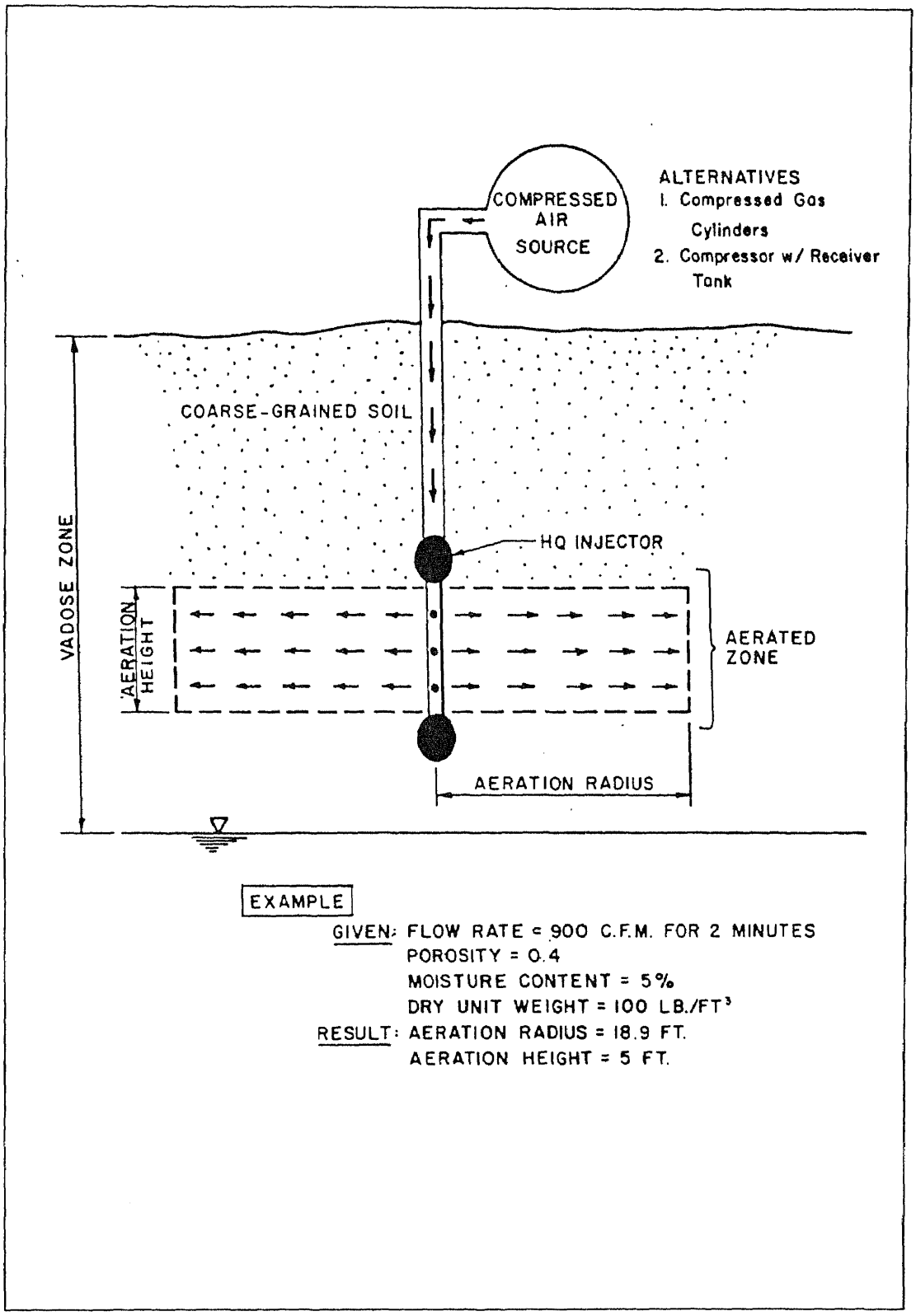

Figure 4 Pneumatic Aeration Concept for Coarse-Grained Soils.

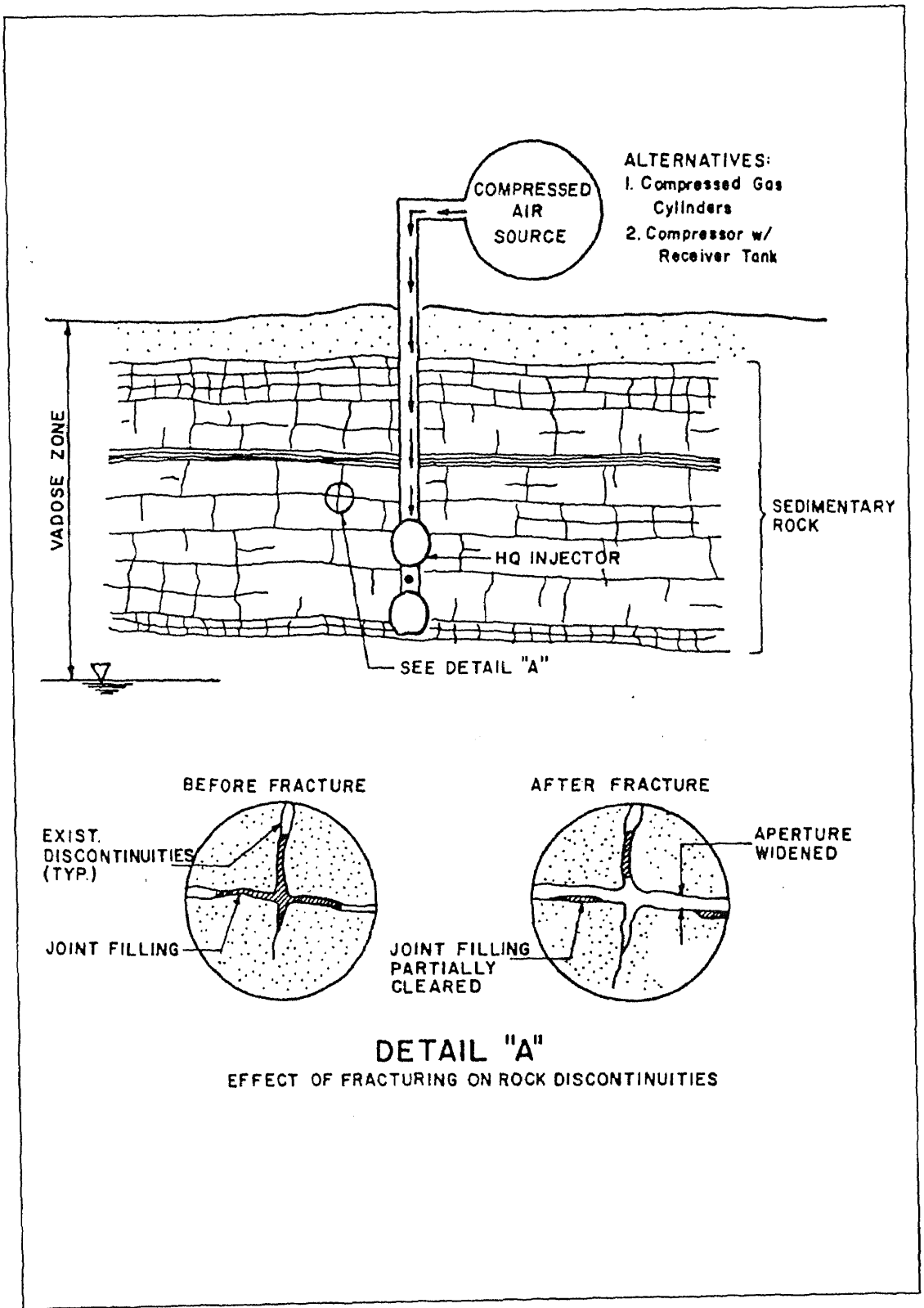

Figure 5 Pneumatic Fracturing Concept for Rock Formations.

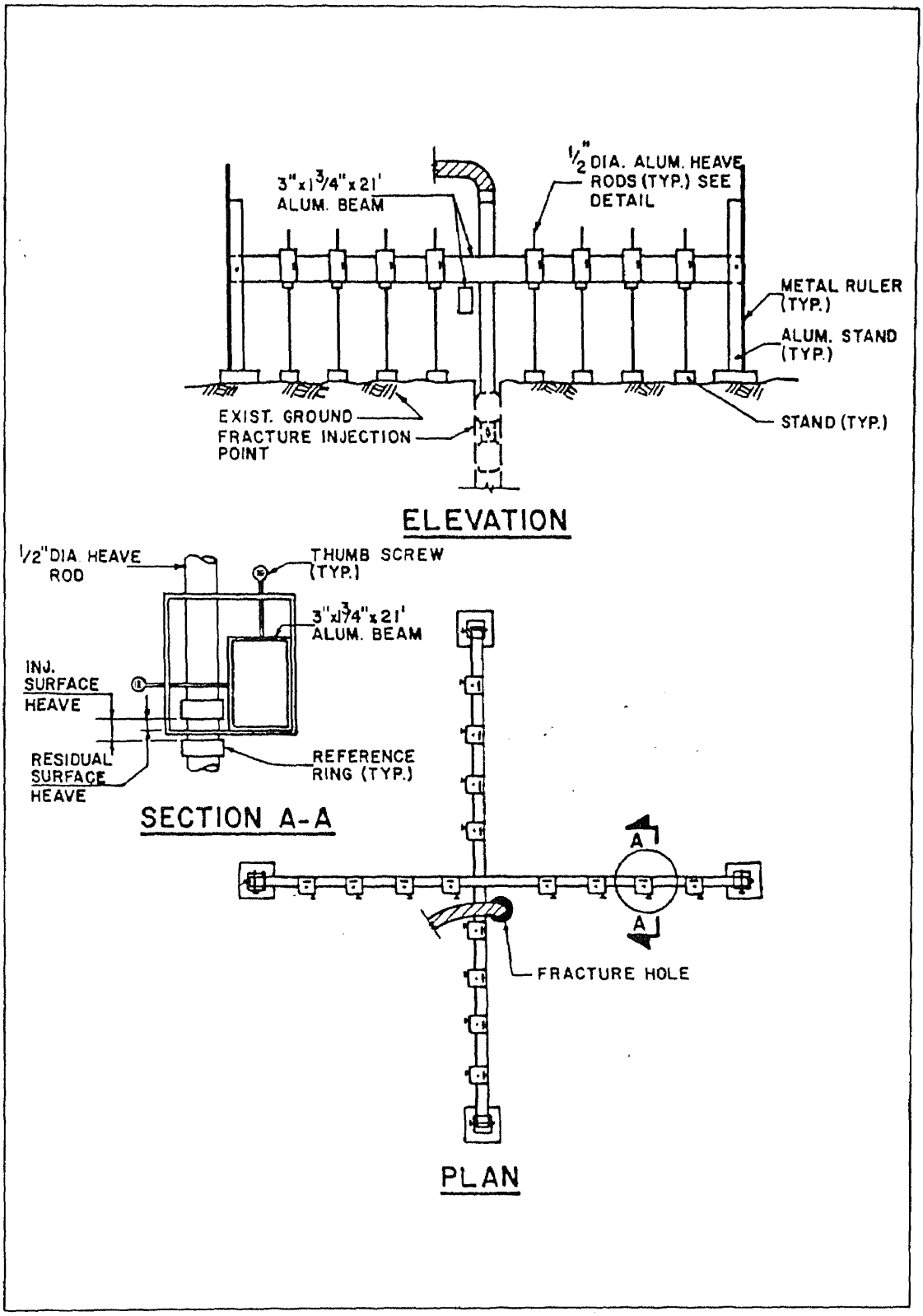

Figure 6 Reference Beam System.

surface heave. By design, the heave rods and sliding rubber indicators record changes of ground surface movements at 1 foot intervals throughout the length of the beam. The rods at the end of the beam were monitored for movement independently with the use of engineering levels. This system improved the accuracy of monitoring the ground surface heave during injection since a larger number of readings in the affected grid could be recorded.

Since soil is a deformable medium, the observed surface heave represents the lower limit of fracture aperture and radius. The data obtained with the reference beam was used to develop heave diagrams from which calculations of pertinent fracture dimensions such as radius and aperture were made. A typical heave diagram is shown in Figure 7, and additional heave diagrams for the various sites are contained in Appendix A1 to A33.

A limitation of this method of surface heave measurement is, as the depth of injection increases, the magnitude of the observed surface effects becomes smaller, since heave is absorbed by the formation as elastic strain. A second limitation is the inability to record the time history of the fracture propagation, since the reference beam records maximum movement only. These limitations were addressed in the development of the electronic tiltmeter system which is described in the following section.

2.3.2 Tiltmeters

In order to refine the system of fracture detection, an electronic tiltmeter system was designed and assembled. This system has increased the confidence and accuracy of surface heave measurements. Tiltmeters now serve as the primary method of measurement of ground surface heave, as they provide a dynamic time history of fracture propagation. The heave rods and optical levels are used to calibrate the tiltmeter data and also provide a backup measurement system. Ground surface heave is measured during pneumatic injection to observe fracture propagation, and also to record the dimensions of residual fractures.

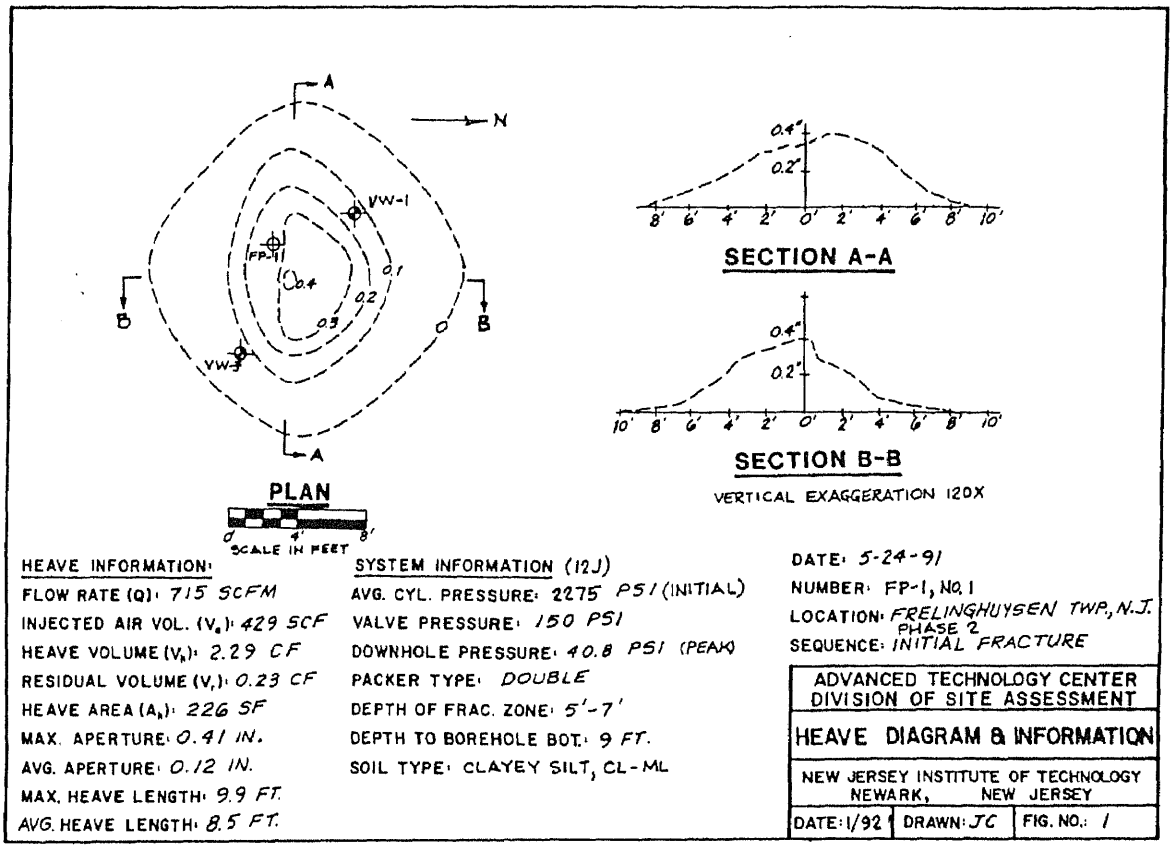

Figure 7 Typical Heave Diagram for Frelinghuysen Township.

In a typical survey, an array of twelve biaxial tiltmeters manufactured by Applied Geomechanics are positioned in a cross-pattern with the injection well located at the center, as shown in Figure 8. The tiltmeters are placed on 12 x 12 x 2 in. thick concrete pads which are founded on tamped sand bedding to assure intimate contact with the ground surface.

Each biaxial tiltmeter contains two electrolytic sensors, which provide tilt sensing in the **X-** and **Y-** axes, respectively. The tiltmeters are connected in a common electronic network which downloads to an automatic data logger. This can then be accessed and controlled by a laptop microcomputer. The combined data acquisition system has the capability to sample each tiltmeter every 0.5 seconds during the injection. A slower 5 minute sampling run is made before and after each fracture to establish baseline behavior, and to check for sensor stability.

Tiltmeters measure differential tilt, i.e. they measure the change in angular deformation of the ground surface. The tiltmeters have a sensitivity range of 0.6 arc seconds to 3 degrees (high gain), and a noise level of approximately 2 arc seconds. The digital tilt values recorded during injections are "curve fitted" to generate the deformation surface using a computer program. The deformation surface is then converted to contours of ground surface heave. These contour maps represents an approximation of the surface movement. A typical ground surface heave contour diagram is shown in Figure 9.

2.3.3 Borehole Camera

A high resolution borehole video camera has been used on a limited basis for direct examination of pneumatically induced fractures. The 1 5/8 inch diameter black and white camera is lowered into the borehole via an armored support cable. The camera height is controlled with a winch system, and a CRT monitor. A video record of the borehole walls is made for future analysis.

Prior to any fracture injections, a baseline record of the borehole is established. The

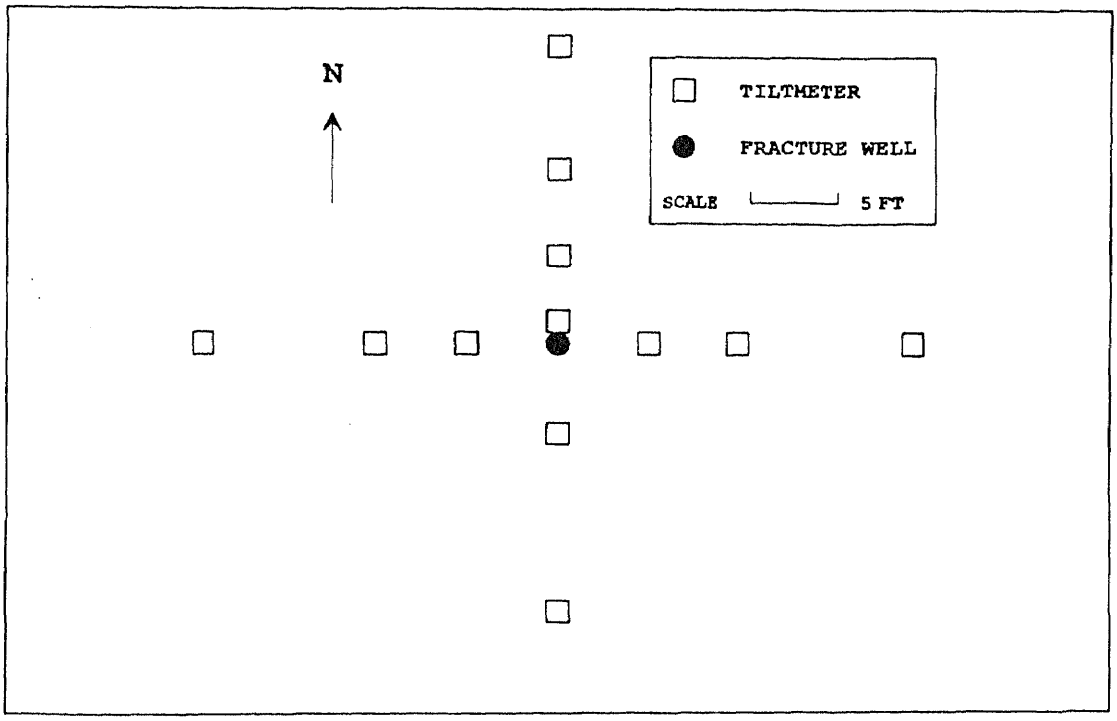

Figure 8 Typical Tiltmeter Array for Fracture Monitoring during Pneumatic Fracturing Injection.

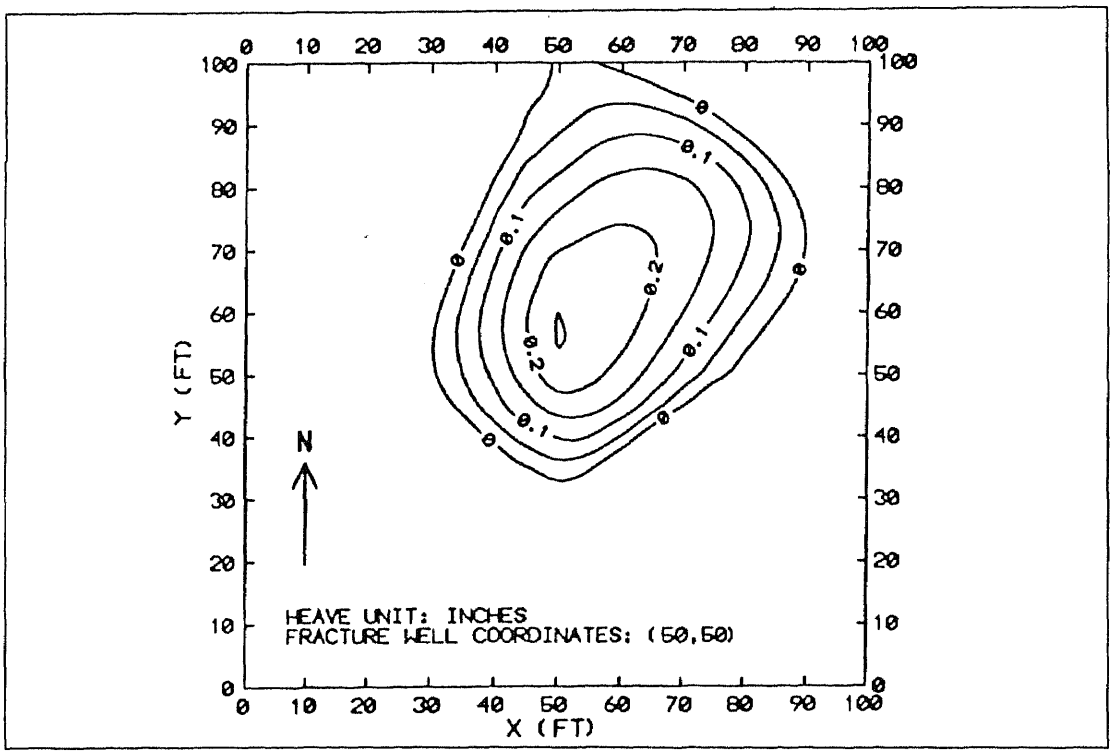

Figure 9 Typical Tiltmeter Ground Surface Heave Contour.

condition of the borehole is again examined after completion of the fracture injection. Comparison of the "before" and "after" videos provide insight into the effects of pneumatic fracturing on the borehole at fracturing.

2.3.4 Borehole Pressure Transducer

A borehole pressure transducer system has been developed to monitor the pressures required to initiate, propagate and maintain pneumatic fractures. The system is shown schematically in Figure 10. The transducer used is Model TH-FV manufactured by T-Hydronics Corporation with a usable range of 0-200 psig. The sensing diaphragm of the transducer is positioned approximately four inches above the outlet ports of the injection nozzle. As pressurization of the interval occurs, the borehole pressure is continually sensed and recorded and is considered representative of the formation's pressures during the various stages of fracture creation and propagation.

The signal output from the transducer is sent to an Elexor Model XL-1900 data logger system which performs the analog to digital conversion. These data are used to generate the pressure-time history of the formation during injection, and to determine the breakdown pressure, reopening pressure, and maintenance pressure.

2.3.5 Monitoring Wells

Monitoring wells are typically established in a grid around the injection well and are used to estimate the extent of horizontally induced fractures. To quantify the extent of air communication between wells, a device called a pressure-flow (PF) indicator has been custom fabricated, as shown in Figure 11. The device is designed for two modes of detection. The first method of detection is used during the injection process with the PF indicator arranged as shown in Figure 11(a). In this configuration, both the pressure and air flow due to the injection process can be monitored at the outlying wells. The second detection method is used during the vacuum extraction process. In this configuration the

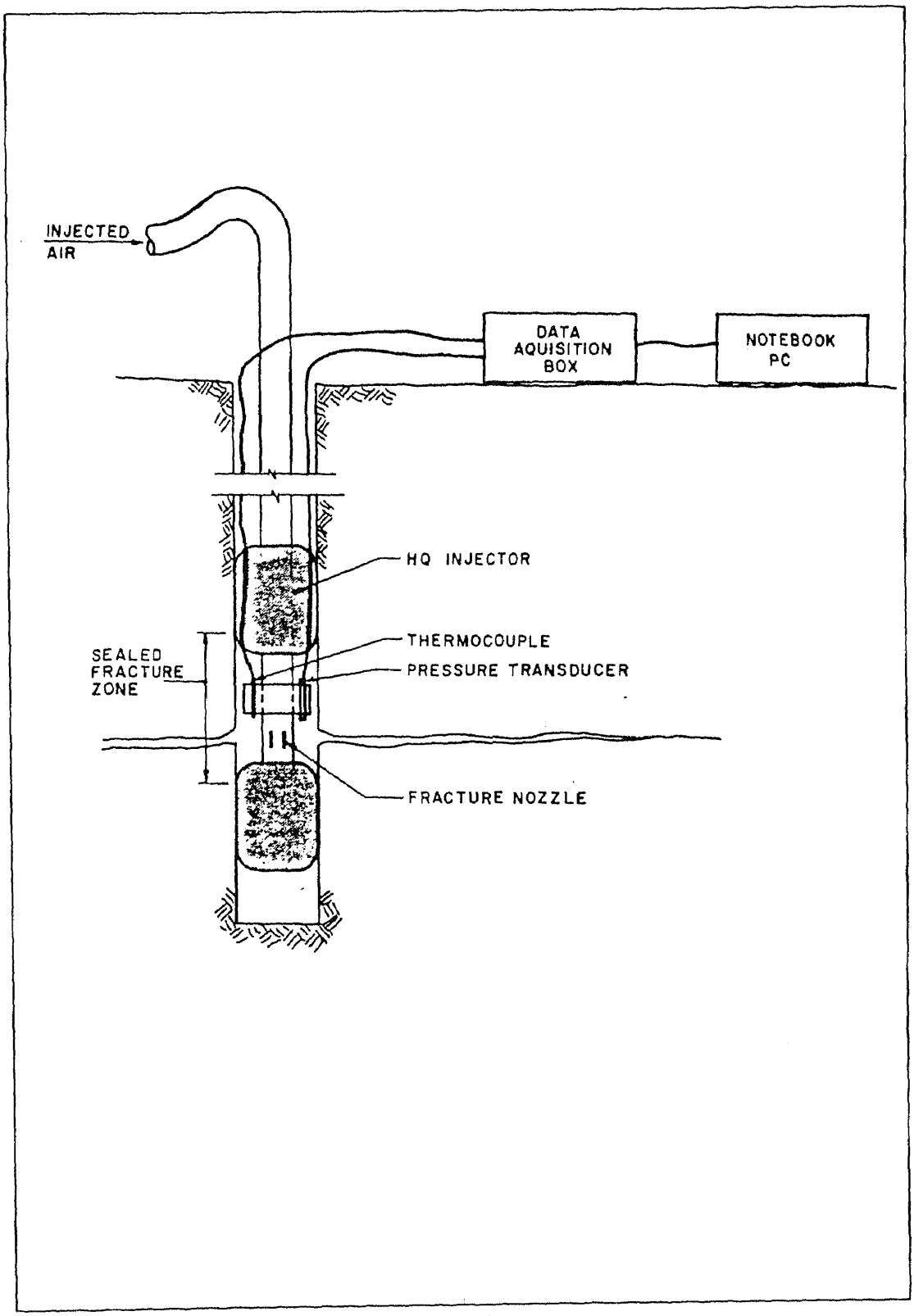

Figure 10 Borehole Instrumentation Schematic.

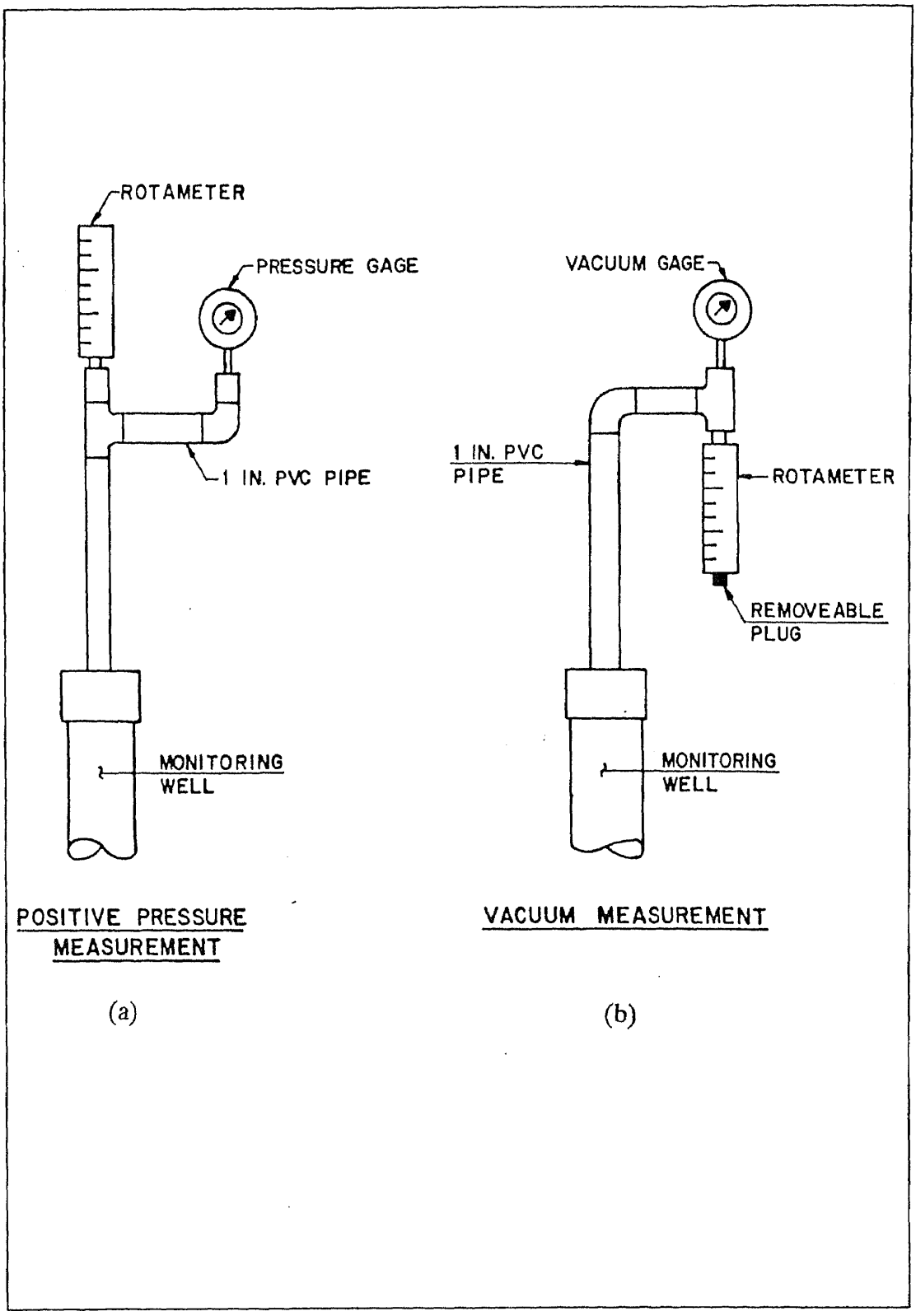

Figure 11 Pressure-Flow Indicator.

PF indicator is arranged as shown in Figure 11(b). As vacuum is established at the extraction wells, vacuum pressure and flow readings are measured at the affected wells. The extent of the fracturing process can be estimated by conducting this test before and after pneumatic injection of the formation.

This system, in addition to detecting fractures, can provide data to develop pressure contours at the site. These contours have shown the preferred direction of fracture propagation and have been useful in the decision making process related to pneumatic fracturing.

2.4 Geology of Test Sites

2.4.1 State of In-Situ Stress

Geologic evidence suggests that the loading history, and the state of stress in a formation can affect the orientation of mechanical fractures. Therefore, in the development of a pneumatic fracturing model, understanding the conditions related to the state of stress is very important. For normally consolidated soils the stress distribution in the formation favors vertical fractures, whereas the tendency is towards horizontal fractures in overconsolidated soils (Leach, 1977; Bjerrum and Anderson, 1972; Bjerrum et al, 1972;). The following section describes how these conditions develop, and the stresses they impose on the formation.

The basic formation process for soil and rock begins with the physical and chemical weathering of rocks over long periods of time. These weathered products are then transported and sedimented in beds, with water acting as the most common agent for transport. Soil deposits within recent fillings or in areas of rapid natural deposits are slowly consolidated under the prevailing overburden pressures. As more soil is deposited and the depth of the overburden is increased, the effective stresses acting on the soil mass is also increased. This results in continuous changes in the engineering properties of the soil at various elevations, e.g., increases in the shear strength, decreases in volume of the mass, permeability and compressibility.

These changes in engineering properties continue until the primary consolidation process stops and the excess pressure in the pore water becomes zero. The condition when the consolidated mass reaches a stable stress is known as normal consolidation. In this state, the vertical stress has reached its maximum value and is equal to the weight of the overburden. The principal stress ratio, K, for this consolidation state approximately 0.5 (depending on the soil type), as indicated in Figure 12.

With geologic time, the process may be reversed as the depth of overburden and ultimately the overburden pressure reduces. This reduction may be due to one of several principal agents: (1) natural elements such as weathering, chemical alterations or erosion; (2) human activity such as, excavation of overburden deposits and removal of pre-loads due to structures which may have been erected in the past; and (3) glacial ice which advances over an area and then retreats.

The rates at which the vertical and horizontal principal stresses relax are different, and geologic evidence shows that the vertical stresses decrease at a faster rate than that of the horizontal stresses. This is due to the horizontal stresses being "locked in" by the previous additional overburden prior to removal. This process continues until stabilization occurs. In this state the soil will be in equilibrium under a stress which is greater than the overburden pressure, but less than the preconsolidation stress. The soil mass can be described as overconsolidated when it has a principal stress ratio greater than approximately 0.5 (depending on soil type), as indicated in Figure 12.

The same principles of overconsolidation apply to sedimentary rock, except in rock the state of stress corresponding to normal consolidation is known as "normal faulting", and overconsolidation corresponds to "thrust faulting." The induration of rock into soil requires much greater depths of burial, and subsequently larger amounts of overburden erosion and uplift. This process require many million of years to occur, and a particular formation may be subjected to more than one cycle of burial and erosion. The tendency of a sedimentary rock formation to be "overconsolidated" is accentuated by the pressures of

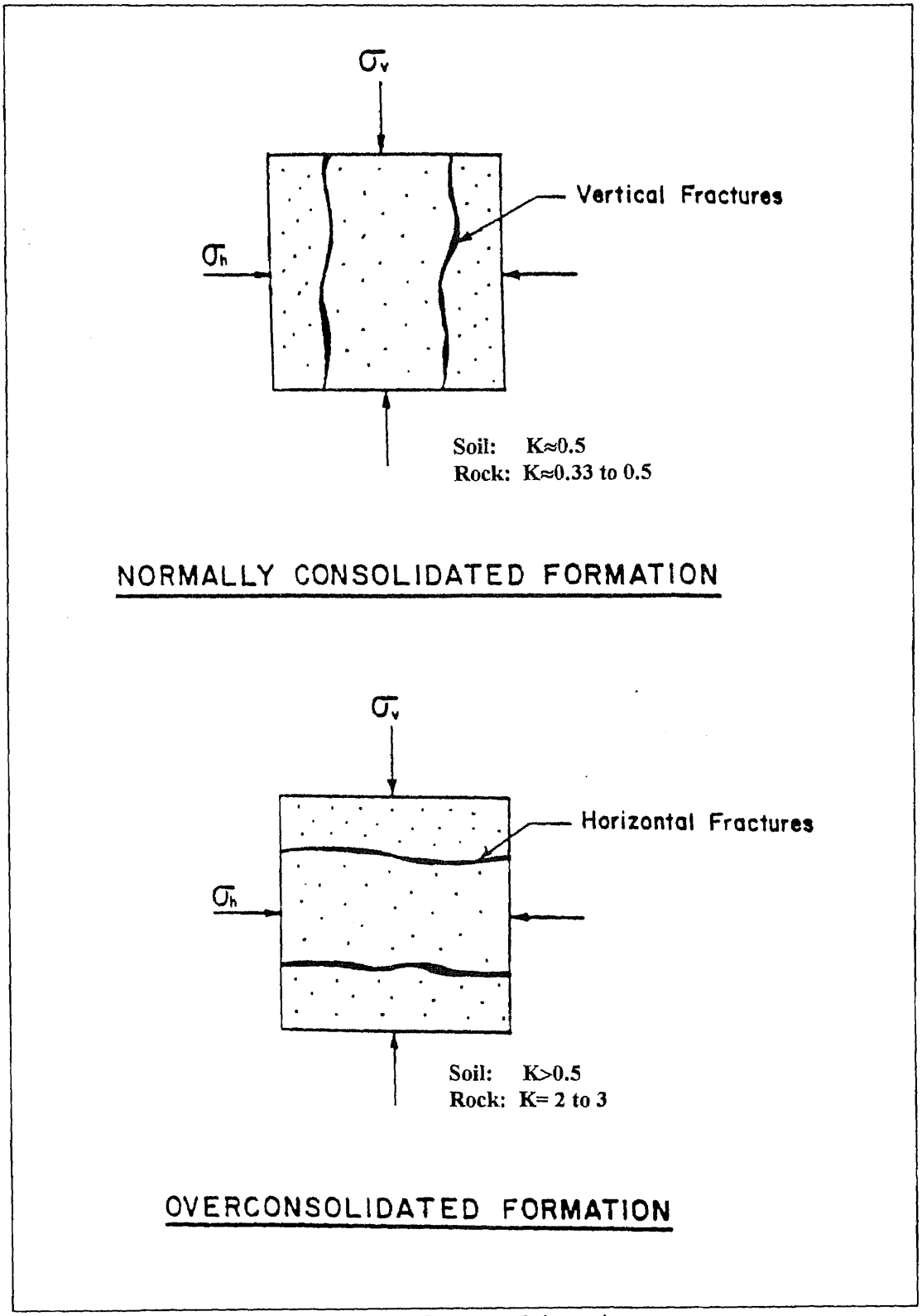

Figure 12 Effects of Consolidation on Fracture Orientation.

lateral tectonic stresses in the crustal rock. As indicated in Figure 12, normal faulting is characterized by a principal stress ratio of 0.33 to 0.5, and thrust faulting is characterized by a ratio of 2 to 3.

To date, most of the field tests of pneumatic fracturing have been performed in overconsolidated formations. Since the minimum principal stress in these formations has been vertical, horizontal separation or fracturing was anticipated. Field observation to date have confirmed that the direction of propagation of pneumatic fracturing in overconsolidated formation is predominantly horizontal.

2.4.2 Geologic Summary

Pneumatic fracturing has been conducted at seven sites and in geologic formations ranging from soil to rock. To optimize the effects of the injection process, experience has shown that physical properties such as moisture content and plasticity can influence fracture formation and orientation. It has therefore been a standard practice to conduct geotechnical assessments at sites. These assessments include reconnaissance soil surveys, soil borings, soil sampling, rock cores, and laboratory analyses of samples.

Reconnaissance soil surveys are conducted by consulting state and county geologic references and are confirmed by site visits. Soil samples and rock cores are obtained from borings drilled by commercial drillers or the HSMRC research team. Each boring is carefully logged to stratify the formation, and to identify bedding or fracture planes. Laboratory tests are conducted on selected samples to determine the engineering properties of the soils. The tests include: natural moisture content, grain size analysis (sieve and hydrometer), Atterberg limits, and unconfined compression.

The geotechnical assessments of the various test sites are summarized in Table 1. The table includes a qualitative description of the site geology and formation texture, as well as engineering properties of the samples tested in the HSMRC laboratory. Also included is a qualitative description of the observed fracturing at the site. A more detailed

Table 1 Summary of Geologic Properties at Demonstration Sites

Site Location	Geology	Texural Description	Unified Symbol	Moisture (%)	Atterberg Limits P.I.	Atterberg Limits L.L.	Unconf. Comp. Strength (ksf)	Est. OCR	Fracture Observation
Frelinghuysen Township, NJ Phases 1 and 2	Glacial Lacustrine	Clayey Silt to Sandy Silt	CL-ML	12-29	20	27	6.4-13.5	>35 (High)	Generally good
	Glacial Fluvial	Sand, tr. Silt	SP-SM	15	-	-	-	-	Not Detected
Richmond,VA	Miocene Sediments	Silty Clay	CH-MH	26	32	62	2.4-5.5 (disturbed samples)	8-18 (High)	Good fracturing
Roseland, NJ FP-1	Fill overlying recent fluvial sediments	Clayey Sand	SC	20	19	30	-	-	Good fracturing
Roseland, NJ FP-2		Silty Sand tr. Clay, Gravel	SM-SC	37	29	36	-	-	Good fracturing
Hillsborough, NJ	Residual soils overlying Triassic Sedimentary Rocks	Siltstone	-	-	-	-	-	-	Good fracturing
Newark, NJ (NJIT)	Fill and Glacial Till overlying Triassic Sedimentary Rocks	Sandstone	-	-	-	-	-	-	Good fracturing
Newark, NJ (Chem Fleur)	Urban fill overlying natural Silts,Clay and Sand.	Sandy Silt (saturated)	SM	-	-	-	-	-	Limited Fracturing
Marcus Hook, PA	Cretaceous sediments	Clayey Silt	CL-ML	18.5	20	25	6.8	>39 (High)	Good fracturing

discussion of the geology of each site is presented in Appendix B.

A review of the data contained in the table indicates that a wide variety of formations have been tested by pneumatic fracturing. The geologies have included glacial soils, marine sediments, urban fill, and sedimentary rock. The soils tested have typically contained high percentages of fine grained clays and silts, which exhibited low to moderate permeabilities. The clays have been classified with low to moderate plasticity, and a wide range of moisture contents have been tested.

Of particular interest in evaluating the sites was the determination of the degree of overconsolidation. This was established by measuring the unconfined compression strength, and comparing it with the overburden stress present at the test depth. At the sites where this determination was made, it was found that the soils were highly overconsolidated. Overconsolidation ratios (OCR's) ranged from 8 to 39+.

CHAPTER 3

Hydraulic Fracturing Theories

3.1 Hydraulic Fracturing Overview

The concept of generating fractures in geologic media by pumping in a liquid is a proven concept. It is known as hydraulic fracturing and has been successfully demonstrated in the petroleum and other industries for decades. The new technology of pneumatic fracturing is similar in concept, except that there are significant differences in the properties of the injection fluid, the rate of fracture propagation, and the resulting formation response. It is nevertheless useful to review the mechanics of hydraulic fracturing, as they will provide an insight into the development of a pneumatic fracturing model. This section will present an overview of the mechanics of hydraulic fracturing as developed over the last several decades.

The basic principle of hydraulic fracturing involves pumping large volumes of fracture forming fluids under pressure into a borehole. This results in the generation of a fracture or a network of fractures. For fractures to be successfully created and propagated, the pressure of injection must be greater than the in-situ stresses of the formation, and the time of injection must be long enough to ensure fracture extension.

The first documented application in the petroleum industry was in 1932 at the Pure Fox Oil Well, in Michigan (Howard and Fast, 1970). At this site, an acid was used to increase the productivity of the well by dissolving the limestone formation and enlarging existing cracks. The process of hydraulic fracturing as it is know today, was first tested in 1947 at Hugoton Gas Field in Kansas, and has since been successfully applied in many locations (Howard and Fast, 1970).

By the 1960's, hydraulic fracturing had developed from a simple (low-volume, low-rate) fracture stimulation method to a highly engineered complex procedure. The benefit of the process was recognized and adopted by other disciplines such as civil engineering,

hydrogeology and the mining industry. As of now some of the main applications of hydraulic fracturing are:

- Injection of water to enhance oil well production or disposal of oil field brines.
- Injection of water to increase water well production by aiding in secondary recovery operations.
- Injection of grout to increase soil/rock strength and decrease permeability.
- Injection of water into clay formations to measure in-situ stresses.
- Injection of water to enhance certain mining operations.
- Deep geologic waste disposal, such as radioactive waste mixed with grout.

In some of the above applications, hydraulic fracturing is performed at great depths.

In an attempt to understand the mechanics of hydraulic fracturing, several theories were proposed. It was recognized that the success of the fracturing process depended on how well crack propagation in the rock mass was understood. From these theories, important physical parameters which may affect the fracture response were identified. These include in-situ geologic stresses, type of geologic formation, moisture content, and the depth of injection. Operational process parameters are also important and typically include injection pressures, injection flow rates and injection times (Howard and Fast, 1970).

During development of these theories, several of the key assumptions are:

- Elastic versus plastic versus brittle behavior.
- The state of geostatic stresses in the formation.
- Penetrating versus non-penetrating fluids.

Card (1962) reviewed a number of these fracturing theories and concluded that failure of geologic materials due to fracturing could be classified as: the theories of strength and theories concerned with the fracture mechanism. The main difference between the two groups of theories lies in the basic approaches taken. The former is a study of the macroscopic phenomenon, and describes the ultimate condition leading to failure. The

latter theory addresses the microscopic aspects involved in failure initiation and propagation.

Howard and Fast (1970) provided an original state-of-the-art review of hydraulic fracturing as it relates to the petroleum industry. As an update to this work, Gidley, et al. (1989) published a monograph which described the latest advances in hydraulic fracturing. Both publications provide an excellent overview of the development, theory, and application of hydraulic fracturing in the petroleum industry. The use of hydraulic fracturing for water well stimulation has been summarized by Smith (1988).

The following section will summarize the work of several investigators who have contributed to the understanding of fracture initiation pressures in the hydraulic fracturing industry. This review will emphasize concepts which can serve as a background for the development of a pneumatic fracturing initiation model.

3.2 Literature Reviews on Fracture Mechanism

Griffith (1921) pioneered the work on fracture mechanics and proposed a theory of "brittle strength". This theory has had a profound effect on the study of fracturing phenomena. Although the theory is applicable for isotropic materials, it can be used for anisotropic materials with modification. In his work he analyzed how the cohesive forces between molecules contribute to fracture initiation and extension. He concluded that, for fracture extension to occur, the surface tension forces must be overcome. Griffith's theory on "brittle strength" was able to explain the observed higher calculated tensile strengths of simple crystals compared to experimentally determined values. In the original, study a flat plate containing an elliptical hole was subjected to a varying stress field. From this work a relationship for the occurrence of the maximum stress, σ_{max}. It is given by

$$\sigma_{max} = \bar{\sigma}\sqrt{\frac{b}{r}} \tag{3.1}$$

where

r = radius of the end of the ellipse

$\overline{\sigma}$ = average stress

b = one-half major axis of ellipse

A limiting condition of this expression is r $\rightarrow$ 0, $\sigma_{max} \rightarrow \infty$

Orowan (1950) further developed Griffith's theory, and by accounting for the tensile strength of the material, the criteria of failure was written as

$$(\sigma_{11} - \sigma_{33})^2 - 8t_o(\sigma_{11} + \sigma_{33}) = 0 \qquad (3.2)$$

where

σ_{11} = major principal stress

σ_{33} = minor principal stress

t_o = tensile strength of the material

This expression is only valid for $\sigma_{11} + 3\sigma_{33} > 0$.

If it is less than zero, then the following criterion will govern:

$$\sigma_{33} + t_o = 0 \qquad (3.3)$$

Cambefort (1955) studied the grouting of soils and the formation of fractures and claquages. By preparing test blocks and subjecting them to various stresses, he confirmed the hypothesis that fractures always develop perpendicular to the minor principal stress direction. Cambefort also observed that fracturing pressures did not always attain a peak level before stabilizing at a constant value, and concluded that pressure monitoring is therefore not a conclusive indicator of fracture development.

From this work, Cambefort presented a relationship for the fracture pressure of the liquid, P_b, at which a borehole wall in a cohesive soil will fail. This relationship is expressed as

$$P_b = \frac{\gamma_s h}{\nu - 1} + t_s \tag{3.4}$$

where

γ_s = unit weight of the soil

ν = Poisson's ratio

h = height of overburden

t_s = cohesive strength of the soil

For a loose soil (assumed to be homogeneous and isotropic), Cambefort presented relationships that predict the fracture pressure for horizontal and vertical fractures on the borehole wall as expressed by

$$P_b = \frac{\gamma_s h}{\nu}(1 + \sin\theta) \tag{3.5}$$

where

θ = angle of internal friction

and

$$P_b = (\nu - 1)\gamma_s h \tag{3.6}$$

Cambefort concluded that fracture pressures depend solely on the geotechnical properties of the soil and depth of the grouted section. Variables such as the permeability of the medium, viscosity of the mix, borehole diameter, and radius of influence of the grouting mix had no effect on the fracture pressure in these studies.

Hubbert and Willis (1957) conducted theoretical and laboratory studies on the mechanics of hydraulic fracturing and were the first to forward a comprehensive explanation for the fracturing mechanism involved in soil and rock. Using a Mohr-Coulomb analysis, they demonstrated the importance of regional tectonic stress directions on the orientation of fracture planes. By the analysis of various failure envelopes, they presented the following relationships to describe the principal stress ratio, K.

$\frac{\sigma_v}{\sigma_h}$ = 2 to 3, for normal faulting (tension state)

and

$\frac{\sigma_v}{\sigma_h} = \frac{1}{3}$ to $\frac{1}{2}$, for thrust faulting (compression state)

These relationships were found to satisfy conditions which are favorable for the formation of vertical and horizontal fractures, respectively.

They also analyzed the stress distribution around boreholes using an elastic analysis. By superimposing the compressive stresses surrounding the borehole with the tensile stresses caused by hydraulic injection, they were able to predict the minimum stresses required to initiate failure (see Figure 13). This analysis showed that in an infinitely long borehole placed in an isotropic medium, the injection of fluids could result in vertical fractures only. However, due to the presence of existing fractures, irregularities in the borehole walls and the axial stresses applied to the ends of the borehole (e.g. use of packers, bottom of hole), horizontal fractures are possible.

By combining the results of the Mohr-Coulomb failure envelope and the borehole stress analysis, several important conclusions were reached. The orientation of hydraulically induced fractures depends on local stress fields, variations of in-situ stresses in different rock layers, initial ground water conditions of the formation and the elastic nature of the medium. It was also concluded that under conditions where the three in-situ principal stresses are unequal, fractures would only occur along planes normal to the minor principal stress (see Figure 14). These fractures would also be independent of the fracturing fluid, penetrating or non penetrating.

It follows that horizontal fractures can be expected in areas of compression, such as overconsolidated soil, sedimentary rock, or in regions characterized by active thrust faulting. Under these conditions, hydraulic fractures can be created when the minimum injection pressure is equal to or greater than the overburden pressure.

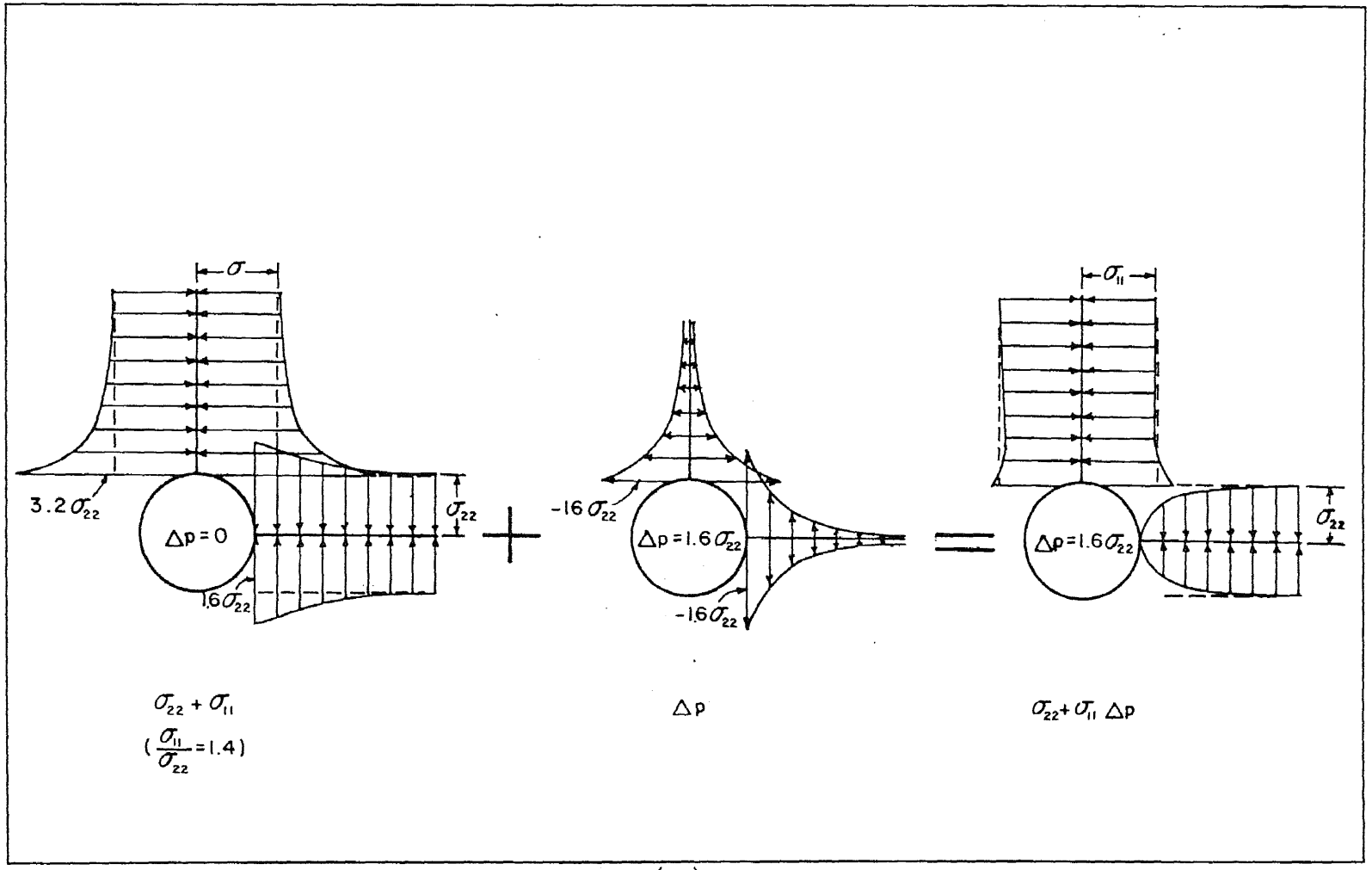

Figure 13 Superposition of the Stresses due to a Pressure (Δp) of $1.6\sigma_{22}$ upon the Stresses around a Wellbore when $\sigma_{11}/\sigma_{22} = 1.4$

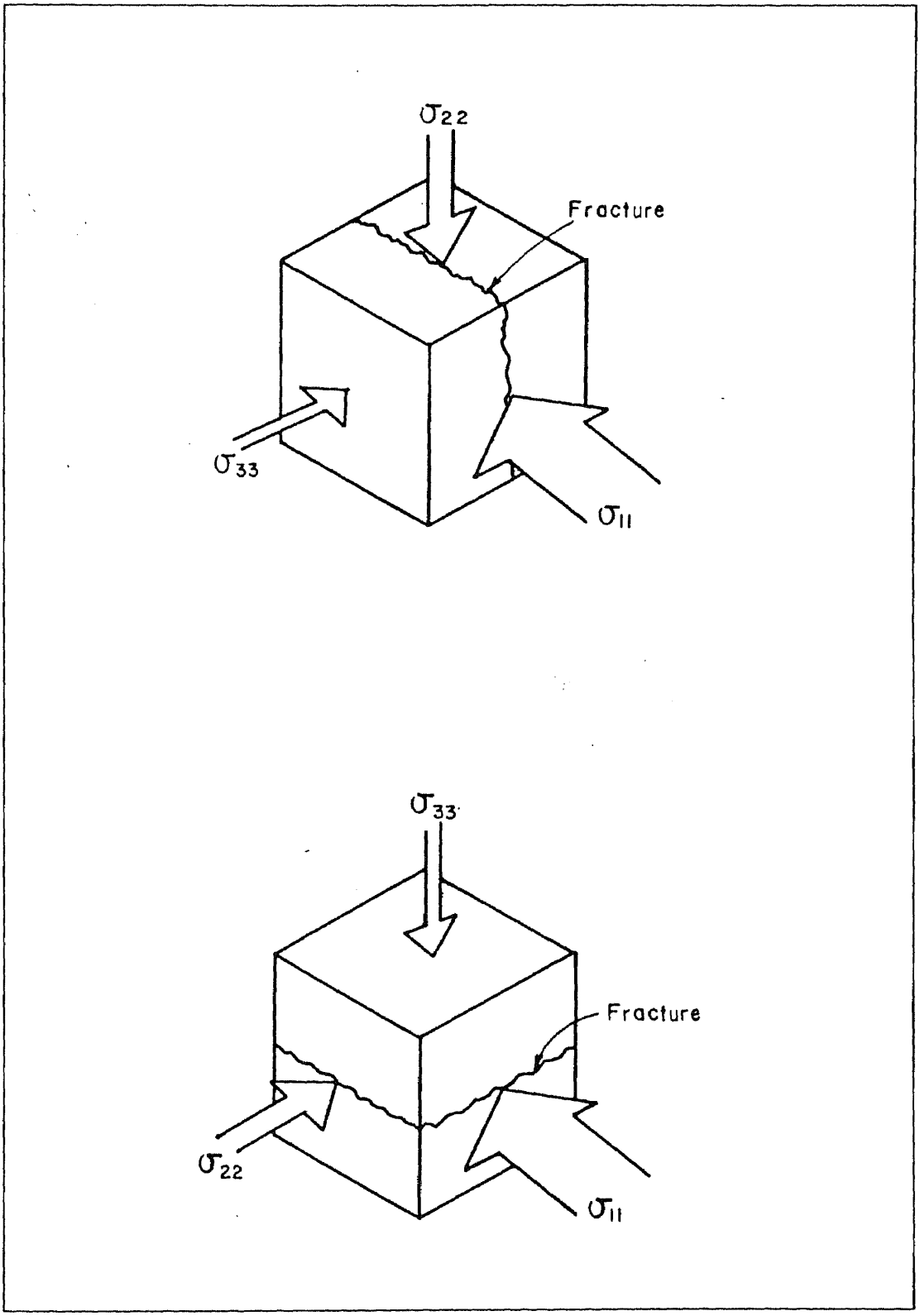

Figure14 Effect of In-Situ Stresses on Preferred Fracture Planes

For tectonic conditions characterized by normal faulting, the minor principal stress would be horizontal. Under these conditions, vertical fractures are produced with injection pressures less that the overburden pressure.

On comparing the breakdown pressures required to fracture a formation with the pressure used during injection, Hubbert and Willis (1957) found that two types of pressure behavior were possible (see Figure 15). These pressures depend on the ratio of the horizontal stresses in the formation and the use of penetrating or non-penetrating fluids. In the first case (see Figure 15 (a)), breakdown pressures may be higher than injection pressures. This behavior can be caused by either the production of horizontal fractures inside a smooth borehole, or by the production of vertical fractures under conditions when horizontal stresses are nearly equal. In the latter case (see Figure 15(b)), there is no distinct pressure breakdown during pressurization of the borehole. This may be possible when horizontal or vertical fractures initiate from pre-existing openings, or when a vertical fracture is produced in an anisotropic formation. Under these conditions the ratio of the horizontal stresses is greater than 2.

Lower breakdown pressures were also observed when penetrating fluids were used. This was attributed to the fluid entering the formation surrounding the borehole and reducing the local stress concentration prior to breakdown. In both cases, the minimum pressure required to fracture a formation when a penetrating or non penetrating fluid is used, must be greater than the minimum in-situ stresses acting around the borehole.

Scheidegger (1962), continued the work of Hubbert and Willis (1957), and used the elastic theory approach to derive equations for borehole fracture initiation pressures for penetrating and non-penetrating fluids. The principal difference between these investigators was, Scheidegger considered the tensile strength of the formation and assumed that failure occurred when the tensile stresses exceeded the tensile strength of the formation.

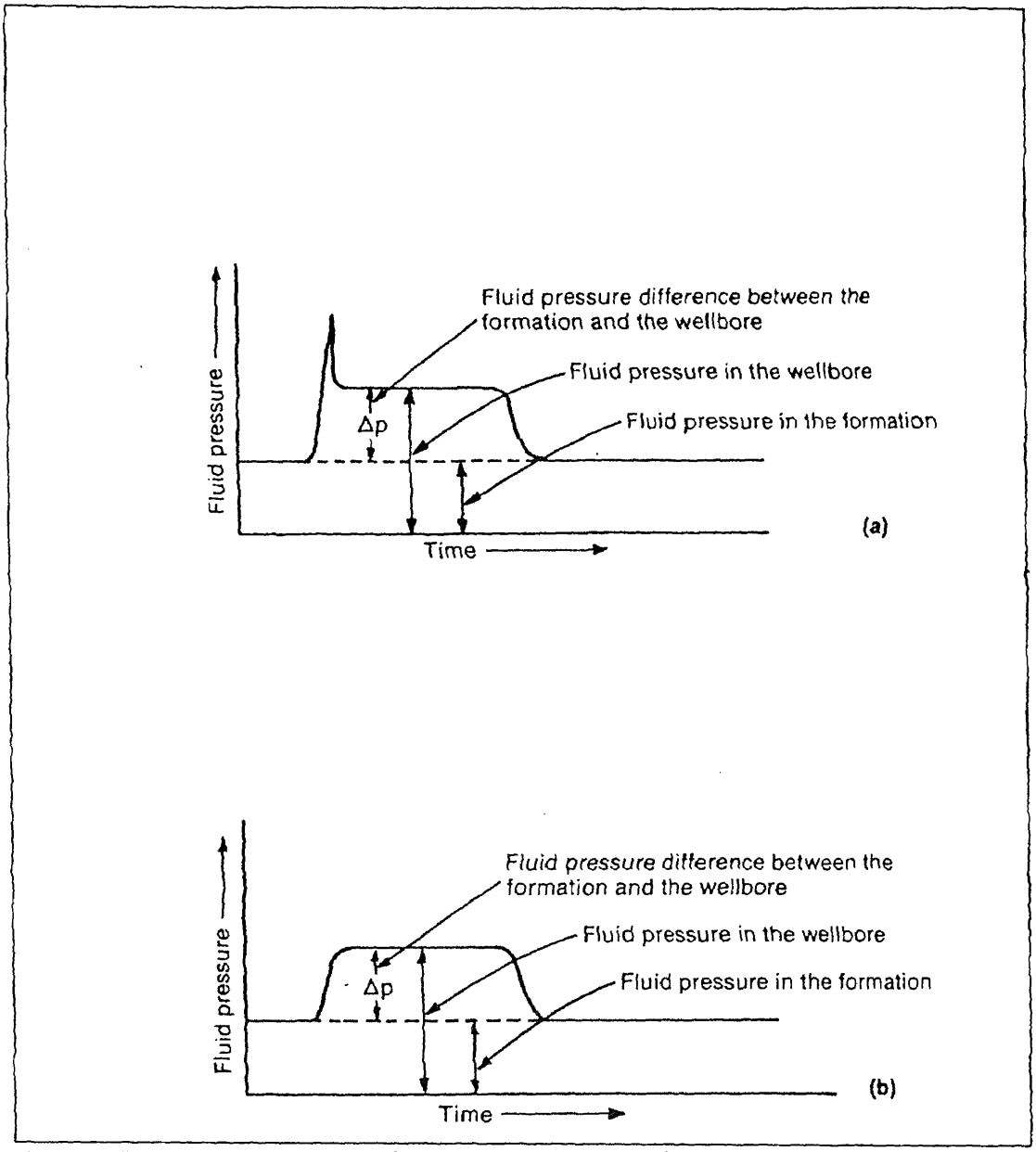

Figure 15 Two possible types of Borehole Pressure behavior.
(Howard and Fast 1957, pg 161)

Scheidegger's work resulted in the classic equation for fracture initiation pressure in hydraulic fracturing, and it is often used in the determination of in-situ stresses. The equation that describes the initiation of vertical fractures for a non-penetrating fluids is given as

$$P_b = 3\sigma_{22}^h - \sigma_{11}^h + t_r - P_o \tag{3.7}$$

where

P_b = fracture initiation pressure

σ_{22}^h = minimum horizontal principal stress

σ_{11}^h = maximum horizontal principal stress

t_r = tensile strength of rock

P_0 = initial pore-pressure of the formation

The main advantage of Scheidegger's approach over other in-situ stress determinations is its simplicity. This method does not require sophisticated instrumentation inside the borehole (Haimson and Fairhurst, 1967), and stresses can therefore be measured at any depth in the formation. If the formation is impermeable to the fracturing fluid, the elastic constants of the rock are neglected in the analysis. This approach has simplified the predictions for fracture initiation pressures and has also made their results more realistic.

Morgenstern and Vaughan (1963) conducted a theoretical study on the mechanics of fracture creation in rocks under high pressures, and also field and laboratory tests to determine the effects of formation variables. Their objective was to determine the allowable injection pressure that could be used to successfully pressure grout soil and rock formations. At the time of this study, the methods for estimating grouting pressures were largely experimental, and were often based on a "rule of thumb". For example, Lippold (1958) recommended a pressure range from 0.75 to 2.5 psi. per foot of overburden depth, and Grundy (1955) recommended using twice the weight of the overburden. The most

common "rule of thumb" for estimating hydraulic fracturing at grouting pressures which remain in use today is 1 psi. per foot of overburden depth. The derivation of this approximate relationship is shown in Figure 16.

In their approach, they supported the belief that the pressure required to induce fractures in the strata around the borehole depends upon the strength of the rock, existing in-situ tectonic stresses and initial ground water conditions. Using the theory of hydraulic fracturing, as discussed by Hubbert and Willis (1957), and applying a principal stress analysis, they determined the allowable grouting pressures for three special cases: an isotropic normally consolidated formation, isotropic overconsolidated formation, and anisotropic formation with horizontal planes of weaknesses.

Assumptions made in the Morgenstern and Vaughan's analysis were:

- The principal stresses could be vertical or horizontal.
- Stress distributions resulting from the creation of the boreholes are localized and would not influence fracture extension.
- Only penetrating fluids were considered since it approximates grouting behavior. Its effects on the borehole stress conditions are however neglected.
- The pore pressure in the potential fracture zone is equal to the injection pressure as measured at the fracture hole.

For the isotropic case, the geology was assumed to conform to the Mohr-Coulomb failure criterion and the effective stresses were expressed as

$$\frac{\sigma'_{11}+\sigma'_{33}}{2}\sin\phi = \frac{\sigma'_{11}-\sigma'_{33}}{2} - c\cos\phi \qquad (3.8)$$

where

σ'_{11} = major principal stress

σ'_{33} = minor principal stress

ϕ = angle of internal friction

c_i = cohesive strength

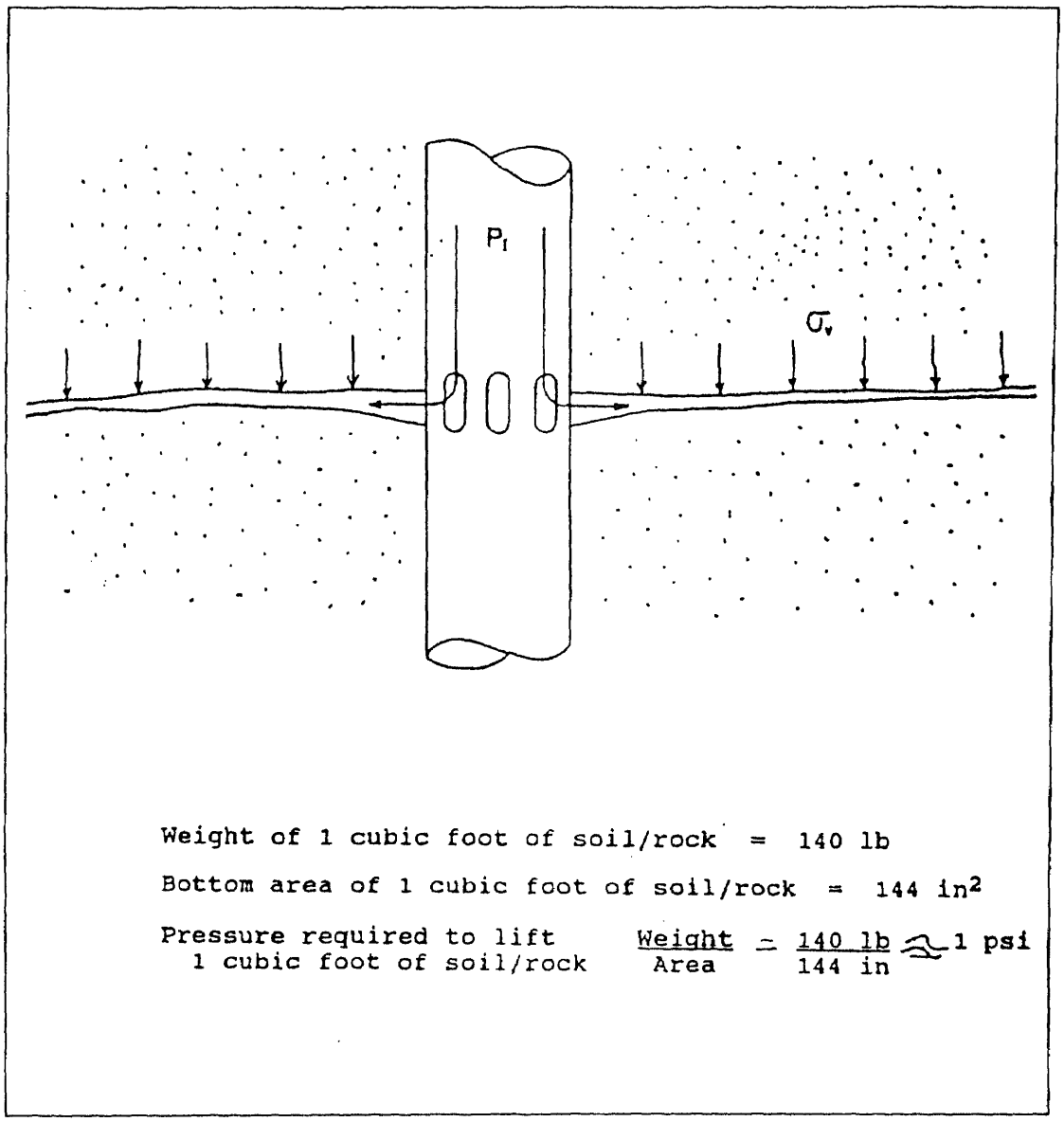

Figure 16 Fracture Initation Pressure.(Hydraulic Fracturing)

For an isotropic normally consolidated condition, the vertical stress is the major principal stress, i.e. K < 1. The initial effective stresses are a function of the formation density and depth of overburden. They are given by

$$\sigma'_{11} = \gamma_r h - \gamma_w h_w \tag{3.9}$$

and

$$\sigma'_{33} = K\sigma'_{11} = K(\gamma_r h - \gamma_w h_w) \tag{3.10}$$

where

γ_r = unit weight of overburden

γ_w = unit weight of water

h = the height of the overburden

h_w = the piezometric level of the ground water above the zone of consideration

K = the principal stress ratio ($\frac{\sigma_h}{\sigma_v}$).

Increasing the pressure in the borehole by a factor P_e, decreases the effective stresses by a similar amount until at formation breakdown, the principal stresses becomes

$$\sigma'_{11} = \gamma_r h - \gamma_w h_w - P_e \tag{3.11}$$

and

$$\sigma'_{33} = K(\gamma_r h - \gamma_w h_w) - P_e \tag{3.12}$$

By substitution into Equation 3.9 and rearrangement of the above formulas an expression for the excess injection pressure was developed as

$$P_e = \frac{(\gamma_r h - \gamma_w h_w)(1+K)}{2} - \frac{(\gamma_r h - \gamma_w h_w)(1-K)}{2\sin\phi} + c_i \cot\phi \tag{3.13}$$

By a similar analysis for an isotropic overconsolidated formation, where the horizontal stress is the major principal stress, i.e. K > 1, the injection pressure can be expressed as

$$P_e = \frac{(\gamma_r h - \gamma_w h_w)(1+K)}{2} - \frac{(\gamma_r h - \gamma_w h_w)(K-1)}{2\sin\phi} + c_i \cot\phi \tag{3.14}$$

The analysis was also extended to the anisotropic case, where there exists a number of

planes of weaknesses in the geologic formation. The Mohr-Coulomb failure criterion for a single plane as stated by Jaeger (1962) was adapted

$$\sigma_{11}'\left[\sin(2\beta+\phi)-\sin\phi\right]-\sigma_{33}'\left[\sin(2\beta+\phi)+\sin\phi\right]=2c_i\cos\phi \qquad (3.15)$$

where β is the angle of inclination of the weak plane to the direction of the major principal stress.

For conditions where the weak plane is horizontal, the major principal stress equals the overburden pressure and $\beta = 90^0$. Then Equation 3.14 reduces to

$$-\sigma_{11}' = c_i \cot\phi \qquad (3.16)$$

At fracture,

$$\sigma_{11}' = \gamma_r h - \gamma_w h_w - P_e \qquad (3.17)$$

The injection pressure, P_b for an anisotropic case can therefore be written as

$$P_b = P_e + \gamma_w h_w = \gamma_r h + c_i \cot\phi \qquad (3.18)$$

The relationships of Morgenstern and Vaughan (1963) for allowable grouting pressures are summarized in Table 2 at the end of this section. However, it will be observed that the piezometric head term due to the water table has been removed, since it is assumed that fracturing is occurring in the unsaturated zone.

Field tests were conducted to observe fracture initiation pressures and their variation with depth. This investigation was made by monitoring surface heave and the variation of flow rates into the formation with pressures. Core logs taken from the site were also laboratory tested to determine soil properties such as tensile strengths of the rocks. For the shale tested, the unconfined compression strength was found to vary between 2000 - 6000 lbs/sq. in.

Based on the theoretical analysis and the field studies conducted, a number of conclusion were made and are summarized below:

- The equations developed are useful in illustrating ranges of injection pressures, and the effects of various formation parameters.

- In-situ stresses and strengths are difficult to determine.
- If the injection pressure is greater than the weight of the overburden, then the material must have cohesion.
- The criterion of 1 psi/ft is only valid if the principal stress ratio is equal to one and there is no cohesion in the formation.
- For unconfined compression tests, the strength of a homogenous and isotropic rock was twelve times the tensile strength.
- Formation conditions are varied and no single pressure criterion can be adopted.
- Unlike conditions for deeper depths, the grouting pressure at shallow depths is influenced by the presence of joints and existing fractures, and is strongly dependent on the value of cohesion.

The investigators concluded that the cohesion intercept from their graphs could be used to represents the strength of the rock. These values were found to be more reliable than the observed field values and lower than the results from the shear box tests.

Kehle (1964) investigated conditions of horizontal fracture initiation near the ends of a pressurized hole. His model included the pressurization of an interval created by two rigid packers, and the transmittance of a shear load to the borehole wall by the borehole pressure. His relationships are summarized as follows:

For a horizontal fracture in a permeable rock formation

$$P_b^p - P_o = \frac{t_r - \sigma'_{33}}{1.94 - a\frac{1-2\nu}{1-\nu}} \tag{3.19}$$

and

For a horizontal fracture in an impermeable rock formation

$$P_b^i - P_o = \frac{t_r - \sigma'_{33}}{0.94} \tag{3.20}$$

where

P_b^p = fracture initiation pressure in a permeable formation

P_b^i = fracture initiation pressure in an impermeable formation

t_r = tensile strength of rock

a = constant of porous-elastic material

ν = Poisson's ratio

A limitation of Kehle's model is that the packer is assumed to be a rigid cylinder in full contact with the borehole wall. Under this condition, when an axial load is applied at one end, it results in a shear stress applied to the rock which tends to initiate horizontal fractures near the ends of the packers under normal tectonic conditions. In practice, however, flexible packers are frequently used and Kehle's assumed stress condition will not develop.

Haimson and Fairhurst (1967) continued the work done by their predecessors and sought to determine in-situ stresses in geologic formations which were both permeable and impermeable to hydraulic fluid. They extended the criteria for hydraulic fracturing and were able to establish theoretical relationships for stress distribution in formations subjected to hydraulic fracturing pressures. These relationships were then compared with results from laboratory tests on hydraulically fractured cubical and cylindrical rock samples. The findings were significant in respect that they were able to determine the necessary fluid pressure to initiate a fracture and the flow rates that would extend this fracture.

In their study, the material under investigation was assumed to be brittle elastic, homogenous, isotropic, linear and porous. It was also assumed that one principal tectonic stress acts in the vertical direction and the other principal tectonic stresses which acts in the horizontal direction may be equal. They also adopted Nowacki's (1962) solution to describe the distribution of tectonic stresses around a borehole. The complete principal

stresses σ_{rr}, $\sigma_{\theta\theta}$, and σ_{zz} can be represented by

$$\sigma_{rr} = -P_w \tag{3.21}$$

$$\sigma_{\theta\theta} = \sigma_{11} + \sigma_{22} - 2(\sigma_{11} - \sigma_{22})\cos 2\theta + P_w - a\frac{1-2\nu}{1-\nu}(P_w - P_o) \tag{3.22}$$

$$\sigma_{zz} = \sigma_{33} - 2\nu(\sigma_{11} - \sigma_{22})\cos 2\theta . a\frac{1-2\nu}{1-\nu}(P_w - P_o) \tag{3.23}$$

where

P_w = pressure at borehole wall due to injected liquid

P_0 = initial pore fluid pressure in the formation

θ = angle measured clockwise from the radius in the direction of the smaller horizontal tectonic stress

ν = Poisson's ratio of the rock

a = porous-elastic parameter which is given by $1 - \left(\frac{C_r}{C_b}\right)$

and

C_r = rock matrix compressibility.

C_b = rock bulk compressibility.

These relationships are supported by the understanding that in a vertical borehole, the tectonic stresses redistribute themselves around the cylindrical cavity. As pressurization of the borehole takes place, two additional stress fields arise. They are due to the borehole pressure, P_w, acting on the walls of the interval and the fracturing fluid penetrating the formation and flowing through the pores. The result is, the pore pressure in the immediate vicinity of the borehole becomes equal to the borehole pressure, P_w, but at some distance away from the borehole it remains P_o. The above equations can then be rewritten in terms of effective stresses

$$\sigma'_{rr} - P_w = -P_w \tag{3.24}$$

$$\sigma'_{\theta\theta} - P_w = \sigma'_{11} + \sigma'_{22} - 2P_o - 2(\sigma'_{11} - \sigma'_{22})\cos\theta + P_w - a\frac{1-2\nu}{1-\nu}(P_w - P_o) \tag{3.25}$$

$$\sigma'_{zz} - P_w = \sigma'_{33} - P_o - 2\nu\left(\sigma'_{11} - \sigma'_{22}\right)\cos 2\theta - a\frac{1-2\nu}{1-\nu}(P_w - P_o) \qquad (3.26)$$

The gradual increase in borehole pressure as the fracturing fluid is injected results in tangential and vertical effective stresses being tensile. For a maximum tangential effective stress, where $\theta = 0,\ \pi$

$$\sigma'_{\theta\theta} = 3\sigma'_{22} - \sigma'_{11} + \left(2 - a\frac{1-2\nu}{1-\nu}\right)(P_w - P_o) \qquad (3.27)$$

A vertical tensile fracture can occur at $\theta = 0,\ \pi$, when the borehole pressure P_w reaches a critical pressure, P_b^P. Under these conditions the effective tensile stress, in Equation 3.27 becomes equal to, or greater than the tensile strength of the rock, t_r in the horizontal plane. For this condition $P_b^P - P_o$ is expressed as

$$P_b^P - P_o = \frac{t_r - 3\sigma'_{22} + \sigma'_{11}}{2 - a\frac{1-2\nu}{1-\nu}} \qquad (3.28)$$

where

P_b^P is the breakdown pressure in permeable rock.

For rock the pore elastic parameter varies between zero and one, and the Poisson's ratio varies between zero and one half.

Therefore

$$1 \le 2 - a\frac{1-2\nu}{1-\nu} \le 2 \qquad (3.29)$$

For conditions where it can be assumed that the effective stresses on the horizontal plane are equal, Equation 3.28 can be reduced to

$$P_b^P - P_0 = \frac{t_r - 2\sigma'_h}{2 - a\frac{1-2\nu}{1-\nu}} \qquad (3.30)$$

which gives a rough approximation of the breakdown pressure.

where

σ'_h = horizontal effective stress

For vertical fractures to be formed in a rock formation which is impermeable to the fracturing fluids and the pore pressure, P_0 is the same throughout the formation, Equation 3.28 and 3.30 becomes

$$P_b^p - P_o = t_r - 3\sigma_{22}^{'} + \sigma_{11}^{'} \tag{3.31}$$

or

$$P_b^i - P_o = t_r - 2\sigma_h \tag{3.32}$$

if $\sigma_{11}^{'} = \sigma_{22}^{'}$.

It is noted that Equation 3.31 is identical with the classic equation developed by Scheidegger (see Equation 3.7).

For horizontal fractures in a permeable rock formation, Equation 3.26 can be modified to give the relationship

$$P_b^p - P_o = \frac{t_r - \sigma_{33}^{'}}{1 - a\dfrac{1-2\nu}{1-\nu}} \tag{3.33}$$

If the rock is impermeable to the fracturing fluid, P_o will be the pore pressure throughout the formation and P_w will not influence the vertical effective stress at the borehole wall. The implies that no horizontal fractures can be initiated unless the borehole wall within the interval is precracked or pre-notched. From Equation 3.30 and 3.33, it is apparent that the horizontal fractures can be initiated in porous rock if the average horizontal effective stress, $\sigma_{11}^{'}$, is much larger than the vertical stress, $\sigma_{33}^{'}$.

In the interpretation of pressure versus time plots for a typical hydraulic fracturing operation, Haimson and Fairhurst concluded that pressure levels can be used to determine fracture orientation. Specifically, measurement of the fracture maintenance pressure, P_m, and the fracture shut-in pressure, P_s, indicate the following fracture orientation.

If

$$P_m \geq P_s \geq -\sigma_{\theta\theta}^{'}, \text{ the fractures are vertical.} \tag{3.34}$$

and

If

$$P_m \geq P_s \geq -\sigma'_{zz} \text{ , the fractures are horizontal} \qquad (3.35)$$

where

P_m is the bottom hole injection pressure which represents the maintenance pressure after fracture breakdown.

To predict whether a vertical or horizontal fracture is feasible and to estimate the value of the tectonic stresses in the formation, Haimson and Fairhurst suggested that the critical parameters, e.g. breakdown pressure , pore pressure , extension pressure and shut-in pressure be obtained from pressure-time history plots. For an accurate determination of the initial fracture directions, the use of a borehole camera or orientation packers can be used. However, it was their opinion that no reliable method was available which could accurately predict fracture orientations or directions away from the borehole. It is noted that subsequent improvements in instrumentation, e.g. tiltmeters, now assist in the prediction of fracture orientation and extent.

To test these relationships, Haimson and Fairhurst (1967) conducted hydraulic fracturing tests on five rock types in the laboratory. They fractured cubical and cylindrical samples of permeable and impermeable rock, onto which various stress levels were imposed. By this method, they were able to study the orientations of fractures and the factors which affect these orientations. Based on the agreement found between the theoretical relationships, laboratory tests and field data, they concluded that hydraulic fracturing can be used to determine the state of stress at greater depths.

They further concluded that when fracturing of permeable rock, the two additional parameters of the porous-elastic rock (a, ν) are required. This contrasts with the case for impermeable rock as described in Equation 3.31. Although theoretically possible, horizontal fractures in permeable rock formations are unlikely at great depths. This is due to the unlikely hood that tectonic stress distributions, would favor a condition where horizontal principal stresses would be less than the stress due to the weight of the

overburden.

To complement this study, laboratory tests were conducted. The results of hydraulic fracturing tests on simulated boreholes for both cases of permeable and impermeable rock, showed that only tensile fractures could be created. For conditions when rubber packers were used, and they independent of the loading conditions, only vertical fractures were obtained. This contrasts with findings using steel packers, where horizontal fractures could be initiated.

Vertical fractures were always observed perpendicular to the minor principal stress, and the breakdown pressures in impermeable rock were similar to the theoretically determined values. For permeable rock, the theoretical breakdown pressures represent the lower limit of the experimental values.

They also reported that the breakdown pressure for vertical fracturing, increases with the rate of pressurization of the borehole. They observed that the borehole pressure decreases with increasing borehole diameter and concluded that these trends could be attributed to changes in the tensile strength of the material. These findings are significant for intact rock at shallow depths, since the tensile strength parameter is significant.

Massarsch (1978) looked at a different aspect of soil fracturing in clays. He first reviewed the main uses of hydraulic fracturing and cites the work of Howard and Fast (1970), Leach (1977) and others. In the review special emphasis was made of the effects of hydraulic fracturing in fine-grained soils. For example Bjerrum, et al.,(1974) had presented a theoretical analysis on the effects of piezometer installations in cohesive soils, and Massarsch and Broms (1977) had investigated the effects of soil fracturing due to pile driving in cohesive soils. In both studies, theoretical analyses and field measurements showed that hydraulic fracturing occurs in almost all cohesive soils.

In the main study, Massarsch (1978) presented a theoretical approach for the mechanics of soil fracturing using the concept of an expanding cylindrical cavity. His

findings were then applied to practical problems such as pile driving, installation of sand drains in clays, field permeability and hydraulic fracturing tests. He also evaluates the significance of piezometric installations and the direction of fracture propagation on the effects of stresses surrounding a borehole.

The expanding cylindrical cavity approach used by Massarsch (1978) was first introduced by Bishop, et. al.(1949) for frictionless materials and was subsequently expanded to soil by Vesic (1972). It assumes that the expansion of a cavity of infinite length takes place in an ideal, elasto-plastic, isotropic material, and by accounting for the pore pressure in the formation, it is possible to assess the changes in effective stresses.

Utilizing this theory, a relationship describing the excess pressure, P_e , that affects the stresses in the plastic zone and causes the expansion of the cavity was presented. This relationship was

$$\frac{P_e}{\tau_f} = \ln\left[\frac{1.36E}{\tau_f(1+\nu)}\right] \tag{3.36}$$

Massarsch and Broms (1977), in their previous work, had shown that fractures were created in the plastic zone during pile driving in cohesive soils. The critical condition under which fractures are created around a driven pile depends on Skempton's pore pressure parameter, A_f, and the effective stresses around the borehole.

For vertical fractures,

$$\frac{\sigma_v' K_o}{\tau_f} \leq 1.73A_f + 0.43 \tag{3.37}$$

and for horizontal fractures,

$$\frac{\sigma_v'}{\tau_f} \leq 1.73A_f - 0.577 \tag{3.38}$$

These relationships apply to soils whose tensile strengths are insignificant and can therefore be neglected. Determination of geotechnical properties is made by standard field

and laboratory tests.

In evaluating the effects of piezometric installations, i.e. pushing or driving piezometers into the ground, it was observed that hydraulic fracturing could be initiated at very low excess pressures. In clay it was found to be $0.2\sigma_v^{'}$ and when repeated in a Norwegian clay, which was normally consolidated, and where arching was not possible, the value was found to range between $0.67\sigma_v^{'}$ and $0.86\sigma_v^{'}$. These values contrasted with those obtained from piezometers which were installed in augured holes and which were noticeably higher. This is due to the creation of fractures around the borehole. Apparently the process of pushing or driving piezometers into the plastic zone creates fractures, and also has the effect of lowering the fracture initiation pressure in that zone. A similar effect occurs during the installation of sand drains, and is responsible for increased drainage efficiencies.

Based on the relationships given in Equations 3.36 and 3.37, the maximum pressure at which fractures in a drilled borehole can occur is given by

$$\frac{P_b}{\sigma_v^{'} K_o} = \frac{\ln\left[\dfrac{1.36E}{\tau_f(1+\nu)}\right]}{1.73A_f + 0.43} \tag{3.39}$$

The direction of fracture propagation depends on the ratio of the critical stresses as given in Equation 3.37 and 3.38. This ratio, R, is expressed by

$$R = \frac{1.73A_f + 0.43}{K_o\left(1.73A_f - 0.577\right)} \tag{3.40}$$

where K_O = coefficient of lateral earth pressure. If $R>1$, then vertical fractures are likely to occur whereas for values of $R<1$, horizontal fractures should be generated.

On testing this condition in normally consolidated and overconsolidated cohesive soils in the plastic zone of clays, it was found that generally $R>1$. This implies that vertical fractures are likely to occur for both cases under these conditions, during

hydraulic fracturing. It can also offer an explanation as to why the coefficient of lateral earth pressure, K_o is often significantly greater than 1 during these tests.

Callanan (1980) analyzed the state of stresses around a borehole at failure during hydraulic fracturing. In the analysis it was assumed that the geologic medium would behave plastically in the near vicinity of the borehole, but would exhibit elastic behavior at larger radii. The values of this transition zone would depend on the magnitude of the borehole pressure. In the analyses, he used the Mohr-Coulomb failure criteria combined with equations of equilibrium to investigate two configurations of principal stresses at failure. These corresponded to cases in which vertical fractures were initiated. Some of the assumptions that were made are: the material was homogeneous, isotropic, non-penetrating nature, and the borehole access was symmetrical. For the first condition which considers the elastic zone, the effective stress was expressed as

$$\sigma'_{rr} - \eta\sigma'_{\theta\theta} = \psi \tag{3.41}$$

where

$\sigma'_{rr} = \sigma'_{11}$ and $\sigma'_{\theta\theta} = \sigma'_{33}$

A relationship for the failure pressure can be expressed as

$$P_b = \frac{2\eta K_o \sigma'_{22} + \psi}{1+\eta} \tag{3.42}$$

For the second case, which considers the plastic zone, the failure criteria due to the effective stresses satisfied the condition

$$\sigma_{zz} - \lambda\sigma'_{\theta\theta} \geq \psi \tag{3.43}$$

where

σ_{zz} = total vertical stress.

$\sigma'_{\theta\theta}$ = effective tangential stress.

$$\eta = \frac{1+\sin\theta}{1-\sin\theta} ..or.. \tan^2\left(\frac{\pi}{4}+\frac{\theta}{2}\right)$$

$$\psi = 2c_i \cdot \tan\left(\frac{\pi}{4} + \frac{\theta}{2}\right)$$

The prediction made for fracture initiation pressure was given as

$$P_b = \frac{(2\eta K_o - 1)\sigma_{zz} + \psi}{\eta} \tag{3.44}$$

Callanan's (1980) key conclusion was that the initiation of hydraulic fractures can be the result of a shear failure instead of a tensile failure. Predictions for the derived relationship were compared with actual field pressure measurements for two sedimentary rock formations, and good agreement was shown between the predicted and field values.

Jaworski, et al., (1980) performed a laboratory study to develop and improve the understanding of the mechanics of hydraulic fracturing around boreholes. The aim was to clarify the influence of factors which affect the fracturing pressure and to relate these results to conditions which promote hydraulic fracturing in the cores of embankment dams.

As background, investigators cited a study initiated by Haimson (1968) which suggested that the pressure required to fracture an impermeable rock formation was considerably higher than that required to fracture a permeable rock formation. The latter was also found to be less predictable. Additional insight was provided by Nobari, et al. (1973) who studied failure modes, fracture plane orientation and their progressions. They concluded that tensile strength of soils resist fracturing, but these values are relatively small, and therefore have a negligible effect on dams more than 15 ft. high.

Jaworski, et al. (1981), performed laboratory tests on different soil samples. They were tested using a cubical stress apparatus subjected to independent principal stresses. The applied stresses were adjusted so that the major principal stress σ_{11} was always parallel to the axis of the borehole and perpendicular to the compaction planes of the soil cubes. Major principal stress was always equal to twice the minor principal stress σ_{33},

with the exception of one test where the intermediate principal stress σ_{22} was equal to σ_{33}. Under laboratory conditions, they were able to control and monitor the effects of a number of parameters such as the composition, moisture content, density, tensile strength, test duration and preexisting fractures on the hydraulic fracture behavior of the soil samples.

The investigators reached a number of conclusions based on these studies. For soils a significant variation in hydraulic fracturing pressures were observed. These pressures depended on localized stress conditions surrounding the borehole, moisture content, compactive effort, and the presence of non-uniformities such as cracks. Although the significance of all the individual effects were not clearly demonstrated in this study some trends were quite apparent Soils with high moisture contents subjected to increasing pressures, behaved in a more ductile manner. This was consistent with the cylindrical cavity theory described by Ladanyi (1963). For uncracked soil, the fracturing pressure was significantly greater than its minor principal stress and this contrasts with the case for a cracked soil where the fracturing pressure was approximately equal to the minor principal stress.

They also related the fracturing initiation pressure, P_b, to the simulated minor principal stress and the tensile strength of the soil. This result was presented as a linear function, given by

$$P_b = m\sigma_h + t_a \tag{3.45}$$

where

t_a = apparent tensile strength

$\sigma_h = \sigma_{33}$ (the minor principal stress)

m = rate of change in fracture pressure with horizontal stress

The slope, m, and the apparent tensile strength, t_a, appeared to depend on the material properties and the localized stress conditions surrounding the borehole. For these tests, values of m for different groups of soils varied from 1.5 to 1.8. These values compared

well with the previously cited study by Vaughan (1971). According to Vaughan (1971), the value of *m* varied from 1 to 2 for an uncracked soil, and for a cracked soil, a minimum value of 1 may be expected.

The apparent tensile strength for the samples tested ranged from 2.82 to 39 psi. These values were generally larger than the tensile strengths determined by the indirect splitting tensile test. This disparity was attributed to the stress conditions in the borehole.

Other notable contributions to the theory of hydraulic fracturing which are summarized in Table 2 include: (1) the single-plane-of-weakness theory proposed by **Jaeger (1960)**; (2) **Walsh-Brace theory (1964)** which is a modification of Jaeger (1960) theory and is useful for anisotropic materials; and (3) fracturing of materials with elastic and plastic properties as an expanding spherical cavity conducted by **Ladanyi (1963)**. The summaries of these theories are limited to Table 2 only, and will not be discussed in further detail.

Recently, **Murdoch (1989, 1991)** has applied hydraulic fracturing technology as an innovative delivery/recovery system for environmental remediation. This application extends conventional hydraulic fracturing in two important respects. First, it can be applied at relatively shallow depths and second, it is being used primarily to remove contaminants from soil. Murdoch (1991) has tested this technology at sites which have been characterized as overconsolidated, silty clay glacial till. Tests were performed by injecting a sand slurry into a borehole which had been pre-notched. Typical areas affected by this fracturing process were 215 to 320 square feet, and most of the fractures were observed to be flat lying to gently dipping and slightly elongated in plan. These fractures extended 15 to 35 feet from the point of injection and were sand filled with apertures ranging from 0.2 to 0.4 inches.

Table 2 Summary of Fracture Mechanism Theories

Investigators	Failure Criterion	Conditions	Relationship	Remarks
Griffith (1921)	———	Brittle elastic	(1) $(\sigma_{11}-\sigma_{33})^2 - 8t_0(\sigma_{11}+\sigma_{33})=0$ if $\sigma_{11}+\sigma_{33}>0$ (2) $\sigma_{33}+t_0=0$ if $\sigma_{11}+\sigma_{33}<0$	Based on stress concentration theory
Cambefort (1955)	Mohr-Coulomb	Isotropic, Homogeneous (1) Cohesive soil (2) Loose soil	(1) $P_b=\frac{\gamma_s h}{\nu}(1+\sin\phi); K<1$ (2) $P_b=(\nu-1)\gamma_s h; K>1$	Originated for pressure grouting of soils
Hubbert and Willis (1957)	Mohr-Coulomb $\tau=t_0+\sigma_n\tan\phi$	(1) Normal faulting $\sigma_1=\sigma_v$ (2) Thrust faulting $\sigma_1=\sigma_h$	(1) $P_b=\frac{\sigma_v}{3}$ (2) $P_b>\sigma_v$	Vertical fractures Horizontal fractures
Lippold (1958)	Empirical	———	P_b = 0.75 to 2.5 psi/ft of overburden	Based on field observations
Scheidegger (1962)	———	Brittle elastic	$P_b=3\sigma_{22}^h-\sigma_{11}^h+t_r-P_0$	Classic equation for in-situ stress determination
Morgenstern and Vaughan (1963)	Mohr-Coulomb $\tau=t_0+\sigma_n\tan\phi$	(1) Isotropic normally consolidated (2) Isotropic overconsolidated (3) Anisotropic	(1) $P_b=\frac{\gamma_r h(1+K)}{2}-\frac{\gamma_r h(1-K)}{2\sin\phi}+c_1\cot\phi$ (2) $P_b=\frac{\gamma_r h(1+K)}{2}-\frac{\gamma_r h(K-1)}{2\sin\phi}+c_1\cot\phi$ (3) $P_b=\gamma_r h+c_1\cot\phi$	Originated for pressure grouting application

Table 2 Continued...

Investigators	Failure Criterion	Conditions	Relationship	Remarks
Kehle (1964)	———	Brittle elastic (1) Permeable formation (2) Impermeable formation	(1) $P_b^p - P_0 = \frac{t_r - \sigma'_{33}}{1.94 - a\frac{1-2\nu}{1-\nu}}$ (2) $P_b^i - P_0 = \frac{t_r - \sigma'_{33}}{0.94}$	Horizontal fractures
Haimson and Fairhurst (1967)	———	Brittle elastic, permeable (1) Horizontal fracture (2) Vertical fracture	(1) $P_b^p - P_0 = \frac{t_r - \sigma'_{33}}{1 - a\frac{1-2\nu}{1-\nu}}$ (2) $P_c^p - P_0 = \frac{t_r - 2\sigma_h}{2 - a\frac{1-2\nu}{1-\nu}}$	———
Massarsch (1978)	Elastoplastic	Saturated clays, normally and overconsolidated	$P_b = \frac{\sigma_v K_0 \ln\left(\frac{1.36E}{\tau_f(1+\nu)}\right)}{1.73A_f + 0.43}$	Horizontal fracture (R<1) Vertical fracture (R>1)
Callanan (1980)	Mohr-Coulomb and Brittle elastic	(1) Elastic Zone (2) Plastic Zone	(1) $P_b = \frac{2\eta K_0 \sigma'_{22} + \psi}{1+\eta}$ (2) $P_b = \frac{(2\eta K_0 - 1)\sigma_{zz} + \psi}{\eta}$	Stress around the borehole

Table 2 Continued...

Investigators	Failure Criterion	Conditions	Relationship	Remarks
Jaworski (1980)	Quasi-tensile Strength	Normally consolidated	$P_b = m\sigma_h + t_a$	Recommended values for m =1.0 to 2.0

CHAPTER 4

4.1 General Approach

This section describes an original approach to predict fracture initiation pressures for pneumatic fracturing. Consideration has been given to hydraulic fracturing theory, with appropriate modifications to account for the uniqueness of air as an injection fluid. The first section will begin with a qualitative assessment of fracture measurements which is used to describe the mechanism of pneumatic fracturing. Next, an analytical model for predicting fracture initiation pressure will be presented, followed by a regressive analysis to establish coefficients for the proposed model.

4.2 Pneumatic Fracturing Initiation

In the development of an analytical model for pneumatic fracturing, it is first necessary to analyze pressure-time histories of the injection process. Useful background information was obtained from previous work done in hydraulic fracturing, since it was observed that pressure-time histories in pneumatic fracturing are similar. After reviewing the pressure-time histories generated during numerous pneumatic fracturing injections, it was observed that the fracturing event can be divided into several distinct stages:

- Breakdown of the formation.
- Fracture extension.
- Fracture maintenance.
- Fracture residual.
- Fracture reopening.

These stages are illustrated in Figure 17, and they apply to an idealized geologic formation. It is noted that the shape of the pressure-time history curve depends on a number of factors including in-situ stress fields and geologic characteristics of the medium.

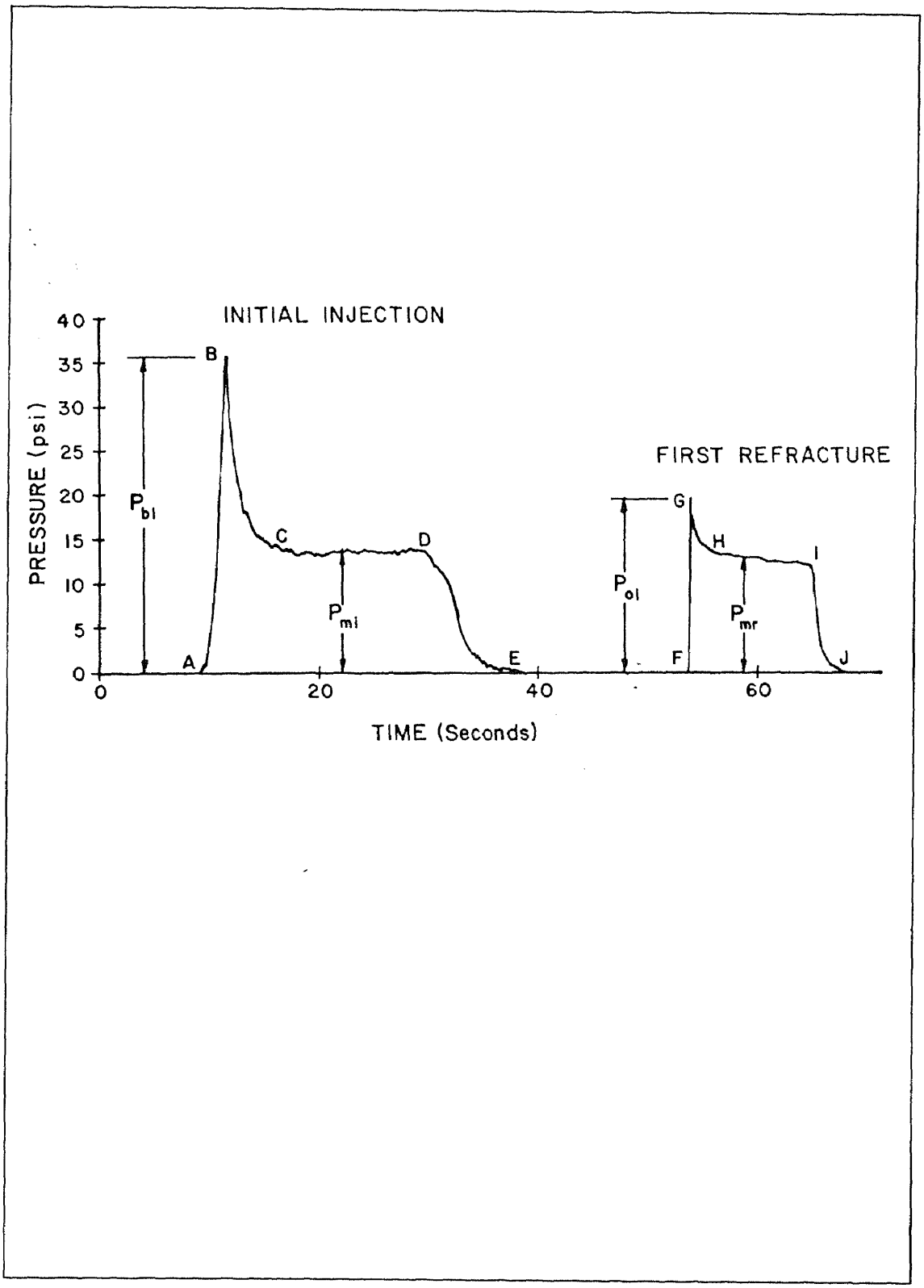

Figure 17 Schematic of an Idealized Pressure-Time history for an Initial Fracture and a Refracture

The following section describes each stage as it relates to the pneumatic fracturing mechanism shown in Figure 17.

During the first stage known as "breakdown", the pressure rapidly builds up as air is injected into the sealed portion of the borehole. This stage is indicated by curve segment A-B. It is possible to develop these elevated pressures because the formation is not yet fractured and still has a low permeability. This stage is relatively short and typically lasts 2 to 3 seconds.

Once the pressure exceeds the in-situ stress conditions and media strength prevailing around the pressurized borehole, breakdown of the formation occurs. The pressure at this instant is known as the breakdown pressure, P_b, which is the minimum pressure that can initiate fractures at a particular depth for a given geologic formation. At the depths and for the soil types tested, pneumatic fracture initiation pressures were found to range between 20 to 50 psi, and for the rock formations, they ranged from 100 to 160 psi. The higher values for rock can be attributed to higher tensile strengths and densities in the formations.

Following breakdown, the pressure decreases rapidly in the borehole and eventually stabilizes at a pressure "plateau" as injection continues. During this time period, air rushes out of the pressurized interval and fractures propagate radially into the formation. This accounts for the rapid decline in the borehole pressure as represented by the curve segment B-C. Based on observations of ground surface heave during injection, fracture extension is quite rapid and typically continues for 3 to 6 seconds only.

The pressure "plateau" C-D represents a period of fracture maintenance which is nearly constant for the remainder of the injection period. This is designated as the initial maintenance pressure, P_{mi}. This pressure indicates that an equilibrium state has been attained for that particular injection flow rate. During this equilibrium state, crack propagation ceases and the affected overburden area can be visualized as "floating" on a cushion of air. During this period, the flow rate into the fractured formation exactly

equals the leak-off into the formation from the fracture surfaces and tips. This contrasts with the earlier stages of fracture formation, i.e. breakdown, and propagation, during which the flow rate into the fractured formation is greater than that leakoff.

As the injection pressure is terminated, the maintenance pressure declines rapidly from D to E. This decline is due to the natural tendency of the formation to return to its original state and also the continuing leak-off of the air into the formation. This process continues until a state is reached where no further closures take place. The residual fractures are then supported by a combination of asperities and block shifting along the fracture network. This phenomenon is known as "self-propping", and the pressure at which this occurs is represented by the change in slope at E.

During the refracture of a formation, the trends of the pressure-time histories are similar as indicated by curves F-J in Figure 17. There are however differences in the magnitude of the pressures which are summarized as:

- The pressure , P_o, at which reopening occurs is less than the breakdown pressure, P_b.
- The reopening pressure, P_o, is greater than the maintenance pressure, P_{mi}.
- Subsequent maintenance pressures, P_{mr}, decline progressively compared with previous maintenance pressures.

The difference between P_b and P_o is attributed to the initial cohesion and/or tensile strength that originally exists in a formation. During subsequent injections these initial strengths have already been overcome, thereby resulting in lower reopening pressures P_o. It is probable, however, that some residual cohesion and/or tensile strength may still have to be overcome in subsequent refracture injections.

It is significant to note that a pressure spike was obtained during reinjection, to reopen the fracture, designated as curve segment F-G-H. This spike was consistently observed during all field tests, and indicates that when reopening a previously fractured formation, it is not sufficient to just overcome the overburden stress, i.e. inject at the

maintenance pressure, P_{mi}. It is believed that the spike is caused by one or more of the following factors. First, even a fractured formation can exhibit a residual cohesion and/or tensile strength. Possible sources of this residual value could be rehealing of the solid fractured surface or surface tension effects due to moisture. A second factor which may also contribute to the pressure spike is gas compressibility. During the first one to two seconds of injection, the gas in the packed off interval becomes highly compressed. During this period , the compressed gas is behaving elastically and is storing any work done as strain energy. As the formation reopens, the strain energy is released and the maintenance pressure is attained.

Another factor which may contribute to a pressure spike is formation inertia. Since the pneumatic injection is very rapid, the mass of the overburden will initially resist dilation of the existing fracture network. Upon reopening, the inertia is overcome and the pressure then reduces to maintenance levels. Of notable interest in the data, is the successive decrease in maintenance pressure with each injection. This is attributed to the progressive weakening of the formation each time it is refractured and disturbed. Progressive extension and cleaning (removal of loose deposits)of fractures may also contribute to this phenomena. The observed reduction in surface heave during reinjection compared with initial injections supports the above hypothesis.

The actual pressure-time histories for the geologic formations studied are given in Appendix C_1 to C_{20}. A review of these curves have led to the following general conclusions:

- Fracture breakdown pressure, P_b, is proportional to the overburden pressure (formation depth and density).
- Fractures become fully established within the first 5 to 10 seconds of injection. Continued injection after this period at the same flow rate, does not significantly increase fracture growth, but may instead contribute to cleaning of the fractures.
- Less pressure is required to refracture the formation.

- Tensile or cohesive strengths of the geologic formation are most significant during initial fractures.
- Maintenance pressures decrease slightly with each successive injection.

The general conclusions drawn from the pressure-time histories were useful in formulating the model described later in this chapter.

4.3 Direction of Fracture Propagation

A review of the field data collected to date indicate that the direction of pneumatic fracture propagation has been predominantly horizontal. This correlates well with the geologic properties of the test sites described in Section 2.4.2, which indicated that the formations were typically overconsolidated. For this reason, the present pneumatic fracture pressure model will be developed on the assumption that the fracture propagation is horizontal.

As discussed in the literature review of Section 3.2, Hubbert and Willis (1957) were the first to propose a criterion which predicts the direction of fracture propagation. They indicated that horizontally induced fractures are formed when the least compressive stress is vertical, and the fracture pressure is equal to or greater than the weight of the overburden. If the injection pressure necessary to form a fracture is less than overburden, then a vertical fracture must be forming. Hubbert and Willis observed that the fracturing pressure necessary to form a vertical fracture is approximately three quarters of the overburden pressure. Thus, if the direction of the least compressive stress is known, the orientation of pneumatically induced fractures, i.e. horizontal or vertical, can be predicted. A geologic reconnaissance prior to any fracturing process will therefore be a valuable asset and can be used as a guide to help in the prediction of fracture orientations.

By correlating the field observations with the theoretical considerations of (e.g. Kehle (1964)), the following possibilities exist for pneumatically induced fractures in an overconsolidated formation:

- The fractures may be horizontal. This means that the smallest compressive stress, σ_{zz} which is perpendicular to the direction of the fractures, can be determined.
- The fracture may initiate vertically but extend horizontally. This type of fracture is possible when the borehole wall is smooth and not pre-cracked or pre-notched. It may also occur, if the packers used do not allow a vertical stress concentration at the ends.
- The fractures may initiate horizontally, but curve upwards and subsequently "daylight" the ground surface. A possible explanation for this behavior is; as the fractures propagate out of the stress field imposed by the packers and well installation, they are affected by the regional stress field. The result is, they may extend vertically or nearly so.

Permeability tests performed on intervals above and below the fracture interval where a horizontal fracture has been formed do suggest that there is some influence in the vertical direction. This is illustrated in Table 3 and Figure 18 which summarizes the results of permeability tests performed at two feet intervals on the sandstone formation at the Newark (NJIT) site. As expected, the largest increase in permeability was recorded in the fractured zone. Some permeability increase was also observed above the zone of injection, suggesting some upward vertical influence. The downward influence was minimal.

Table 3 Summary of Permeability Influences due to Fractures

Fracture			Air Flows(acfm) at 20" H_2O Vacuum				
Interval (ft)	Date	Condition	7'-9'	9'-11'	11'-13'	13'-15'	15'-17'
9'-11'	3/8/91	Pre	0.45	2.1	4.4	4.6	-
9'-11'	3/8/91	Post	2.6	10.5+	5.0	5.0	-
15'-17'	4/5/91	Pre	2.75	11.0+	7.3	5.3	0.5
15'-17'	4/12/91	Post	2.5	11.0+	10.5	9.5+	7.25

NEW JERSEY INSTITUTE OF TECHNOLOGY

AIR PERMEABILITY LOG

PROJECT: HSMRC SITE 21 PNEUMATIC FRACTURING DATE: 3/8/91

LOCATION: ATC PARKING LOT, NEWARK, N.J.

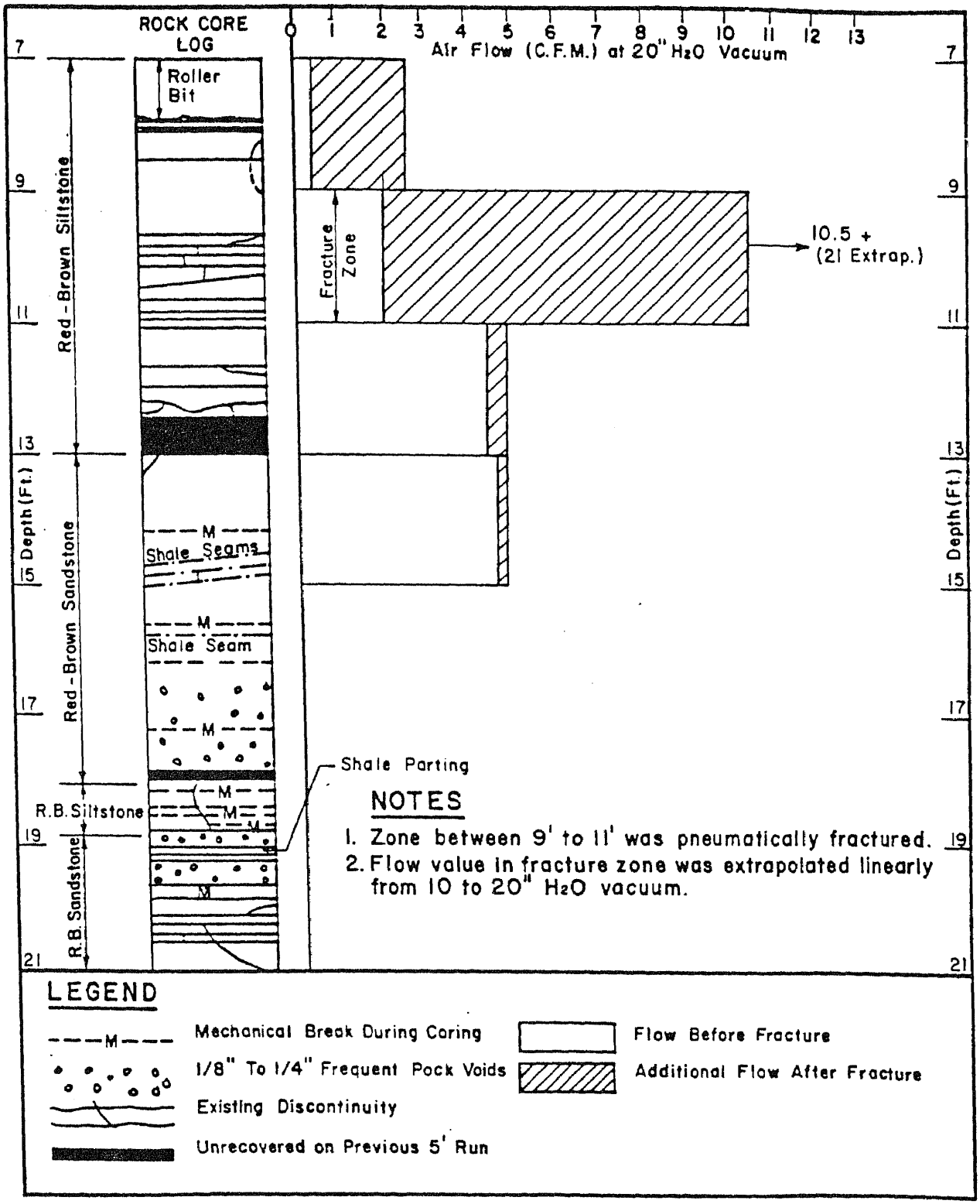

Figure 18 Air Permeability Log for a Sandstone Formation Fractured at a Zone of 9.0-11.0 (ft)

The investigator Kehle (1964) also concluded that horizontal fractures can be generated at the borehole ends if rigid packers are used. In commenting on Kehle's model, Haimson and Fairhurst (1967) suggest that formation of horizontal fractures would be difficult when using flexible packers, such as the kind used in the pneumatic fracturing process. This contrasts with experience to date, since surface heave and air communication data have confirmed that horizontal fractures have been predominant. This is attributed to: (1) good friction and load transfer between the rubber packer element and the borehole wall; and (2) the ability of the packers to move apart independently during pressurization of the interval. The actual orientation of fractures as they intersect the borehole will be studied in future, since it is planned to purchase a borehole video camera.

It is noted that the in-situ stress conditions at shallow depths favor horizontal fractures, since the least compressive stress is typically vertical. As the depth range of pneumatic fracturing is extended, the tendency to form vertical fractures may increase since the principal stress ratio, K, decreases with depth in most geologic formations. As a result, techniques such as notching may become more necessary at deeper depths when horizontal fractures are desired.

4.4 Model Assumptions

In developing an analytical model for pneumatic fracturing initiation pressures, a number of assumptions are made. These assumptions have been carefully chosen to reflect the physical properties of the geologic media, as well as the effects of the equipment on the mechanism of pneumatic fracturing.

The assumptions are:

1) Since the area of influence of pneumatic fracturing is localized, e.g., radius of approximately 25 feet radius, the formation is either homogeneous or uniformly stratified.
2) The formation is overconsolidated, and may contain horizontal planes of

weakness along which fractures can propagate.

3) The tectonic stresses in the formation are horizontally isotropic.

4) The formation is semi-porous so that the applied borehole pressure extends a short distance into the formation. The elasticity of the formation is described by the pore elastic parameter, a, and Poisson's ratio, ν.

5) A hydrostatic pore pressure, P_o, may exist in the formation.

6) The depth of fracture will be relatively shallow, e.g. less than 100 ft.

7) The packers at the ends of the borehole do not slip, but do transfer the full end pressure to the formation.

8) The packers are able to move apart independently a slight amount, i.e. they are not rigidly connected.

9) Due to the rapidity of injection, momentum is developed by the packer moving apart and it is transferred to the borehole wall.

10) The effects of stress disturbance due to drilling of the borehole are ignored.

4.5 Development of Model

The development of the model begins with a discrete section of the borehole which is subjected to an injected air pressure, P_a. The assumed stress condition in and around a borehole during pressurization is shown in Figure 19 (a). It is noted that the applied pressure is not yet sufficient to initiate failure. A relationship which describes the effective stresses during this initial period can be written in a manner similar to Haimson and Fairhurst (1967) (refer to Equation 3.26). The vertical effective stress in the vicinity of the borehole is:

$$\sigma'_{zz} - P_a = \sigma'_{33} - P_o - 2\nu\left(\sigma'_{11} - \sigma'_{22}\right)\cos 2\theta - a\frac{1-2\nu}{1-\nu}\left(P_a - P_o\right) \qquad (4.1)$$

where

σ'_{zz} = vertical effective stress at borehole wall, which is compressive initially.

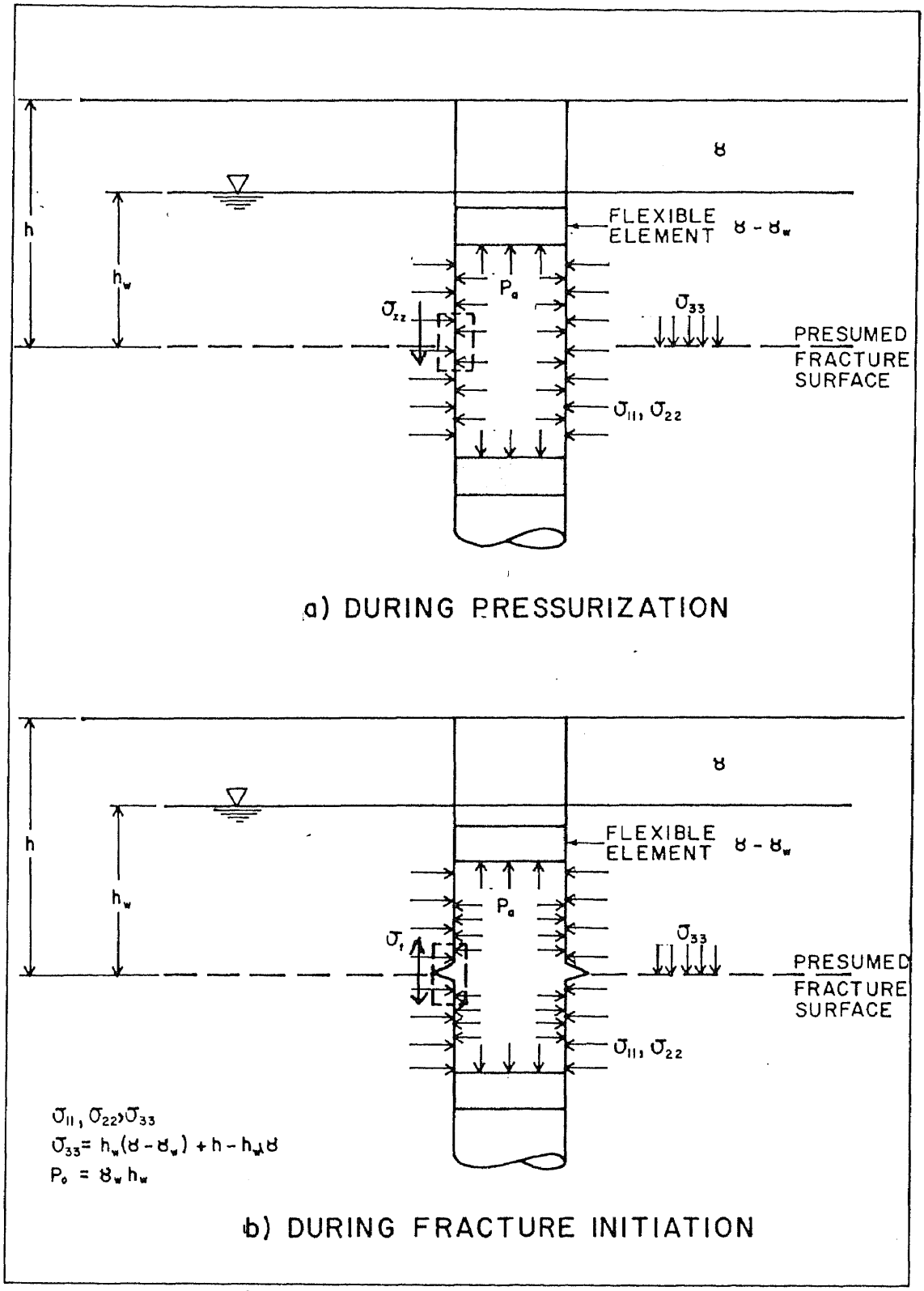

Figure 19 Stress Conditions for Pneumatic Initiation Fracture Model

σ'_{11} = maximum horizontal stress, which is compressive.

σ'_{22} = minimum horizontal stress, which is compressive.

σ'_{33} = vertical effective stress due to overburden, which is compressive.

P_o = pore pressure.

P_a = pressure due to injected air.

ν = Poisson's ratio.

a = pore elastic parameter.

θ = angle measured clockwise from the radius in the direction of the smaller horizontal tectonic stress.

As stated in the previous section, it will be assumed that the tectonic stresses in the horizontal plane are isotropic, i.e. $\sigma'_{11} = \sigma'_{22}$. The reference angle for the plane of interest will be assumed in the direction of σ'_{11}, so θ is equal to zero.

Under these conditions the effective stress now becomes:

$$\sigma'_{zz} - P_a = \sigma'_{33} - P_o - a\frac{1-2\nu}{1-\nu}\left(P_a - P_o\right) \tag{4.2}$$

As P_a is increased, the vertical effective stresses, σ'_{zz}, will become tensile. At this point, the compressive stress due to the weight of overburden is overcome. If pressurization is continued even further, the effective stress at the borehole wall will eventually reach the tensile strength of the geologic formation, i.e. $\sigma_{zz} = \sigma_t$. At this instant, P_a is said to have reached the breakdown pressure, P_b, for the geologic formation. This condition is illustrated in Figure 19 (b). Equation 4.2 can then be written as:

$$P_b - P_o = \frac{\sigma'_{33} + \sigma_t}{1 - a\frac{1-2\nu}{1-\nu}} \tag{4.3}$$

or

$$P_b = \lambda\sigma'_{33} + \lambda\sigma_t + P_o \tag{4.4}$$

where $\lambda = \dfrac{1}{1 - a\dfrac{1-2\nu}{1-\nu}}$

The rational for "lumping" the elasticity parameters into a single constant is that they are not easily determined during the investigation of a site. It is anticipated that in field applications, a single empirical constant can be established based on standard geotechnical classification and properties testing. An initial attempt to determine the values of constants for the various geologic formations tested to date is made in Section 4.6.

In view of the relative shallow depths, i.e.(<100 ft) at which pneumatic fracturing will most commonly be applied, the influence of heterogeneities in geologic structure will be significant. This will result in poor correlation between the apparent strength of the formation and the overburden stress at the same location. For this reason, separate constants λ_1 and λ_3 will be maintained for the overburden stress and tensile strength terms. Equation 4.4 can then be written as:

$$P_b = \lambda_1 \sigma'_{33} + \lambda_3 \sigma_t + P_o \qquad (4.5)$$

The above equation can be rewritten with standard geotechnical parameters which can be easily measured for various geologic conditions. Specifically, the overburden stress can be written as :

$$\sigma_{33} = (h - h_w)\gamma + h_w(\gamma - \gamma_w)$$

$$P_o = \gamma_w h_w$$

and

$$\sigma_t = \sigma_{ta}$$

where σ_{ta} is defined as the "apparent" breakdown tensile strength of the formation. This distinction is made since soil formation and fractured rock do not exhibit a true tensile strength as would intact rock. By making the above substitution, the equation becomes

$$P_b = \lambda_1(h - h_w)\gamma + \lambda_1 h_w(\gamma - \gamma_w) + \lambda_3 \sigma_{ta} + h_w \gamma_w \qquad (4.6)$$

which is a general relationship for saturated conditions. In the vadose zone, the pore pressure effects can be neglected, and the expression reduces to

$$P_b = \lambda_1 \gamma h + \lambda_3 \sigma_{ta} \tag{4.7}$$

In summary, Equation 4.6 and 4.7 form the basic analytical model for fracture breakdown pressure. It can be seen that the two dominant influences on fracture pressure are overburden stress and apparent tensile strength.

In the following section, a regression analysis will be used to determine coefficients for this model. First, the coefficients for the overburden term will be estimated by analyzing the pressure-time history for the various formations. Specifically, the overburden term will be equated with the observed maintenance pressure, P_m. Once the overburden coefficients are established, the apparent breakdown tensile strength will be calculated as the difference between total breakdown pressure, P_b, and the observed maintenance pressure P_{mi}. Using this approach, the coefficient λ_3 will be equal to 1.0 by definition.

4.6 Regressive Analysis of Data.

In order to validate the model developed in the previous section, an analysis of the field fracturing data collected over the last four years was performed. This data has been summarized in Table 4. The analysis involved plotting pertinent graphs of fracturing pressure data from the various sites. This provided an opportunity to identify data trends for model validation, and determine the model coefficients by regression.

4.6.1 Fracture Maintenance Pressure - Soil.

Fracture maintenance pressure is the minimum pressure which is required to dilate the formation after the fracture has been initiated. It represents an equilibrium condition, when the injection flow rate and pressure exactly balances the overburden pressure.

Data for fracture maintenance pressure has been collected from three sites for

Table 4 Summary of Data From the Demonstration Sites

Site	Date	Geology	Avg. Depth (ft)	Inj. No.	Inj. P (psi)	Inj. Q (scfm)	Inj. T (s)	Initial Max. Heave (in.)	Initial Avg. Heave (in.)	Residual Max. Heave (in.)	Residual Avg. Heave (in.)	Max Radi (ft.)	Avg. Radi (ft.)	Bd. Pressure (psi)	Reopen Pressure (psi)	Maint. Pressure (psi)	Shut-in Pressure (psi)	Dry Density. (pcf)	Vert. Stress (psf)	App. Bd. T.Strength (psi)	App. Reop. Strength (psi)
Frelinghuysen	4/18/90	Clayey Silt	3.5	1-1	150	300		0.95	0.28	0.11	0.06	7	4.2			10*		105	368		
Phase 1	4/18/90	Clayey Silt	3.5	1-2														105			
	4/18/90	Clayey Silt	3.5	1-3	150	300		0.64	0.25			7	4.2			10*		105	368		
	4/18/90	Clayey Silt	3.5	1-4	150	300		0.75				4						105	368		
	4/18/90	Clayey Silt	3.5	1-5	150	300												105	368		
	4/27/90	Clayey Silt	3.5	1-6	150	300		0.75	0.26			7	4.2					105	368		
	4/27/90	Clayey Silt	3.5	1-7	150	300		0.25	0.11			7	4.2			7*		105	368		
	4/27/90	Clayey Silt	3.5	1-8	150	300		0.38	0.16			7	4.2			8*		105	368		
	11/16/90	Clayey Silt	4	2-1	150	619		0.56	0.095	0.22	0.02	9.5	6.1					105	420		
Frelinghuysen	5/24/91	Clayey Silt	6	3-1	150	715	36	0.41	0.12	0.13	0.012	9.9	8.5	36		13		105	630	23.0	
Phase 2	5/24/91	Clayey Silt	6	3-2	200	1227	22	0.44	0.18	0		10	8.5		21	11		105	630		10.0
	5/24/91	Clayey Silt	6	3-3	200	270	20	0.41	0.16	0		11	8.6		18/17	10.0/8.0		105	630		8/9
	5/24/91	Clayey Silt	6	3-4	NR	690	90											105	630		
	9/20/91	Clayey Silt	6	4-1	175	1157	20	0.09	0.02			8.5	5.7	34		15		105	630	19	
	9/20/91	Clayey Silt	8.3	4-2	NR	1500	12	0.28	0.06			15.5	11.7	45		18		105	872	27	
	9/20/91	Clayey Silt	6	5-1	175	1500	10	0.45	0.06	0.14	0.013	11	8.6	56		17		105	630	39	
	9/20/91	Clayey Silt	6	5-2			10	NR				NR			20	17					3
	9/20/91	Clayey Silt	8.6	5-3	225	1339	20	0.47	0.11			16	11.3	35		17		105	903	18	
	9/20/91	Clayey Silt	8.6	5-4			20	NR				NR			22	17/15/13					5/7/9
Frelinghuysen	5/29/92	Clayey Silt	6	5-1	200	858	15	0.2	0.04			6.5	4.16	22		15.0		105	630	7	
Phase 3	5/29/92	Clayey Silt	6	5-2	200	964	15	0.33	0.05			18	12.6		13.2	11.4		105	630		1.8
	5/29/92	Clayey Silt	6	5-3	250	1000	15	0.3	0.05			15.3	9.6		13.0	11.0		105	630		2.0
	5/29/92	Clayey Silt	9	5-4	200	943	15	0.22	0.06			21.3	14.1	23.5		16.5		105	945	7	
	5/29/92	Clayey Silt	9	5-5	250	1114	16	0.18	0.04			24	16.1		17	14.7	1	105	945		2.3
	6/3/92	Clayey Silt	6	6-1	150	722	12	0.33	0.07			21	11.7	19.5		12.5		105	630	7	
	6/3/92	Clayey Silt	8.4	6-2	250	984	12	0.19	0.04			14.5	11.4	22.2		17	0.2	105	882	5.2	
	6/3/92	Clayey Silt	8.4	6-3	280		20								16	15	0.2	105	882		1.0
Richmond	6/13/90	Silty Clay	7.5	1-1	150	864	20	1.06	0.35	0.19	0.05	14	8.2								
	6/13/90	Silty Clay	7.5	1-2	150	864	20	0.44	0.22			14	8.6								
	6/14/90	Silty Clay	9.8	1-3	150	864	20														
	6/14/90	Silty Clay	9.8	1-4	150	864	20														
	6/14/90	Silty Clay	7.5	1-5	150	864	20	0.31	0.14			14	8.6								
	6/14/90	Silty Clay	8	2-1	150	864	20	0.38	0.13			14	8.6								

Table 4 Continued...

Site	Date	Geology	Avg. Depth (ft.)	Inj. No.	Inj. P (psi)	Inj. Q (scfm)	Inj. T (s)	Initial Max. Heave (in.)	Initial Avg. Heave (in.)	Residual Max. Heave (in.)	Residual Avg. Heave (in.)	Max Radi (ft.)	Avg. Radi (ft.)	Bd. Pressure (psi)	Open Pressure (psi)	Maint. Pressure (psi)	Shut-in Pressure (psi)	Dry Density. (pcf)	Vert. Stress (psf)	App. Bd. T.Strength (psi)	App. Tensil Strength (psi)
Newark	03/08/91	Sandstone	10	1-1	180	771	52	0.16	0.12	0.03		>10		80		37.5	21	140	1400	42.5	
(NJIT)	04/05/91	Sandstone	16	1-2	180	857	28	0.13	0.06	0.03		>10		105		53	5	140	2240	52	
Roseland	7/23/91	Clayey Sand	5	1-1	150	1018		0.86	0.34	0.05		27	16								
	7/23/91	Silty Sand	6	2-1	175	1714		1.83	0.59	0.09		22	14.5								
Hillsborough	6/22/92	Siltstone		1-1																	
Phase 1	6/22/92	Siltstone		1-2																	
	6/22/92	Siltstone	13	1-3										57		20		140	1820	37	
Hillsborough	8/20/92	Siltstone	10.1	2-1	200	1500	20	0.38				>20		140		21	2	140	1400	119	
Phase 2	8/20/92	Siltstone	12.2	2-2	200	1607	20	0.31				>20		155		25	5	140	1680	130	
	8/21/92	Siltstone	14.2	2-3	200	1886	20	0.38				>20		100		20	4	140	1960	80	
	8/22/92	Siltstone	15.5	2-4	200		20											140	2100		
Hillsborough	4/6/93	Siltstone	14.3	3-1	250	1029	20							82		23	10			59	
Phase 3	4/6/93	Siltstone	18.5	3-2	250	1114	20							82		24	10			58	
	4/6/93	Siltstone	23	3-3	250	1229	30							210		31	10			179	
	4/6/93	Siltstone	20.8	3-10	250	1131	25	0.12						90		40	10			50	
Newark	9/18/92	Sandy Silt	5	1-1	(100)	(1028)	5	(0.19)						30		8		105	525	24	
(Chem Fleur)	9/18/92	Sandy Silt	5	1-2	(100)	(1113)	5	(0.06)							14.5	5.5		105	662		9
	9/18/92	Sandy Silt	6.3	1-3	(150)	(1113)	5	(0.03)						50		10	3			40	
Marcus Hook	10/21/92	Clayey Silt	6	1-1	150	1200	20							72		12		105	630	60	
	10/22/92	Clayey Silt	6	1-2	150	-	5								38	18		105	630		40
	10/22/92	Clayey Silt	6	1-3	150	1276	20								21	19		105	630		2
	10/22/92	Clayey Silt	6**	1-4	150	1400	20								24	14		105	630		10
	10/22/92	Clayey Silt	4	1-5	150		20							22		9		105	420	13	

analysis including Frelinghuysen, Marcus Hook and Chem Fleur. The soils at the first two sites were similar, and consisted of stiff overconsolidated clayey silts. The soils at Chem Fleur site will be discussed separately since they were a mixture of soft silt and fill.

Plots of the maintenance pressure vs. the average depth for the Frelinghuysen and Marcus Hook sites are presented in Figures 20 and 21 respectively. As indicated, numerous data were available for Frelinghuysen since the majority of developmental research has been conducted at this site. Lines of linear data regression are shown on each plot. The following observations were made upon review of the data for these sites:

- Maintenance pressure generally increases with the depth of overburden.
- The Frelinghuysen data shows that maintenance pressure for refracture is always less than for the original fracture. Both trends exhibits a similar slope, however.
- Some data scatter is apparent although the linear regression lines are relatively consistent.

Based on the trends for these two sites, the use of a linear relationship between maintenance pressure with average depth appears justifiable. It is recognized, however, additional data will be necessary over a wide range of depth to confirm this tentative trend. From a theoretical perspective, it is possible that the intercept shown in these data may be caused by relatively shallow fracture depths. It may also be attributed to the existence of a residual tensile resistance (λ_2) in the formation, even after it is fractured.

For the purpose of selecting model coefficients, a combined graph for clayey silt is presented in Figure 22. As indicated, the slope of the line which represents the value of the pressure gradient $\lambda_1\gamma$, is 1.5 psi per foot of overburden depth. Assuming an average soil unit weight of 105 pcf, (Goodman 1980), this translates to a λ_1 value of 2.1. The y-intercept, which represents a residual tensile resistance λ_2, is 4.7 psi. See Table 5 for a summary of these values.

For comparative purposes, the maintenance pressure data for the Chem Fleur site is presented in Figure 23. It can be seen that the slope is similar although the y-intercept is

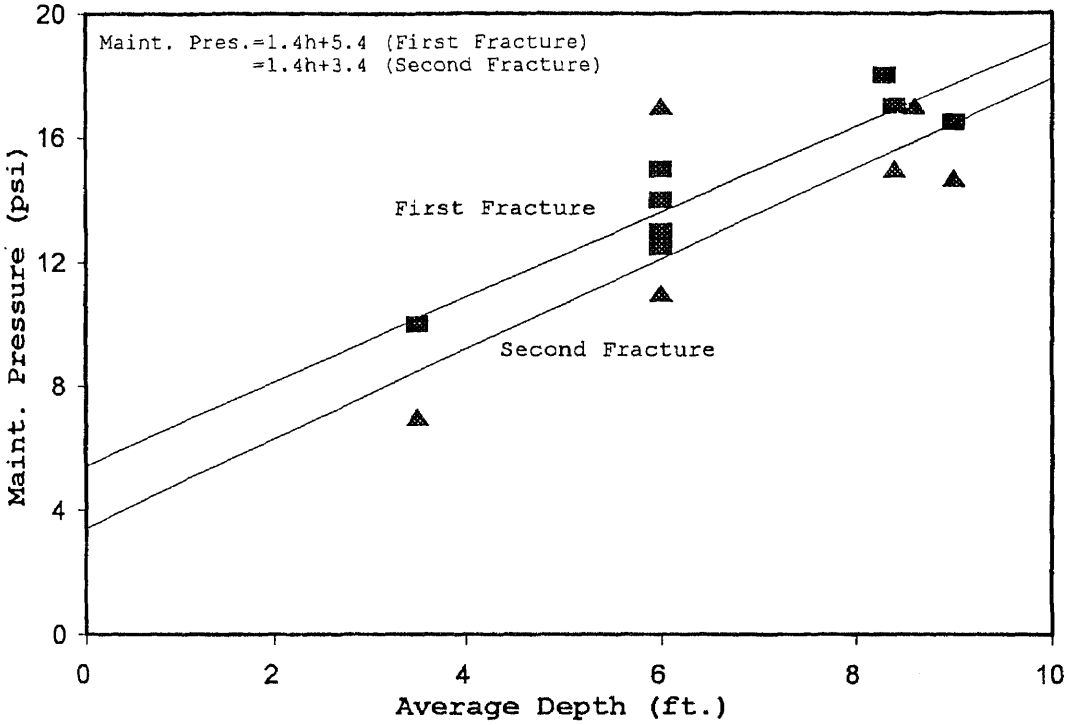

Figure 20 Graph of Maintenance Pressures vs. Average Depth for Frelinghuysen Site

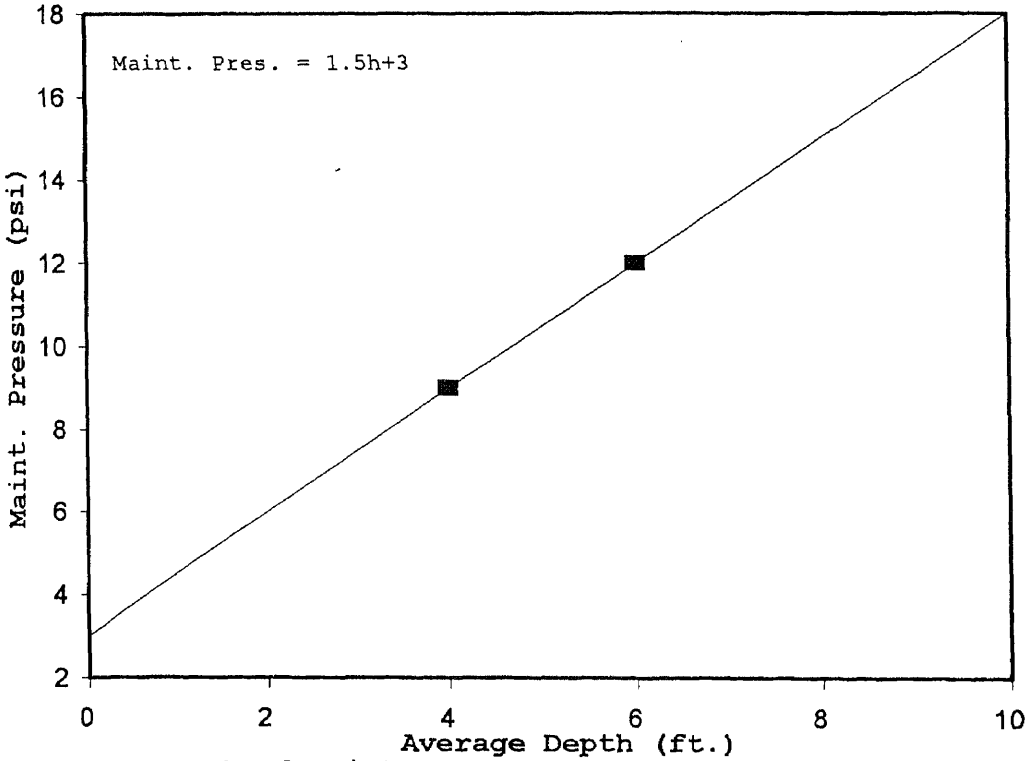

Figure 21 Graph of Maintenance Pressure vs. Average Depth for Marcus Hook Site

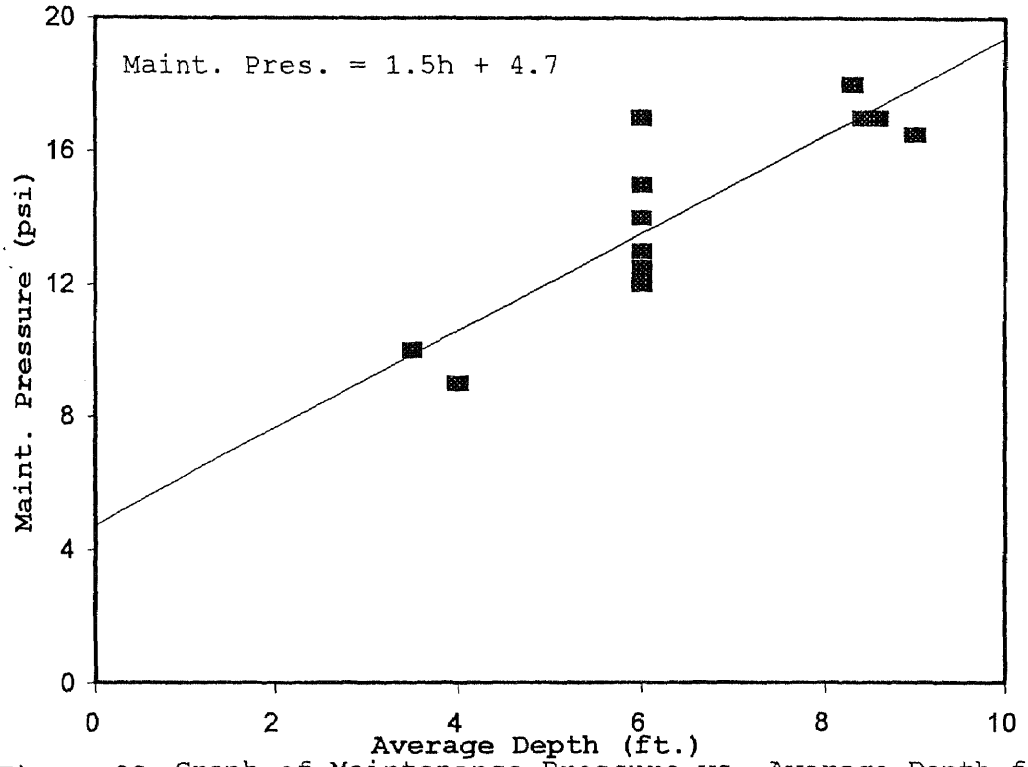

Figure 22 Graph of Maintenance Pressure vs. Average Depth for Clayey Silt Formations

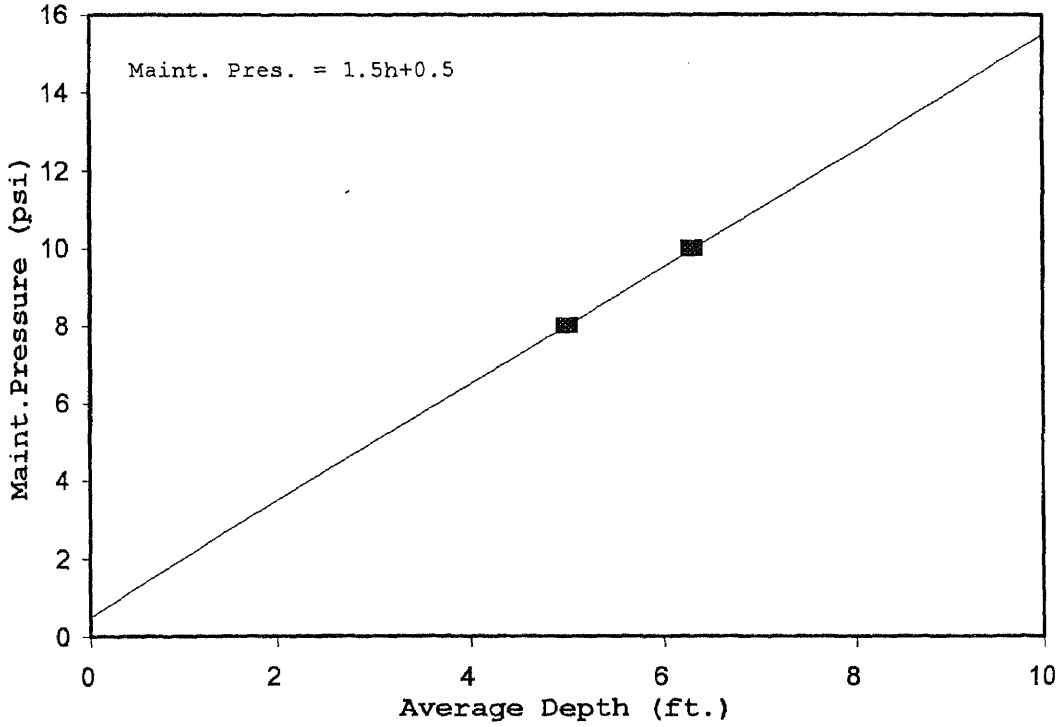

Figure 23 Graph of Maintenance Pressure vs. Average Depth for Newark (Chem Fleur) Site

nearly zero. This deviation from the previously presented data may be due to the soft nature of soil at the depth tested at this site. These data are too limited (only two points) to establish any definitive trend for this geology.

4.6.2 Fracture Maintenance Pressure - Rock.

Data for fracture maintenance pressure for rock formations has been collected from two sites for analysis. These are the Hillsborough and Newark(NJIT) Site. Both of these sites are part of the Brunswick formation, but the lithologic texture at each site is slightly different. The Hillsborough site consists of primarily siltstone, while the Newark site is mostly of fine grained sandstone. This textural differences may influence their response to pneumatic injection pressure.

Plots of maintenance pressure vs. average depth of injection for the sites are shown in Figure 24 and Figure 25. From Table 4, it can be seen that most of the information in rock formations has been collected at the Hillsborough site. At this site fracturing has taken place at three separate locations over the period of a year. This contrasts with the data collected at the Newark Site, where fracturing was limited to one location.

The approach taken in the analysis of rock formations is similar to that of soil, i.e. lines of linear data regression are shown in the plots to identify trends and determine model coefficients.

On review of these plots the following observations are made:

- Maintenance pressure generally increases with depth of overburden, a trend which was also observed in soil. Some data scatter is apparent at the Hillsborough site.
- The slope of the line for the siltstone formation is (1.14) lower than the value in the sandstone formation (2.5), and the clayey silt. (1.5) formation.
- The intercepts for Siltstone and Sandstone are (7.7) and (13) respectively

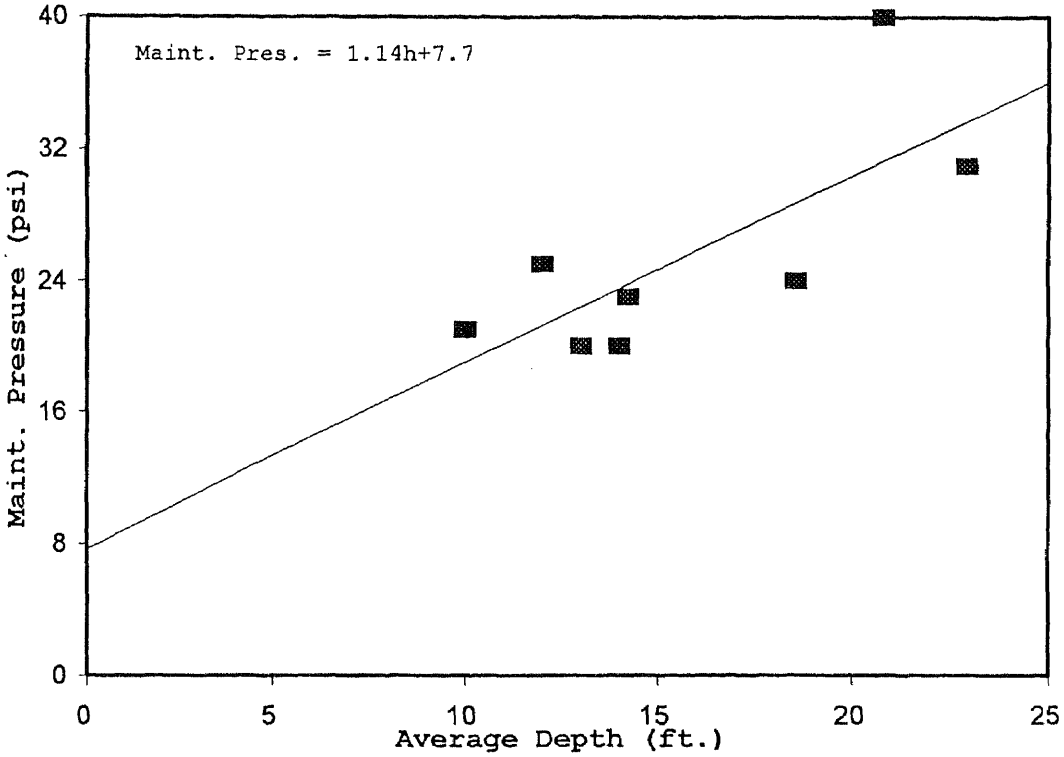

Figure 24 Graph of Maintenance Pressure vs. Average Depth for Hillsborough Site

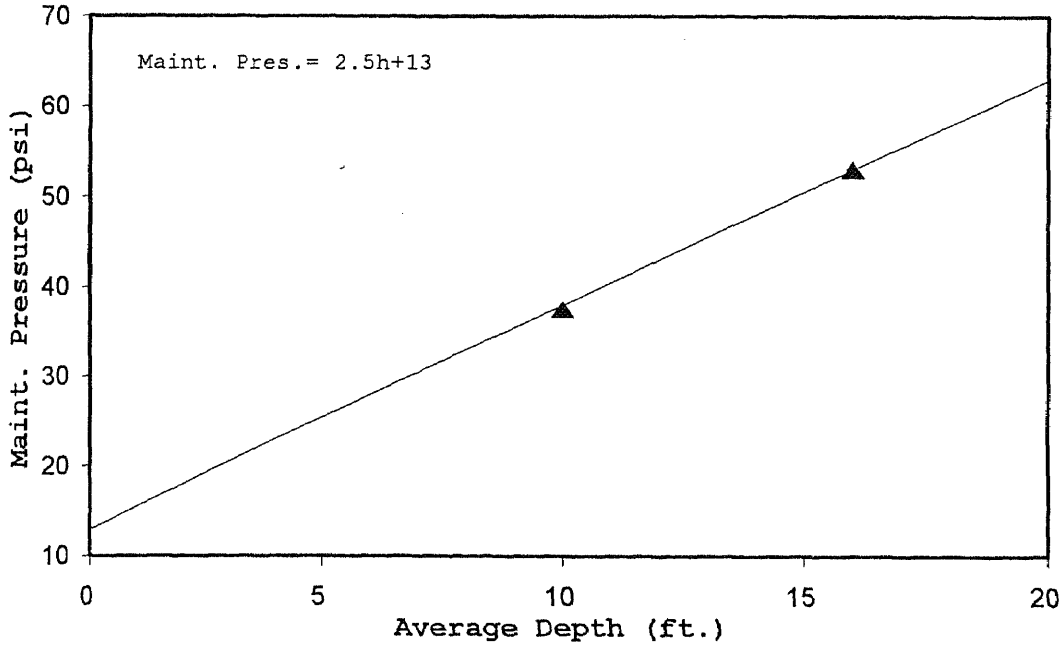

Figure 25 Graph of Maintenance Pressure vs. Average Depth for Newark (NJIT) Site

As with soil, a linear relationship between maintenance pressure and average depth is indicated. The slope of the line ($\lambda_1\gamma$) for siltstone is 1.14, which corresponds to a pressure gradient of approximately 1.2 psi per foot of depth. For an assumed unit weight of 140 pcf., (Goodman 1980) the value of λ_1 for siltstone is approximately 1.2. For sandstone, the slope is 2.5 psi per foot of depth, and λ_1 for sandstone is 2.6. The residual tensile resistance of the formations are 7.7 psi and 13 psi for siltstone and sandstone respectively. See Table 5 for a summary of these values.

Figure 26 shows a summary graph of the lines of regression for the combined soil and rock formations. It is seen that the maintenance pressure and the residual tensile resistance for soil is generally lower than that for rock. This is expected since soil behaves more plastically than rock and is therefore more deformable.

4.6.3 Breakdown Pressures - Soil and Rock

Fracture breakdown pressure is the minimum injection pressure required to overcome the in-situ stresses at the borehole wall to initiate new fractures or dilate existing fractures. Breakdown pressure is always higher than maintenance pressure, since the tensile strength of the formation has to be overcome during the first fracture.

The first plot of breakdown pressure vs. average depth is presented in Figure 27. These data are for clayey silt at the Frelinghuysen site, and are interesting since it suggests that soil moisture influences breakdown pressure. As indicated, breakdown pressure for the saturated soil condition is greater than for unsaturated soil conditions. This behavior is probably due to the fact that for higher moisture contents, the soil behaves more plastically or ductilily. Therefore, the formation is able to absorb more energy before fracture initiation, resulting in higher breakdown pressures.

Figure 28 shows a combined summary of breakdown pressures for the various sites tested. It is seen that the trends are quite similar to the maintenance pressures shown in Figure 22, except that the values are much higher. The following observations are made:

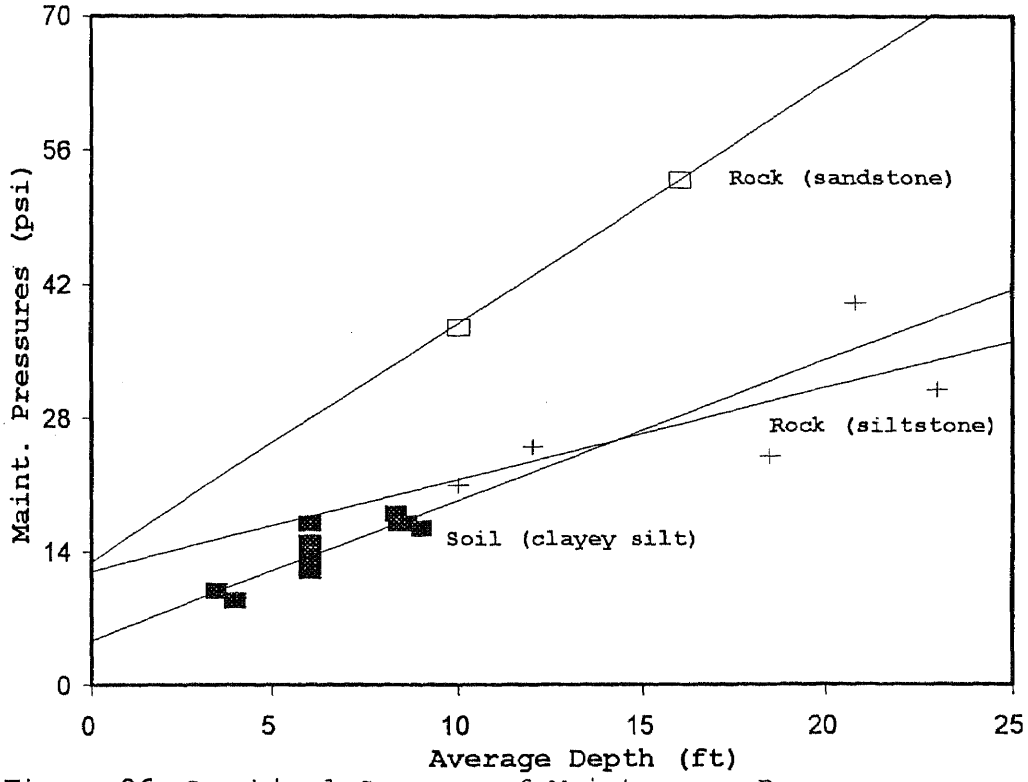

Figure 26 Graphical Summary of Maintenance Pressure vs. Average Depth

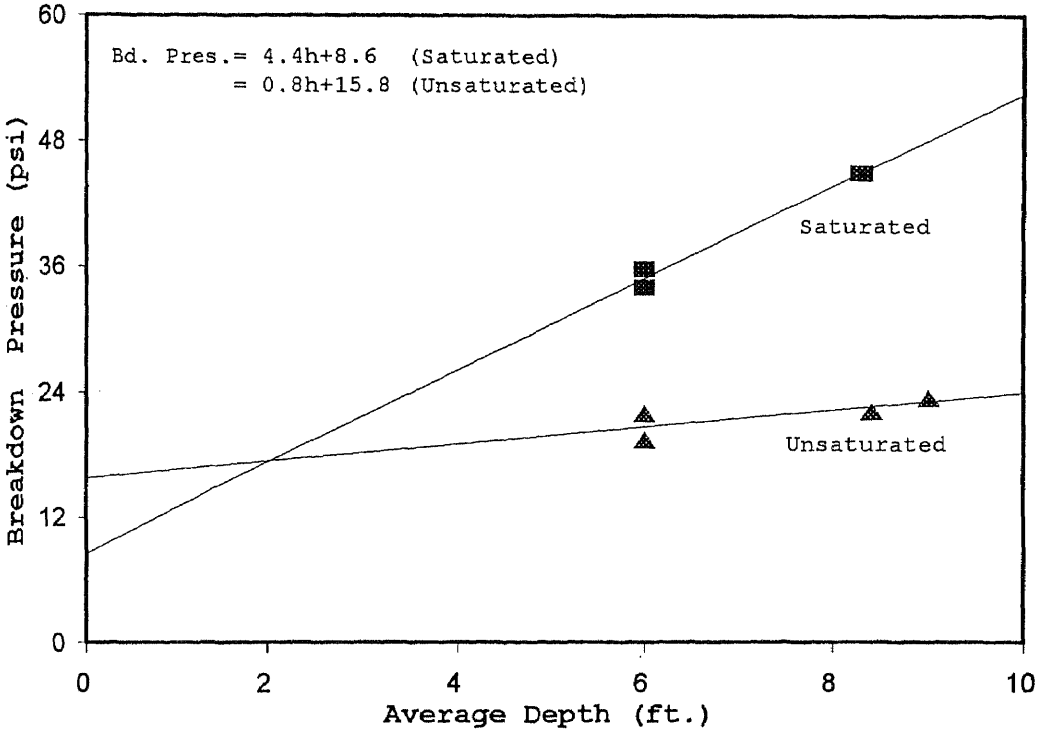

Figure 27 Graph of Breakdown Pressure vs. Average Depth for Frelinghuysen Site

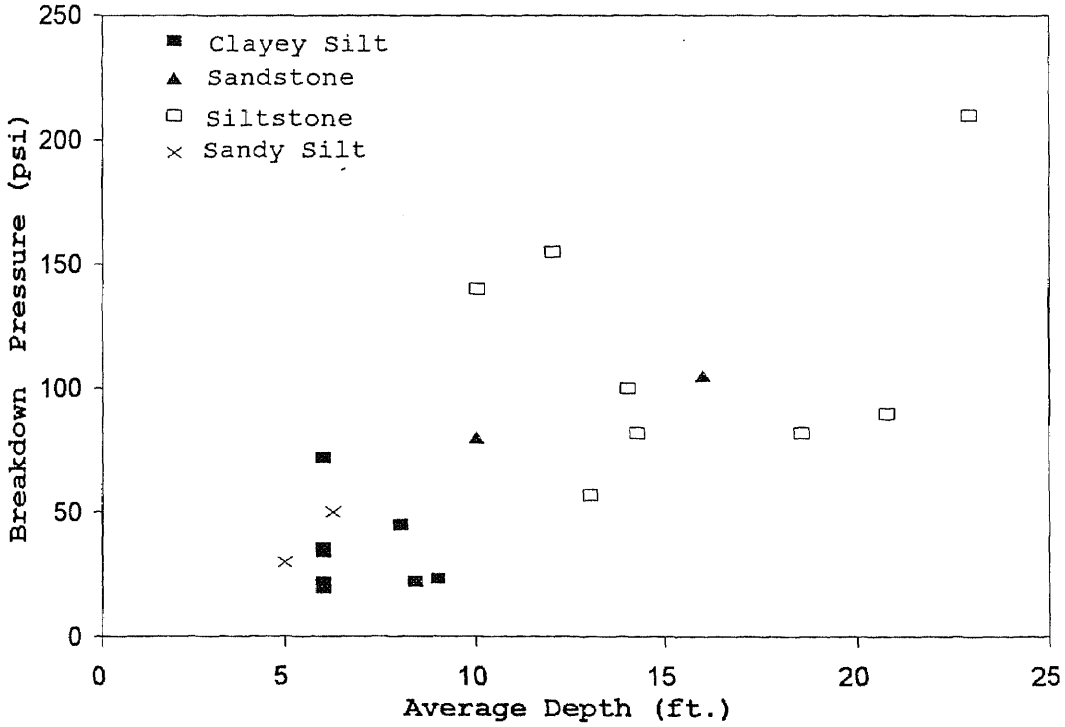

Figure 28 Summary Graph of Breakdown Pressure vs. Average Depth

- There is a general trend of increasing breakdown pressure with depth, except the data scatter is very wide.
- The breakdown pressure for rock is higher than for soil.
- The apparent breakdown tensile strength of the siltstone is higher than that of sandstone.

The wide variation of breakdown pressures for similar conditions are consistent with the observations of previous investigators, e.g. Jaworski (1980), Jumikis (1975), and Lippold (1958). It is attributed to the local heterogeneities, e.g. existing cracks and fractures, textural changes, and moisture variations which exists in all geologic formations, and which can profoundly affect tensile strength. These variations in tensile strength are accentuated at shallow depths since the weight of overburden is not as influential.

Finally, a plot of apparent breakdown tensile strength vs. average depth of injection is presented for soil and rock in Figure 29. This parameter which corresponds to $\lambda_3\sigma_{ta}$, was obtained by taking the difference between the peak breakdown pressure and maintenance pressure for each pressure-time history. The value of apparent breakdown tensile strength is important since it is the dominant term in the breakdown pressure model relationship. As may be expected, it exhibits the same trends as the total breakdown pressure presented in Figure 28. As indicated, in Figure 29 the ranges of apparent breakdown tensile strengths are 8 to 39 psi, 42 to 52 psi. and 40 to 180 psi, respectively for clayey silt, sandstone and siltstone. Since the coefficient λ_3 is assumed to be one, the above ranges also represent the value of σ_{ta}. See Table 5 for a summary of these values.

4.7 Summary of Proposed Relationships and Model Coefficients

Based on the regressive analysis in the previous Section, the proposed relationship for the clayey silt and siltstone/sandstone are presented below:

Clayey Silt:

For breakdown pressure,

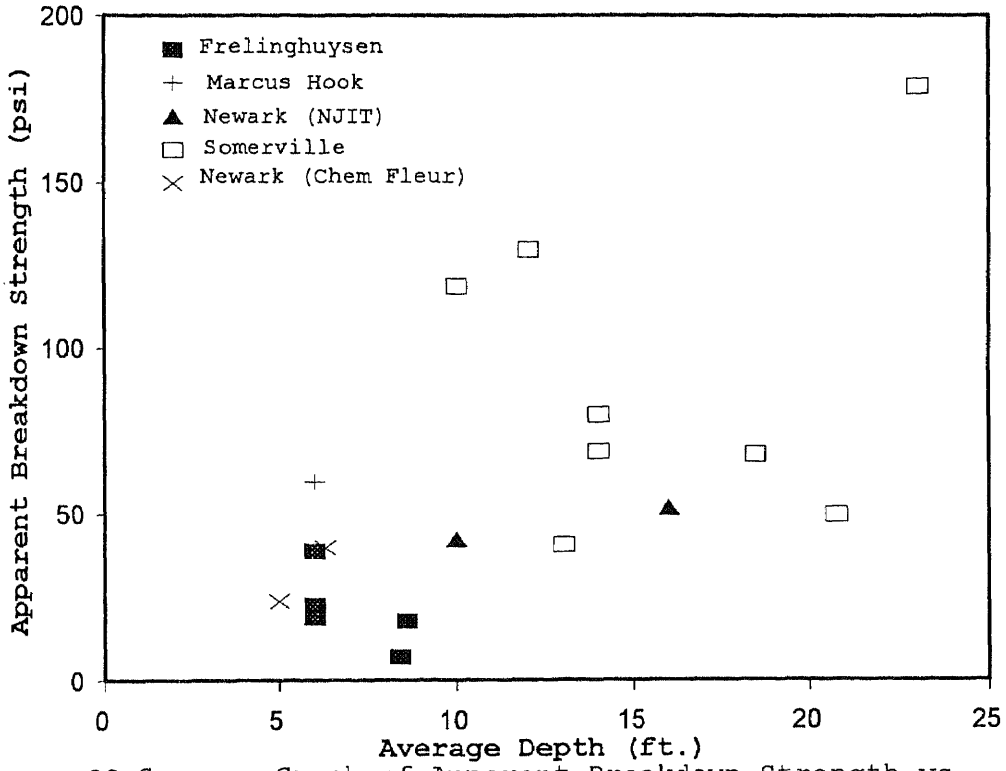

Figure 29 Summary Graph of Apparent Breakdown Strength vs. Average Depth

Table 5 Summary of Related Geologic Formation Strength Data

Geologic Formation	Location	Geology	Maintenance Pressure		Formation Strength (psi)		
			Gradient, $\lambda_1\gamma$ (psi/ft)	Intercept, λ_2 (psi)	Apparant Tensile, $\lambda_3\gamma_{ta}$	Other Apparant Tensile*	Cohesion*
Soil	Frelinghuysen	Clayey Silt	1.4	5.4	5-23	Jaworski (1980) 39-78	11-26.5
Soil	Marcus Hook	Clayey Silt	1.5	3.0	13-60		11-26.5
Soil	Summary	Clayey Silt	1.5	4.7	7-60		-
Soil	Newark (Chem Fleur)	Sandy Silt	1.5	0.5	24-40		-
Soil	Roseland	Clayey Sand	-	-	-		-
Rock	Richmond	Silty Clay	-	-	-		-
Rock	Hillsborough	Siltstone	0.6	15.4	41-179		Jumikis (1975) 320-3270
Rock	Newark (NJIT)	Sandstone	2.5	13	42-52		

* measured in the laboratory

$$P_b = \lambda_1\left(h-h_w\right)\gamma_s + \lambda_1 h_w\left(\gamma_s-\gamma_w\right) + \lambda_2 + \lambda_3\sigma_{ta} + h_w\gamma_w$$

where

$\lambda_1 \approx 2.0$

$\lambda_2 \approx 5$ psi

$\lambda_3 = 1.0$(assumed)

$\sigma_{ta} \approx 10$ to 60 psi

The above equation can also be used for estimating maintenance pressure, by neglecting the term $\lambda_3\sigma_{ta}$.

Siltstone/Sandstone:

For breakdown pressure,

$$P_b = \lambda_1\left(h-h_w\right)\gamma_r + \lambda_1 h_w\left(\gamma_r-\gamma_w\right) + \lambda_2 + \lambda_3\sigma_{ta} + h_w\gamma_w$$

where

$\lambda_1 \approx 1.0$ to 2.5

$\lambda_2 \approx 15$ psi

$\lambda_3 = 1.0$(assumed)

$\sigma_{ta} \approx 40$ to 180 psi

The above equation can also be used for estimating maintenance pressure, by neglecting the term $\lambda_3\sigma_{ta}$.

Example Calculation:

Problem: Find the breakdown and maintenance pressure for the following soil.

Given: Very Stiff Clayey Silt

Depth to water table = 9 ft

Depth to fracture zone = 14 ft

Estimate: $\lambda_1 \approx 2.0$

$\lambda_2 \approx 5$ psi

$\lambda_3 = 1.0$(assumed)

$\sigma_{ta} \approx 40$ psi

$\gamma = 110$ lb/ft^3

Substituting into the proposed model

$$P_b = \lambda_1\left(h-h_w\right)\gamma_s + \lambda_1 h_w\left(\gamma_s-\gamma_w\right) + \lambda_2 + \lambda_3\sigma_{ta} + h_w\gamma_w$$

$$P_b = (2.0)(9ft)\left(110\,{}^{lb}/_{ft^3}\right)\left(\frac{1ft^2}{144in^2}\right) + (2.0)(5ft)\left(110-62.4\,{}^{lb}/_{ft^3}\right)\left(\frac{1ft^2}{144in^2}\right) + 5psi +$$
$$(1.0)(40psi) + (5ft)\left(62.4\,{}^{lb}/_{ft^3}\right)\left(\frac{1ft^2}{144in^2}\right)$$

$= 13.8+3.3+5+40+2.1$

$P_b = 64.2$ psi

and the maintenance pressure,

$P_m = 64.2 - 40 = 24.2$ psi

CHAPTER 5

CONCLUSIONS AND RECOMMENDATIONS

5.1 Conclusions

(1) This thesis has examined the mechanism of pneumatic fracturing in geologic media including soil and rock. Pneumatic fracturing is an innovative technique for increasing the permeability of geologic formations by the controlled injection of high pressure air or other gas. It has been developed at the Hazardous Substance Management Research Center (HSMRC) located at New Jersey Institute of Technology (NJIT) over the last several years. Present applications are focusing on the in-situ remediation of contaminated soil and ground water, although pneumatic fracturing has other geotechnical uses such as pumping well enhancement.

(2) A number of methods and monitoring techniques were developed to investigate the initiation and propagation of pneumatic fractures. These include pressure measurements made in the zone of injection with a transducer, and the ground surface heave data recorded with electronic tiltmeters. Data collected from these instruments have provided valuable insight into the mechanism of pneumatic fracturing, and a comprehensive data summary is contained in this thesis.

(3) As background for development of a pneumatic fracturing model, a literature review of a related technique known as hydraulic fracturing was undertaken. The review indicated that the pneumatic and hydraulic fracturing technologies have some similarities, and also some differences. The significant differences include properties of the injection fluid, rate of fracture propagation, and resulting formation response.

(4) Pressure-time histories from actual pneumatic injections were analyzed in detail to understand the failure mechanism. Several distinct stages of a typical fracture event are identified which were common to all injections including: fracture initiation, fracture extension, fracture maintenance, and fracture residual. The entire fracture event was consistently found to be quite rapid, lasting only several seconds, leading to the conclusion that the formations will respond brittlely to fracture injection. Refracture behavior of previously fractured formations was also investigated. In general, fracture pressures were found to decline for each successive reinjection.

(5) Based on these pressure-time analyses, an original analytical model was developed for predicting fracture pressure. The model describes the stress conditions leading to failure in and around a discrete section of borehole during pneumatic injection. The model assumes the geologic medium is brittle-elastic, uniformly stratified, overconsolidated, horizontally isotropic, and semi-porous. The model also reflects the characteristics of the pneumatic injection equipment, by assuming that end pressures are fully transferred to the borehole walls, i.e. there is no packer slippage, and that the upper and lower packers can move independently.

(6) The model was developed by consideration of the two dominant influences on fracture pressure: overburden stress and apparent tensile strength. Model variations were developed for predicting fracture initiation pressure (breakdown pressure) and fracture maintenance pressure. The effects of piezometric head are also incorporated, so that the model is applicable to both the vadose zone and saturated zone. To assure maximum applicability, the parameters in the model were purposely selected to reflect standard geotechnical properties which are routinely determined during a site investigation.

(7) Validation of the model was made with actual field data from several different research test sites. The three geologic media evaluated were clayey silt, siltstone, and sandstone. The trends of the data showed reasonable agreement with the model, and tentative numerical coefficients were determined by regression. The results are briefly summarized below:

Clayey Silt:	**Siltstone/Sandstone:**
$\lambda_1 \approx 2.0$	$\lambda_1 \approx 1.0$ to 2.5
$\lambda_2 \approx 0$ to 6 psi	$\lambda_2 \approx 10$ to 15 psi
$\lambda_3 = 1.0$(assumed)	$\lambda_3 = 1.0$(assumed)
$\sigma_{ta} \approx 10$ to 60 psi	$\sigma_{ta} \approx 40$ to 180 psi

An example calculation was presented for a typical subsurface condition consisting of clayey silt.

5.2 Recommendations for Future Study

1) Since this model has been developed using a limited amount of data, further refinement and calibration may be necessary. This can be done as more data is collected for various geologic formations and as the technology is extended to the saturated zone.

2) A systematic approach to the collection and management of pneumatic fracturing data and design parameters is necessary. This will assist in determining the influence of various parameters on fracture dimensions and mechanisms. Some of these parameters may include moisture content at the time of fracturing, borehole diameter and borehole

preparation. For example, there may be a correlation between borehole diameter, and borehole preparation on the breakdown pressure of the formation.

3) The following effects should be investigated to optimize fracture dimensions in formations.

a) Pre-stressing of the fracture interval - This can be achieved by first pressurizing the borehole at a lower pressure than that predicted to cause fractures. Next, the pressure in the borehole will be rapidly increased to initiate fractures. In this state, the isolated interval may respond more effectively to pneumatic injection.

b) Two stage injection process - The objective of such a system will be to design the first injection, such that the minimum pressure to initiate fracturing will be applied for 2 to 3 seconds. Next a rapid increase in injection flow rate and pressure from the control system can be made. The advantage of this approach will be to enable geologic formations to be fractured safely, as the high flow rates and pressures necessary for fracture propagation will be attained in the second injection cycle.

4) In geologic formations which are not stratified, preferential horizontal fractures can be initiated by use of flexible sliding head packers. Further enhancement may be possible by notching of the borehole at design intervals. This may also be advantageous when pneumatic fracturing is done at great depths. At these depths the effective in-situ stresses around the borehole may favor the establishment of vertical fractures. However, the dynamics of the injection process and the notch may initiate horizontal fractures.

5) The effects of a directional nozzle on fracture direction and mechanism should also be investigated. This information will be very useful as fracturing is conducted around utilities and structures.

APPENDIX

A: Heave Diagrams and Information.

B: Geologic Description of Test Sites.

C: Pressure - Time Histories.

Appendix A: Heave Diagrams and Information.

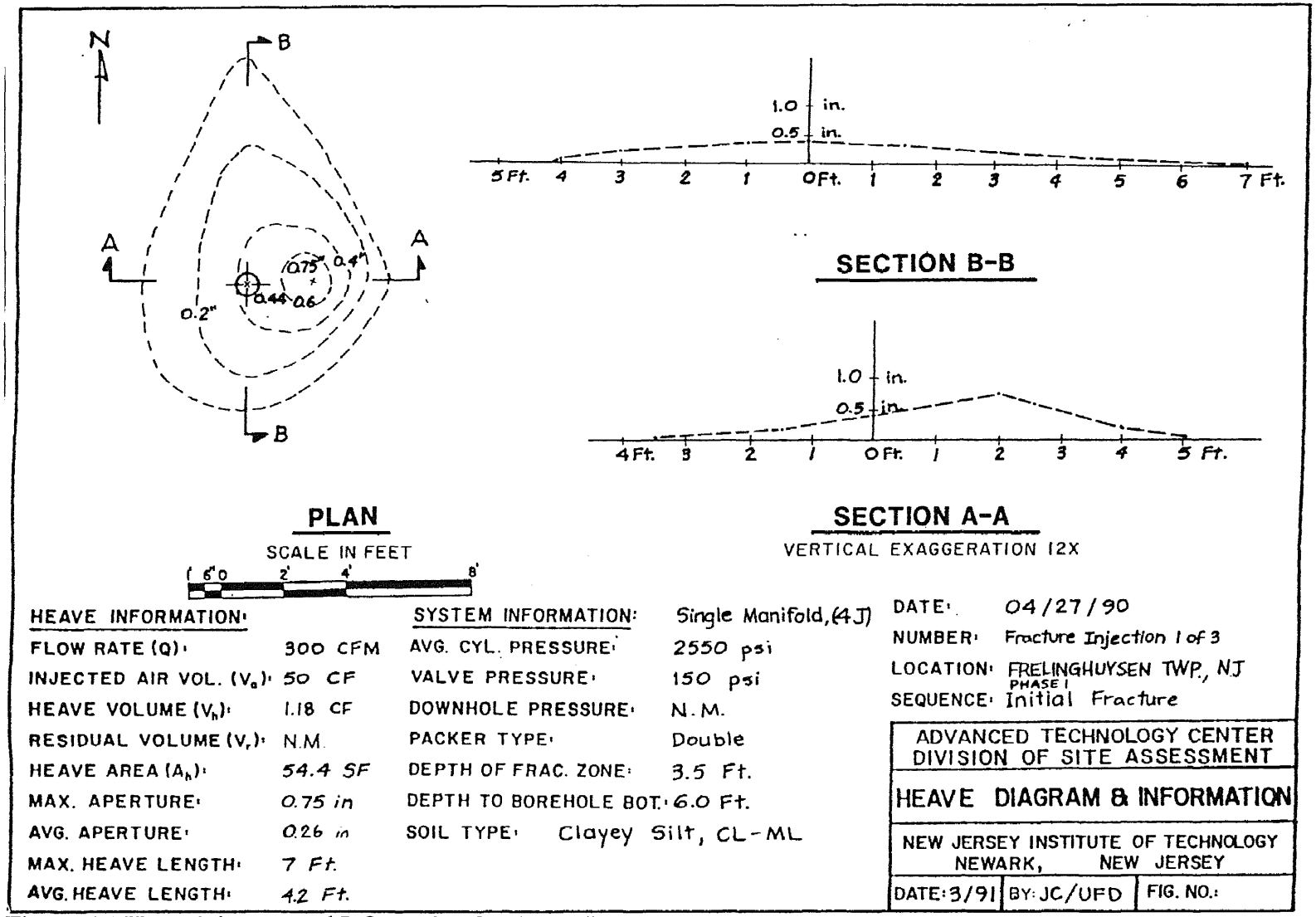

Figure A1 Heave Diagram and Information for the Frelinghuysen Site.

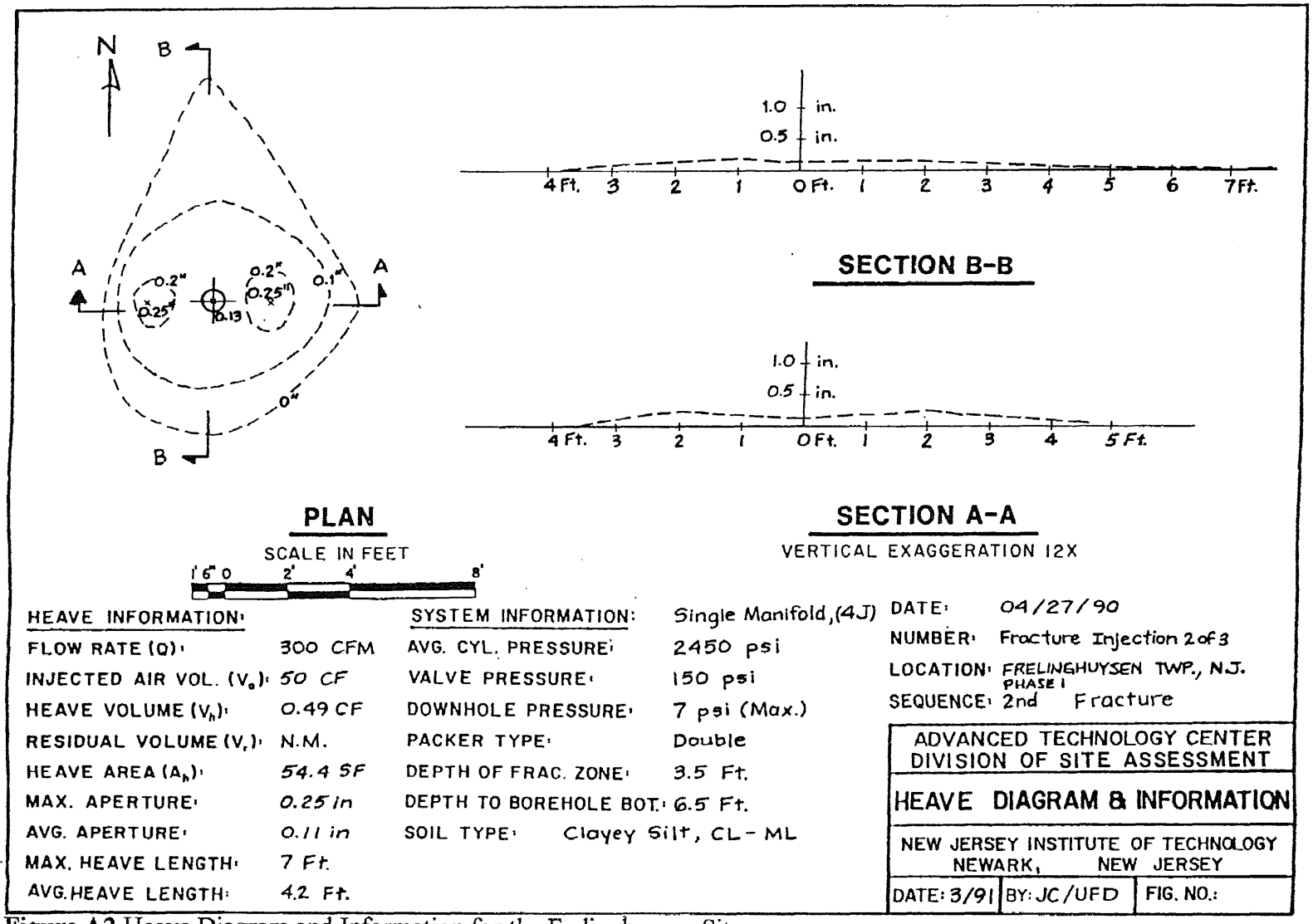

Figure A2 Heave Diagram and Information for the Frelinghuysen Site.

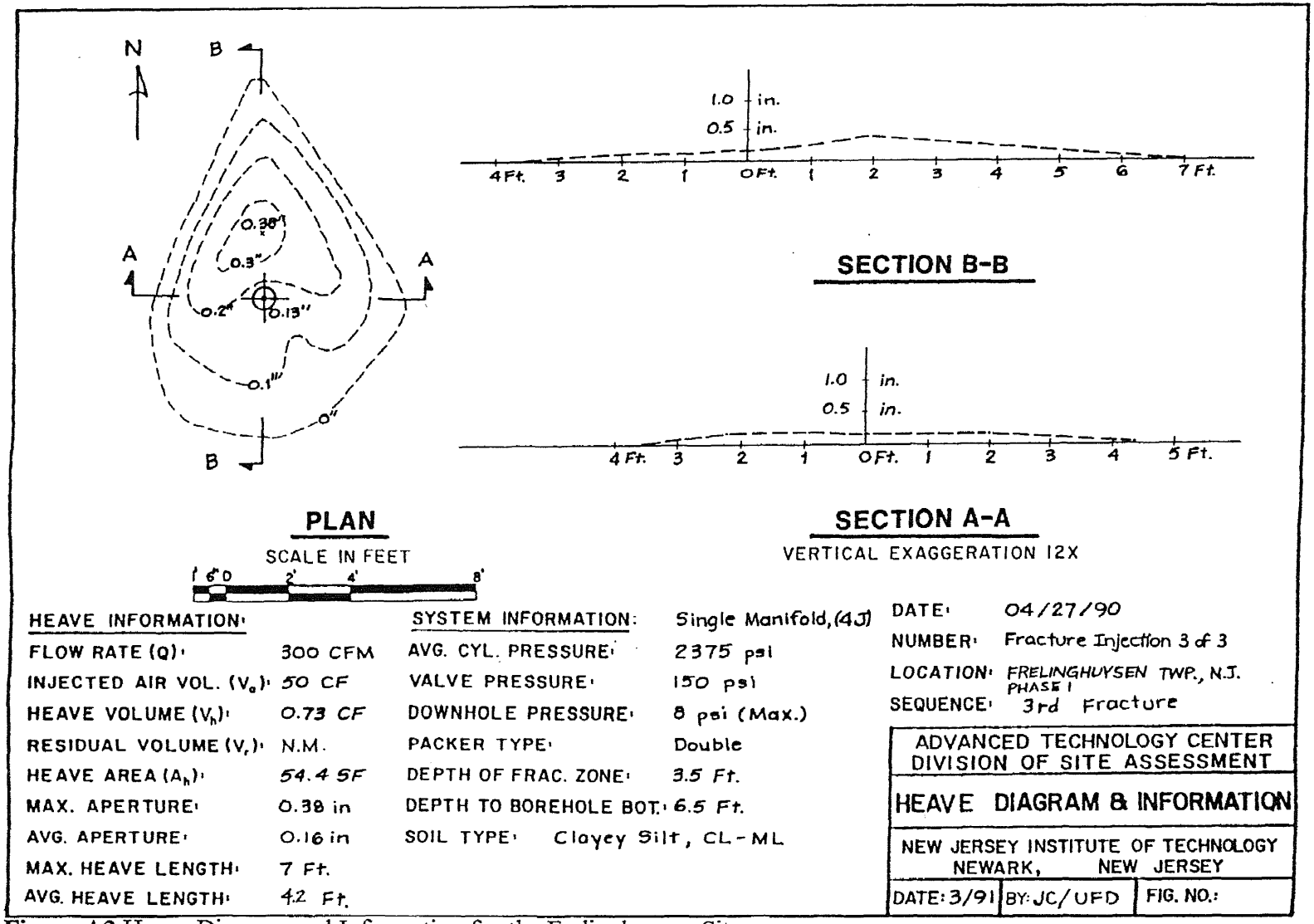

Figure A3 Heave Diagram and Information for the Frelinghuysen Site.

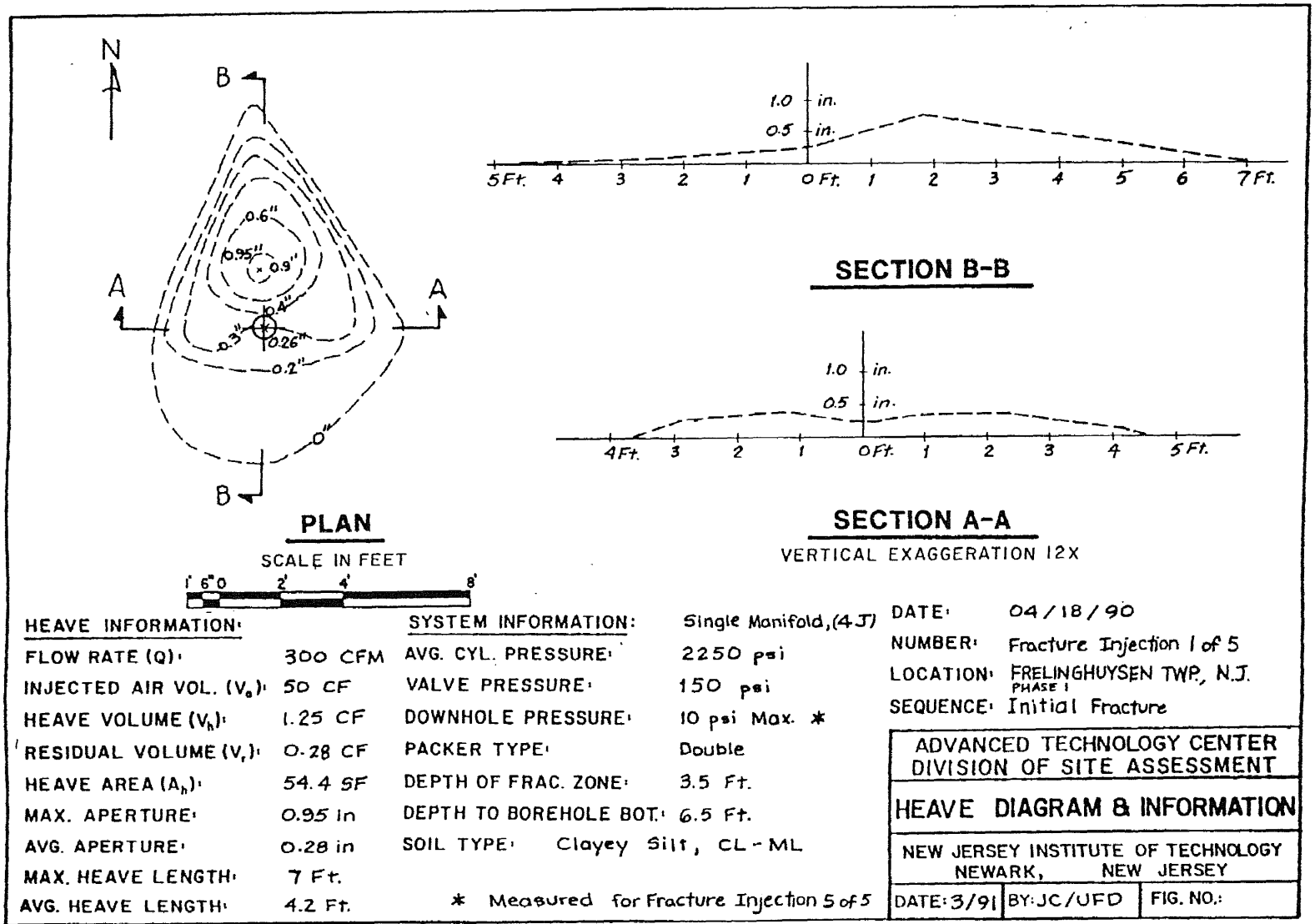

HEAVE INFORMATION:		SYSTEM INFORMATION:	
FLOW RATE (Q):	300 CFM	AVG. CYL. PRESSURE:	2250 psi
INJECTED AIR VOL. (V_a):	50 CF	VALVE PRESSURE:	150 psi
HEAVE VOLUME (V_h):	1.25 CF	DOWNHOLE PRESSURE:	10 psi Max. *
RESIDUAL VOLUME (V_r):	0.28 CF	PACKER TYPE:	Double
HEAVE AREA (A_h):	54.4 SF	DEPTH OF FRAC. ZONE:	3.5 Ft.
MAX. APERTURE:	0.95 in	DEPTH TO BOREHOLE BOT.:	6.5 Ft.
AVG. APERTURE:	0.28 in	SOIL TYPE:	Clayey Silt, CL-ML
MAX. HEAVE LENGTH:	7 Ft.		
AVG. HEAVE LENGTH:	4.2 Ft.		

SYSTEM INFORMATION: Single Manifold, (4-J)

* Measured for Fracture Injection 5 of 5

DATE: 04/18/90
NUMBER: Fracture Injection 1 of 5
LOCATION: FRELINGHUYSEN TWP., N.J. PHASE I
SEQUENCE: Initial Fracture

ADVANCED TECHNOLOGY CENTER
DIVISION OF SITE ASSESSMENT

HEAVE DIAGRAM & INFORMATION

NEW JERSEY INSTITUTE OF TECHNOLOGY
NEWARK, NEW JERSEY

DATE: 3/91 | BY: JC/UFD | FIG. NO.:

Figure A4 Heave Diagram and Information for the Frelinghuysen Site.

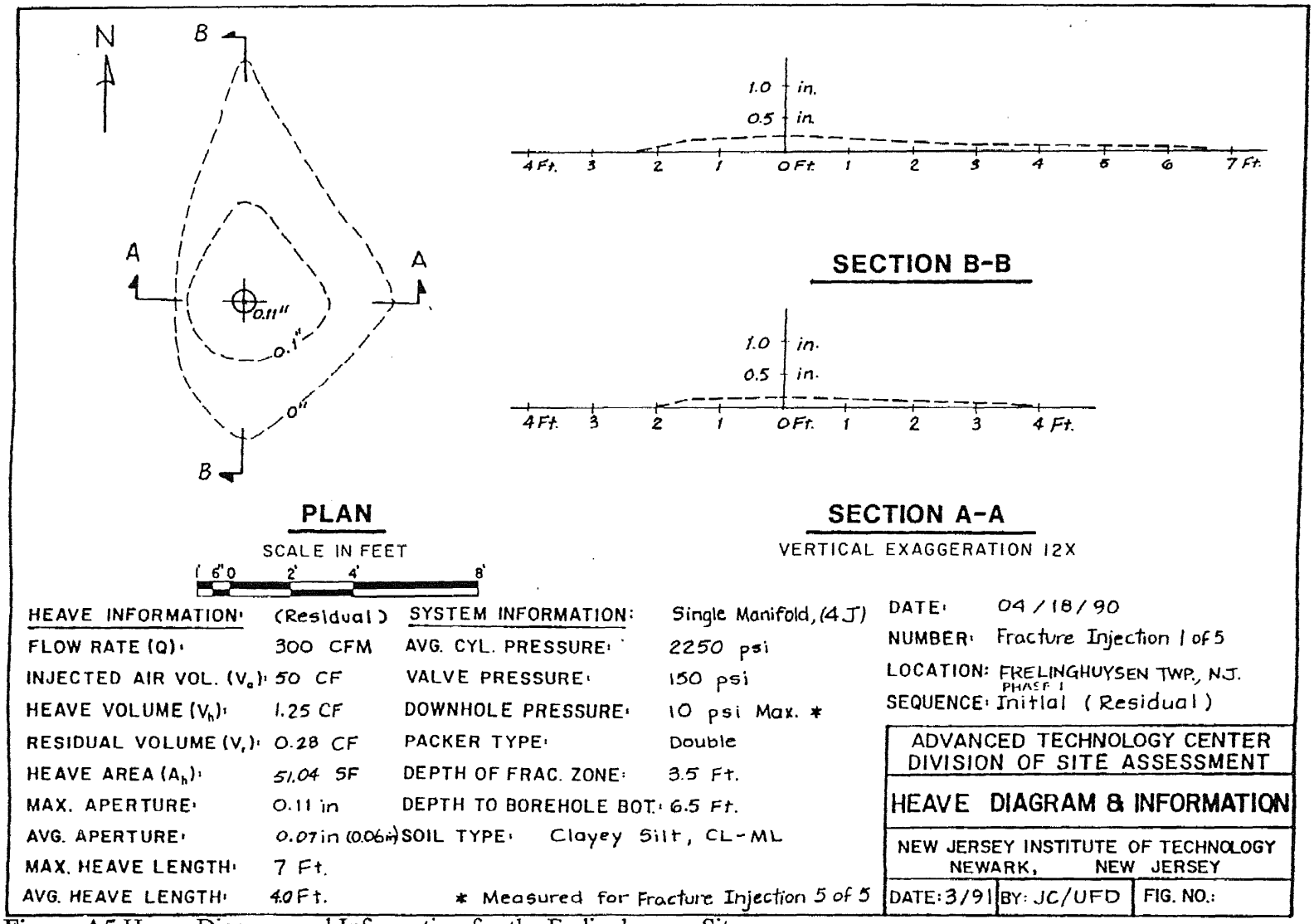

Figure A5 Heave Diagram and Information for the Frelinghuysen Site.

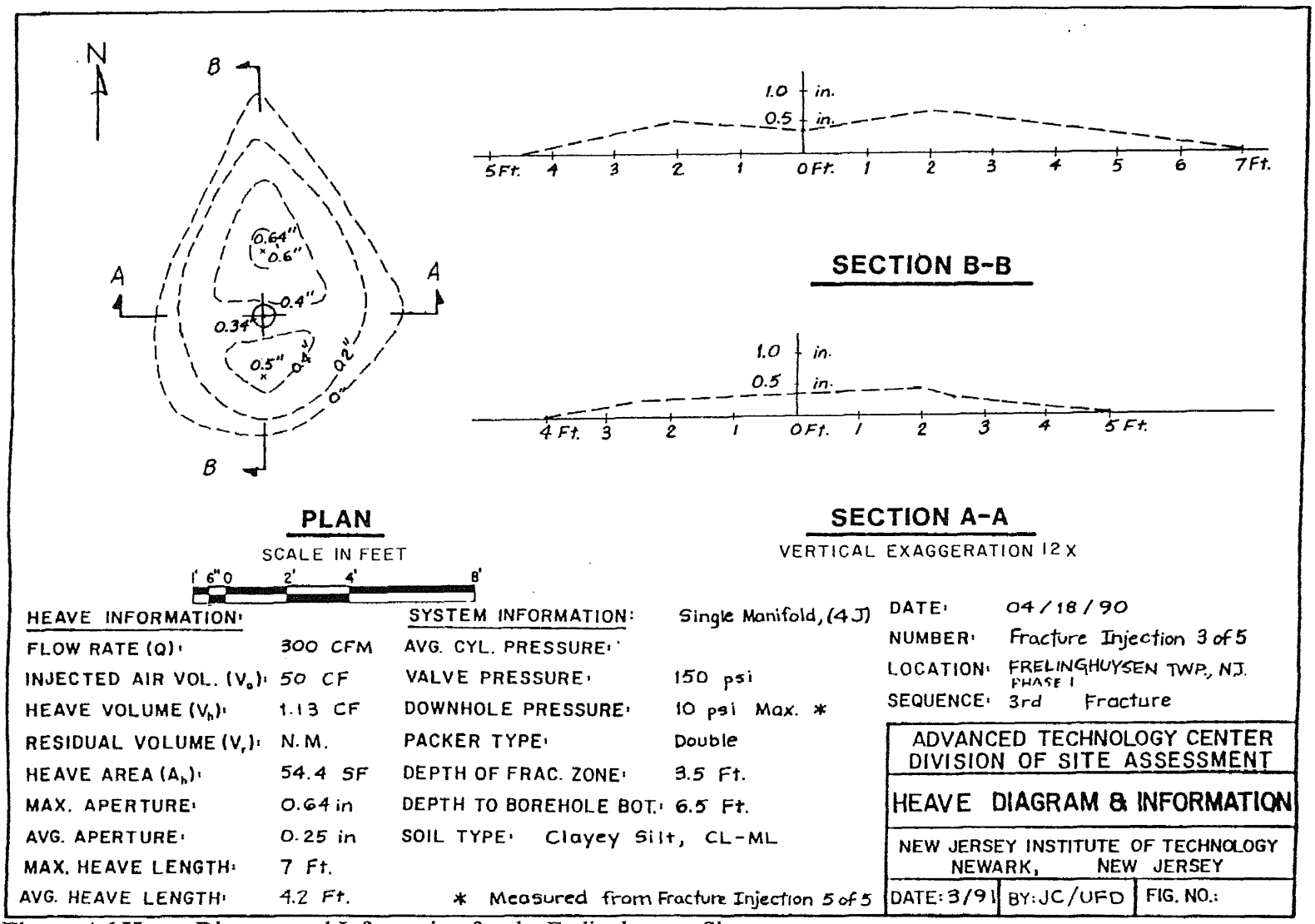

Figure A6 Heave Diagram and Information for the Frelinghuysen Site.

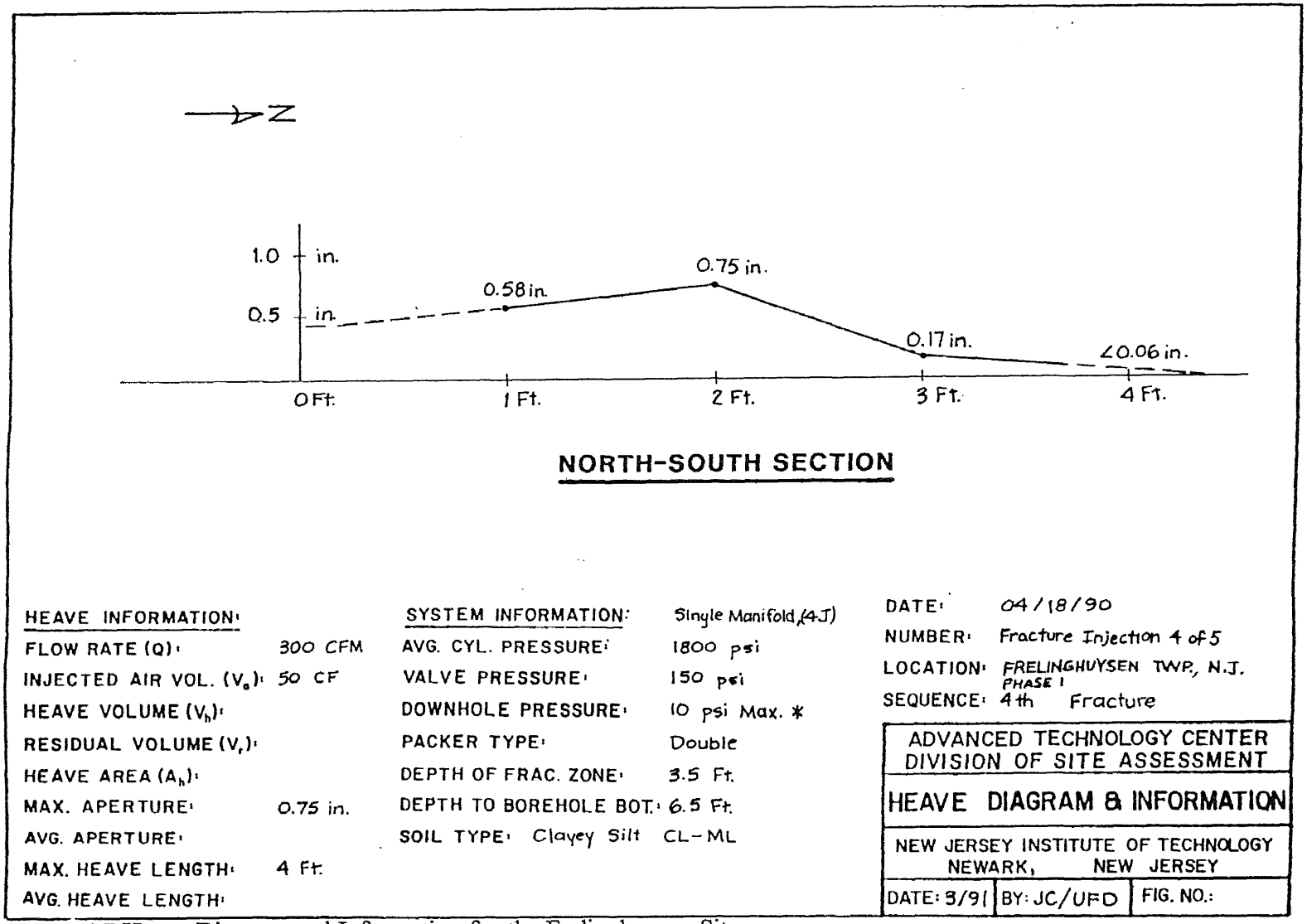

Figure A7 Heave Diagram and Information for the Frelinghuysen Site.

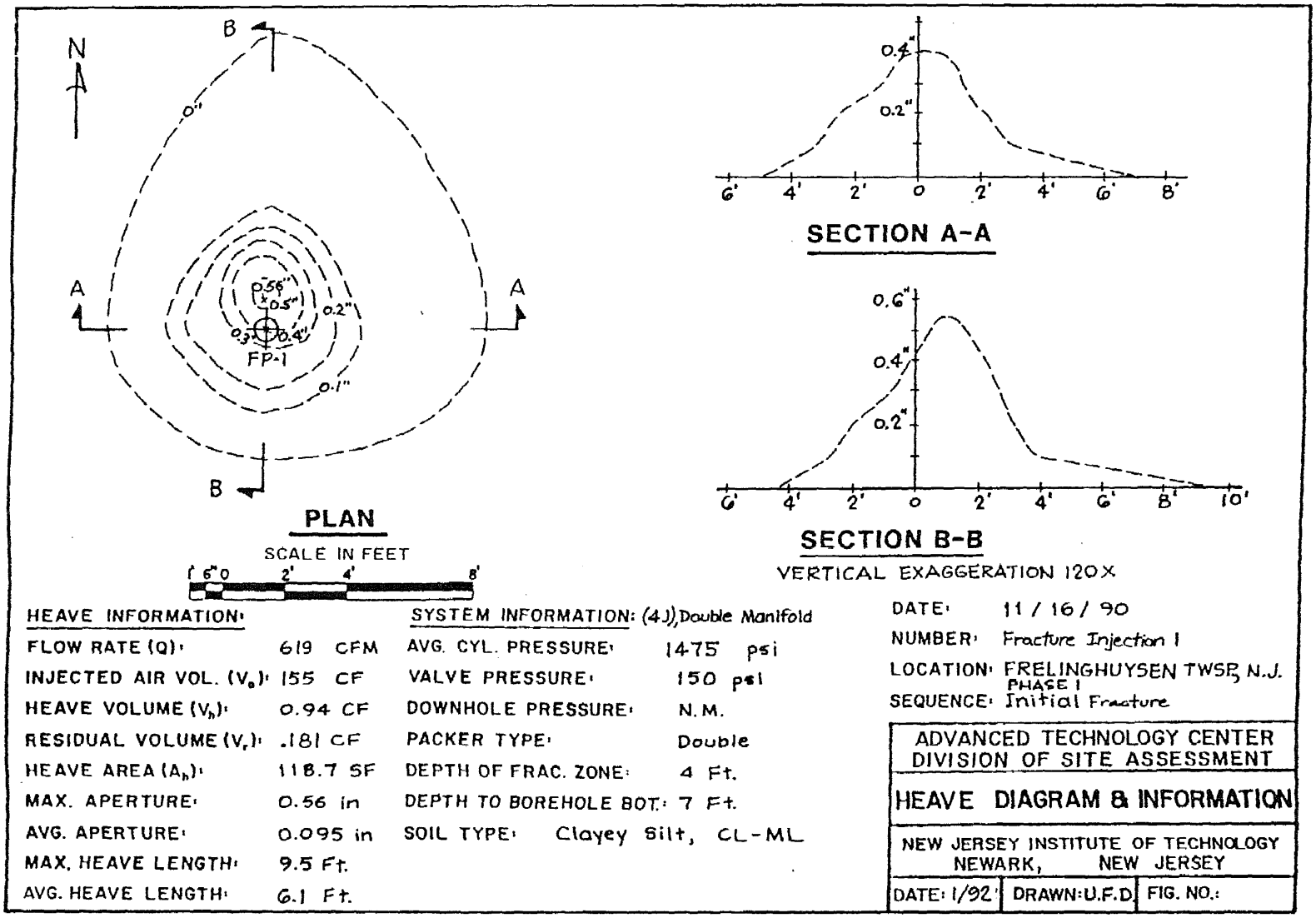

Figure A8 Heave Diagram and Information for the Frelinghuysen Site.

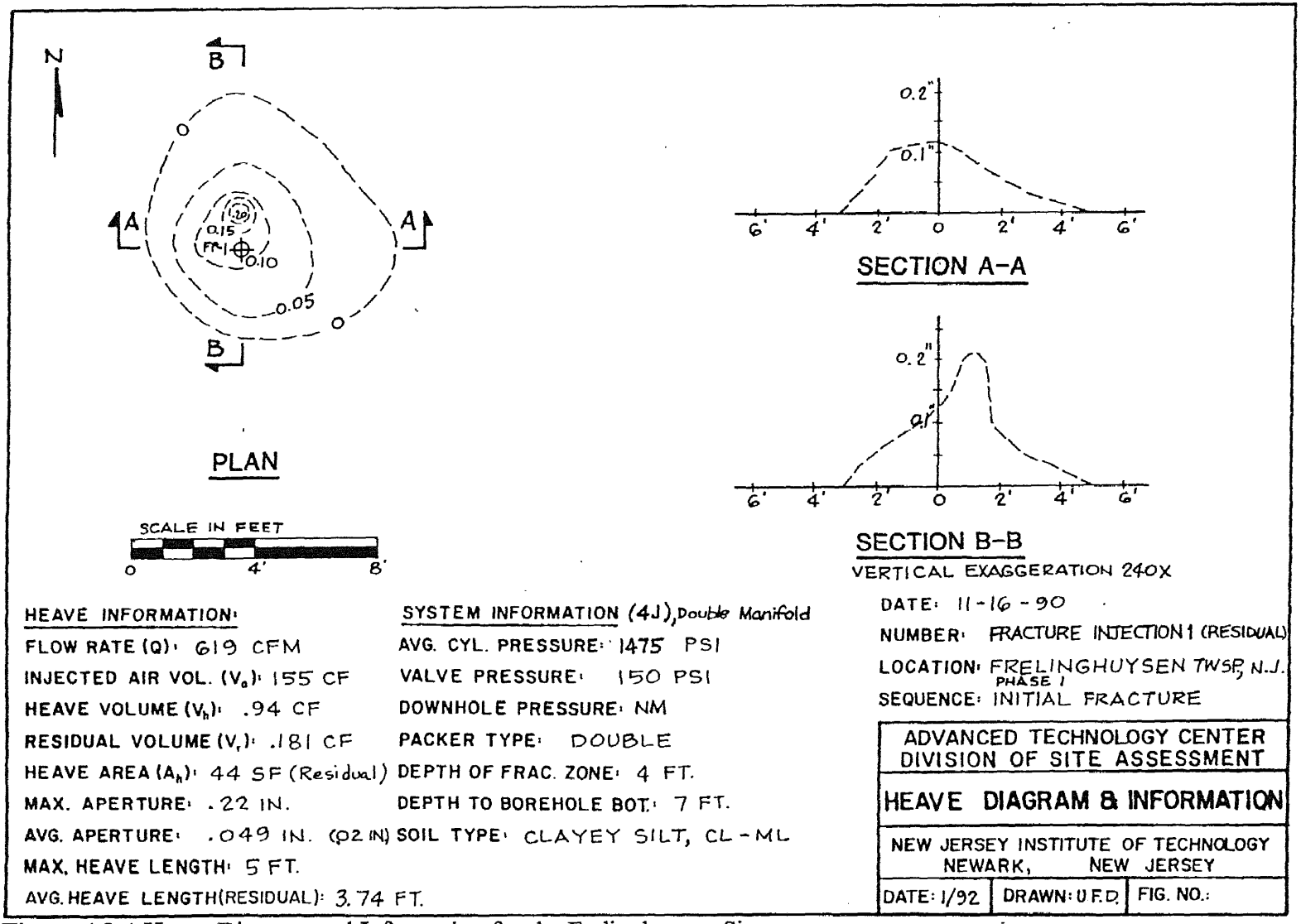

Figure A8-1 Heave Diagram and Information for the Frelinghuysen Site.

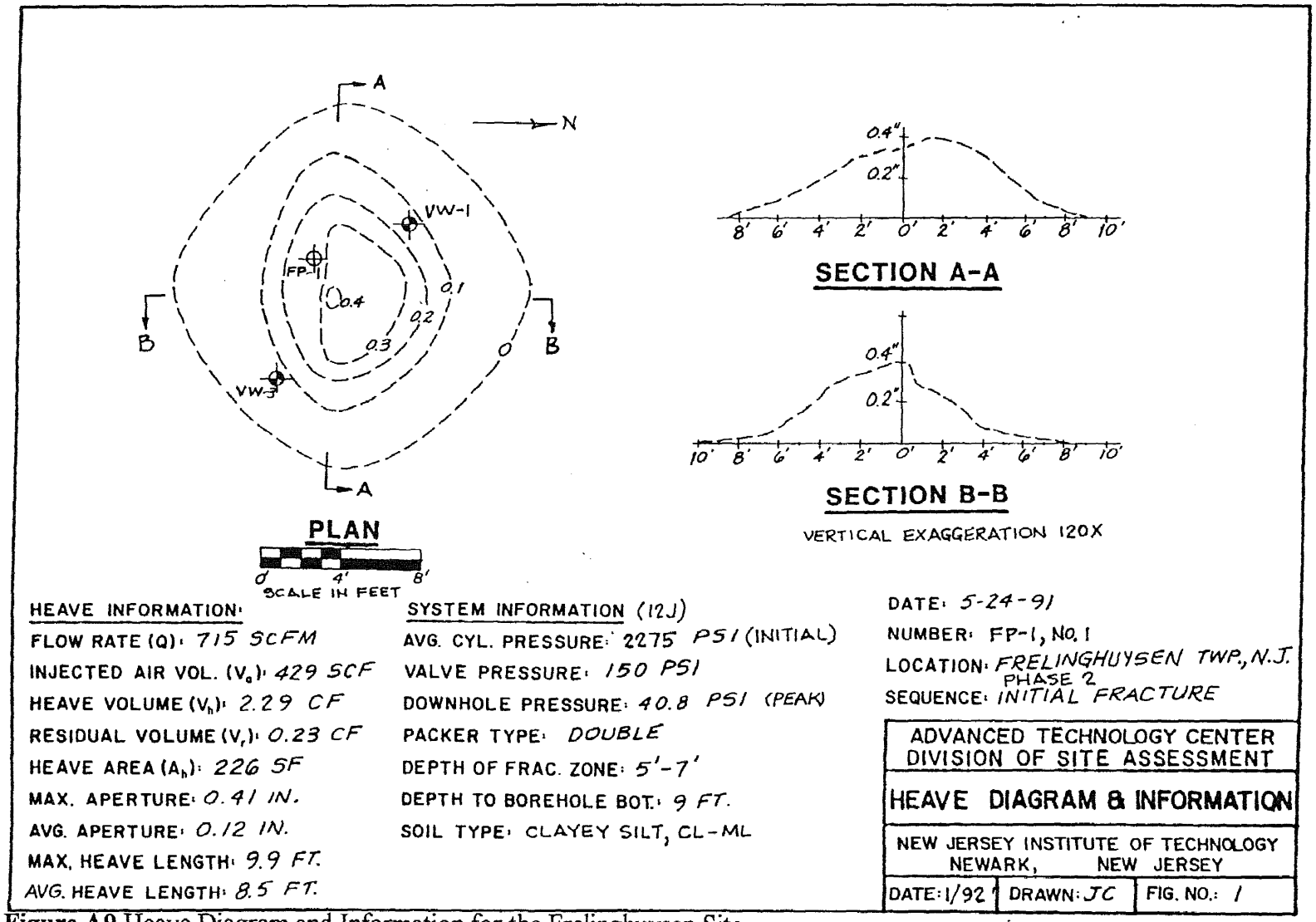

Figure A9 Heave Diagram and Information for the Frelinghuysen Site.

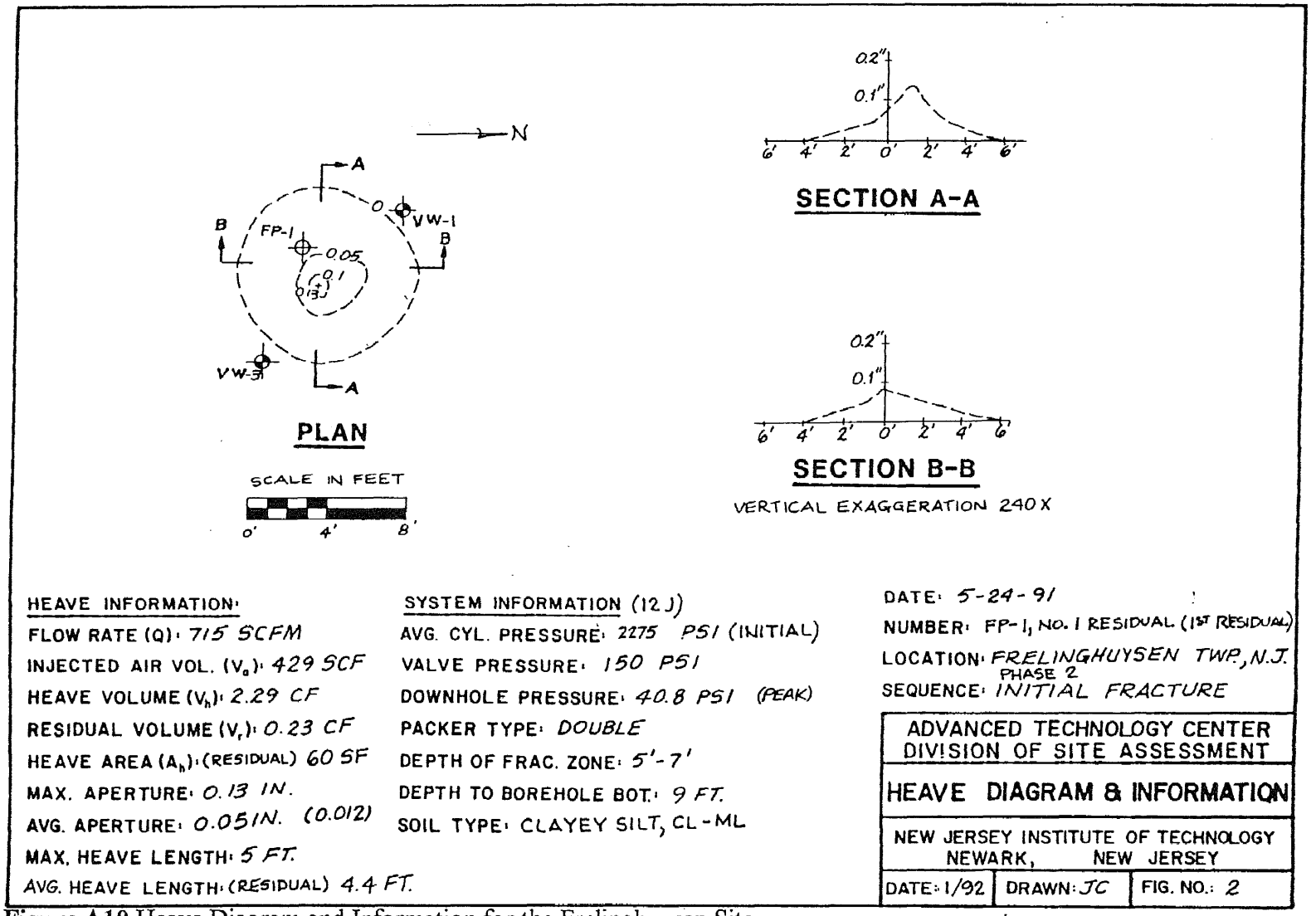

Figure A10 Heave Diagram and Information for the Frelinghuysen Site.

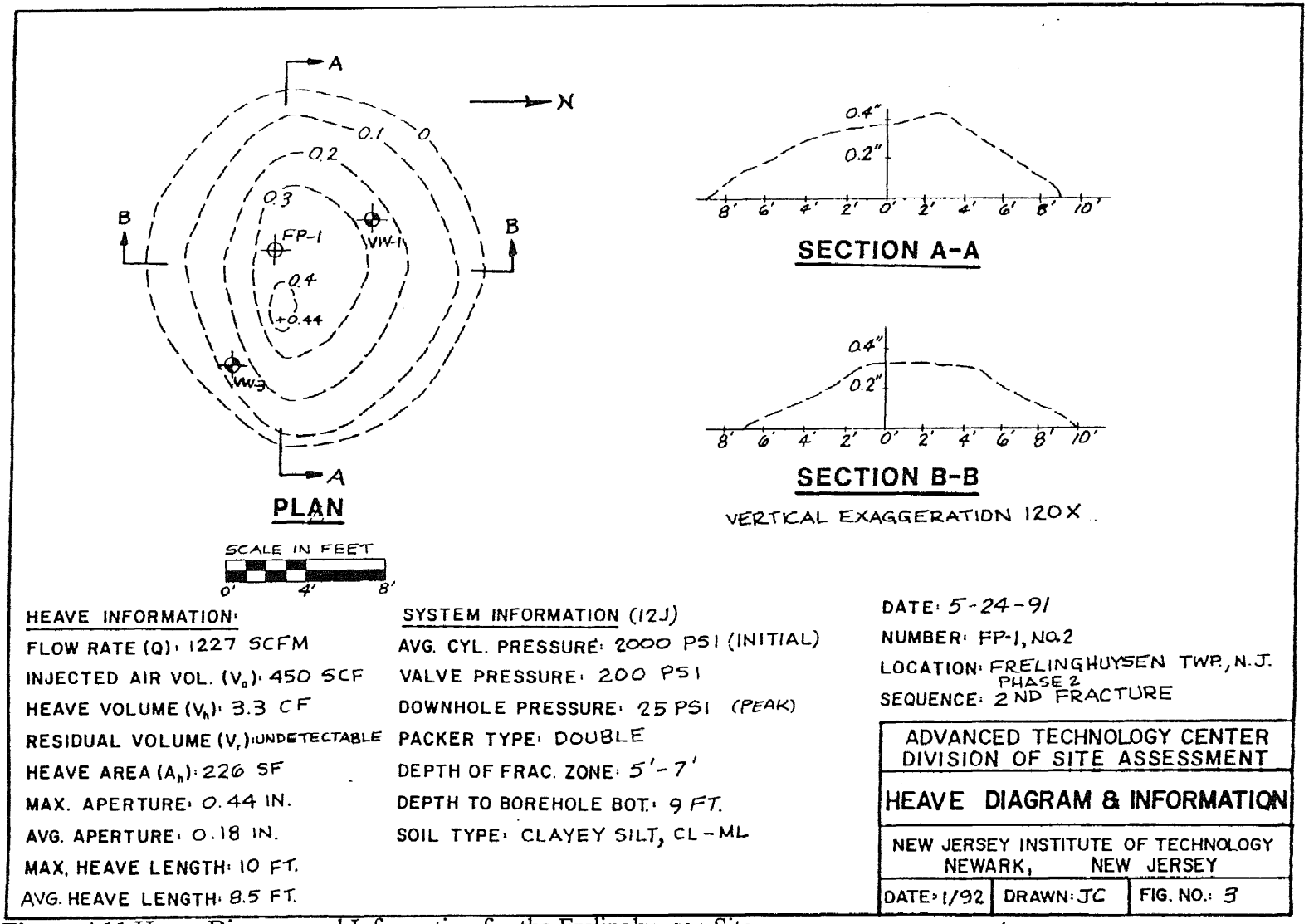

Figure A11 Heave Diagram and Information for the Frelinghuysen Site.

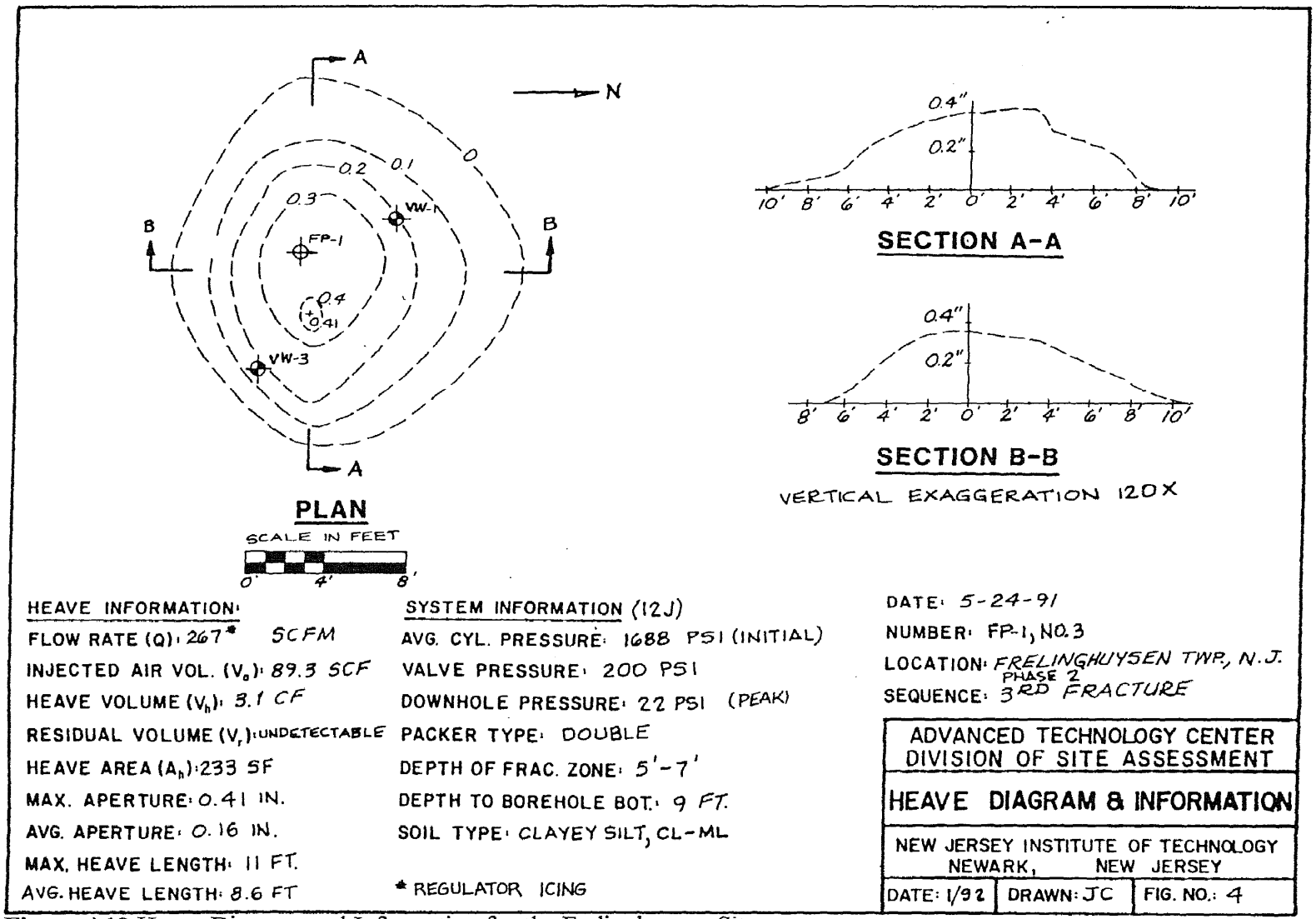

Figure A12 Heave Diagram and Information for the Frelinghuysen Site.

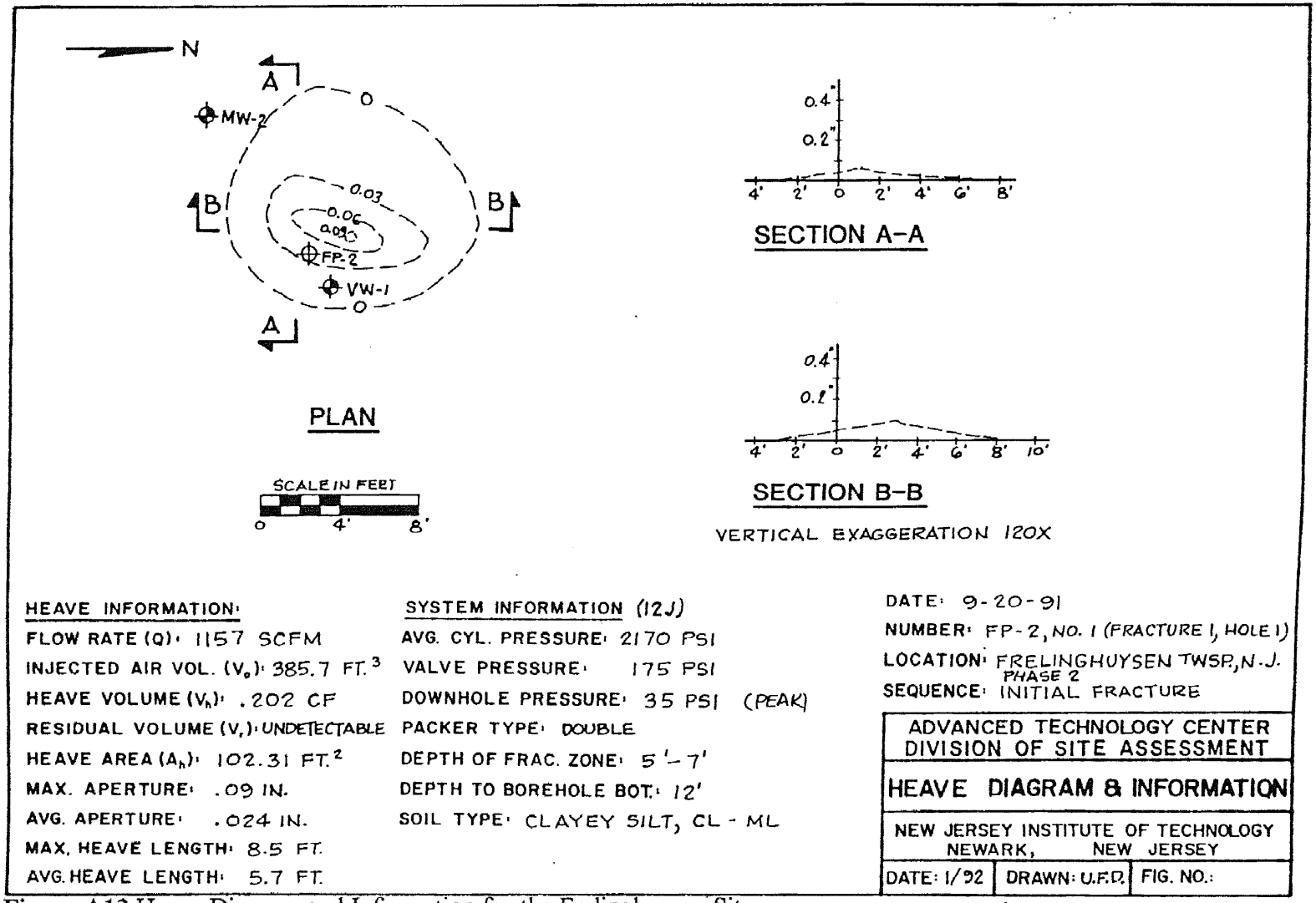

Figure A13 Heave Diagram and Information for the Frelinghuysen Site.

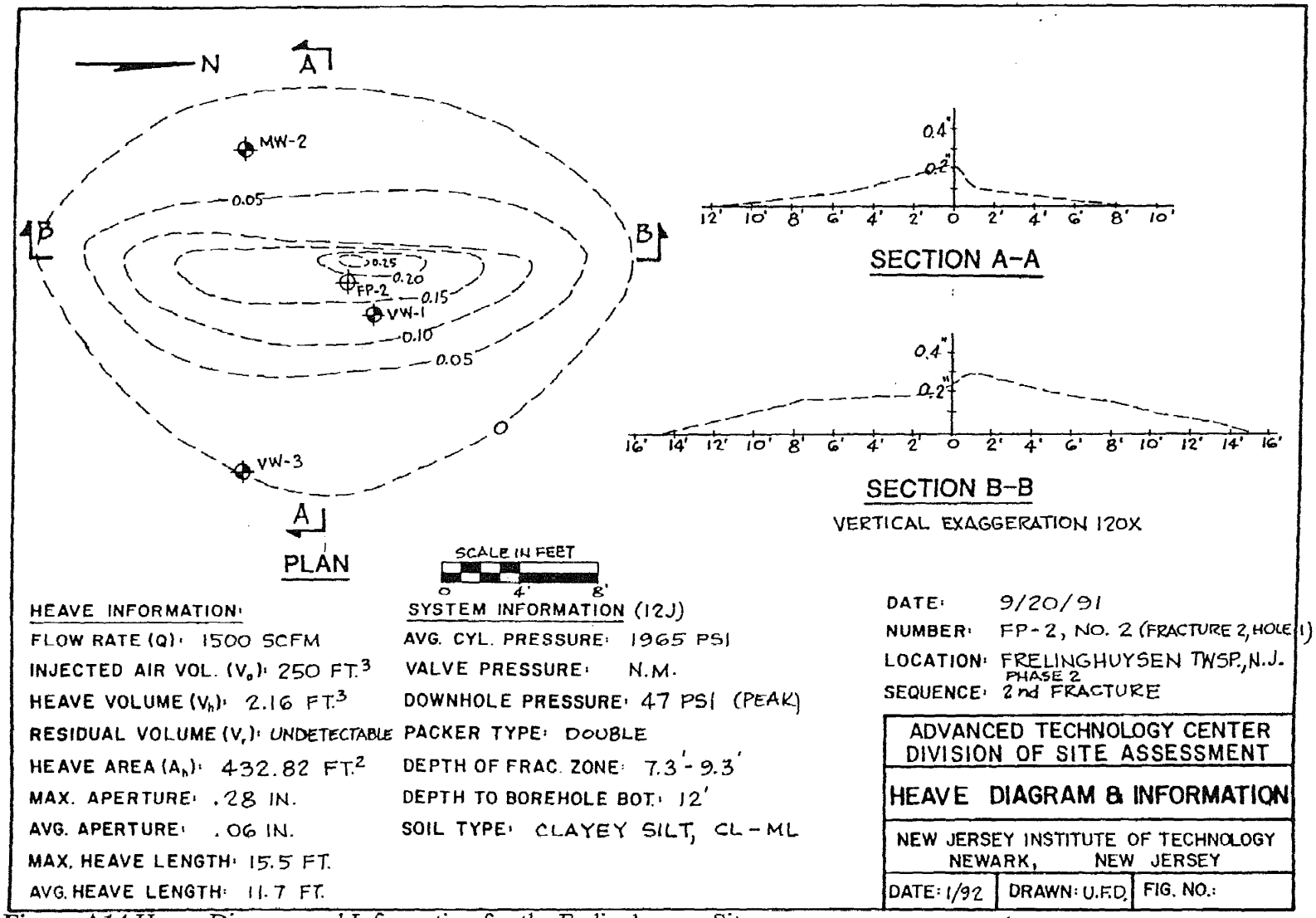

Figure A14 Heave Diagram and Information for the Frelinghuysen Site.

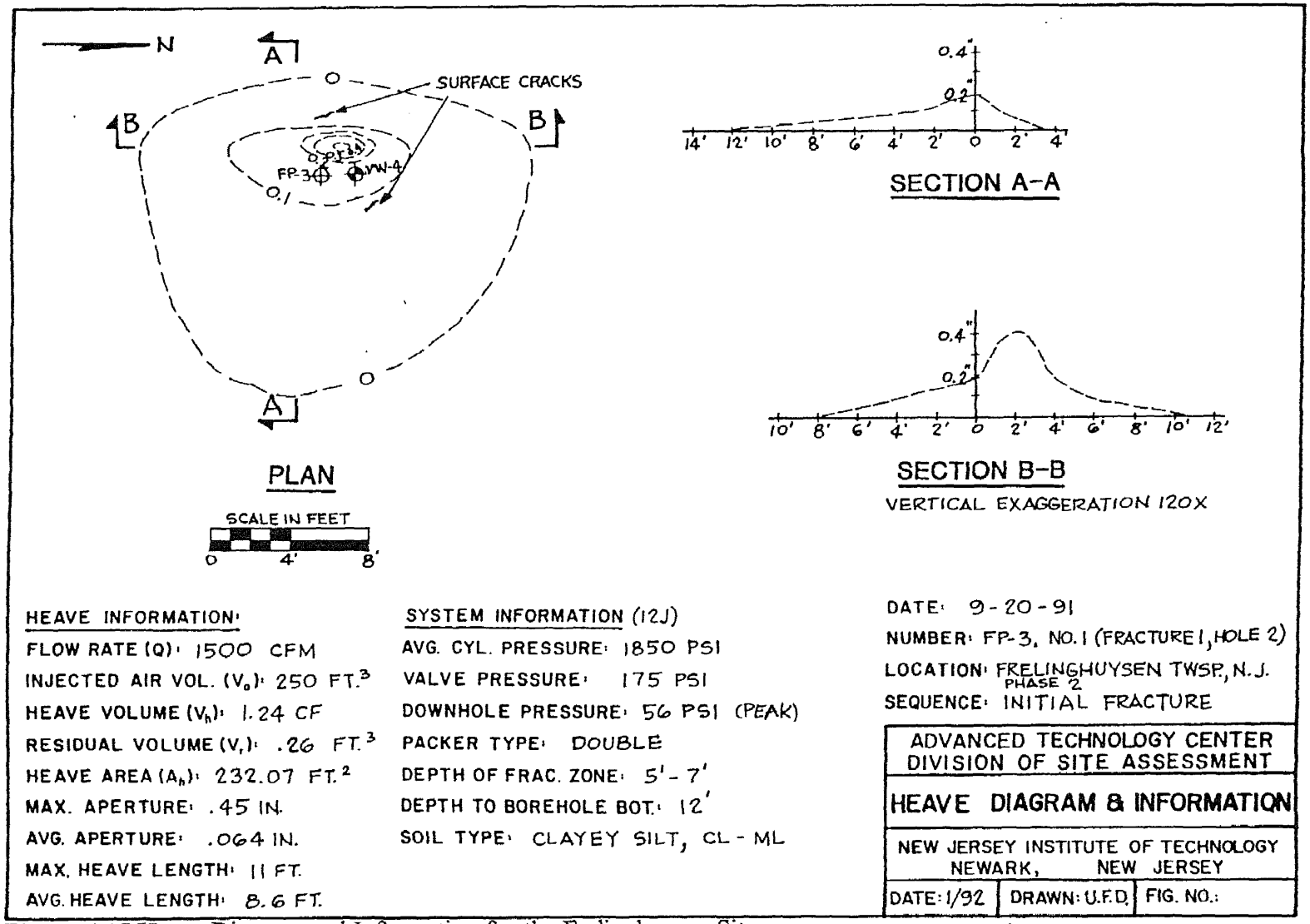

Figure A15 Heave Diagram and Information for the Frelinghuysen Site.

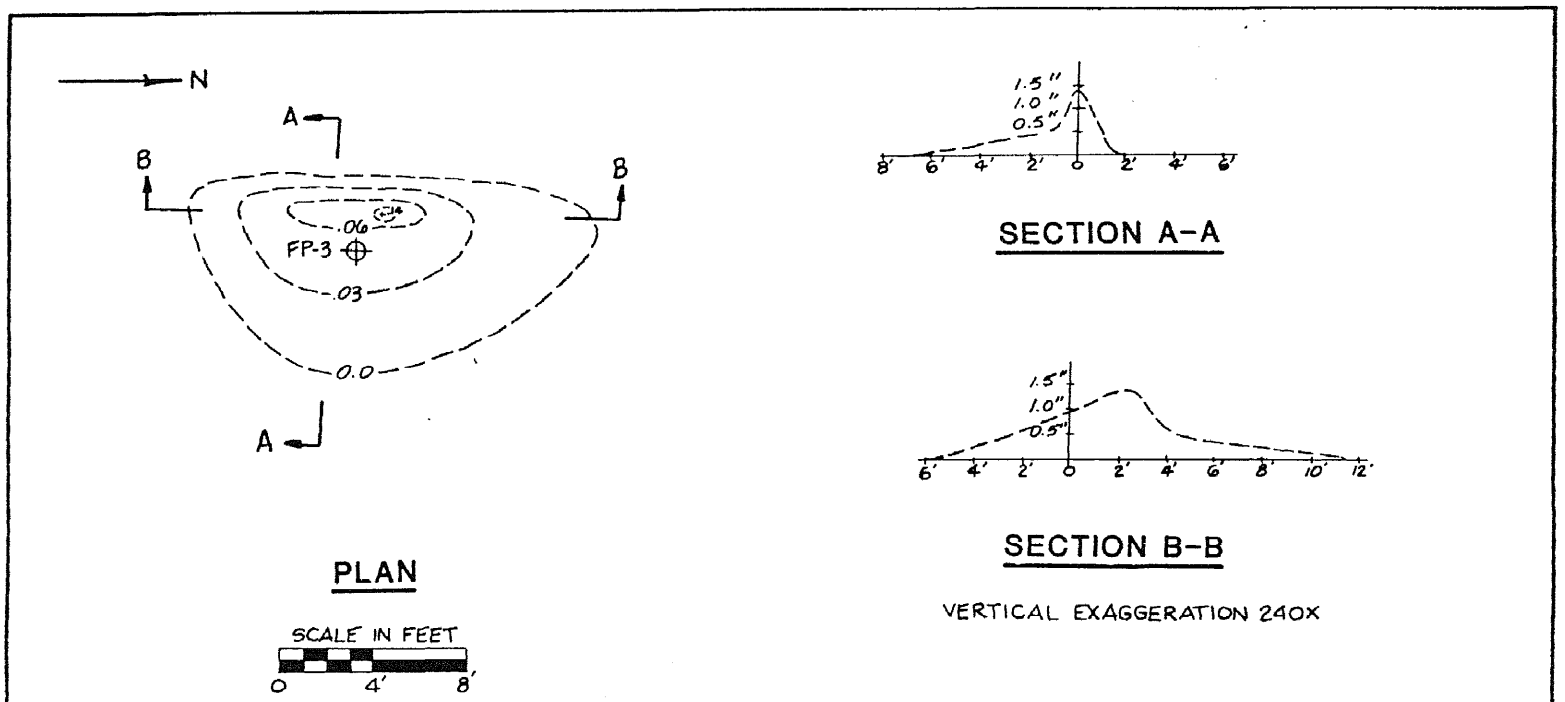

HEAVE INFORMATION:		SYSTEM INFORMATION (12 J)	
FLOW RATE (Q):	1500 SCFM	AVG. CYL. PRESSURE:	1850 PSI
INJECTED AIR VOL. (V_o):	250 CF	VALVE PRESSURE:	175 PSI
HEAVE VOLUME (V_h):	1.24 FT.^{3}	DOWNHOLE PRESSURE:	56 PSI
RESIDUAL VOLUME (V_r):	.26 FT.^{3}	PACKER TYPE:	DOUBLE
HEAVE AREA (A_h):	104.48 FT.^{2} (Residual)	DEPTH OF FRAC. ZONE:	5'-7'
MAX. APERTURE:	.14 IN.	DEPTH TO BOREHOLE BOT.:	12'
AVG. APERTURE:	.030 IN. (.013 IN.)	SOIL TYPE:	CLAYEY SILT, CL-ML
MAX. HEAVE LENGTH:	9.9 FT.		
AVG. HEAVE LENGTH:	5.8 FT. (Residual)		

DATE: 9-20-91 (RESIDUAL 1ST, HOLE 2)
NUMBER: FP-3, NO. 1 RESIDUAL
LOCATION: FRELINGHUYSEN TWP., N.J.
SEQUENCE: PHASE 2 INITIAL FRACTURE

ADVANCED TECHNOLOGY CENTER DIVISION OF SITE ASSESSMENT		
HEAVE DIAGRAM & INFORMATION		
NEW JERSEY INSTITUTE OF TECHNOLOGY NEWARK, NEW JERSEY		
DATE: 1/92	DRAWN: UFD	FIG. NO.:

Figure A16 Heave Diagram and Information for the Frelinghuysen Site.

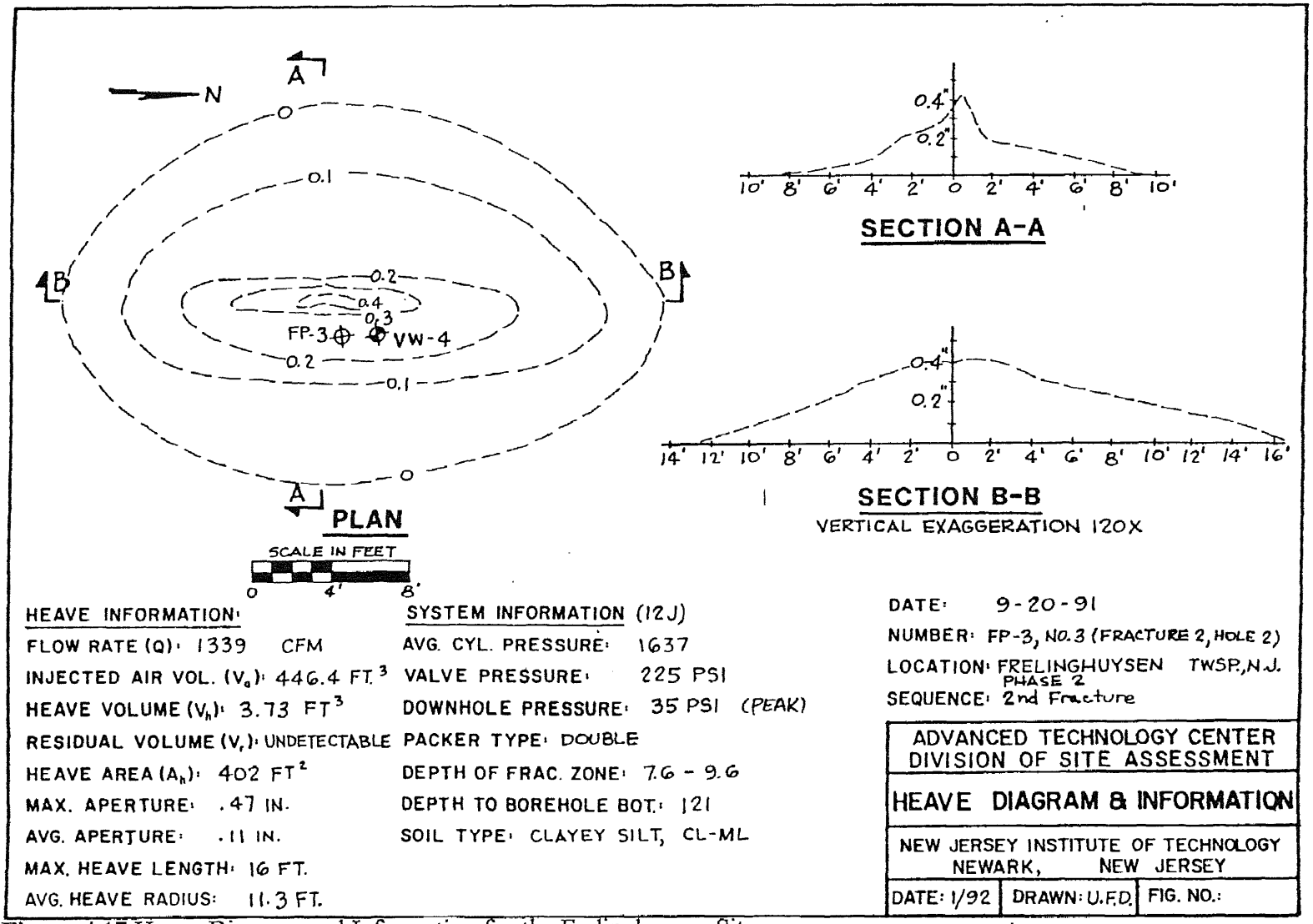

HEAVE INFORMATION:

FLOW RATE (Q): 1339 CFM
INJECTED AIR VOL. (V_a): 446.4 FT^3
HEAVE VOLUME (V_h): 3.73 FT^3
RESIDUAL VOLUME (V_r): UNDETECTABLE
HEAVE AREA (A_h): 402 FT^2
MAX. APERTURE: .47 IN.
AVG. APERTURE: .11 IN.
MAX. HEAVE LENGTH: 16 FT.
AVG. HEAVE RADIUS: 11.3 FT.

SYSTEM INFORMATION (12J)

AVG. CYL. PRESSURE: 1637
VALVE PRESSURE: 225 PSI
DOWNHOLE PRESSURE: 35 PSI (PEAK)
PACKER TYPE: DOUBLE
DEPTH OF FRAC. ZONE: 7.6 - 9.6
DEPTH TO BOREHOLE BOT.: 121
SOIL TYPE: CLAYEY SILT, CL-ML

DATE: 9-20-91
NUMBER: FP-3, No.3 (FRACTURE 2, HOLE 2)
LOCATION: FRELINGHUYSEN TWSP, N.J. PHASE 2
SEQUENCE: 2nd Fracture

ADVANCED TECHNOLOGY CENTER
DIVISION OF SITE ASSESSMENT

HEAVE DIAGRAM & INFORMATION

NEW JERSEY INSTITUTE OF TECHNOLOGY
NEWARK, NEW JERSEY

DATE: 1/92 | DRAWN: U.F.D. | FIG. NO.:

Figure A17 Heave Diagram and Information for the Frelinghuysen Site.

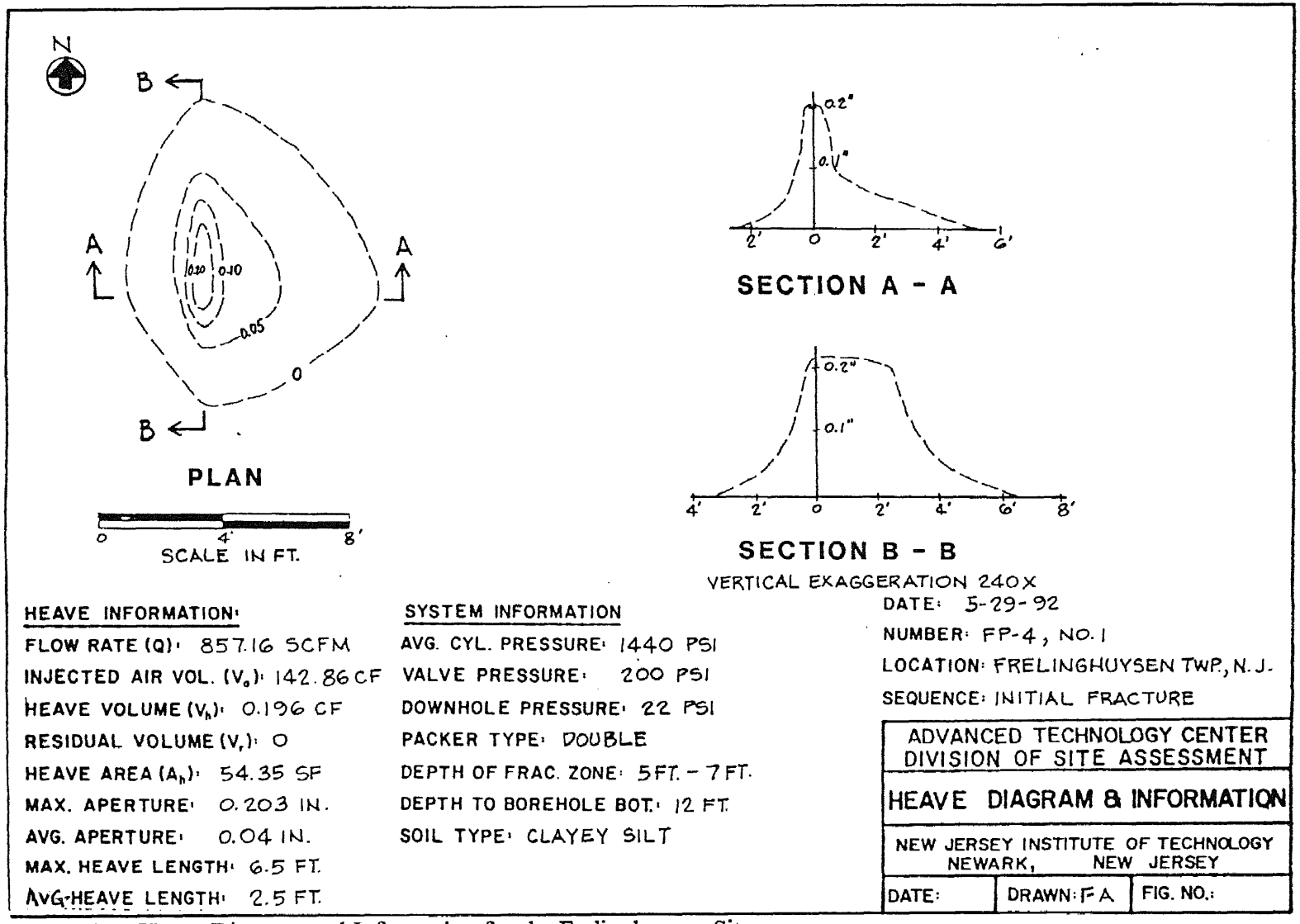

Figure A18 Heave Diagram and Information for the Frelinghuysen Site.

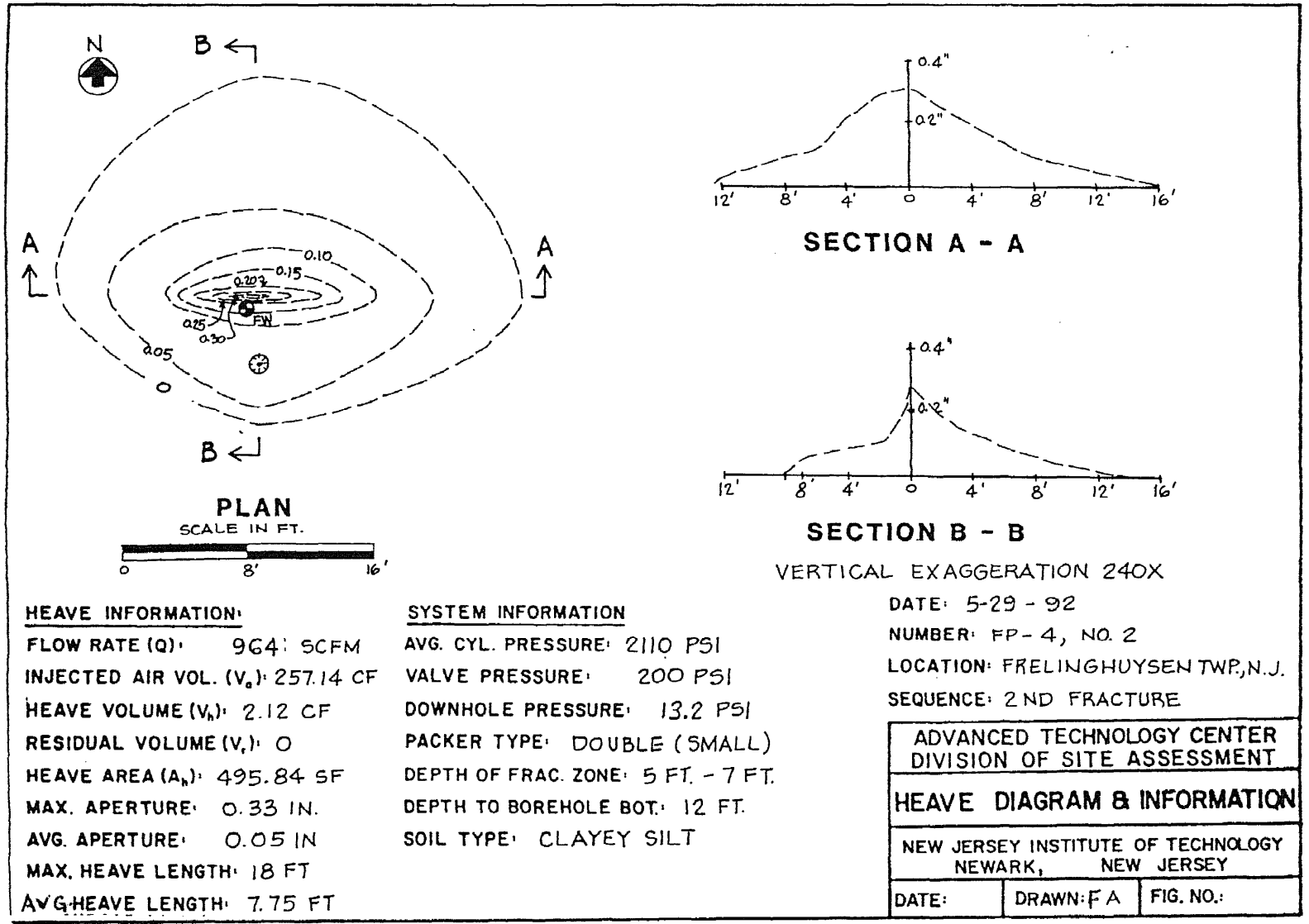

Figure A19 Heave Diagram and Information for the Frelinghuysen Site.

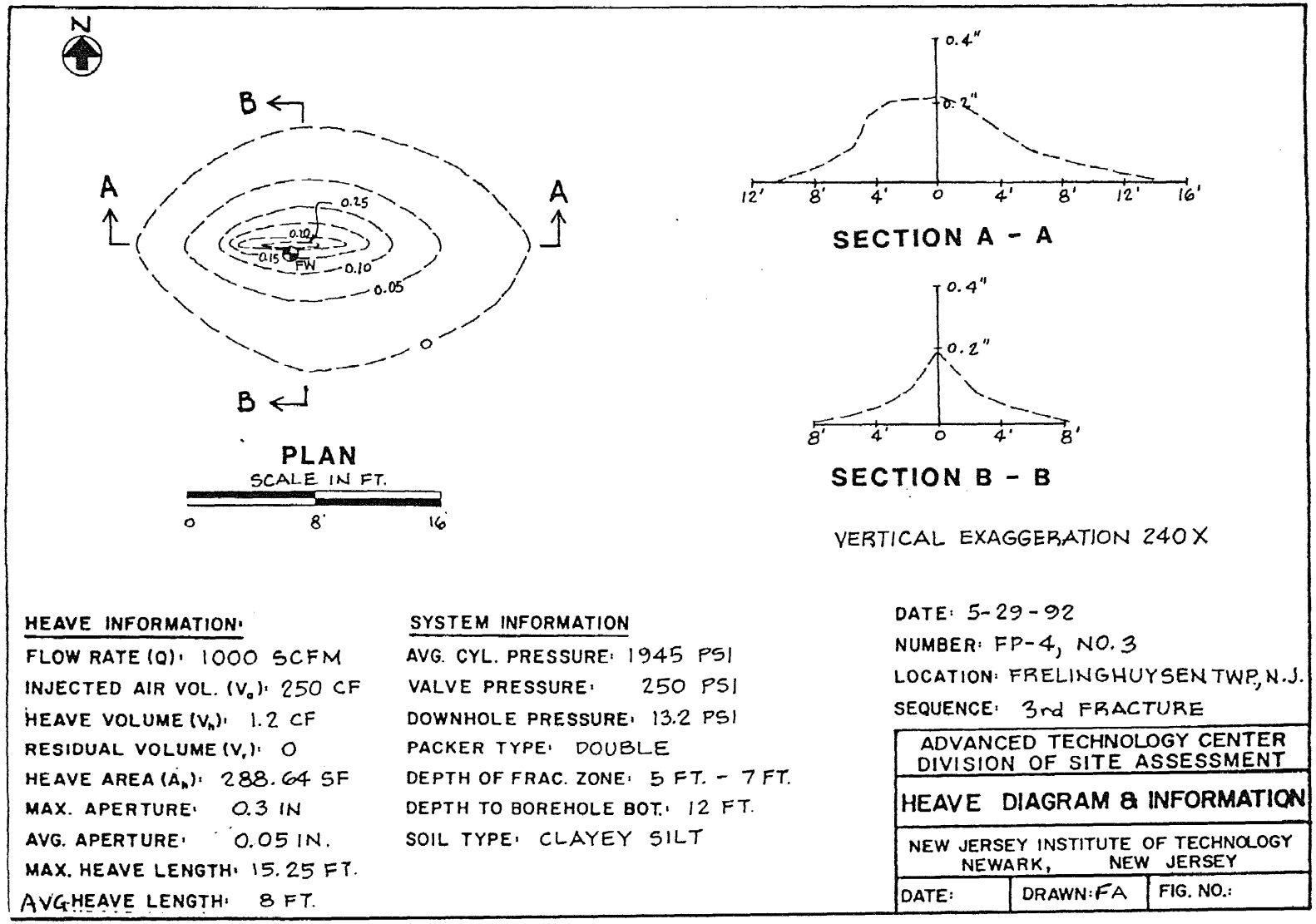

Figure A20 Heave Diagram and Information for the Frelinghuysen Site.

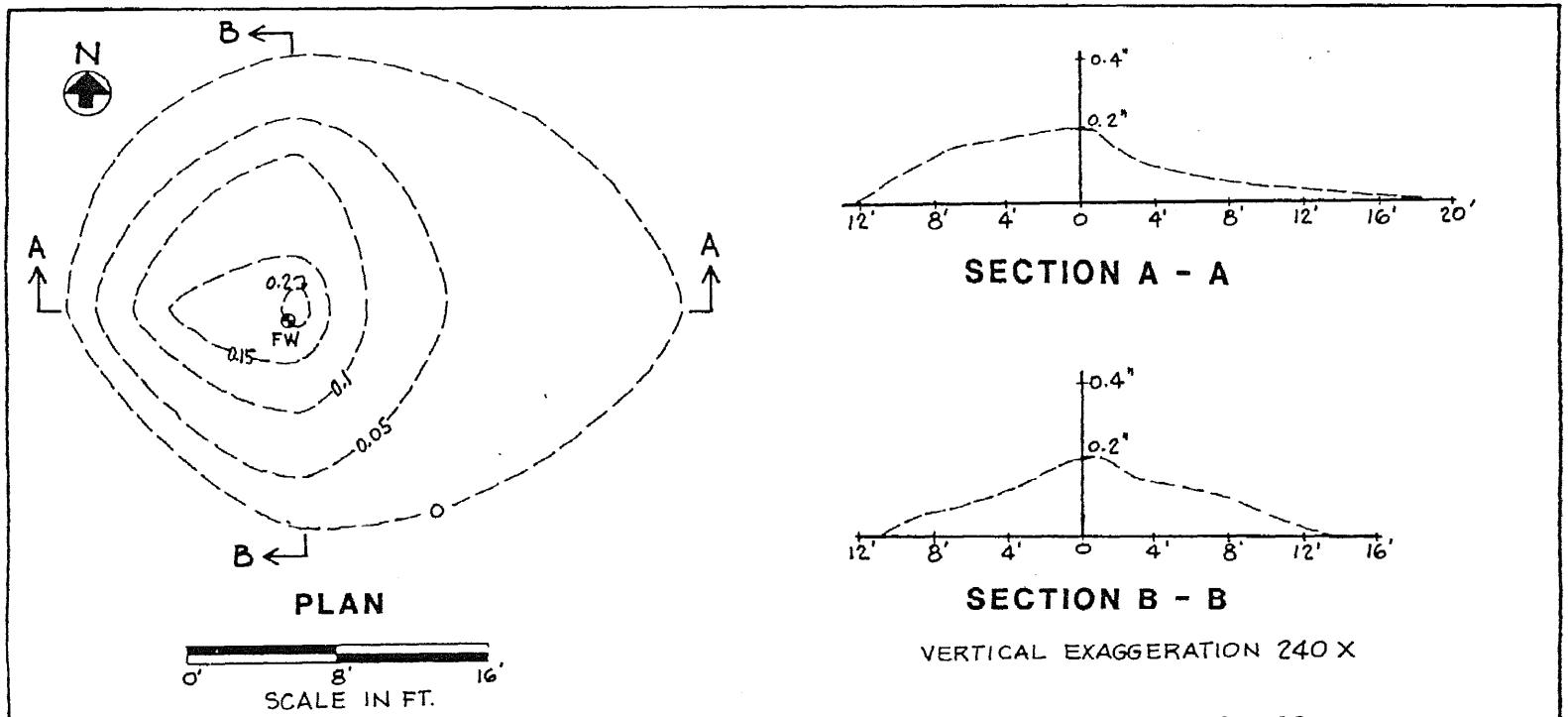

HEAVE INFORMATION:

FLOW RATE (Q): 943 SCFM
INJECTED AIR VOL. (V_a): 235.75
HEAVE VOLUME (V_h): 3.12 CF
RESIDUAL VOLUME (V_r): 0
HEAVE AREA (A_h): 624 SF
MAX. APERTURE: 0.22 IN.
AVG. APERTURE: 0.06 IN
MAX. HEAVE LENGTH: 21.3 FT
AVG HEAVE LENGTH: 11.2 FT

SYSTEM INFORMATION

AVG. CYL. PRESSURE: 1785 PSI
VALVE PRESSURE: 200 PSI
DOWNHOLE PRESSURE: 23.5 PSI
PACKER TYPE: DOUBLE
DEPTH OF FRAC. ZONE: 8 FT. - 10 FT.
DEPTH TO BOREHOLE BOT.: 12 FT.
SOIL TYPE: CLAYEY SILT

DATE: 5-29-92
NUMBER: FP-4, NO. 1
LOCATION: FRELINGHUYSEN TWP., N.J.
SEQUENCE: INITIAL FRACTURE

ADVANCED TECHNOLOGY CENTER
DIVISION OF SITE ASSESSMENT

HEAVE DIAGRAM & INFORMATION

NEW JERSEY INSTITUTE OF TECHNOLOGY
NEWARK, NEW JERSEY

DATE:	DRAWN: FA	FIG. NO.:

Figure A21 Heave Diagram and Information for the Frelinghuysen Site.

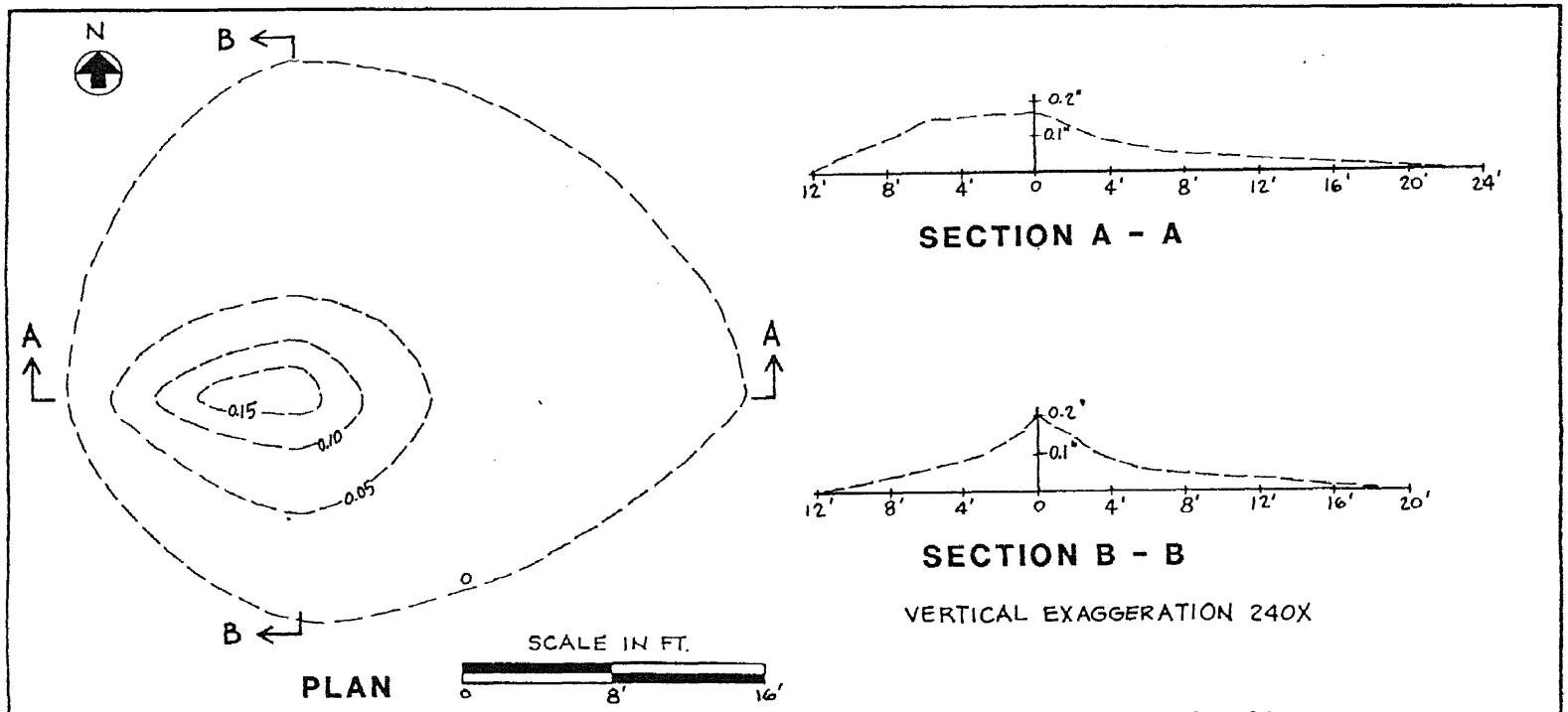

HEAVE INFORMATION:

FLOW RATE (Q): 1114.28 SCFM
INJECTED AIR VOL. (V_o): 278.51 CF
HEAVE VOLUME (V_h): 2.44 CF
RESIDUAL VOLUME (V_r): 0
HEAVE AREA (A_h): 812.59 SF
MAX. APERTURE: 0.18 IN.
AVG. APERTURE: 0.04 IN.
MAX. HEAVE LENGTH: 24 FT.
AVG. HEAVE LENGTH: 12.5 FT.

SYSTEM INFORMATION

AVG. CYL. PRESSURE: 1635 PSI
VALVE PRESSURE: 250 PSI
DOWNHOLE PRESSURE: 17 PSI
PACKER TYPE: DOUBLE
DEPTH OF FRAC. ZONE: 8 FT. - 10 FT.
DEPTH TO BOREHOLE BOT.: 12 FT.
SOIL TYPE: CLAYEY SILT

DATE: 5-29-92
NUMBER: FP-4, NO. 2
LOCATION: FRELINGHUYSEN TWP., N.J.
SEQUENCE: 2nd FRACTURE

ADVANCED TECHNOLOGY CENTER
DIVISION OF SITE ASSESSMENT

HEAVE DIAGRAM & INFORMATION

NEW JERSEY INSTITUTE OF TECHNOLOGY
NEWARK, NEW JERSEY

DATE:	DRAWN: FA	FIG. NO.:

Figure A22 Heave Diagram and Information for the Frelinghuysen Site.

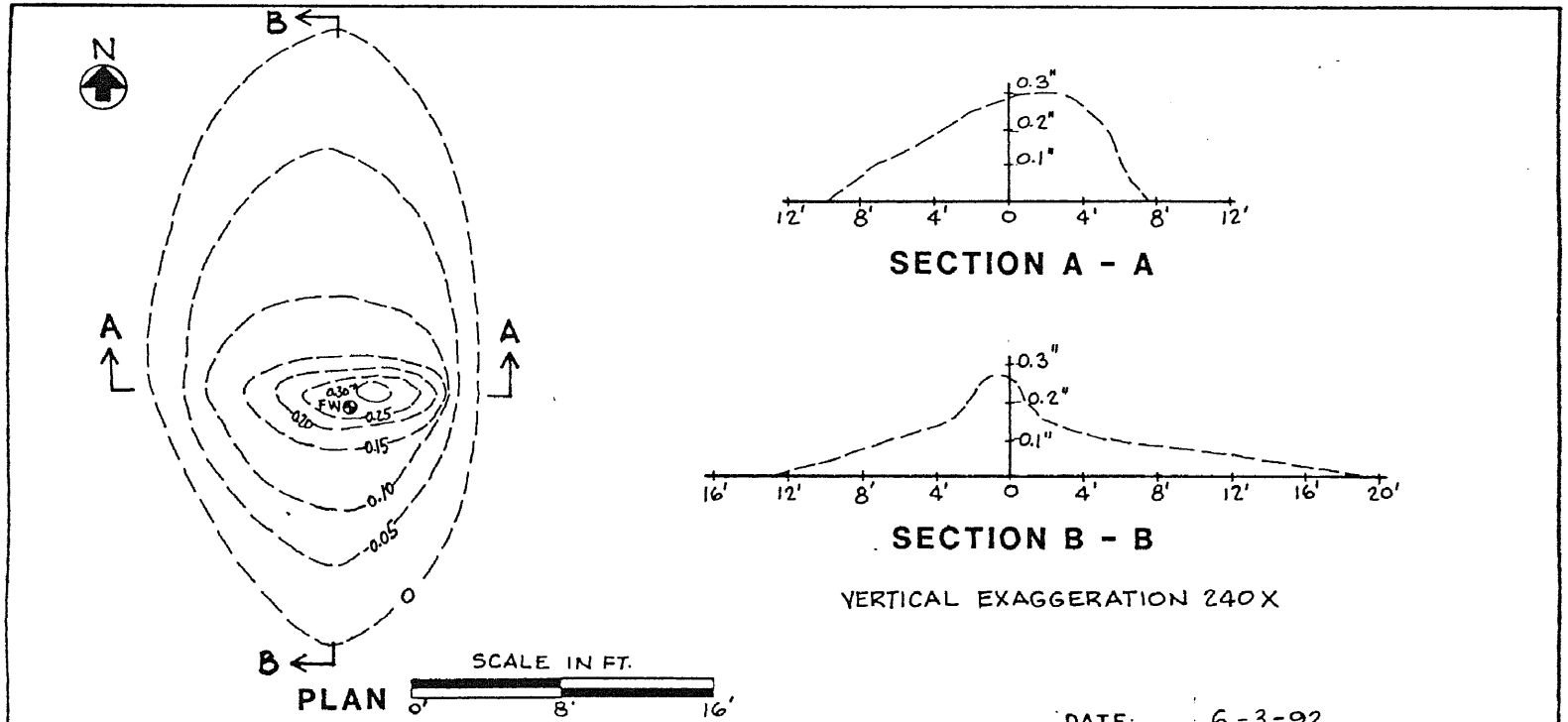

HEAVE INFORMATION:		SYSTEM INFORMATION	
FLOW RATE (Q):	722.3 SCFM	AVG. CYL. PRESSURE:	2315 PSI
INJECTED AIR VOL. (V_o):	192.84 CF	VALVE PRESSURE:	150 PSI
HEAVE VOLUME (V_h):	2.69 CF	DOWNHOLE PRESSURE:	19.5 PSI
RESIDUAL VOLUME (V_r):	0	PACKER TYPE:	DOUBLE (SMALL)
HEAVE AREA (A_h):	438.13 SF	DEPTH OF FRAC. ZONE:	5 FT. - 7 FT.
MAX. APERTURE:	0.33 IN.	DEPTH TO BOREHOLE BOT.:	12 FT.
AVG. APERTURE:	0.07 IN.	SOIL TYPE:	CLAYEY SILT
MAX. HEAVE LENGTH:	21 FT.		
AVG. HEAVE LENGTH:	7 FT.		

DATE: 6-3-92
NUMBER: FP-5, NO.1
LOCATION: FRELINGHUYSEN TWP, N.J.
SEQUENCE: INITIAL FRACTURE

ADVANCED TECHNOLOGY CENTER
DIVISION OF SITE ASSESSMENT

HEAVE DIAGRAM & INFORMATION

NEW JERSEY INSTITUTE OF TECHNOLOGY
NEWARK, NEW JERSEY

DATE:	DRAWN: FA	FIG. NO.:

Figure A23 Heave Diagram and Information for the Frelinghuysen Site.

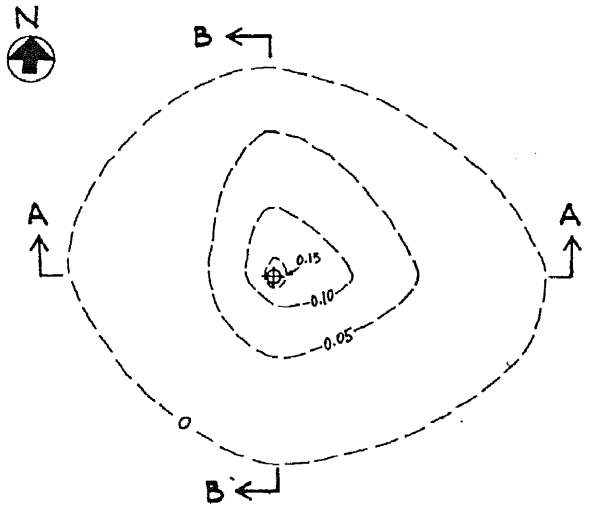

PLAN

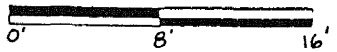

SCALE IN FT.

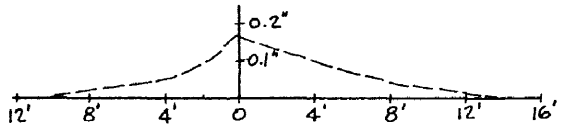

SECTION A - A

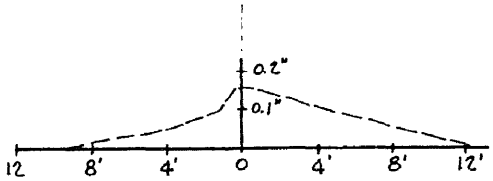

SECTION B - B

VERTICAL EXAGGERATION 240 X

HEAVE INFORMATION:		SYSTEM INFORMATION	
FLOW RATE (Q):	983.77 SCFM	AVG. CYL. PRESSURE:	1345 PSI
INJECTED AIR VOL. (V_o):	164.29 CF	VALVE PRESSURE:	250 PSI
HEAVE VOLUME (V_h):	1.34 CF	DOWNHOLE PRESSURE:	22 PSI
RESIDUAL VOLUME (V_r):	0	PACKER TYPE:	DOUBLE (SMALL)
HEAVE AREA (A_h):	405.87 SF	DEPTH OF FRAC. ZONE:	7 FT. 4 IN. – 9 FT. 4 IN.
MAX. APERTURE:	0.19 IN.	DEPTH TO BOREHOLE BOT.:	12 FT.
AVG. APERTURE:	0.04 IN.	SOIL TYPE:	CLAYEY SILT
MAX. HEAVE LENGTH:	14.5 FT		
AVG. HEAVE LENGTH:	10.25 FT		

DATE: 6 - 3 - 92
NUMBER: FP-5, NO. 2
LOCATION: FRELINGHUYSEN TWP., N.J.
SEQUENCE: 2nd FRACTURE

ADVANCED TECHNOLOGY CENTER DIVISION OF SITE ASSESSMENT		
HEAVE DIAGRAM & INFORMATION		
NEW JERSEY INSTITUTE OF TECHNOLOGY NEWARK, NEW JERSEY		
DATE:	DRAWN: FA	FIG. NO.:

Figure A24 Heave Diagram and Information for the Frelinghuysen Site.

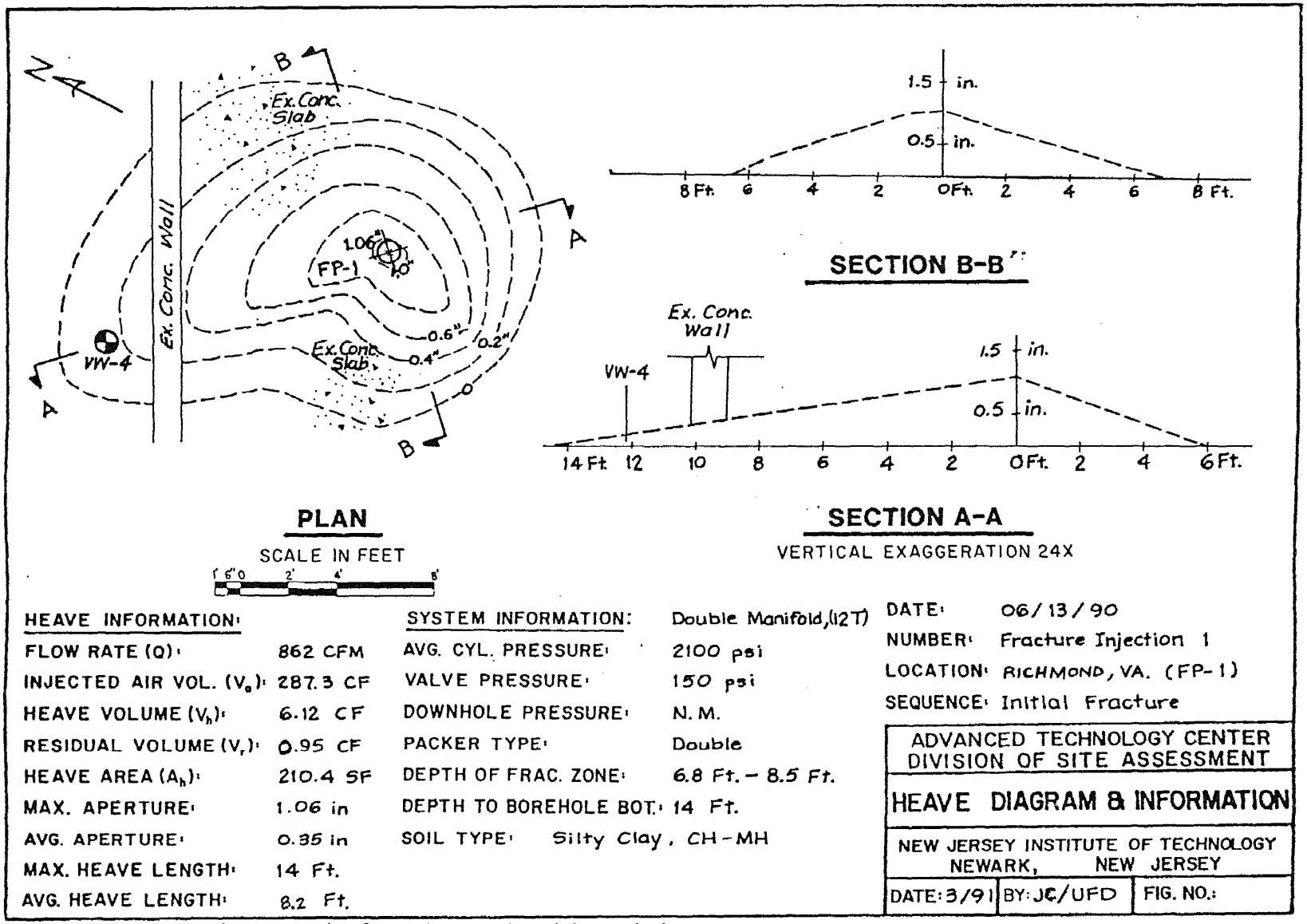

Figure A25 Heave Diagram and Information for the Richmond Site.

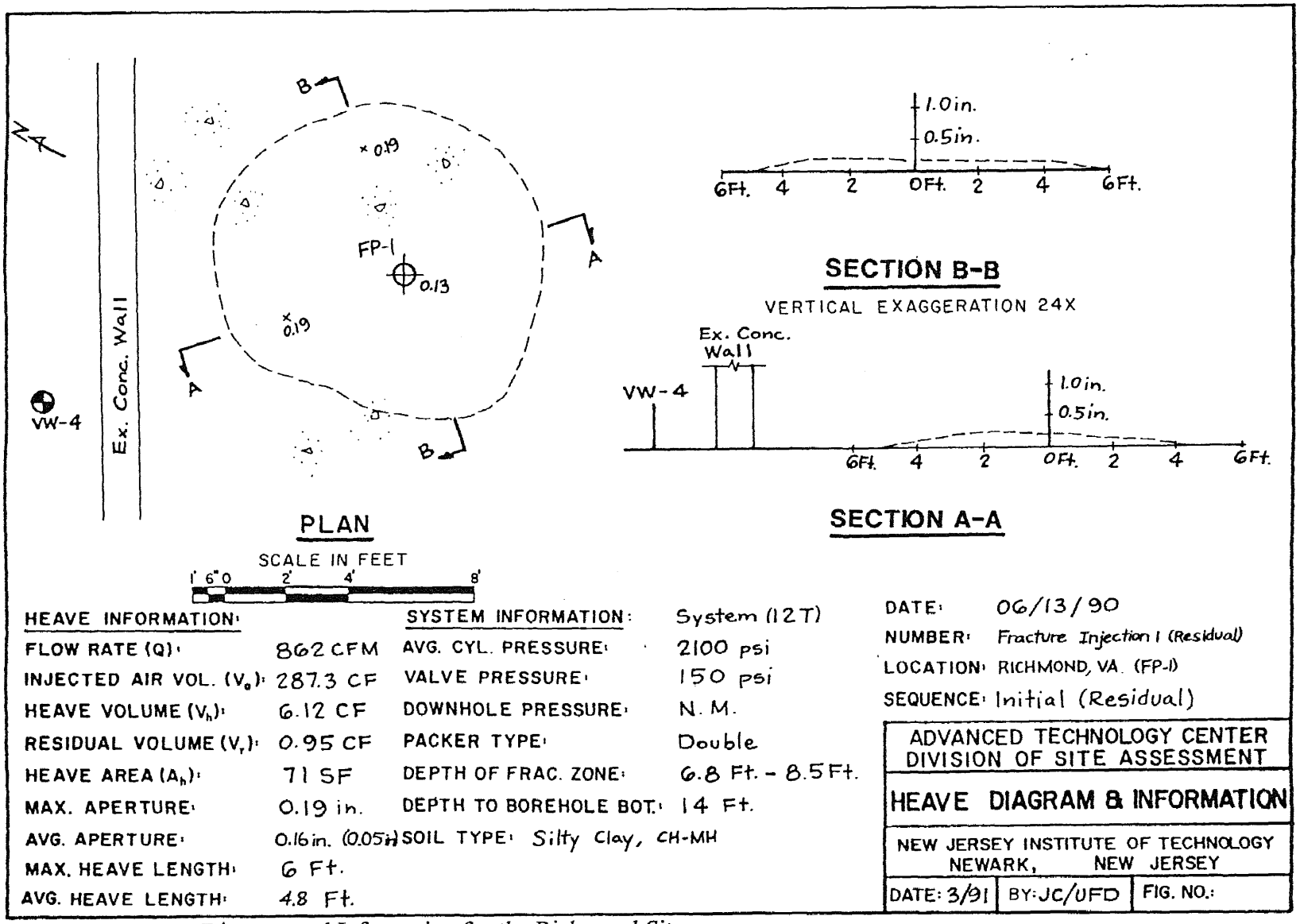

HEAVE INFORMATION:		SYSTEM INFORMATION:	
FLOW RATE (Q):	862 CFM	AVG. CYL. PRESSURE:	2100 psi
INJECTED AIR VOL. (V_o):	287.3 CF	VALVE PRESSURE:	150 psi
HEAVE VOLUME (V_h):	6.12 CF	DOWNHOLE PRESSURE:	N. M.
RESIDUAL VOLUME (V_r):	0.95 CF	PACKER TYPE:	Double
HEAVE AREA (A_h):	71 SF	DEPTH OF FRAC. ZONE:	6.8 Ft. - 8.5 Ft.
MAX. APERTURE:	0.19 in.	DEPTH TO BOREHOLE BOT.:	14 Ft.
AVG. APERTURE:	0.16 in. (0.05 in)	SOIL TYPE:	Silty Clay, CH-MH
MAX. HEAVE LENGTH:	6 Ft.		
AVG. HEAVE LENGTH:	4.8 Ft.		

DATE: 06/13/90
NUMBER: Fracture Injection 1 (Residual)
LOCATION: RICHMOND, VA. (FP-1)
SEQUENCE: Initial (Residual)

ADVANCED TECHNOLOGY CENTER
DIVISION OF SITE ASSESSMENT

HEAVE DIAGRAM & INFORMATION

NEW JERSEY INSTITUTE OF TECHNOLOGY
NEWARK, NEW JERSEY

DATE: 3/91 | BY: JC/UFD | FIG. NO.:

Figure A26 Heave Diagram and Information for the Richmond Site.

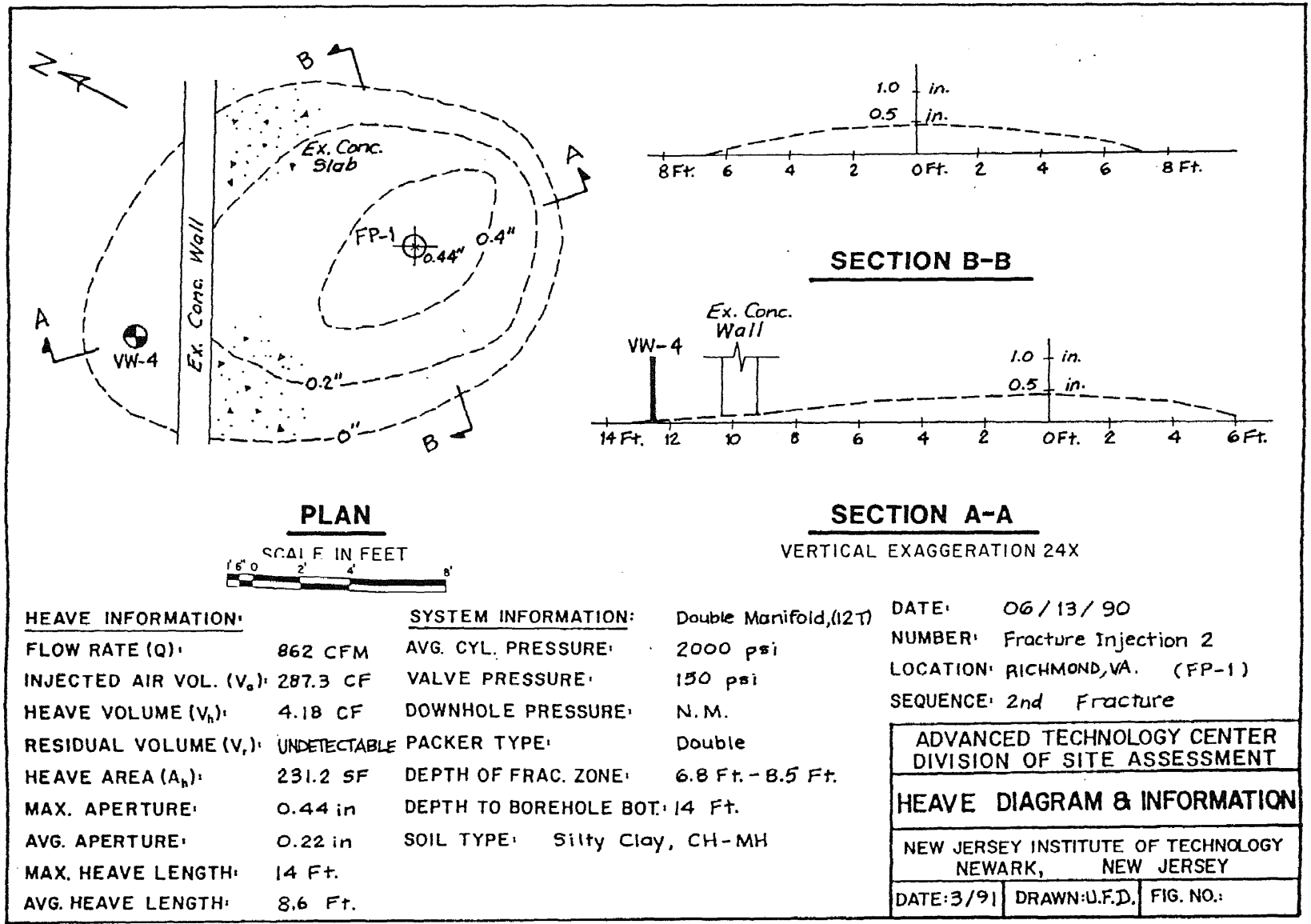

HEAVE INFORMATION:		SYSTEM INFORMATION:	Double Manifold,(12T)
FLOW RATE (Q):	862 CFM	AVG. CYL. PRESSURE:	2000 psi
INJECTED AIR VOL. (V_a):	287.3 CF	VALVE PRESSURE:	150 psi
HEAVE VOLUME (V_h):	4.18 CF	DOWNHOLE PRESSURE:	N.M.
RESIDUAL VOLUME (V_r):	UNDETECTABLE	PACKER TYPE:	Double
HEAVE AREA (A_h):	231.2 SF	DEPTH OF FRAC. ZONE:	6.8 Ft. - 8.5 Ft.
MAX. APERTURE:	0.44 in	DEPTH TO BOREHOLE BOT.:	14 Ft.
AVG. APERTURE:	0.22 in	SOIL TYPE:	Silty Clay, CH-MH
MAX. HEAVE LENGTH:	14 Ft.		
AVG. HEAVE LENGTH:	8.6 Ft.		

DATE: 06/13/90
NUMBER: Fracture Injection 2
LOCATION: RICHMOND, VA. (FP-1)
SEQUENCE: 2nd Fracture

ADVANCED TECHNOLOGY CENTER
DIVISION OF SITE ASSESSMENT

HEAVE DIAGRAM & INFORMATION

NEW JERSEY INSTITUTE OF TECHNOLOGY
NEWARK, NEW JERSEY

DATE: 3/91 | DRAWN: U.F.D. | FIG. NO.:

Figure A27 Heave Diagram and Information for the Richmond Site.

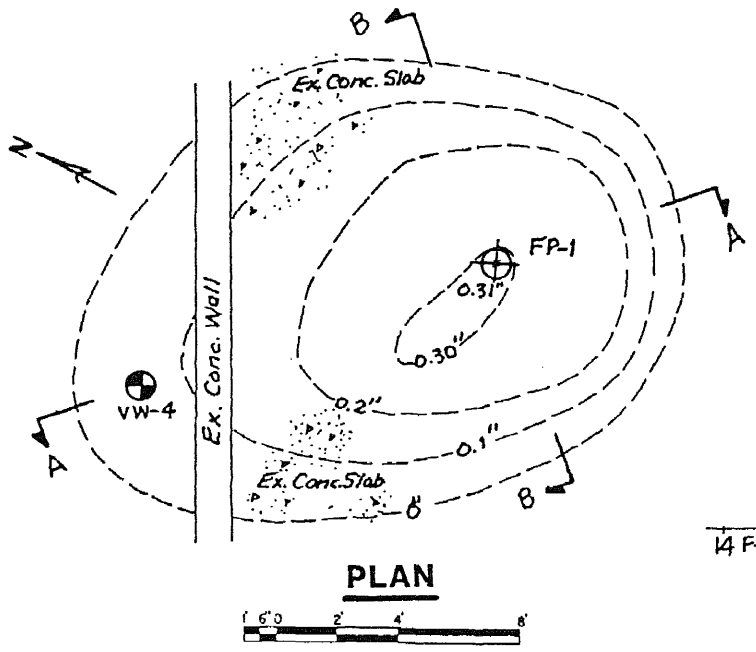

PLAN

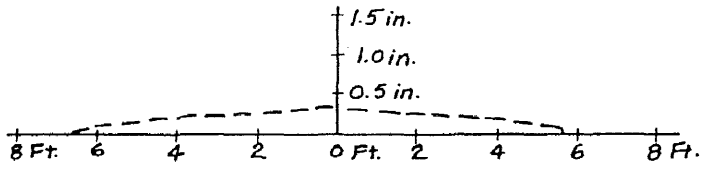

SECTION B-B

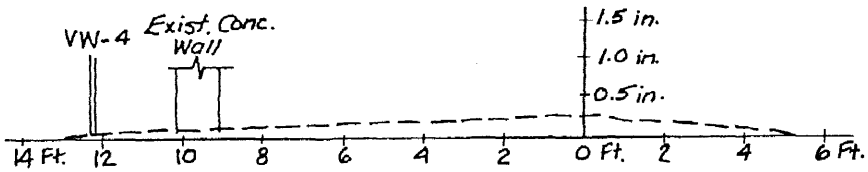

SECTION A-A

HEAVE INFORMATION:		SYSTEM INFORMATION: Double Manifold, (12T)	
FLOW RATE (Q):	862 CFM	AVG. CYL. PRESSURE:	1400 psi
INJECTED AIR VOL. (V_a):	287.3 CF	VALVE PRESSURE:	150 psi
HEAVE VOLUME (V_h):	2.75 CF	DOWNHOLE PRESSURE:	N.M.
RESIDUAL VOLUME (V_r):	UNDETECTABLE	PACKER TYPE:	Double
HEAVE AREA (A_h):	231.2 SF	DEPTH OF FRAC. ZONE:	6.8 Ft. - 8.5 Ft.
MAX. APERTURE:	0.31 in	DEPTH TO BOREHOLE BOT.:	14 Ft.
AVG. APERTURE:	0.14 in	SOIL TYPE:	Silty Clay, CH-MH
MAX. HEAVE LENGTH:	14 Ft.		
AVG. HEAVE LENGTH:	8.6 Ft.		

DATE: 06/14/90
NUMBER: Fracture Injection 5
LOCATION: RICHMOND, VA. (FP-1)
SEQUENCE: 3rd Fracture

ADVANCED TECHNOLOGY CENTER
DIVISION OF SITE ASSESSMENT

HEAVE DIAGRAM & INFORMATION

NEW JERSEY INSTITUTE OF TECHNOLOGY
NEWARK, NEW JERSEY

DATE: 3/91 | BY: JC/U.F.D. | FIG. NO.:

Figure A28 Heave Diagram and Information for the Richmond Site.

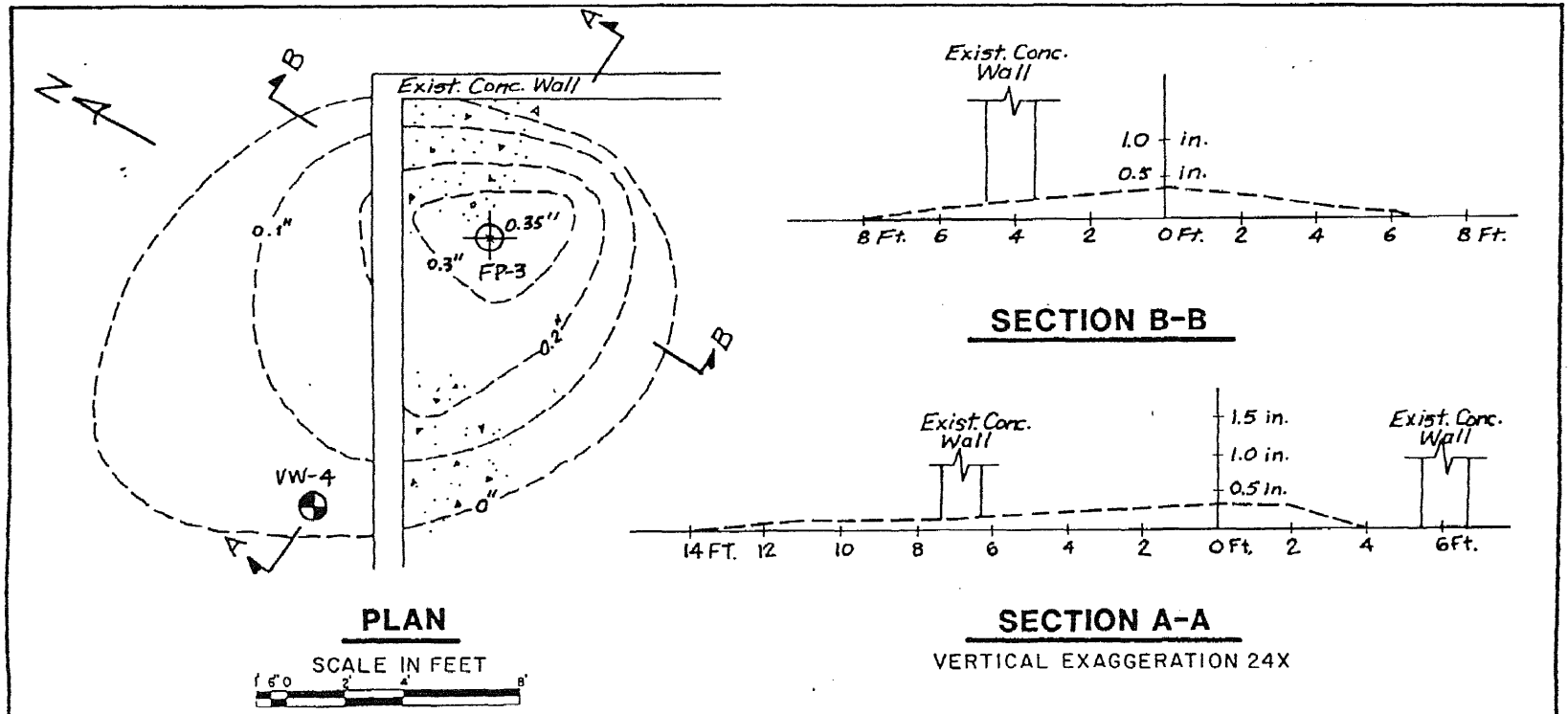

HEAVE INFORMATION:		SYSTEM INFORMATION:	Double Manifold, (12T)
FLOW RATE (Q):	862 CFM	AVG. CYL. PRESSURE:	1200 psi
INJECTED AIR VOL. (V_o):	287.3 CF	VALVE PRESSURE:	150 psi
HEAVE VOLUME (V_h):	2.45 CF	DOWNHOLE PRESSURE:	N.M.
RESIDUAL VOLUME (V_r):	N.M.	PACKER TYPE:	Double
HEAVE AREA (A_h):	231.2 SF	DEPTH OF FRAC. ZONE:	7.1 Ft. – 8.8 Ft.
MAX. APERTURE:	0.38 in	DEPTH TO BOREHOLE BOT.:	14 Ft.
AVG. APERTURE:	0.13 in	SOIL TYPE:	Silty Clay, CH - MH
MAX. HEAVE LENGTH:	14 Ft.		
AVG. HEAVE LENGTH:	8.6 Ft.		

DATE: 06/14/90
NUMBER: Fracture Injection 6
LOCATION: RICHMOND, VA. (FP-3)
SEQUENCE: Initial Fracture

ADVANCED TECHNOLOGY CENTER
DIVISION OF SITE ASSESSMENT

HEAVE DIAGRAM & INFORMATION

NEW JERSEY INSTITUTE OF TECHNOLOGY
NEWARK, NEW JERSEY

DATE: 3/91	BY: JC/UFD	FIG. NO.:

Figure A29 Heave Diagram and Information for the Richmond Site.

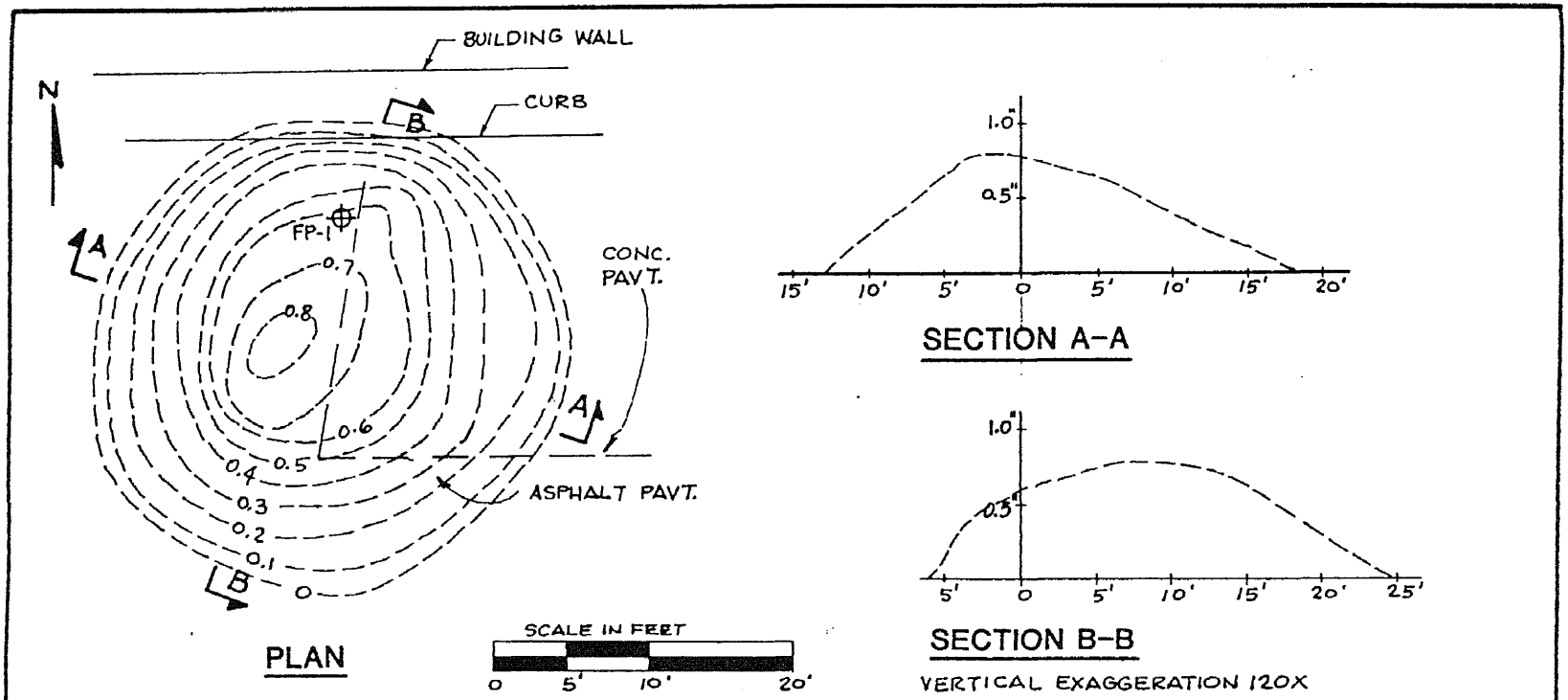

HEAVE INFORMATION:

FLOW RATE (Q):	1018 SCFM
INJECTED AIR VOL. (V_a):	339 SCF
HEAVE VOLUME (V_h):	23.7 CF
RESIDUAL VOLUME (V_r):	3.55 CF
HEAVE AREA (A_h):	821 SF
MAX. APERTURE:	0.86 IN.
AVG. APERTURE:	0.35 IN.
MAX. HEAVE LENGTH:	25 FT.
AVG. HEAVE LENGTH:	16 FT.

SYSTEM INFORMATION (12J)

AVG. CYL. PRESSURE:	2388 PSI
VALVE PRESSURE:	150 PSI
DOWNHOLE PRESSURE:	N/A
PACKER TYPE:	DOUBLE
DEPTH OF FRAC. ZONE:	4-6 FT.
DEPTH TO BOREHOLE BOT.:	9 FT.
SOIL TYPE:	CLAYEY SAND, SC

DATE: 7-23-91
NUMBER: FP-1, NO. 1 (1ST)
LOCATION: ROSELAND, N.J.
SEQUENCE: INITIAL FRACTURE

ADVANCED TECHNOLOGY CENTER
DIVISION OF SITE ASSESSMENT

HEAVE DIAGRAM & INFORMATION

NEW JERSEY INSTITUTE OF TECHNOLOGY
NEWARK, NEW JERSEY

DATE: 1/92	DRAWN: U.E.D.	FIG. NO.:

Figure A30 Heave Diagram and Information for the Roseland Site.

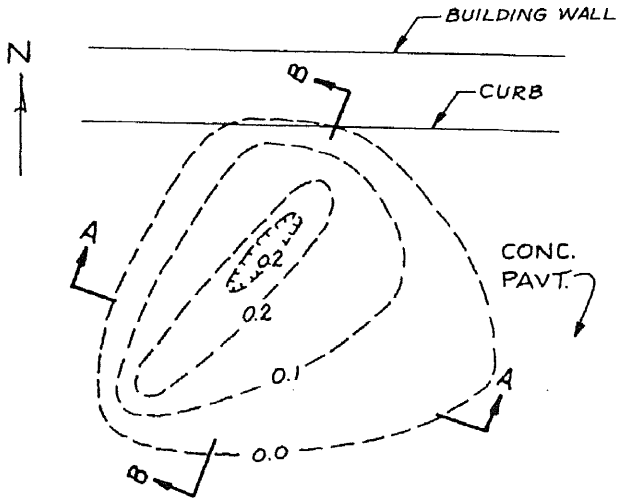

PLAN

SCALE IN FEET

0 5' 10' 20'

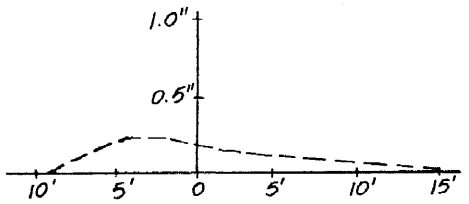

SECTION A-A

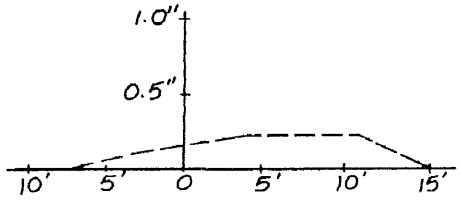

SECTION B-B

VERTICAL EXAGGERATION 120X

HEAVE INFORMATION:

FLOW RATE (Q): 1018 SCFM
INJECTED AIR VOL. (V_a): 339 SCF
HEAVE VOLUME (V_h): 23.7 CF
RESIDUAL VOLUME (V_r): 3.55 CF
HEAVE AREA (A_h): 381.9 SF (Residual)
MAX. APERTURE: 0.34 IN.
AVG. APERTURE: 0.11 IN. (.052 IN.)
MAX. HEAVE LENGTH: 17 FT.
AVG. HEAVE LENGTH: 11 FT.

SYSTEM INFORMATION (12J)

AVG. CYL. PRESSURE: 2388 PSI
VALVE PRESSURE: 150 PSI
DOWNHOLE PRESSURE: N/A
PACKER TYPE: DOUBLE
DEPTH OF FRAC. ZONE: 4'-6'
DEPTH TO BOREHOLE BOT.: 9 FT.
SOIL TYPE: CLAYEY SAND, SC

DATE: 7-23-91
NUMBER: FP-1, NO. 1 RESIDUAL (1ST Residual)
LOCATION: ROSELAND, N.J.
SEQUENCE: INITIAL

ADVANCED TECHNOLOGY CENTER DIVISION OF SITE ASSESSMENT		
HEAVE DIAGRAM & INFORMATION		
NEW JERSEY INSTITUTE OF TECHNOLOGY NEWARK, NEW JERSEY		
DATE: 1/92	DRAWN: U.F.D.	FIG. NO.:

Figure A31 Heave Diagram and Information for the Roseland Site.

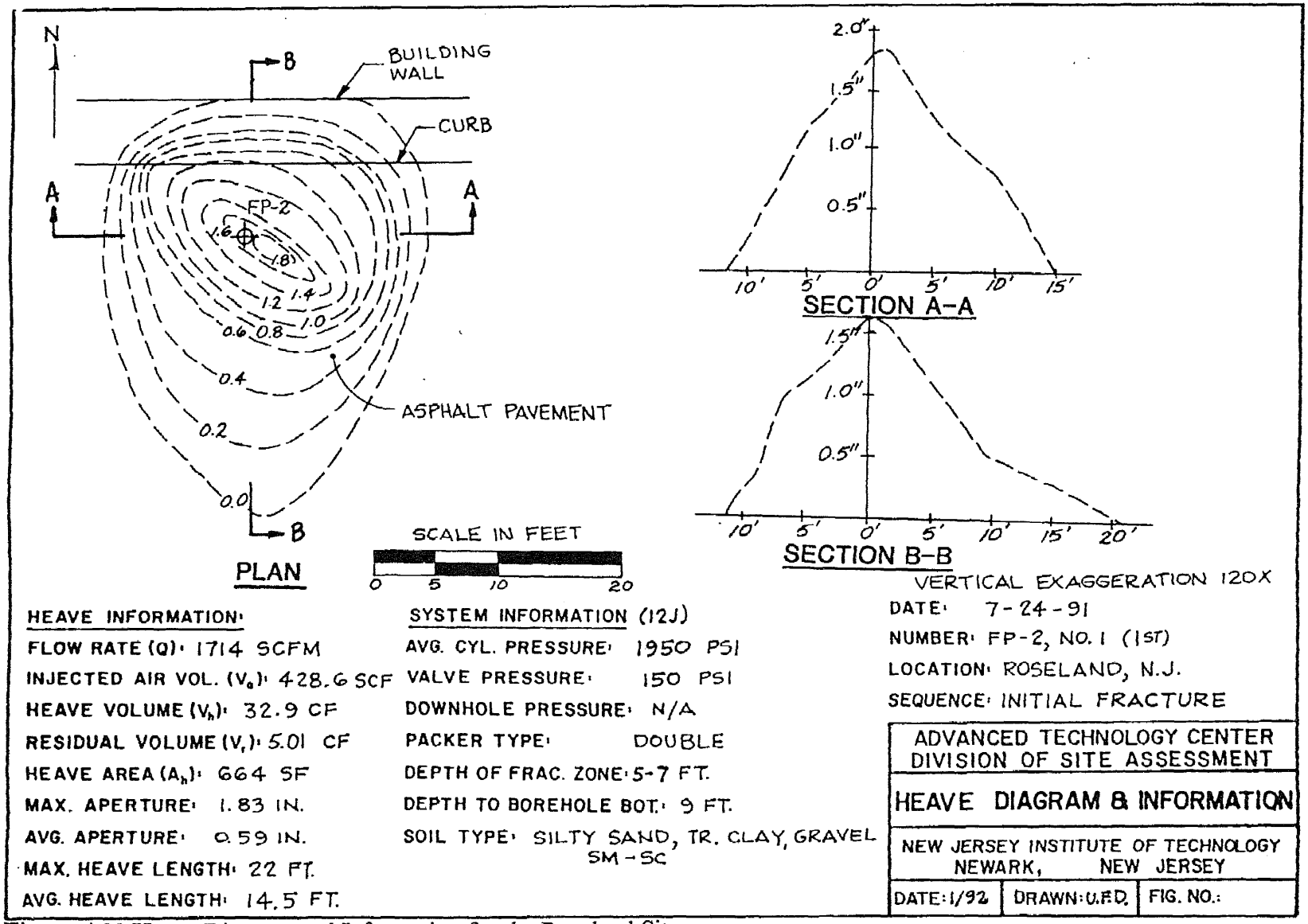

HEAVE INFORMATION:

FLOW RATE (Q):	1714 SCFM
INJECTED AIR VOL. (V_a):	428.6 SCF
HEAVE VOLUME (V_h):	32.9 CF
RESIDUAL VOLUME (V_r):	5.01 CF
HEAVE AREA (A_h):	664 SF
MAX. APERTURE:	1.83 IN.
AVG. APERTURE:	0.59 IN.
MAX. HEAVE LENGTH:	22 FT.
AVG. HEAVE LENGTH:	14.5 FT.

SYSTEM INFORMATION (12J)

AVG. CYL. PRESSURE:	1950 PSI
VALVE PRESSURE:	150 PSI
DOWNHOLE PRESSURE:	N/A
PACKER TYPE:	DOUBLE
DEPTH OF FRAC. ZONE:	5-7 FT.
DEPTH TO BOREHOLE BOT.:	9 FT.
SOIL TYPE:	SILTY SAND, TR. CLAY, GRAVEL SM-SC

DATE: 7-24-91
NUMBER: FP-2, NO. 1 (1ST)
LOCATION: ROSELAND, N.J.
SEQUENCE: INITIAL FRACTURE

ADVANCED TECHNOLOGY CENTER
DIVISION OF SITE ASSESSMENT

HEAVE DIAGRAM & INFORMATION

NEW JERSEY INSTITUTE OF TECHNOLOGY
NEWARK, NEW JERSEY

DATE: 1/92	DRAWN: U.F.D.	FIG. NO.:

Figure A32 Heave Diagram and Information for the Roseland Site.

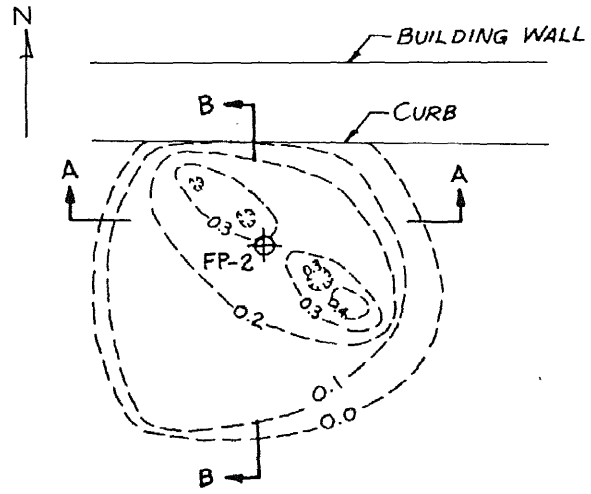

PLAN

SCALE IN FEET

0 5 10 20

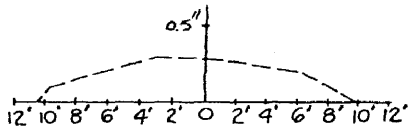

SECTION A-A

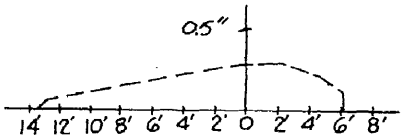

SECTION B-B

VERTICAL EXAGGERATION 120X

HEAVE INFORMATION:

FLOW RATE (Q): 1714 SCFM
INJECTED AIR VOL. (V_a): 428.6 SCF
HEAVE VOLUME (V_h): 32.9 CF
RESIDUAL VOLUME (V_r): 5.01 CF
HEAVE AREA (A_h): 344.32 FT.^{2}
MAX. APERTURE: .49 IN.
AVG. APERTURE: .175 IN. (.09 IN.)
MAX. HEAVE LENGTH: 14.5 FT.
AVG. HEAVE LENGTH: 11 FT.

SYSTEM INFORMATION (12 J)

AVG. CYL. PRESSURE: 1950 PSI
VALVE PRESSURE: 150 PSI
DOWNHOLE PRESSURE: N/A
PACKER TYPE: DOUBLE
DEPTH OF FRAC. ZONE: 5'-7'
DEPTH TO BOREHOLE BOT.: 9 FT.
SOIL TYPE: SILTY SAND, TR. CLAY, GRAVEL SM-SC

DATE: 7-24-91
NUMBER: FP-2, NO-1 RESIDUAL
LOCATION: ROSELAND, N.J.
SEQUENCE: INITIAL FRACTURE

ADVANCED TECHNOLOGY CENTER DIVISION OF SITE ASSESSMENT		
HEAVE DIAGRAM & INFORMATION		
NEW JERSEY INSTITUTE OF TECHNOLOGY NEWARK, NEW JERSEY		
DATE: 1/92	DRAWN: UFD	FIG. NO.:

Figure A33 Heave Diagram and Information for the Roseland Site.

Appendix B: Geologic Description of Test Sites.

Clayey Silt - Frelinghuysen Township, NJ

Frelinghuysen Township is located in the Kittatiny Valley of the Appalachian Ridge and Valley Physiographic Province. The surficial soils were deposited during the Wisconsin Glacial Advance of the Pleistocene Epoch. The primary test site is a glacial lacustrine deposit containing clayey silt and sandy silt. The Unified Classification of the soil texture ranges from CL to ML. Depth to groundwater is variable and ranges from 3 to 10 + feet through out the year.

The soil formation was predominantly fine-grained and fairly uniformed. However, although there was evidence of some horizontal stratification, the formation could not be classified as varved. A geologic section of the site is shown in Figure B.1.

Clayey Silt - Marcus Hook, PA

This test site is a former gasoline blending plant which was destroyed by fire. It is located in Marcus Hook, Pennsylvania, in the Coastal Plain Physiographic Province, approximately one mile north of the Delaware River. The surficial unconsolidated deposits consists of recent surface fill and natural sediments of Cretaceous Age. Proglacial sediments deposited during the retreat of the Pleistocene Glaciers are found in the near vicinity. A basement of mica schist bedrock known as the Wissahickon formation underlies the site at variable depths. Based on reconnaissance geologic data the latter may be found down to 50 feet.

A typical soil boring taken during the installation of wells is shown in Figure B.2. As indicated, the surficial layer of fill was derived from the naturally occurring clayed silt is mixed with varying amounts of imported sand and gravel. The fill extends to approximately 4 feet. Within this zone, there are a number of abandoned concrete formations.

The underlying layer up to approximately 9 to 10 feet can be classified as being predominantly clayey silt, with a number of occasionally sand zones. The consistency of

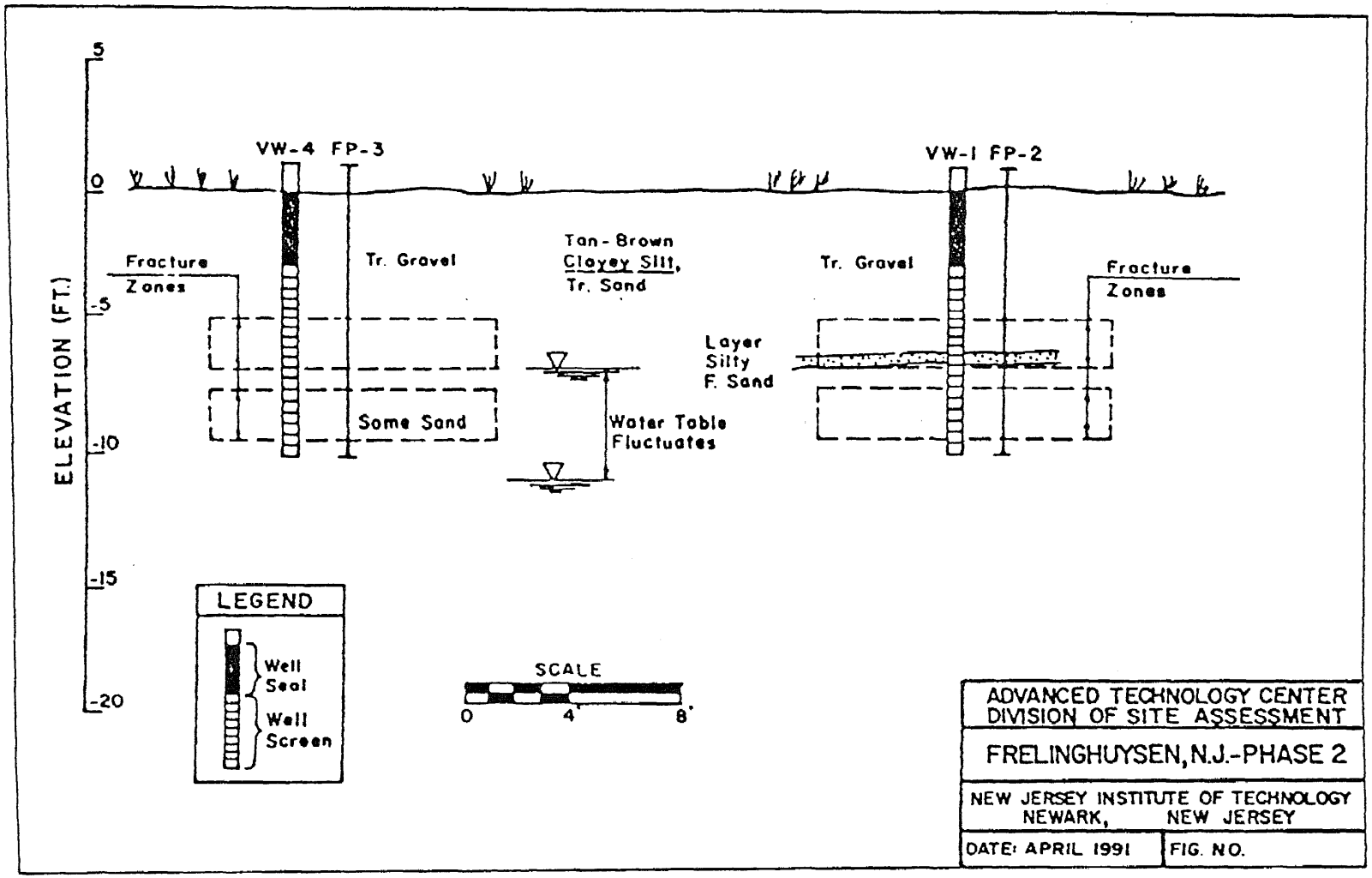

Figure B1 Schematic for a Geologic Section showing a Glacial Lacustrine Deposit at the Site.

BORING LOG

PROJECT - MARCUS HOOK	LOCATION Gravel Parking	RIG TYPE ATV CME 750
PROJECT #	DRILLING CO.	BORING ID 4.25
DATE 12/10/91	DRILLER	BORING O.D. 8 IN.
LOGGED BY	METHOD HSA/SPSP	TOTAL DEPTH 10 FT.

SAMPLED	BLOWS PER 6 IN.	REC. IN.	DEPTH FEET	SAMPLE DESCRIPTION
1	34,15 8,8	18		Top .5" gravel (1.0'). Change to dk. brown med. sand & silt dry, odor. Bottom 6" bk. oily silt & clay, strong odor.
2 (700 ppm)	4,3 2,2	18	2	Bk.-brown coarse sand, silty clay, staining, strong odor, moist.
3	3,8 8,9	18	4	Dk. gray silt & clay, moist, odor.
4	3,3 5,7	22	6	Top 1.5'greenish-brown silty med. sand & clay, strong odor. Bottom 4" greenish-brown silt & clay , odor.
5	3,4 6,8	23	8	Greenish-gray silty clay, moist.
6		18	10	Top 3" same as above. Change to med.-coarse sand, very wet. Change to greenish-gray clay.
			12	TD = 10' SPSP = 12'
			14	
			16	

GROUNDWATER DEPTH (FT) DATE/TIME

REMARKS: TD - TOTAL DEPTH Total of 5 samples collected.
SPSP - SPLIT SPOON SAMPLE
Note: PID readings could not be taken because of windy and freezing conditions.

Figure B2 Typical Boring Log for the Marcus Hook Site.

these zones were found to range from medium stiff to stiff and this deduction was made based on the blow counts during sampling. This confirms that a high degree of overconsolidation exists in this substratum. From around 9 to 10' the clayey silt grades into a gray silty sand.

Of notable interest in this soil zone was the increase of moisture content. A subsequent boring established that the water table varies between the 12 to 15 feet and is classified as an unconfined aquifer.

Sandy Silt - Chem Fleur, Newark, NJ

This test site is a former perfume plant and is located in the Newark Basin. The site is currently paved with concrete. At this site no soil cores were taken, but based on reconnaissance geologic data the following is inferred. A thin blanket of fill common to this area overlies the site and is known to vary in thickness up to several feet. Beneath the fill is natural surficial which essentially consists of a red-brown glacier till deposit. In the zone of interest from 0 to 10 feet, the soil was characterized as being predominantly sandy silt.

Brunswick Sandstone - Newark, NJ

The test site is a parking lot on the NJIT campus which is located in the Newark Basin. The parking lot is paved with asphalt concrete. A thin blanket of fill overlies the site and varies in thickness from a few to several feet. Beneath the fill at most locations is the natural surficial soil which consists of red-brown glacial till. Underlying the till approximately 5 - 10 feet below grade is the Brunswick formation.

The Brunswick formation consists of a monotonous succession of reddish-brown mudstone and siltstone, with local beds of claystone and fine-grained sandstone. The formation has a non-marine origin and is estimated to range in thickness from 6,000 to 16,000 feet through the basin. Based on reconaissance geologic data, the strike is

estimated at North 20 degrees East and the dip 10 degrees West.

A core log of this site is shown Figure B.3 The predominant lithology of the rock is fine sandstone with occasional zones of siltstone and infrequent shale seams and partings. The jointing is predominantly horizontal and coincides with original bedding. Joint frequency varies from very closely spaced to medium spaced. The depth to the ground water fluctuates between 21 - 25 feet.

Siltstone-Hillsburg, NJ

The stratigraphy of the site can be generally described as 3 feet of soil fill overlying sedimentary rock. The rock formation is of Triassic Age and is most commonly known as the Brunswick Formation, although recently it has been renamed as the Passaic Formation of the Newark Supergroup. A core sample recovered during construction of the fracture well showed the bedrock lithology within the treatment zone was predominantly siltstone, with occasional zones which would classify texturally as shale or fine sandstone. The predominant joint set was nearly horizontal, corresponding to the formation dip which is approximately 5 degrees west. The rock structure can be described as intensely jointed, although it increased in competency with depth. The core recoveries were good, with recovery ratios ranging from 90 to 95%. The RQD's (Rock Quality Designator) for the upper and lower 5 ft. core runs were 0% and 26%, respectively, which reflect the intensity of jointing.

The phraetic groundwater surface is encountered at 22 and 25 feet below ground surface across the site. All drilling and fracture operations were limited to the vadose zone, and were carried out above a depth of 18 feet. A perched water zone was encountered between 12 and 18 feet, which necessitated frequent dewatering in the zone of treatment during operations.

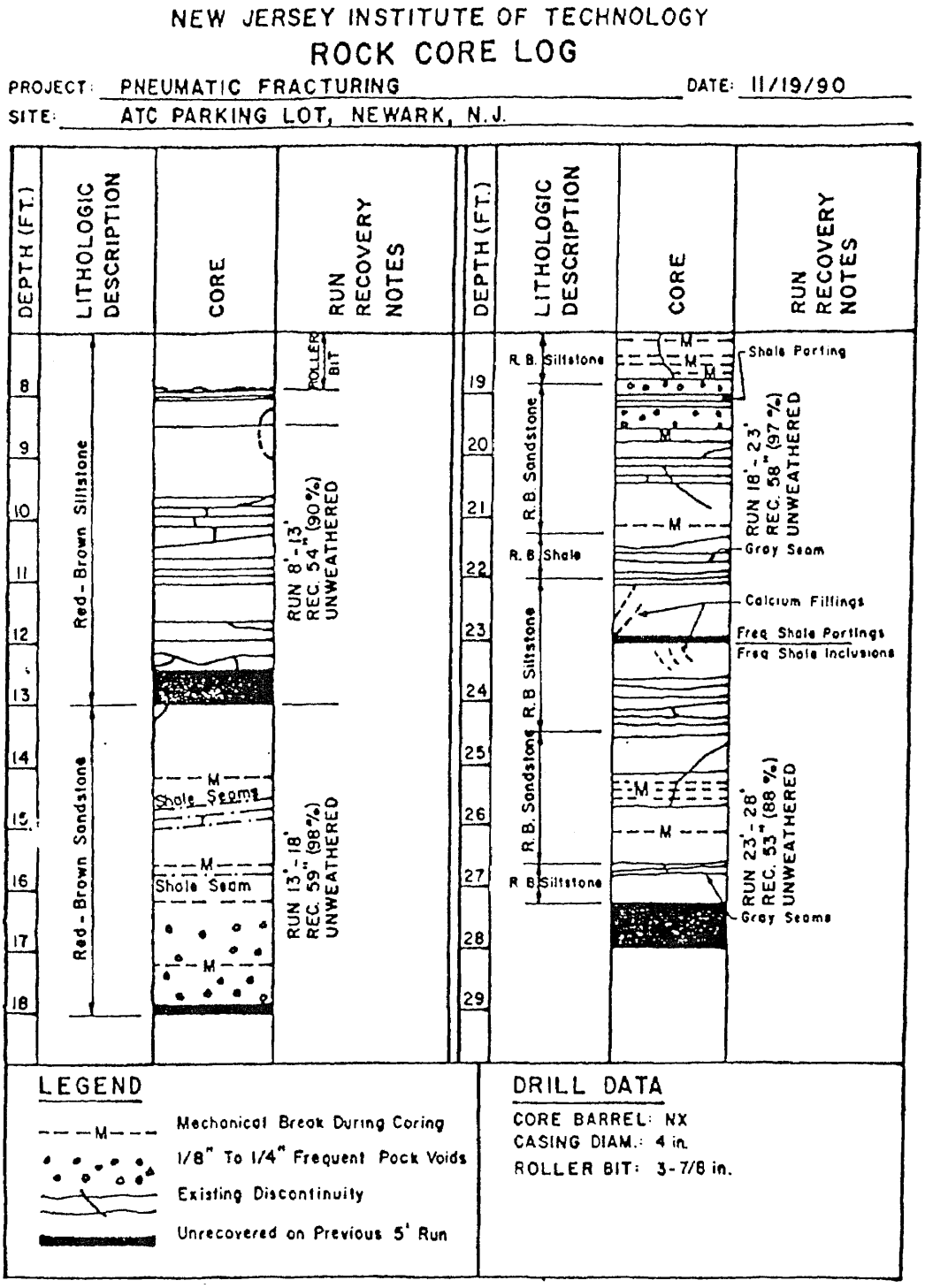

Figure B3 A Rock Core Log for the Newark (NJIT) Site.

Appendix C: Pressure - Time Histories.

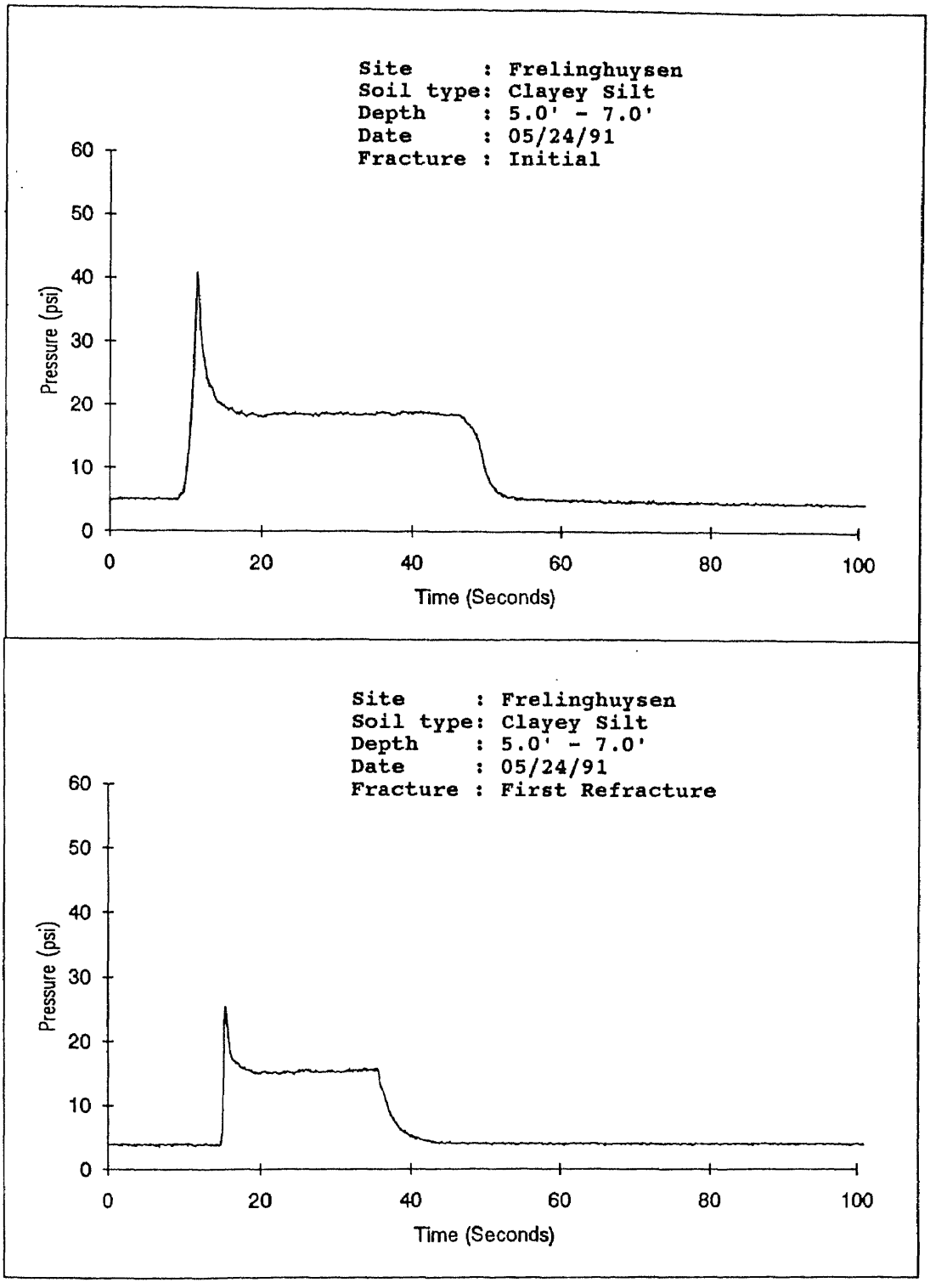

Figure C1 Pressure - Time Histories for the Frelinghuysen Site.

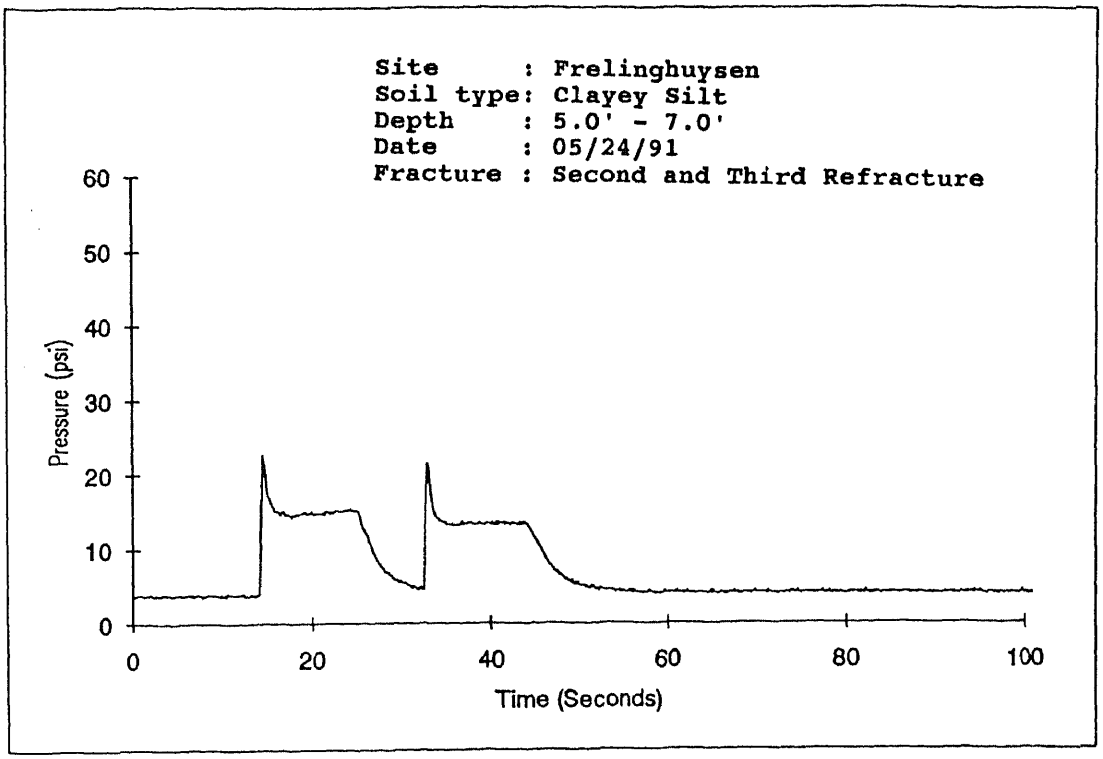

Figure C2 Pressure - Time Histories for the Frelinghuysen Site.

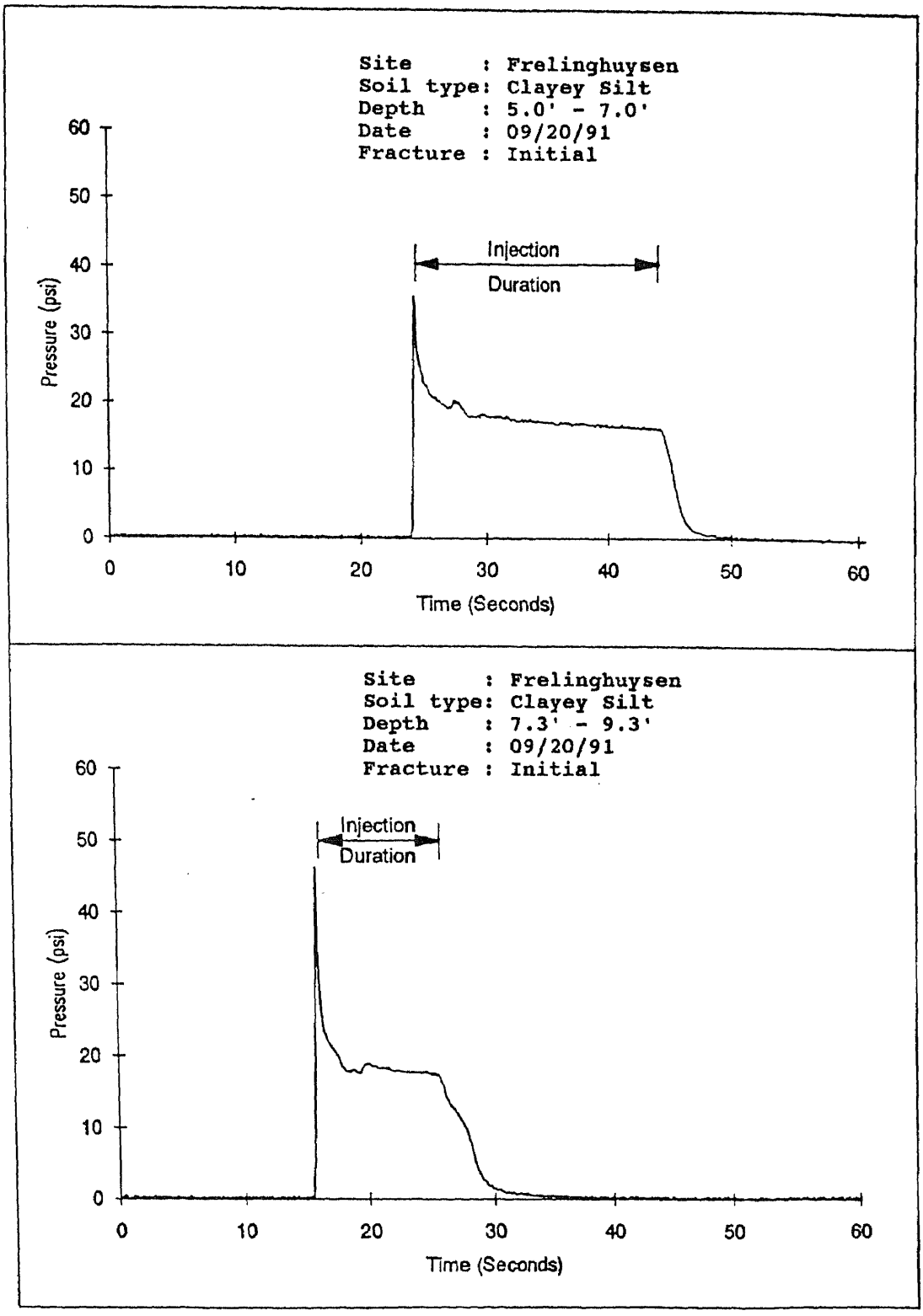

Figure C3 Pressure - Time Histories for the Frelinghuysen Site.

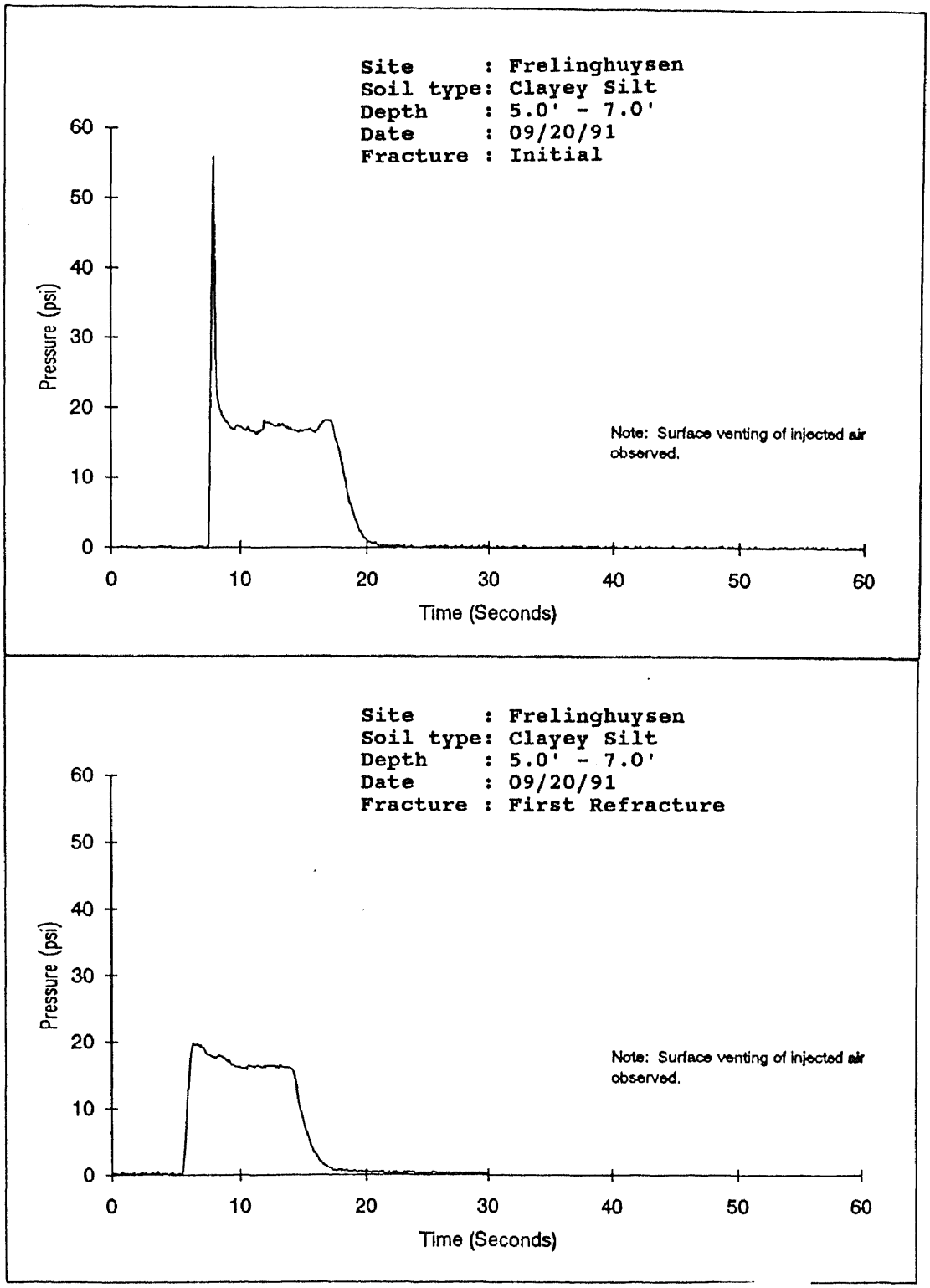

Figure C4 Pressure - Time Histories for the Frelinghuysen Site.

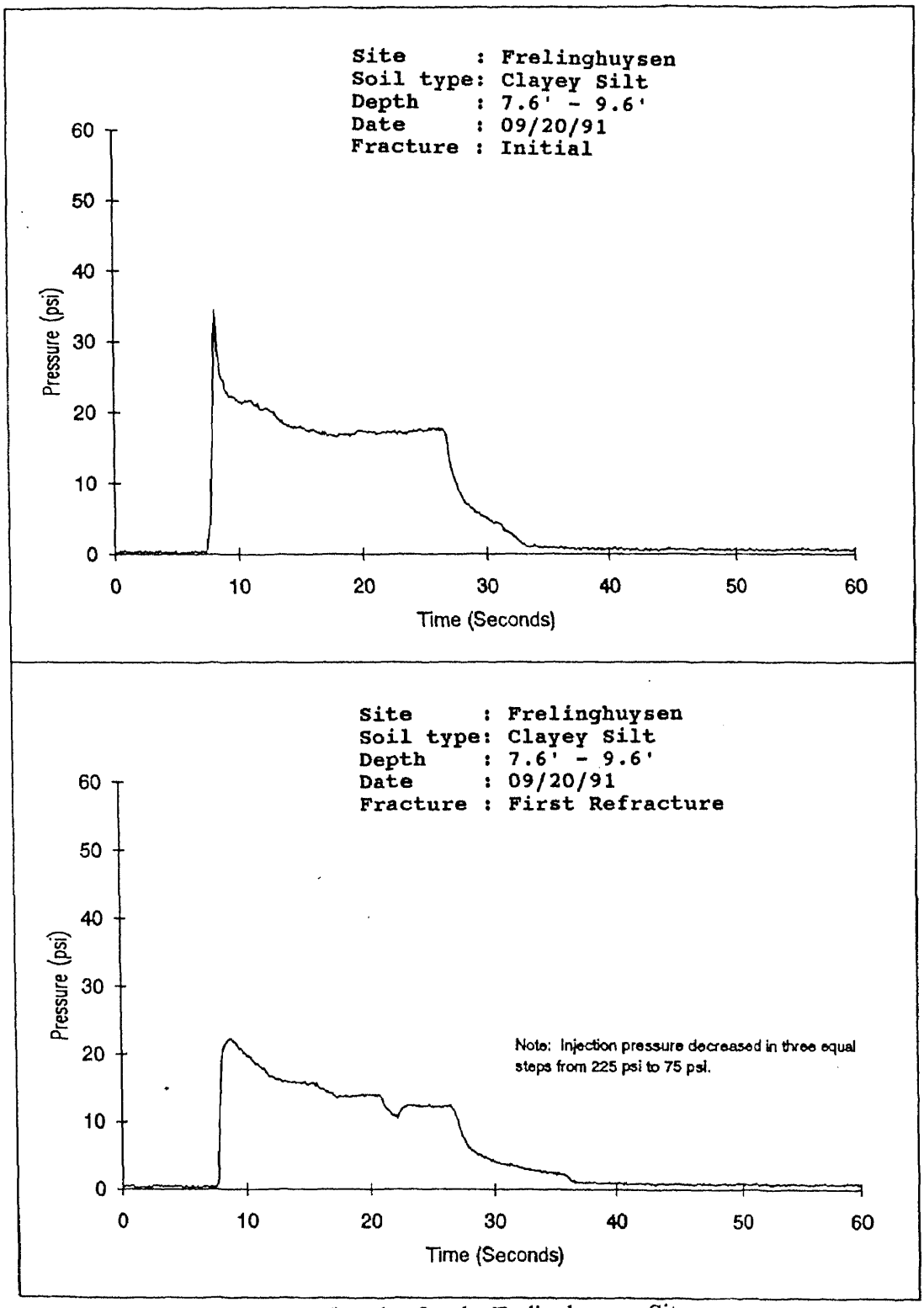

Figure C5 Pressure - Time Histories for the Frelinghuysen Site.

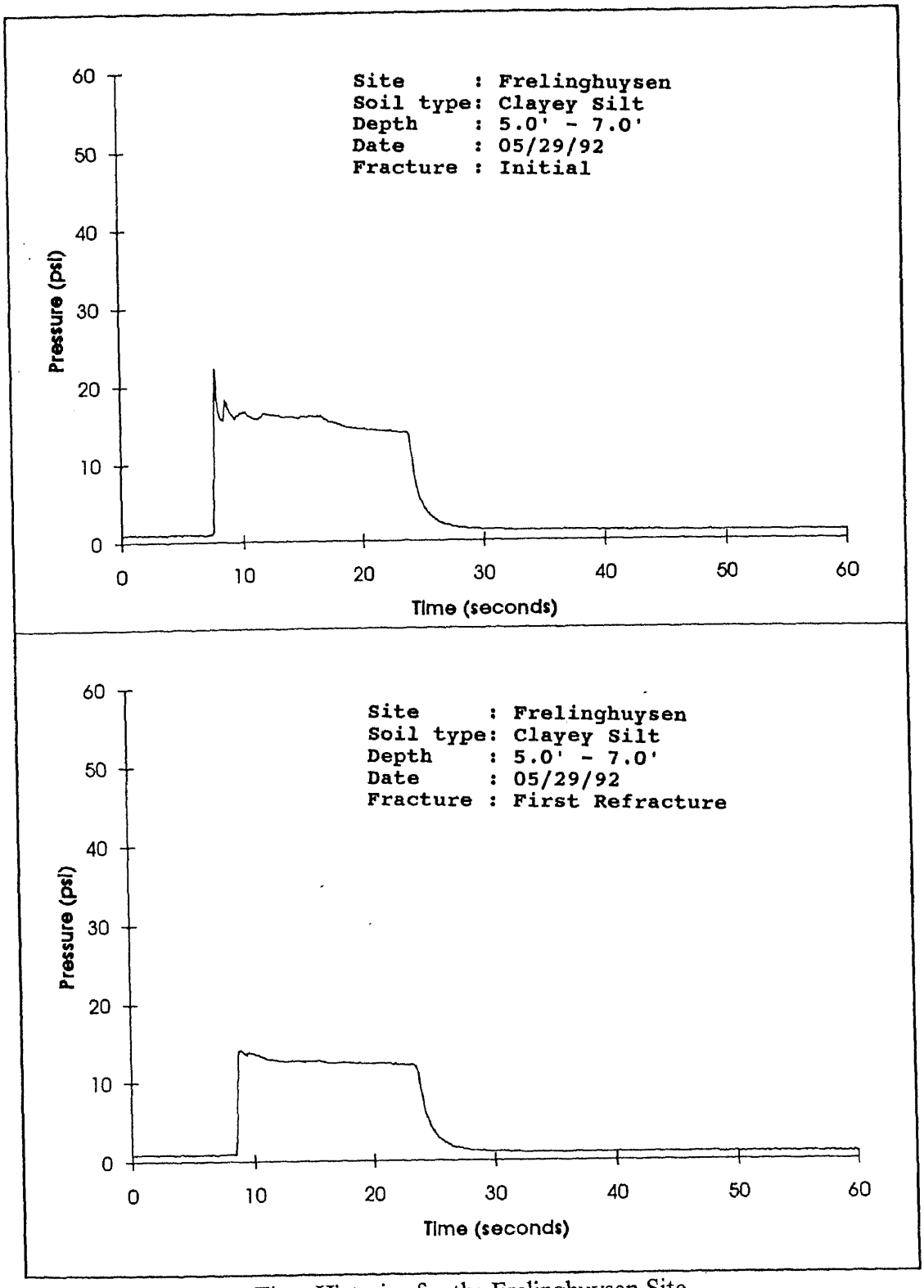

Figure C6 Pressure - Time Histories for the Frelinghuysen Site.

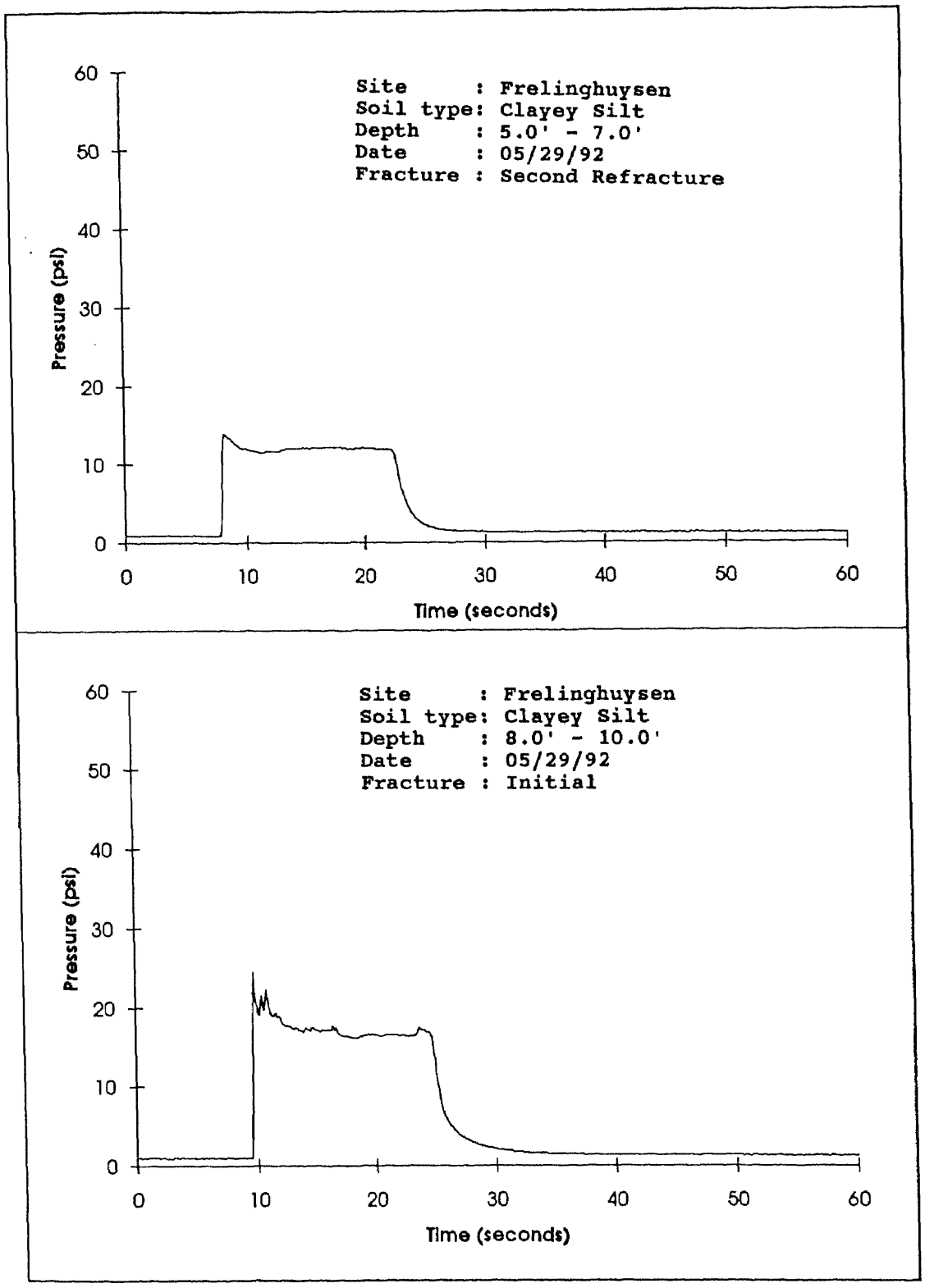

Figure C7 Pressure - Time Histories for the Frelinghuysen Site.

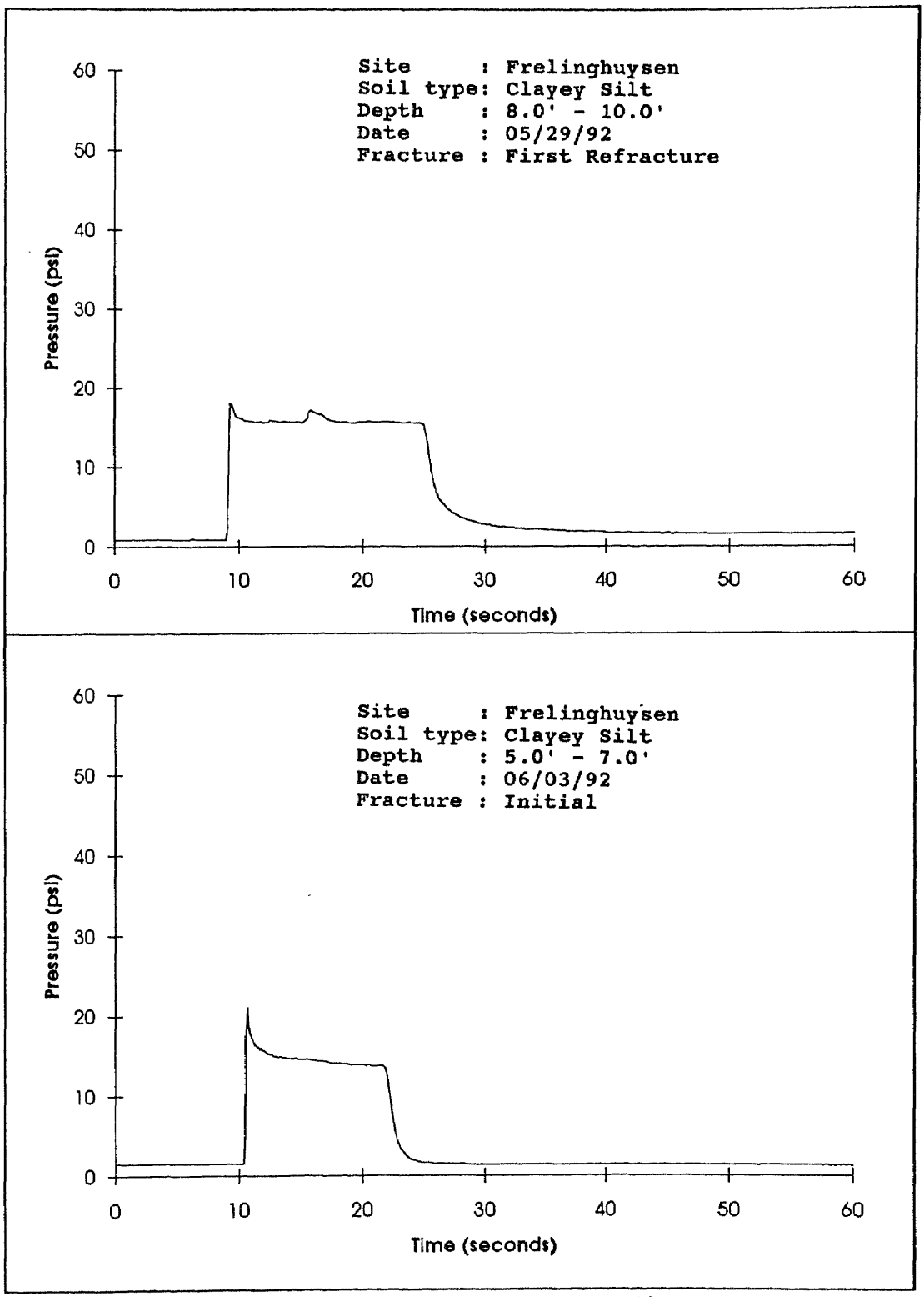

Figure C8 Pressure - Time Histories for the Frelinghuysen Site.

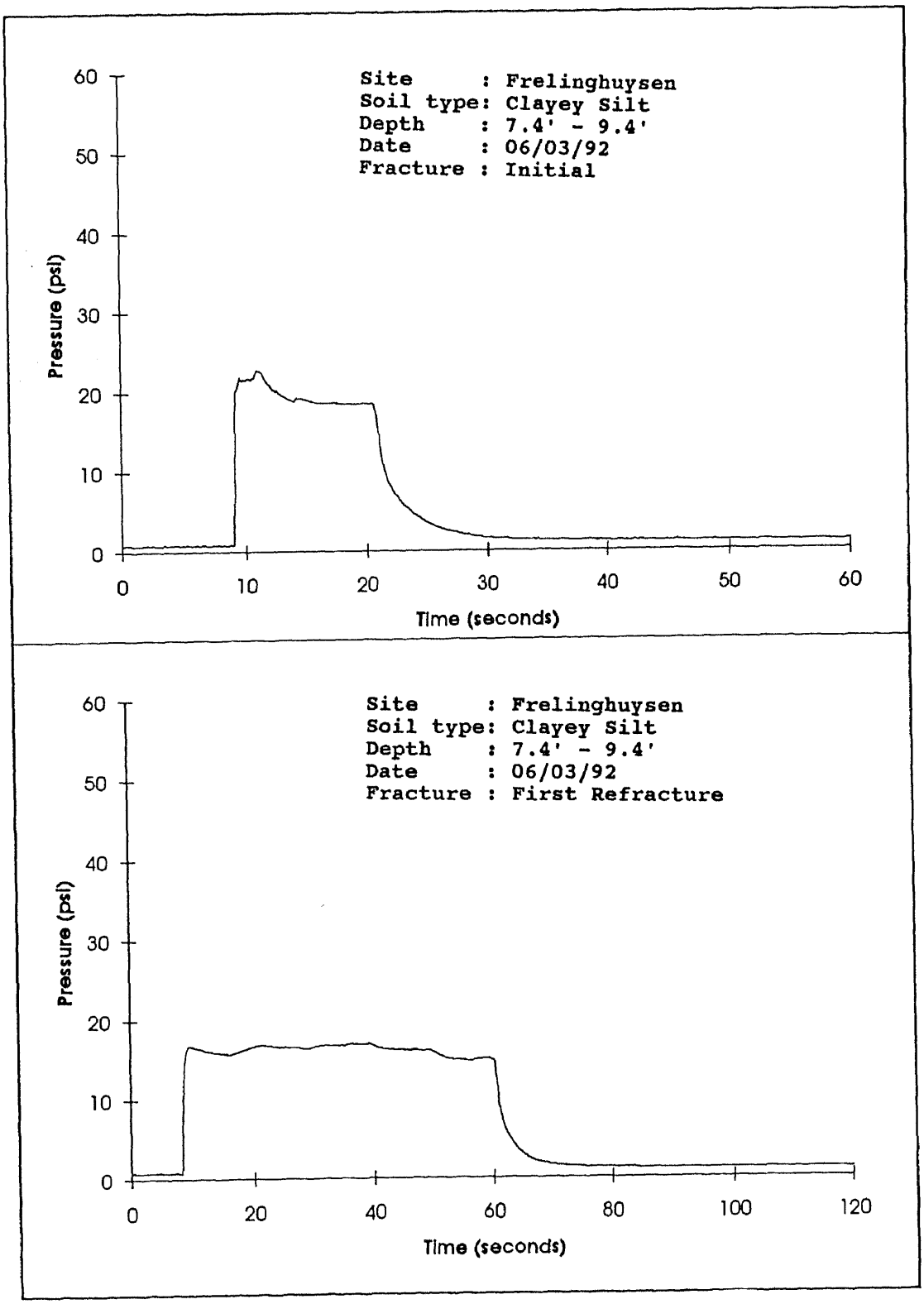

Figure C9 Pressure - Time Histories for the Newark (NJIT) Site.

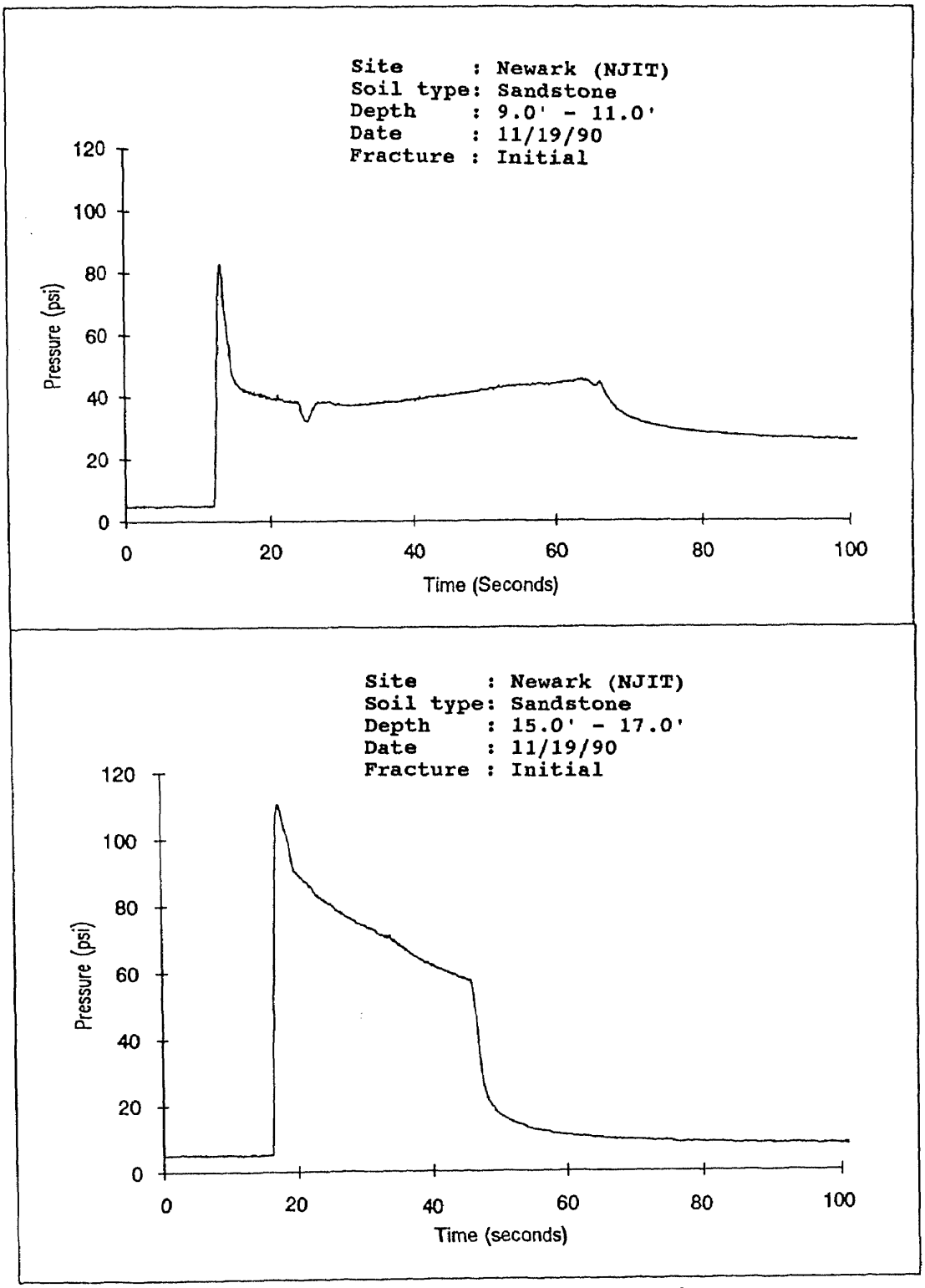

Figure C10 Pressure - Time Histories for the Newark (NJIT) Site

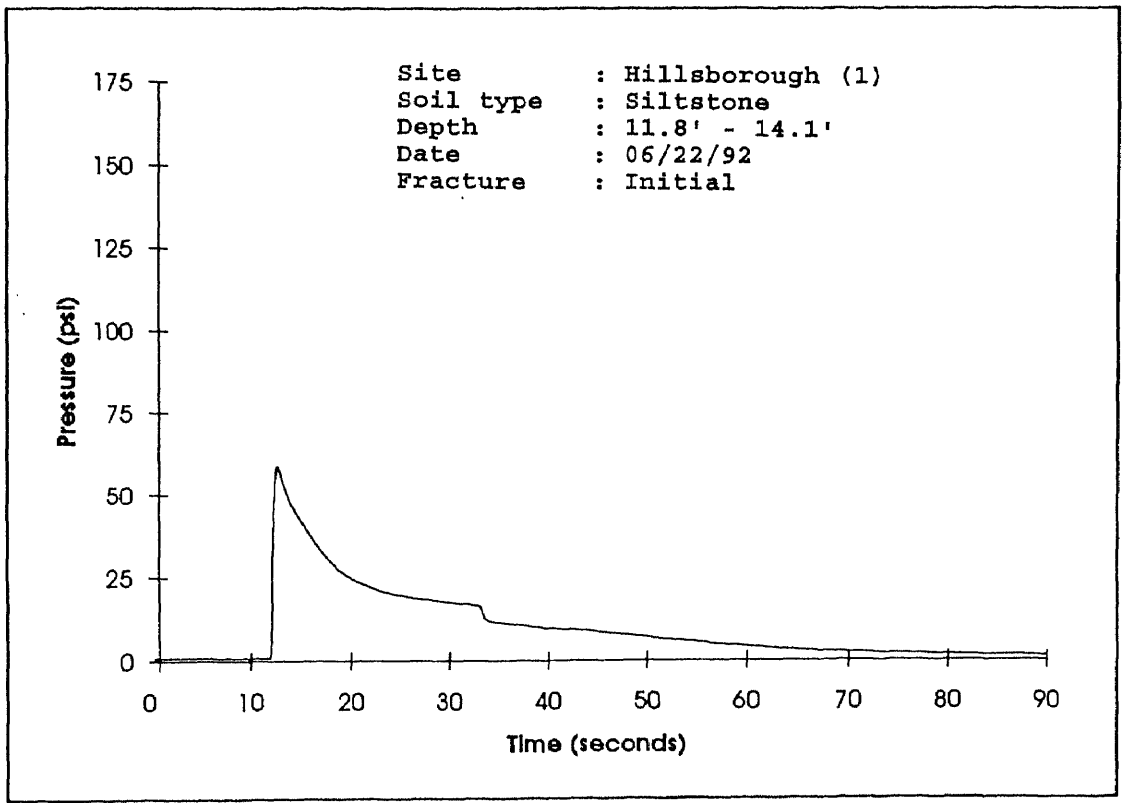

Figure C11 Pressure - Time Histories for the Hillsborough Site (1)

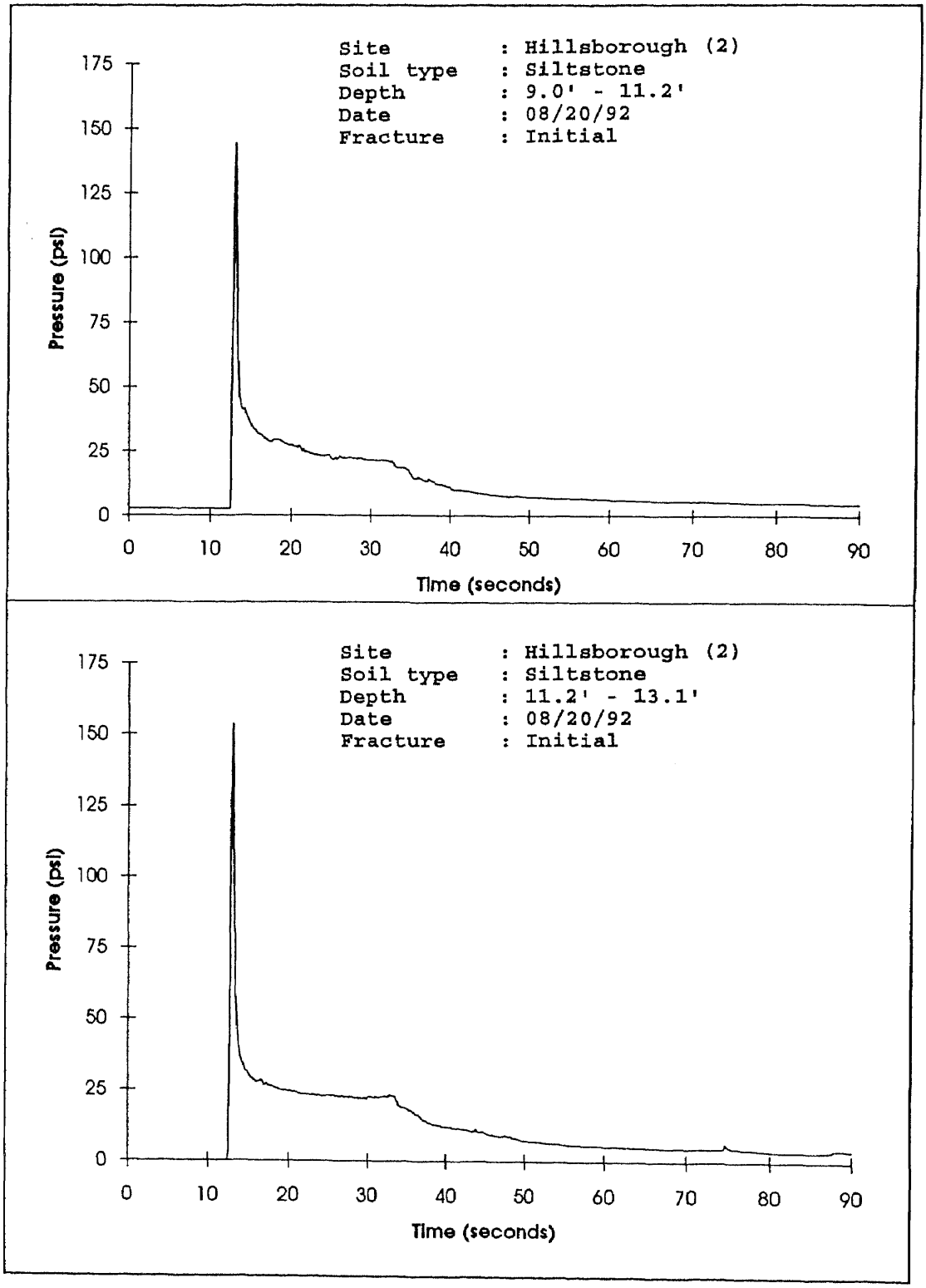

Figure C12 Pressure - Time Histories for the Hillsborough Site (2)

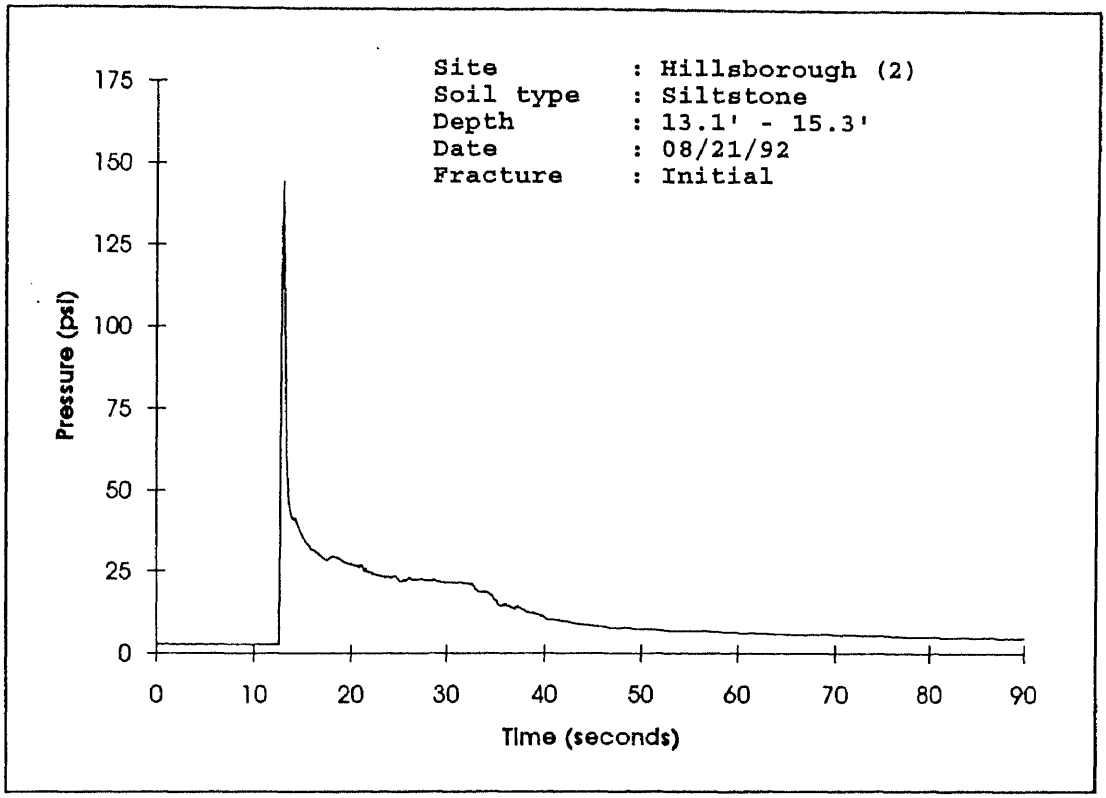

Figure C13 Pressure - Time Histories for the Hillsborough Site (2)

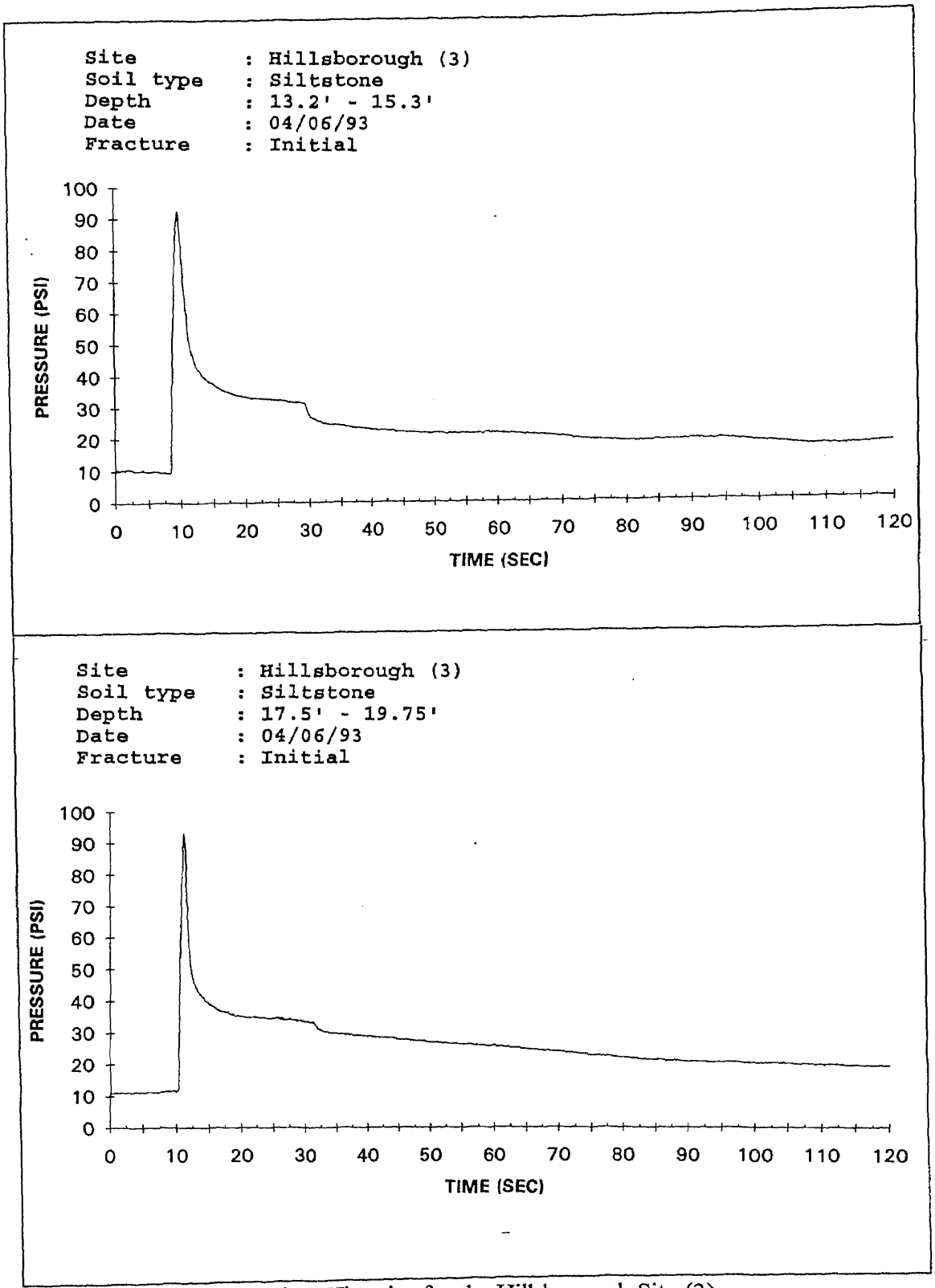

Figure C14 Pressure - Time Histories for the Hillsborough Site (3)

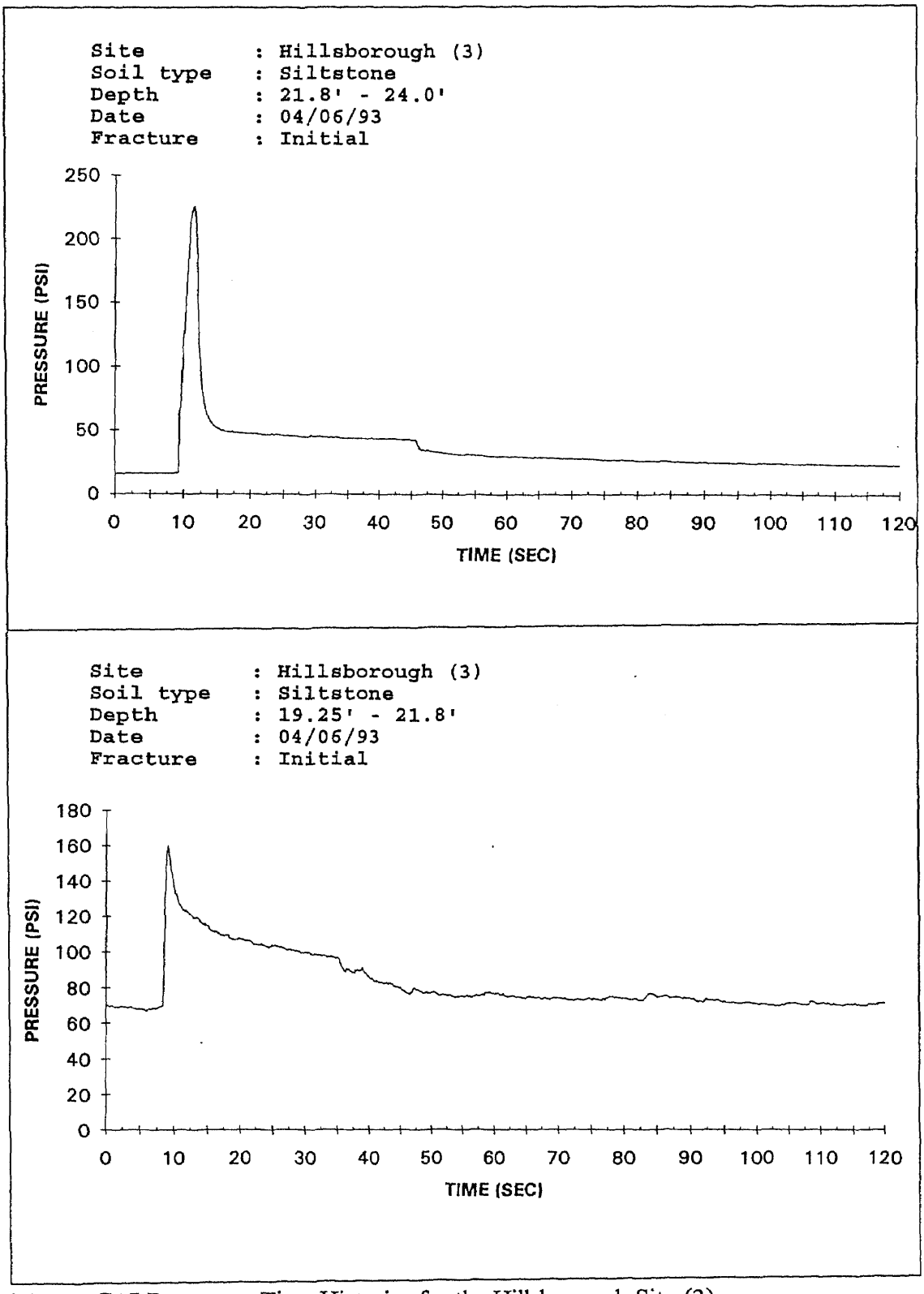

Figure C15 Pressure - Time Histories for the Hillsborough Site (3)

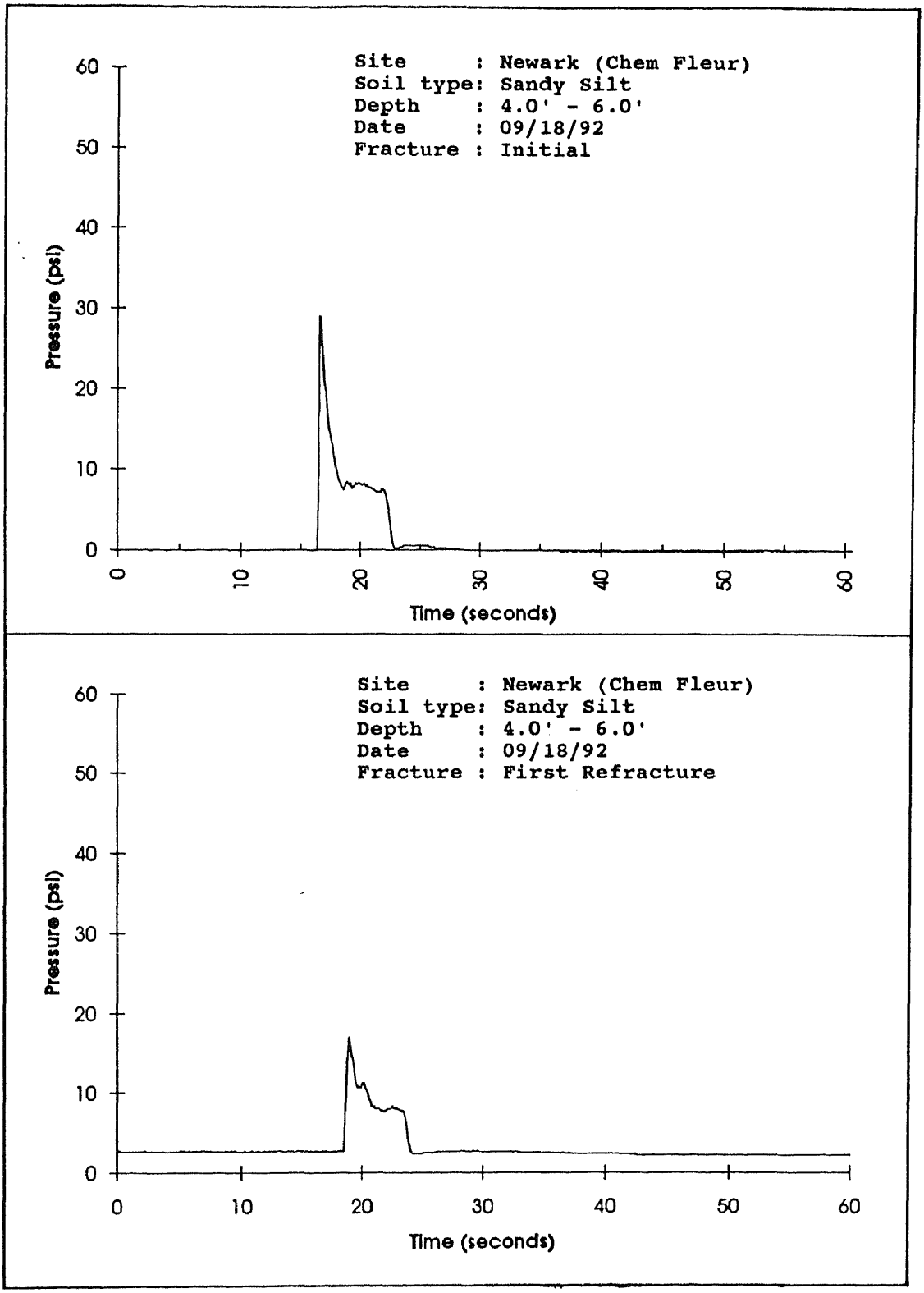

Figure C16 Pressure - Time Histories for the Newark (Chem Fleur) Site

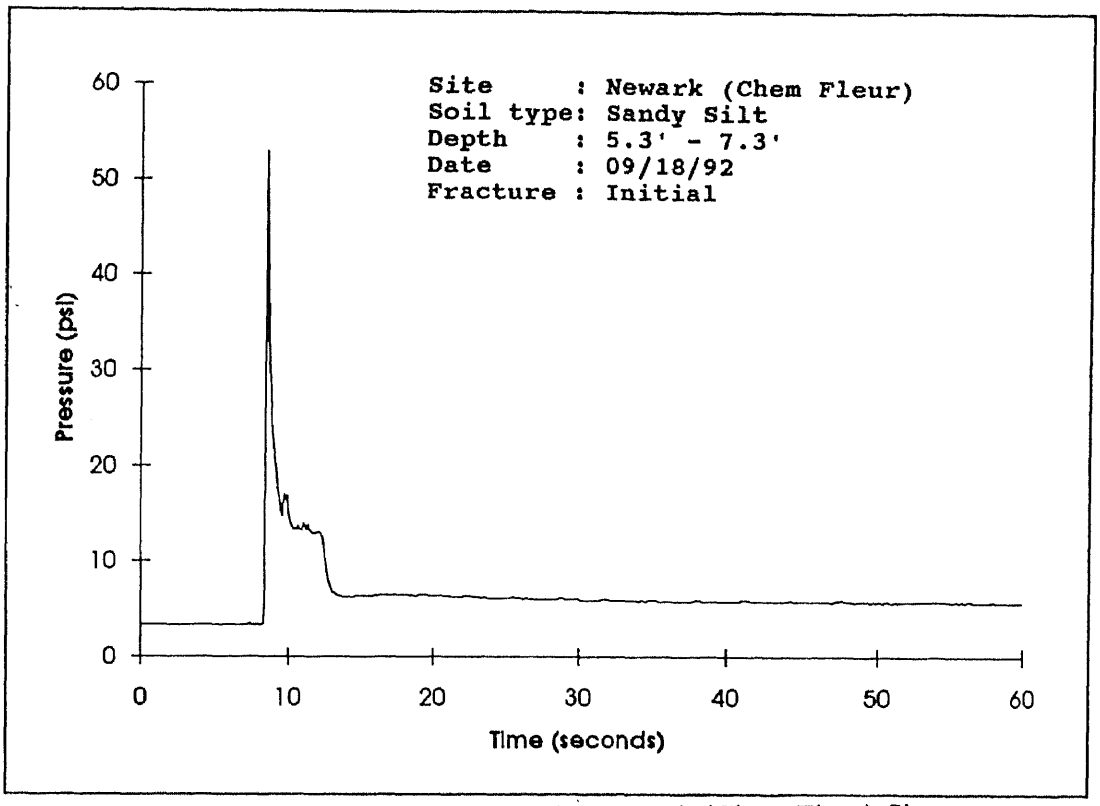

Figure C17 Pressure - Time Histories for the Newark (Chem Fleur) Site

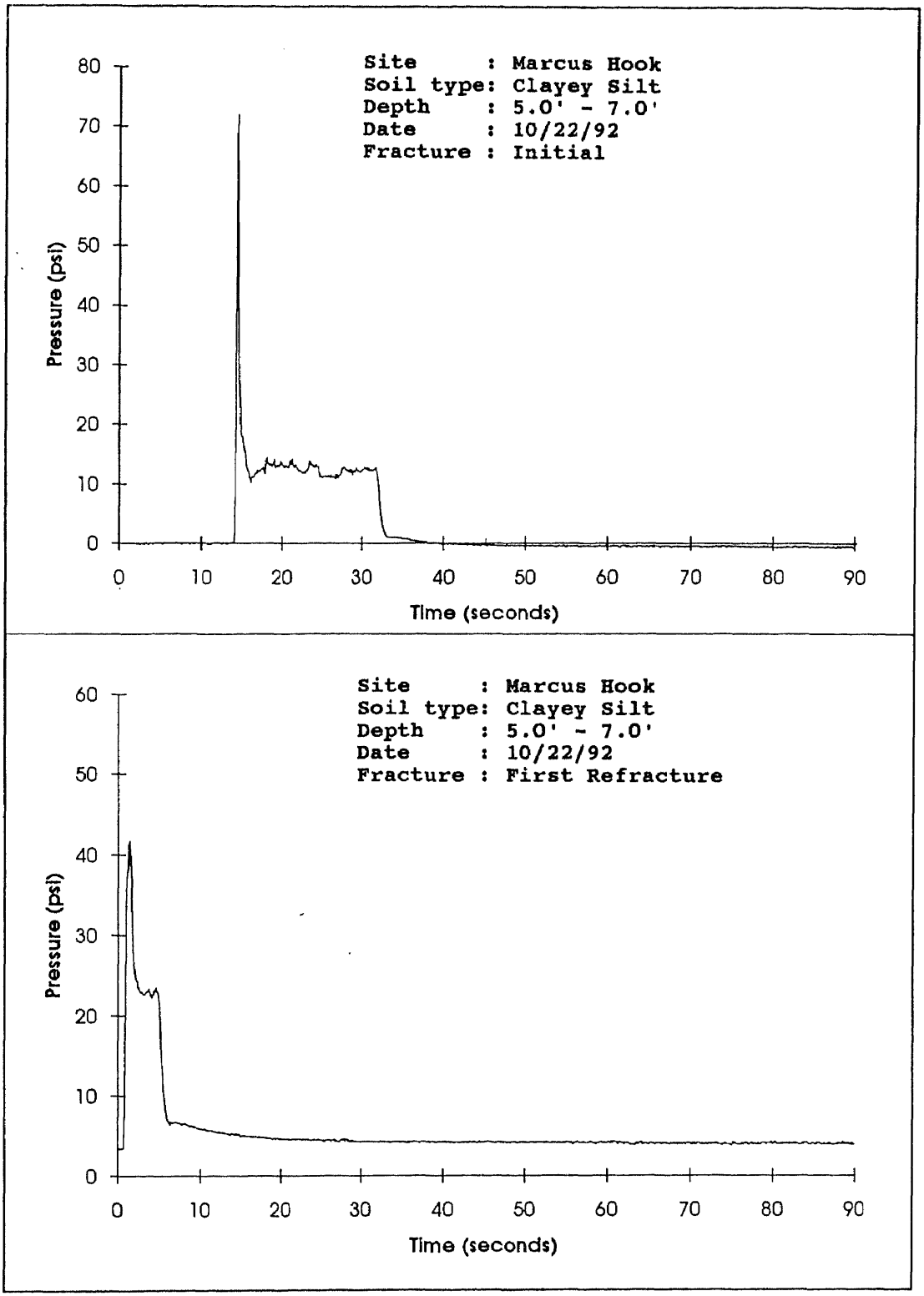

Figure C18 Pressure - Time Histories for the Marcus Hook Site

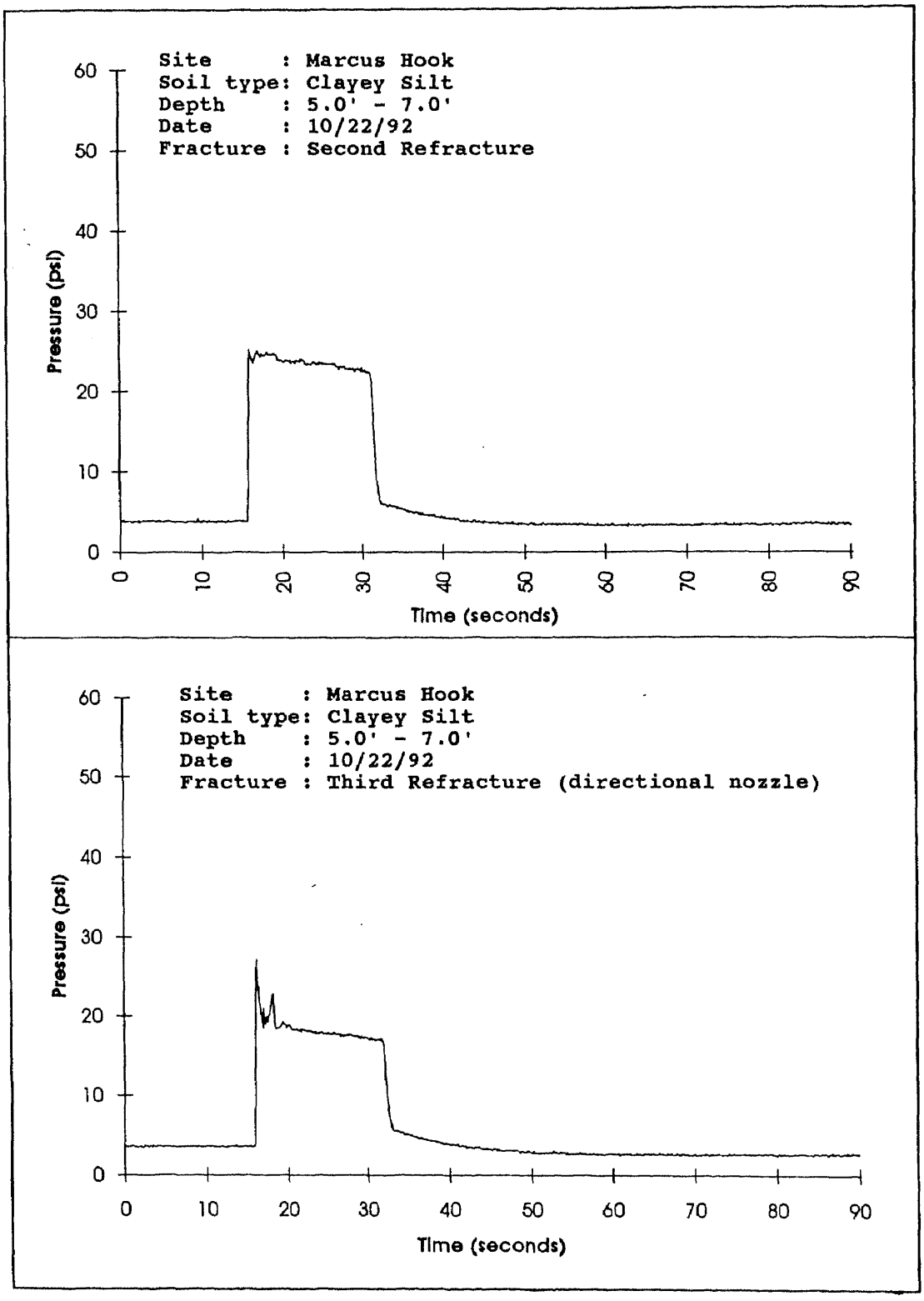

Figure C19 Pressure - Time Histories for the Marcus Hook Site

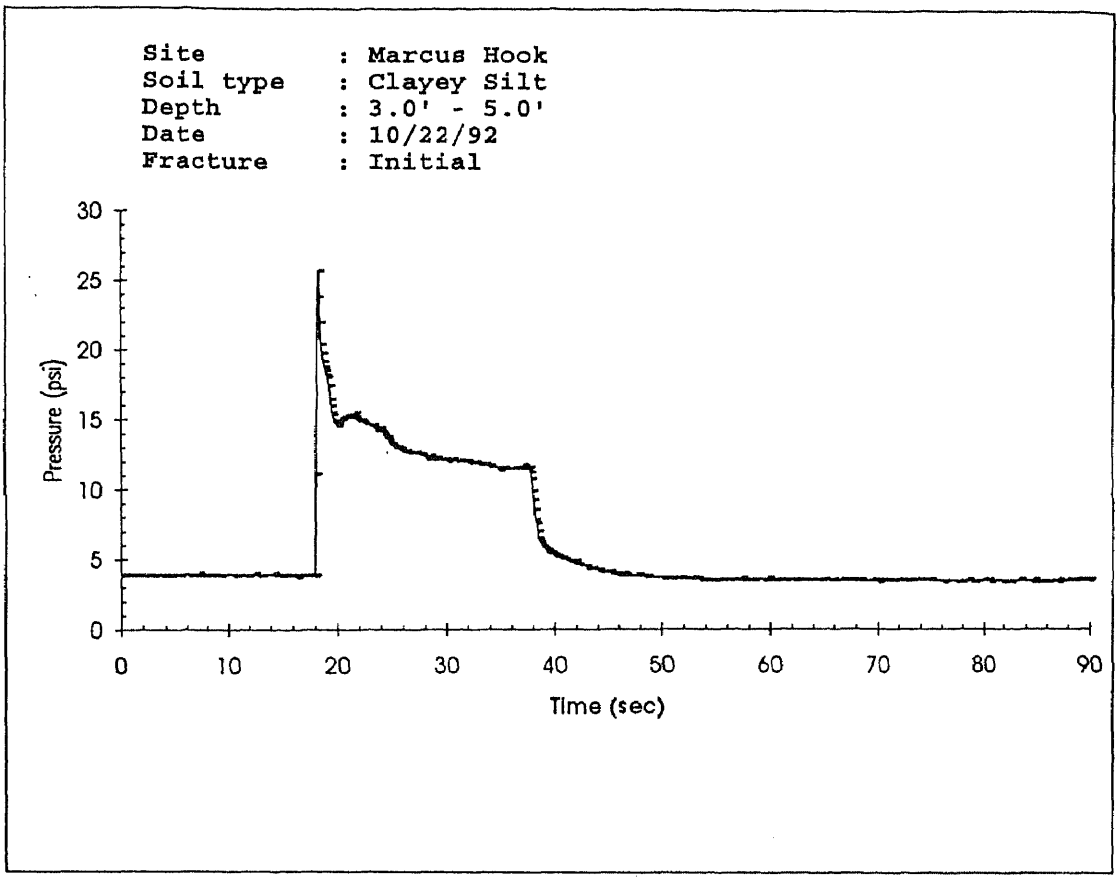

Figure C20 Pressure - Time Histories for the Marcus Hook Site

REFERENCES

Bishop, R. F., . Hill, and N. F. Mott., "The Theory of Indentations and Hardness Test," Proceedings of the British Physical Society, London, England, Vol. 57, No.3, 1949.

Bjerrum, L., and K. H. Anderson., "In-Situ Measurement of Lateral Pressures in Clay," Fifth European Conference on Soil Mechanics and Foundation Engineering, April 1972, Madrid.

Bjerrum, L., et al., "Hydraulic Fracturing in Field Permeability Testing," Geotechnique, London, England, Vol. 22, No. 2, June 1974: 319-332

Callanan, M. J., "Hydraulic Fracture Initiation by Shear Failure in Formations at Great Depth," Hydraulic Fracturing Stress Measurements,1980: 181-189.

Cambefort, H., "Grouting Loose Soils," Rock Grouting and Diaphragm Wall Construction, Developments in Geotechnical Engineering Vol. 55, 1955: 300-303

Card, D. C. Jr., "Review of Fracturing Theories", UCRL 13040, Colorado School of Mines Research Foundation. Inc., Golden Colorado. April 16, 1962: 14-20.

Gidley, J. L., S. A. Holditch, D. E. Nierode, and R. W. Veatch, Recent Advances in Hydraulic Fracturing, SPE, Richardson, TX, 1989.

Goodman, R. E., Introduction to Rock Mechanics, Wiley, NY, 1980: 31

Griffith, A. A., "The Phenomena of Rupture and Flow in Solids", Philos. Trans. Royal Society., London, Vol. 221 A, 1921.

Grundy. C.F., "The treatment by Grouting of Permeable Foundations of Dams," Proceedings of the 5 th Congress on Large Dams, 1: 647-674

Haimson, B. G., "Hydraulic Fracturing in Porous and Non-Porous Rock and its Potential for Determining In-Situ Stresses at Great Depth," Technical Report No. 4-68, United States Army Core of Engineers, Missouri Division Omaha, Neb., 1968

Haimson, B. G. and C. Fairhurst, "In-Situ Stress Determination at Great Depth by Means of Hydraulic Fracturing," Rock Mechanics-Theory and Practice, 1970: 559-584.

Howard, G. C. and C. R. Fast., Hydraulic Fracturing Monograph Series, SPE, Richardson, TX, 1970.

Hubbert, M. K. and ..G. Willis., "Mechanics of Hydraulic Fracturing", Trans. AIME, Vol. 210, 1957: 153-166.

Jaworski, G. W., J. M. Duncan, and H. B. Seed., "Laboratory Study of Hydraulic Fracturing", ASCE, Journal of Geotechnical Engineering, Vol. 107, No. GT6: 1981: 713-732

Jaeger, J. C. and N. J. W. Cook., "Fluid Pressure and Flow in Rocks," in Fundamentals of Rock Mechanics, Methuen and Company Ltd, London EC 4: 213-214

Jumikis, A. R. and A. Jumikis., "Red Brunswick Shale and its Engineering Aspects," Engineering Research Bulletin No. 55. Rutgers State University of New Jersey, 1975.

Kehle, R. O., "Determination of Tectonic Stresses Through Analysis of Hydraulic Well Fracturing," Journal of Geophysical Research, Vol. 69, January 1964: 259.

Ladanyi, B., "Expansion of a Cavity in a Saturated Clay Medium", ,Journal of the Soil Mechanics and Foundation Division, ASCE, Vol. 89, No. SM4, Proc. Paper 3577, July, 1963: 127-161.

Leach, R. E., "Hydraulic Fracturing of Soils-A Literature Review," Miscellaneous Paper S-77-6, U. S. Army Engineer Waterway Experiment Station, March, 1977.

Lippold, F. H., "Pressure Grouting with Packers", ASCE, Soil Mechanics and Foundation Division Journal, Vol. 84, No. SM1, Paper No. 1549, 1958.

Massarsch, K. R., "Soil Movements Caused by Pile Driving in Clay," Report 51, Commission on Pile Research, Stockholm, Sweden, 1976.

Massarsch, K. R., "New Aspects of Soil Fracturing in Clays", ASCE, Journal of Geotechnical Engineering, Vol. 104, No. GT8, August 1978: 1109-1121.

Massarsch, K. R., and B. B. Broms., "Fracturing of Soil Caused by Pile Driving in Clay," 9th International Conference on Soil Mechanics and Foundation Engineering, Vol. 1/40, Tokyo, Japan, 1977: 197-200.

Morgenstern, N. R. and P. R. Vaughan. "Some Observations on Allowable Grouting Pressures. " In Grouts and Drilling Muds in Engineering Practice, Buttersworth, London. 1963: 36-42.

Murdoch, L.C. "Innovative Delivery and Recovery Systems: Hydraulic Fracturing a Field Test,". Presented at USEPA Research Symposium. 1989.

Murdoch, L.C. G. Losonsky, P. Cluxton, B. Patterson, I. Klich, B. Braswell. "The Feasibility of Hydraulic Fracturing of Soil to Improve Remedial Actions". Final Report USEPA 600/2-91-012. NTIS Report PB 91-181818. 298, 1991.

Ng, N,. "Enhancement of Air Flow and Contaminant Removal in Fractured Soil," M.S. Project, Department of Civil and Environmental Engineering, New Jersey Institute of Technology, Newark, NJ, 1991.

Nobari, E. S., K. L. Lee, and J. M. Duncan. "Hydraulic Fracturing in Zoned Earth and Rockfill Dams", Report No. TE 73-1, Vol. 9, No. 8, Office of Research Services, University of California, Berkley, California, 1973: 17-23.

Nordgren, R. P. , "Proprogation of Vertical Hydraulic Fractures", Society of Petroleum Engineers Journal, 1972.

Nowacki, W., Thermoelasticity, Pergamon Press, New York, 1962.

Orowan, E., "Fatigue and Fracturing of Metals," paper presented at MIT Symposium, Boston, Mass. June, 1950.

Papanicolaou, P., "Laboratory Model Studies of Pneumatic Fracturing of Soils to Remove Volatile Organic Compounds", M. S. Thesis, Department of Civil and Environmental Engineering, New Jersey Institute of Technology, Newark, NJ, 1989.

Shah, N. P., "Study of Pneumatic Fracturing to Enhance Vapor Extraction of the Vadose Zone." M. S. Thesis, Department of Civil and Environmental Engineering, New Jersey Institute of Technology, Newark, NJ, 1991.

Scheidegger, A. E., "Stresses in Earth's Crusts as Determined from Hydraulic Fracturing Data," Geologie und Bauwesen, Vol. 27, No. 2, 1962: 45-53.

Schuring, J. and P. Chan, "Removal of Contaminants from the Vadose Zone by Pneumatic Fracturing." U. S. Geological Survey, Dept. of the Interior, U.S.G.S Award 14-08-0001-G1739, January 1992.

Schuring, J., V. Jurka, and P. Chan, "Pneumatic Fracturing of a Clay Formation to Enhance Removal of VOC's." Proceedings Fourteenth Annual Madison Waste Conference, Univ. of Wisconsin-Madison, September 1991.

Vaughan, P. R., "The Use of Hydraulic Fracturing Tests to Detect Crack Formation in Embankment Dam Cores," Interim Report, Department of Civil Engineering, Imperial College, London, England, 1971.

Vesic, A. S.,"Expansion of Cavities in Infinite Soil Mass," Journal of the Soil Mechanics and Foundation Division, ASCE, Vol. 98, No. SM3, Proc Paper 8790, March, 1972: 265-290.

Walsh, J. B. and W. E. Brace., "A Fracture Criterion for Brittle Anisotropic Rocks," J.Geophys. Research. 1964. LXIX, No. 16. 3449.